

Bulletin



N° **50**

December 2013

ISSN 0392-3029

Number 50
December 2013

Editor

Hamid Tagziria

European Commission, Joint Research Centre,
ITU - Nuclear Security Unit
T.P. 800, I-21027 Ispra (VA), Italy
Tel. +39 0332-786324
esarda-bulletin@jrc.ec.europa.eu

ESARDA is an association formed to advance and harmonize research and development for safeguards. The Parties to the association are:

Areva, France; ATI, Austria; CEA, France;
CNCAN, Romania; EDF, France; ENEA, Italy;
European Commission; FZJ, Germany; HAEA,
Hungary; MTA EK, Hungary; IRSN, France;
MINETUR, Spain; NNL, United Kingdom; NRI,
Czech Republic; NRPA, Norway; SCK/CEN,
Belgium; Sellafield Ltd, United Kingdom;
SFOE, Switzerland; SSM, Sweden;
Springfields Fuels Limited, United Kingdom;
STUK, Finland;
University of Hamburg, Germany
University of Liege, Belgium
University of Uppsala, Sweden
UKAEA, United Kingdom; URENCO, Germany;
VATESI, Lithuania;
WKK, Germany; PAA, Poland;
ORNL, USA.

Editorial Committee

K. Axell (SSM, Sweden)
P. Peerani (EC, JRC, ITU, Italy)
E. Radde (ATI, Austria)
A. Reznicek (Uba-GmbH, Germany)
B. Richter (FZJ, Germany)
P. Schwalbach (EC, DG ENER)
F. Sevini (EC, JRC, ITU, Italy)
H. Tagziria (EC, JRC, ITU, Italy) (Chairman)
J. Tushingham (NNL, United Kingdom)

Scientific and technical papers submitted for publication in the peer reviewed section are reviewed by independent authors including members of the Editorial Committee.

Manuscripts are to be sent to the Editor (esarda-bulletin@jrc.ec.europa.eu) following the 'instructions for authors' available on <https://esarda.jrc.ec.europa.eu> where the bulletins can also be viewed and downloaded.

Photos or diagrams should be of high quality.

Accepted manuscripts are published free of charge.

N.B. Articles and other material in the ESARDA Bulletin do not necessarily present the views or policies of neither ESARDA nor the European Commission.

ESARDA Bulletin is published jointly by ESARDA and the Joint Research Centre of the European Commission and distributed free of charge to over 1000 registered members, libraries and institutions Worldwide.

The publication is authorized by ESARDA.

© Copyright is reserved, but part of this publication may be reproduced, stored in a retrieval system, or transmitted in any form or by any means, mechanical, photocopy, recording, or otherwise, provided that the source is properly acknowledged.

Cover designed by Jose-Joaquim Blasco (JRC Ispra in Italy),

Printed in Italy



Bulletin

Table of Content Issue n° 50

Editorial

Hamid Tagziria	1
----------------------	---

Peer Reviewed Section

Particle Size Inhomogeneity Effect on Neutron Resonance Densitometry	2
B. Becker, H. Harada, K. Kauwenberghs, F. Kitatani, M. Koizumi et al.	
Development of Neutron Resonance Densitometry at the GELINA TOF Facility	9
P. Schillebeeckx, S. Abousahl, B. Becker, A. Borella, F. Emiliani et al.	
Expanding the Capabilities of Neutron Multiplicity Measurements: Conclusions from a Four Year Project	18
B. Goddard, W. Charlton, M. Swinhoe and P. Peerani	
Determination of the half-life and specific thermal power of ²⁴¹Pu by nuclear calorimetry	27
S. Croft, P.A. Santi and R.D. McElroy	
The detection of reactor antineutrinos for reactor core monitoring: an overview	34
M. Fallot	
Burnup monitoring of VVER-440 spent fuel assemblies	41
I. Almási, C.T. Nguyen, Z. Hlavathy, J. Zsigrai, L. Lakosi and P. Nagy	
Development of a reference spent fuel library of 17x17 PWR fuel assemblies	48
R. Rossa, A. Borella and K. van der Meer	
Seismic monitoring of an Underground Repository in Salt - Results of the measurements at the Gorleben Exploratory mine	61
J. Altmann	
Intrinsic fingerprints inspection for identification of dry fuel storage casks	79
D. Demyanuk, M. Kroening, A. Lider, D. Chumak and D. Sednev	
State Regulatory Authority (SRA) Coordination of Safety, Security, and Safeguards of Nuclear Facilities: A Framework for Analysis	87
S. Mladineo, S. Frazar, A. Kurzrok, E. Martikka, T. Hack and T. Wiander	
Collection and Analysis of Open Source News for Information Awareness and Early Warning in Nuclear Safeguards	94
G. M. Cojazzi, E. van Der Goot, M. Verile and E. Wolfart	
New Approaches and New Technologies for the Verification of Nuclear Disarmament	106
D. Keir	
Confirmation of Nuclear Treaty Limited Items: Pre-dismantlement vs. Post-dismantlement	116
D. MacArthur, D. Hauck and Morag Smith	

News and Synopses

Panel Discussion: Disarmament Verification – a Dialogue on Technical and Transparency Issues	124
Malte Götsche and Götz Neuneck	
Focused Working Group Activities on the Subject of Measurement Uncertainties and Reference Material Needs	126
J. Tushingham	

Editorial

Dear Readers,

I am pleased to provide you with the 50th edition of the Esarda bulletin, a culmination of hard work by authors and, sometimes strenuous but always serious, review process by reviewers of the papers published to an ever wider community covering an ever wider range of themes and activities. On behalf of the Editorial committee, I am grateful to the authors for allowing their good work to be published in our journal and to the reviewers for their most valuable and important contributions to this process thus ensuring that good quality is maintained and continuously improved. Each paper has generally been peer-reviewed by two independent experts and in some rare cases three when the two opinions were opposing and contrasting on important issues. As in issue 49, the papers published in this 50th edition are predominantly those selected by the chairmen of the previous Esarda symposium in Bruges as best papers in addition to other papers independently submitted by their authors to us. The timing of the publication (i.e. issue 49 or 50?) mostly depended on the timing and readiness as regards the peer-review process. Some remaining papers will be published in issue 51.

In addition to peer reviewed papers section, Issue 50 contains under a new section News and Synopses:

- a summary report on the panel discussion held in Bruges on the topic of *Disarmament Verification – a Dialogue on Technical and Transparency Issues*
- a short editorial followed by the abstracts of two extensive reports by the DA, NDA and NA/NT working groups (WG) which focused on *the subject of measurement uncertainties and reference material needs* following two workshops organised by them and hosted by the IAEA and DG-ENER respectively. The full reports including a list of recommendations can be promptly viewed and downloaded at: <https://esarda.jrc.ec.europa.eu>.

The Esarda Editorial Committee continues to strive to increase the visibility and good citation and referencing of your publications within the Esarda bulletin which will ensure accessibility to a wider and more global audience. In order to achieve that many steps are currently being undertaken.

You may notice that since very recently every bulletin published to date (i.e. since 1976!) has been uploaded to the Esarda library and is accessible on the web site. A heading is added for each individual article in our library which will allow other authors to reference the source of the file correctly and in a standardised fashion. Furthermore, migrating the library to a suitable repository or journal management such as Google Scholar thus allowing an automated and correct indexing of the files is also considered together with the upload of all existing Bulletins files in the open source indexing engines. Requests for some other indexing engines are in progress with the benefits this would bring to both authors and readers especially in terms of visibility and citation of their work.

The technical support of my colleague Andrea de Luca in that endeavour and for his work on the new Esarda website are warmly acknowledged.

I would like to thank all authors for submitting their papers to the bulletin and I encourage everybody to cite the work published in the bulletin whenever appropriate.

I wish you all a very happy and successful new year.

Hamid Tagziria
Editor and Editorial Committee Chairman

<https://esarda.jrc.ec.europa.eu>
Esarda-bulletin@jrc.ec.europa.eu
hamid.tagziria@jrc.ec.europa.eu

Particle Size Inhomogeneity Effect on Neutron Resonance Densitometry

B. Becker¹, H. Harada², K. Kauwenberghs¹, F. Kitatani², M. Koizumi², S. Kopecky¹, A. Moens¹, P. Schillebeeckx¹, G. Sibbens¹, H. Tsuchiya²

¹ European Commission, Joint Research Centre, Institute for Reference Materials and Measurements, Retieseweg 111, B-2440 Geel, Belgium

E-mail: bjorn.becker@ec.europa.eu, peter.schillebeeckx@ec.europa.eu

² Japan Atomic Energy Agency (JAEA) - Tokai-mura, Naka-gun, Ibaraki 319-1195, Japan

E-mail: harada.hideo@jaea.go.jp

Abstract:

Neutron Resonance Densitometry (NRD) represents a possible option to determine the heavy metal content in melted nuclear fuel. This method is based on the well-established methodology of neutron time-of-flight (TOF) transmission and capture measurements. In particular, NRD can measure both the isotopic and the elemental composition. It is a non-destructive method and is applicable for highly radioactive material. The details of this method are explained in another contribution to this bulletin.

The accuracy of NRD depends among other factors on sample characteristics. Inhomogeneities such as density variations in powder samples can introduce a significant bias in the determination of the composition. In this contribution, the impact of the particle size distribution of such powder samples on results obtained with NRD is investigated. Various analytical models, describing the neutron transport through powder, are compared. Stochastic numerical simulations are used to select a specific model and to estimate the introduced model uncertainty. The results from these simulations will be verified by dedicated measurements at the TOF-facility GELINA of the EC-JRC-IRMM.

Keywords: non-destructive assay; densitometry; neutron time-of-flight; resonance analysis; melted fuel; severe accidents; nuclear safeguards

1. Introduction

Neutron Resonance Densitometry (NRD) can be used to determine the isotopic and the elemental composition of unknown samples [1,2]. NRD consists of a combination of Neutron Resonance Transmission Analysis (NRTA) [3,4,5,6] and Neutron Resonance Capture Analysis (NRCA) [5,6]. Both NRTA and NRCA are non-destructive neutron time-of-flight measurement techniques which are based on well-established methods for nuclear cross section determination [7].

In case that the sample consists of particle-like debris of melted nuclear fuel formed in a severe accident, such as happened in the Fukushima Daiichi nuclear power plants, the inhomogeneity of the sample can introduce a significant bias in the result of an NRD measurement. In this

contribution, the impact of the sample inhomogeneity is investigated by comparing different analytical methods with stochastic simulations of the neutron transport through powder samples.

2. Particle Size Models

In the last decades various models have been developed to describe the neutron transport through stochastic media [8]. In this contribution, we consider binary stochastic mixtures of particles (phase α) embedded in a matrix (phase β). The mixture is characterized by the volume fraction of each phase $i = \alpha, \beta$ defined as $\rho_i = V_i / (V_\alpha + V_\beta)$ where V_i is the volume, and by the chord lengths $\lambda_i = 4 V_i / S$ where S is the boundary surface between the different phases. The volume fraction of the particles is also referred to as packing fraction.

In sections 2.1 - 2.3, a brief overview of a number of analytical models available to calculate the neutron transport through a stochastic mixture is given. For detailed information on each of the models and in particular their derivation we refer the reader to the original publications. In section 2.4 two different Monte Carlo methods to calculate the neutron transport through the mixture are briefly discussed.

2.1 Homogeneous Limit

The homogeneous limit, also called atomic mixing, is based on the assumption that the neutron effectively sees a homogenous mixture of particles and matrix material. This assumption holds if the neutron passes multiple particles between interactions, i.e. if the mean free path (*mfp*) of the neutron in the particle is significantly higher than the characteristic particle size l : $mfp = 1 / \Sigma^\alpha \gg l$. In this particular case the macroscopic total cross section of the particle-matrix mixture Σ^{hom} is simply given by the volume fraction weighted sum of the particle and matrix total cross sections Σ^α and Σ^β :

$$\Sigma^{hom} = \bar{\Sigma} = \rho_\alpha \Sigma^\alpha + \rho_\beta \Sigma^\beta.$$

The transmission (T) of neutrons through a sample of thickness (R) is then:

$$T^{hom} = e^{-\Sigma^{hom} R}.$$

2.2 Macroscopic Analytical Model

Kopecky et al. [9] developed a model to describe the transmission of neutrons through a Pu powder sample. Since this model is based on a distribution of the overall thickness of the particle phase rather than on particle properties, the model can be considered as macroscopic.

Within this model it is assumed that the particle phase thickness is log-normal distributed with an additional hole fraction f_h . The transmission through the sample is then given by:

$$T^{Kop} = (1 - f_h) \int e^{-n' \sigma^\alpha x} \rho(x) dx + f_h$$

where n' is related to the areal density n , determined from measurements of the mass and sample area, by: $n' = n / (1 - f_h)$. σ^α is the total microscopic cross section of the particle phase. The variable x is distributed as a log-normal distribution:

$$\rho(x) = \frac{1}{x \sqrt{2\pi s^2}} \exp\left(-\frac{(\ln x + s^2/2)^2}{2s^2}\right)$$

with an average value one and the width parameter s . It is further assumed that the cross section of the matrix material can be neglected. In this model the width parameter and hole fraction are free model parameters. An advantage of Kopecky's model is that both free parameters tend to be uncorrelated parameters in a fitting procedure. In general, Kopecky's model is not restricted to a log-normal distribution of the thickness. Depending on the powder characteristics, a different thickness distribution might be advantageous. The model of Kopecky et al. [9] has been implemented in the least squares fitting program REFIT [10].

2.3 Microscopic Analytical Models

Microscopic model are directly based on properties of the individual particles, such as size and shape distributions rather than on overall properties of the mixture. The following models differ in particular in the underlying stochastic and particle shape assumptions and in complexity. Burrus model for example is quite simple with assumptions inspired from basic reactor physics while Randall's extended model is too complex for practical calculations within the context of this contribution.

• **Burrus's Model:** Burrus [11,12] developed a simple model for the effective total cross section $\Sigma^{eff, Bur.}$ of a binary mixture neglecting the matrix cross section. The effective cross section is given by:

$$\Sigma^{eff, Bur.} = -\frac{1}{\lambda_\alpha} \ln(1 - \rho_\alpha F)$$

where F is the probability that a neutron does not penetrate a particle. F is related to the self-collision probability P_C by $F = \lambda_\alpha \Sigma^\alpha (1 - P_C)$. The self-collision probability can be determined using Wigner's rational approximation:

$$P_C = \lambda_\alpha \Sigma^\alpha / (1 + \lambda_\alpha \Sigma^\alpha).$$

The transmission through the sample is then given by:

$$T^{Bur.} = e^{-\Sigma^{eff, Bur.} R}$$

Burrus investigated the transmission of thermal neutrons through boral slabs made out of a heterogeneous mixture of boron carbide and aluminium.

• **Doub's Model:** Doub's model [13] is based on the calculation of a self-shielding factor f_D for the particles. The average transmission through a mixture of thickness R is then given by:

$$T^{Doub} = e^{-R \rho_\alpha f_D \Sigma^\alpha}$$

In case of $f_D = 1$ Doub's model reduces to the homogeneous limit with a zero cross section matrix. Doub underlying assumption is the number of particles that the neutron passes is given by a binominal distribution. In his model the self-shielding factor of mono-dispersed spheres with radius r is:

$$f_D = \frac{1}{\frac{2}{3} y \rho_\alpha / g} \ln \left(\frac{1}{1 - \rho_\alpha / g (1 - \bar{t})} \right)$$

with $y = 2r \Sigma_\alpha$ and $g = 0.740$. \bar{t} is given by $\bar{t} = 2 / y^2 [1 - (1 + y) e^{-y}]$. Doub extended the model to polydisperse spheres using a volume averaged self-shielding factor $\bar{f}_D = \sum_j f_{Dj} V_j / V_\alpha$ where f_{Dj} and V_j are the self-shielding factor and volume of spheres with a radius r_j . Doub compared his model to measurements of transmission through a mixture of boron-carbide and aluminium spheres [13] with a minimum self-shielding factor of 0.86. He showed that the measured shape of f_D as function of neutron energy is well reproduced with the model.

• **Randall's Model:** While Doub's model is restricted to spherical particles, Randall developed a more general model based on a stochastic description of the integral transport equation (for more details see Refs. [12,14,15]). When all particles have the same characteristics, the average transmission is given by:

$$T^{Ran.} = \{\rho_\beta + \rho_\alpha E'\}^N e^{-R \Sigma^\beta}$$

with $E' = [1 + \lambda_\alpha \Sigma (\sigma_\Delta / \lambda_\alpha)]^{-[\lambda_\alpha / \sigma_\Delta]}$. The particle shape is describe by the average chord length λ_α and the chord length variance σ_Δ^2 . The factor N is given by $N = (Ra) / \lambda_\alpha$ with the effective linear packing factor $a \equiv [(2 - pf) X]^{-1}$ where $X = 1 + \sigma_\Delta^2 / \bar{t}^2$. Values for λ_α and X for different particle shapes are tabulated in Ref. [14]. Randall further extended the description of the transport based on binominal statistics [15]. However, since the final expression involves the calculation of the confluent hypergeometric function, the calculation tends to be slow and sometimes not stable. Therefore Randall's extended expression is not considered in this contribution.

• **LP Model:** Levermore et al. [16] and Vanderhaegen [17] developed a model of the neutron transport through a Markovian statistical mixture. In this case, the line segments in a particular phase along a trajectory of the neutron have a decaying exponential probability distribution. The LP model is therefore not based on spherical particles, unlike Doub's model and to some extent Randall's model. For a stationary process the transmission through a sample with thickness R is given by:

$$T^{LP} = \left\{ \frac{r_+ - \tilde{\Sigma}}{r_+ - r_-} \right\} e^{-r_+ R} + \left\{ \frac{\tilde{\Sigma} - r_-}{r_+ - r_-} \right\} e^{-r_- R}$$

with $\tilde{\Sigma} = \rho_\beta \lambda_\alpha + \rho_\alpha \lambda_\beta + \lambda_\alpha^{-1} + \lambda_\beta^{-1}$ and the decay constants:

$$2r_\pm = \tilde{\Sigma} + \tilde{\Sigma} \pm \sqrt{(\tilde{\Sigma} - \tilde{\Sigma})^2 + 4\theta}$$

The parameter θ is given by:

$$\theta = (\Sigma^\alpha - \Sigma^\beta)^2 \rho_\alpha \rho_\beta$$

The LP model has two free model parameters: λ_α and ρ_α . Both λ_β and ρ_β can be obtained using the equations: $\rho_\beta + \rho_\alpha = 1$ and $\rho_\alpha = \lambda_\alpha / (\lambda_\alpha + \lambda_\beta)$. This model is extensively used in various scientific domains dealing with radiative transfer. In particular, it is applied in climatology to calculate the radiation through cloud fields and in inertial confined fusion and to calculate the radiation transfer through a two-fluid turbulent mixture of liquid water and vapour [8].

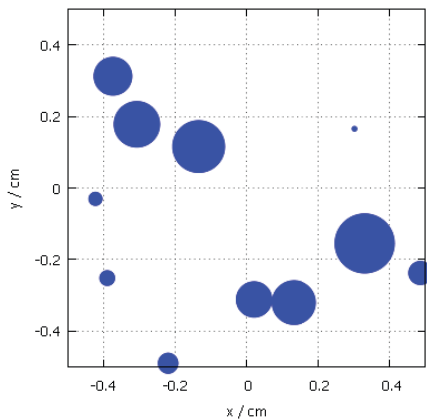


Figure 1: Example of a stochastic geometry based on a polydisperse spherical particle distribution.

2.4 Monte Carlo Simulations

The transmission and capture of neutrons in stochastic media can also be calculated by Monte Carlo (MC) simulations. The idea is to generate multiple stochastic geometries and to track individual neutrons through these geometries. Based on a significant number of histories, the average transmission can be deduced. MC simulations are not suitable to be used in the analysis of NRD measurements due to the significant calculation time. However, since fewer approximations are made in the MC simulations, they can be used to benchmark the different analytical models. In this contribution, we explore two methods to generate the stochastic geometry:

- **MC Method 1:** Spheres are randomly placed into a control volume until a specific packing fraction is obtained similar to the Random Sequential Addition (RSA) algorithm described in Refs. [18,19]. Newly placed spheres are not allowed to overlap with already placed spheres. In case of polydisperse spheres, spheres with a large radius are placed first. A limitation of this method is that the maximum reachable packing fraction is lower than the theoretical one of a closely packed mixture. Figure 1 shows a cut through a polydisperse mixture.
- **MC Method 2:** The algorithm of Switzer [20] is used to generate a 2-dimensional geometry with Markovian characteristics (for details see Refs. [20,21]). Following the method used by Lepage et al. [21] a binary mixture is generated. Figure 2 shows an example of a binary stochastic mixture.

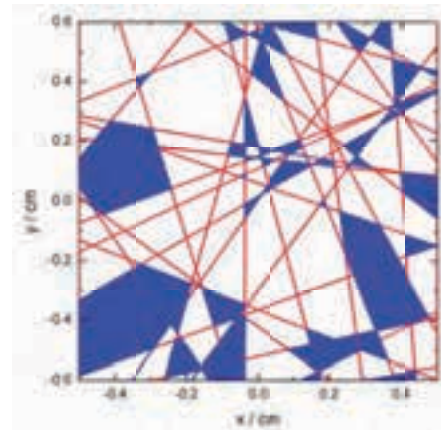


Figure 2: Example of a stochastic Markovian geometry.

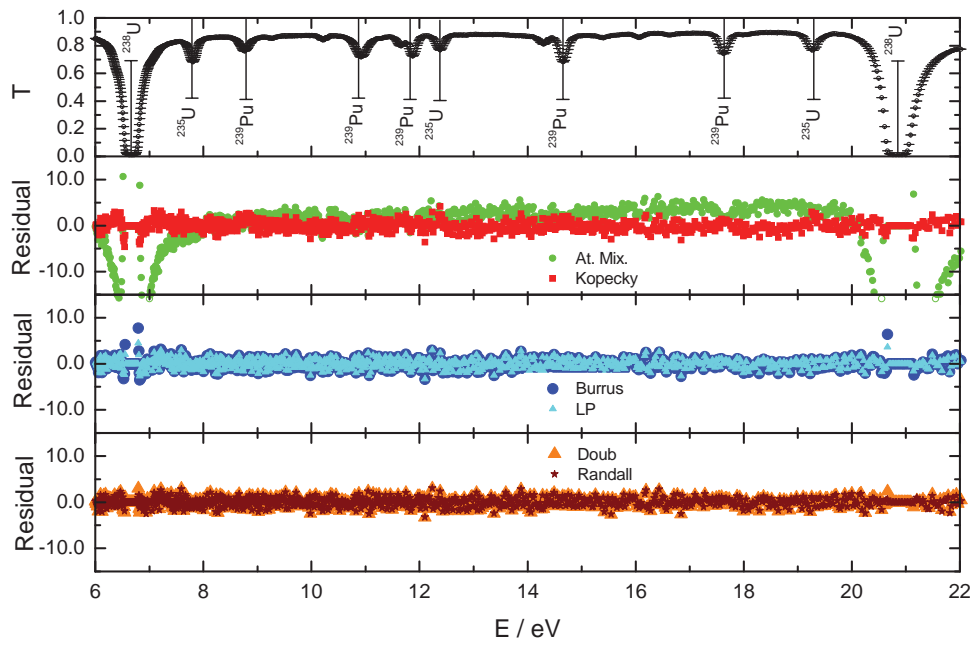


Figure 3: Created transmission spectrum and residual distribution in benchmark case 1.

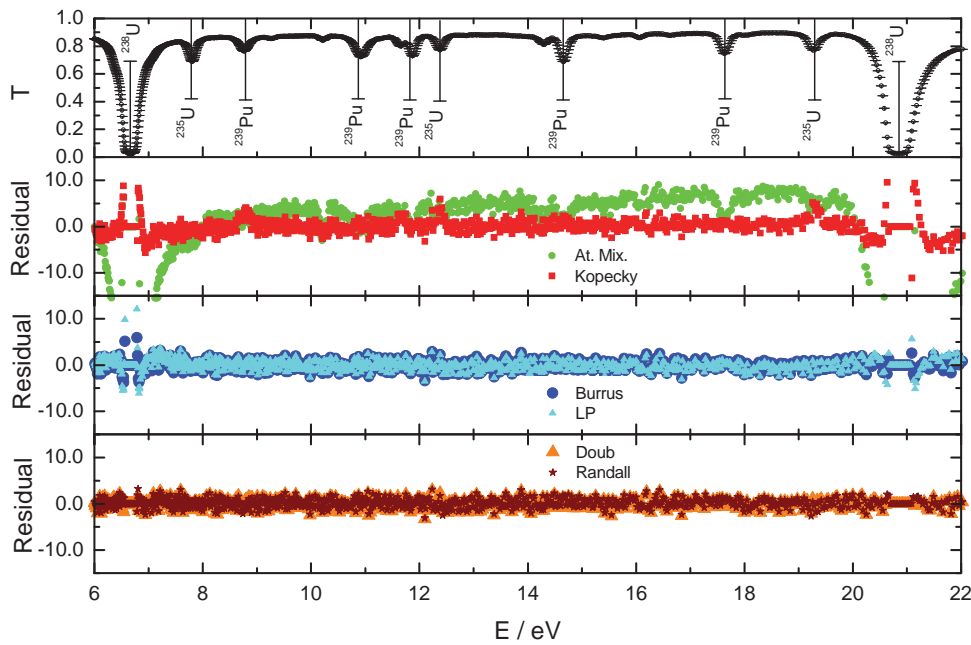


Figure 4: Created transmission spectrum and residual distribution in benchmark case 2.

3. Particle Size Impact on NRTA

A bias introduced by the particle size distribution on results of an NRTA analysis was investigated by comparing analytical model calculations with MC simulations. The two MC methods described in section 2.4 are used to generate a set of synthetic transmission data. In all cases the particle phase consists of uranium and plutonium oxide with a density of 10.97 g/cm³. The particle composition is given in Table 1. The matrix is considered to be void. The packing fraction was assumed to be 30%. The sample thickness was chosen to be 1 cm.

Nuclei	at.%
²³⁵ U	0.6667
²³⁸ U	31.999
²³⁹ Pu	0.6667
¹⁶ O	66.667

Table 1: Assumed particle composition.

The six different analytical methods given in sections 2.1, 2.2 and 2.3 were used to determine by χ^2 minimization the average areal density of the U²³⁵, U²³⁸ and Pu²³⁹ content considering the energy range 6 – 22 eV. In addition, a

normalization factor has been fitted. In a transmission measurement, the contribution of a constant cross section, such as the one of ^{18}O in the considered energy range, leads to an energy independent reduction of the transmission which is equivalent to a scaling with a normalization factor.

All free model parameters (Table 2) are adjusted on the same footing. In a real transmission experiment, the quality of low transmission data is very much dependent on the knowledge of the measurement background and mostly data below an experimental transmission of 0.1 are not considered. Therefore, in this contribution we also do not include data points with a transmission below 0.1 in the parameter adjustment.

Model	Free Parameter	Fixed Parameter
Homogenous limit	-	-
Kopecky	s, f_h	-
Burrus	$\lambda_\alpha, \rho_\alpha$	-
Doub	r, ρ_α	$g = 0.740$
Randall	$\lambda_\alpha, \rho_\alpha$	$X = 9/8$
LP	$\lambda_\alpha, \rho_\alpha$	-

Table 2: Free and fixed model parameters.

3.1 Polydisperse Spheres

Two benchmark cases were generated using MC method 1. A flat particle diameter distribution ($0\text{ mm} < d < 2\text{ mm}$) and a log-normal distribution (with: $\bar{d} = 1.22$ and the width parameter $\sigma = 0.6$) were used for benchmark cases 1 and 2, respectively. Sampled particles were placed in a volume with a thickness of 1 cm and a height and width of 4 cm. About 4600 spheres were sampled to reach the desired packing fraction of 30%. The created geometry was used to evaluate the thickness of the particle path along 40000 different transmission paths. From the obtained thickness distribution a transmission spectrum was created. A 1% uncertainty for transmission $T = 1$ has been associated to the spectrum. The final transmission spectrum was then obtained by adding a Gaussian fluctuation to the spectrum corresponding to the uncertainty.

In case of Burrus's model all parameters were found to be strongly correlated, therefore an initial uncertainty of the packing fraction of 10% was assumed. In case of Randall's model, the parameter X was chosen to be 9/8 which is in principle only correct for monodisperse spheres. Figures 3 and 4 show the created transmission spectrum for cases 1 and 2, respectively, as well as the residual of the parameter adjustments using the different methods. By simply homogenizing particles and matrix, a significant bias is introduced when adjusting the average areal densities. For both cases the bias is up to 5% for ^{235}U and ^{239}Pu and 13% for ^{238}U . The other models perform more or less equally. They all improve the result of the adjustment significantly compared to the homogeneous limit.

3.2 Markovian Geometry

Two additional benchmark cases (case 3 and 4) were created using the second MC method. A mean chord length (λ_A) of 0.067 cm and 0.267 cm were assumed for cases 3 and 4, respectively. 400 different realizations of the stochastic geometry were sampled for each case. 4000 neutron histories per stochastic geometry were simulated. Capture and scattering events were taken into account by neutron weight reduction. Figure 5 and 6 show the two created transmission spectra. The transmission deviates in particular in the region close to the ^{238}U resonances. The uncertainties due to sampling range from 0.002 to 0.006 depending on the transmission. Again, the initial uncertainty of the packing fraction of 10% was assumed for Burrus's model and the parameter X in Randall's model was assumed to be 9/8.

Theoretically, the LP model should describe perfectly the transmission through a stochastic geometry created by MC method 2. This is indeed observed for both cases. The nominal densities and the adjusted densities using the LP model agree within the uncertainty of the fit. For case 3, Doub's and Randall's model give relatively good results with a bias of less than 1.5%. However, the bias increases for case 4 due to the increased particle size. Atomic mixing always leads to an under prediction of the areal densities. For case 3, the bias is up to 6% for ^{235}U and ^{239}Pu and 12% for ^{238}U . For case 4, this bias increases up to 20% for ^{235}U and ^{239}Pu and to 35% for ^{238}U . Even though the fitting residual distribution of Kopecky's or Burrus's model is more or less flat, both models over predict the densities by up to 25% for case 4.

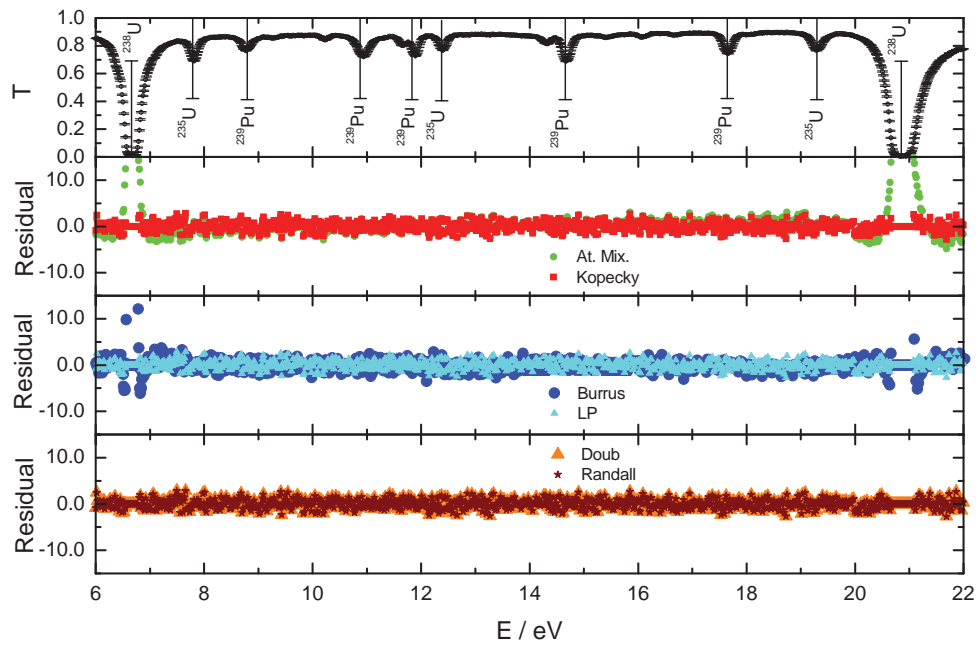


Figure 5: Created transmission spectrum and residual distribution in benchmark case 3.

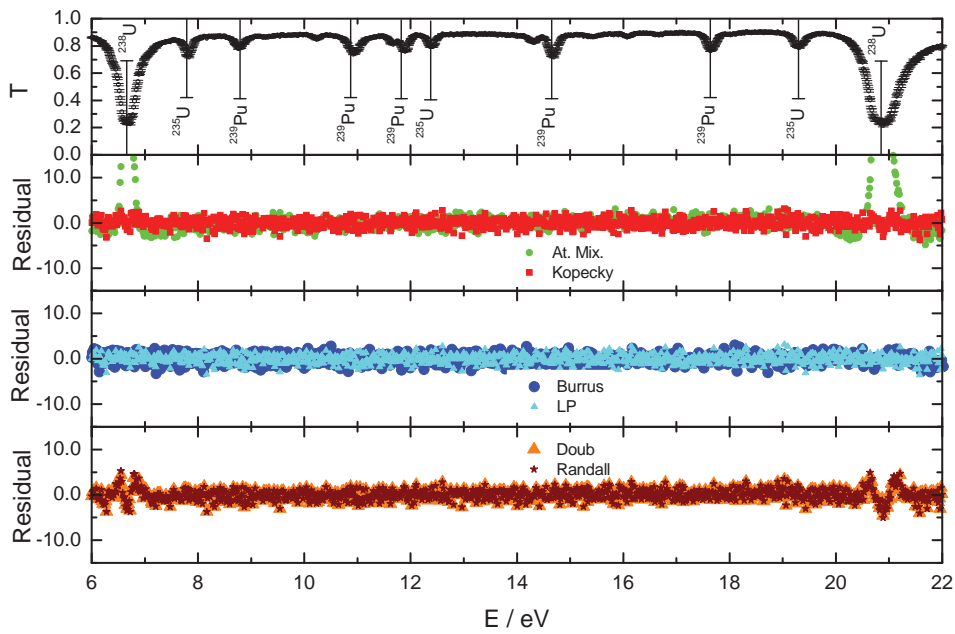


Figure 6: Created transmission spectrum and residual distribution in benchmark case 4.

Sample	Thickness mm	Solid	Powder	Nominal Grain Size μm	Packing Fraction
Cu	0.250	x		-	-
			x	500	31% (pure Cu)
			x	500	5.1% (Cu-S mix.)
Cu	0.125	x	x	150	5.1% (Cu-S mix.)
			x	500	5.0% (Cu-S mix.)
			x	150	5.1% (Cu-S mix.)
W	0.150	x		-	-
			x	50-250	14.5% (W-S mix.)
	0.509		x	50-250	17.0% (W-S mix.)

Table 3: Transmission measurements planned at the GELINA facility of EC-JRC-IRMM.

4. Experimental Measurement Campaign at GELINA

Even though several analytical models can be used to determine accurately the ^{235}U , ^{238}U and ^{239}Pu content by χ^2 minimization in some of the benchmark cases, the question whether the MC realization reflects the transmission through a real powder sample remains. Therefore, several transmission measurements with powder samples are being made at the GELINA facility [22] of EC-JRC-IRMM. While in previous measurements of Doub [13], the transmission of thermal neutrons ($E < 1.23$ eV) through a mixture of boron-carbide and aluminium spheres was studied, the measurements at EC-JRC-IRMM are dedicated to investigate the transmission at higher energies in the resolved resonance range. Samples made out of Cu and W powder mixed with S powder are being used. Transmission spectra of powder and solid metal samples are compared in order to be independent of cross section uncertainties. Table 3 gives an overview of the planned measurements.

5. Conclusion

Four different stochastic benchmark calculations, simulating the neutron transport through a powder sample, have been made to investigate the sensitivity of a NRD measurement on the inhomogeneity of the sample. Different analytical transport models have been used to determine the areal densities of ^{235}U , ^{238}U and ^{239}Pu . It was shown that a simple homogenization of particles and matrix can result in a significant bias depending on the particle size. Depending on the benchmark case, several analytical models can be used to correctly determine the areal densities, i.e. to take into account the inhomogeneity of the sample. Transmission measurements through powder samples are currently being made at the GELINA facility of EC-JRC-IRMM in order to complement the numerical benchmark calculations. Based on these results an analytical method will be implemented in the REFIT code. The developed model and code will be used to study the inhomogeneity effect quantitatively for various conditions of sample.

6. Acknowledgements

This work was done under the agreement between JAEA and EURATOM in the field of nuclear materials safeguards research and development.

7. References

- [1] Harada H., Kitatani F., Koizumi M., Tsuchiya H., Takamine J., Kureta M., Imura H., Seya M., Becker B., Kopecky S., Schillebeeckx P., Proc. of ESARDA35 (2013) presented during the ESARDA 2013 Symposium.
- [2] Schillebeeckx P., Abousahl S., Becker B., Borella A., Harada H., Kauwenberghs K., Kitatani F., Koizumi M., Kopecky S., Moens A., Sibbens G., Tsuchiya H., ESARDA Bulletin **50**, 9-17 (2013) presented during the ESARDA 2013 Symposium.
- [3] Priesmeyer H.G., Harz U., Atomkernenergie **25**; 109-113, 1975.
- [4] Behrens J.W., Johnson R.G., Schrack R.A., *Nuclear Technology* **67**, 162-168, 1984.
- [5] Postma H., Schillebeeckx P., Encyclopedia of Analytical Chemistry (John Wiley & Sons Ltd), 2009; p.1-22;
- [6] Schillebeeckx P., Borella A., Emiliani F., Gorini G., Kockelmann W., Kopecky S., Lampoudis C., Moxon M., Perelli Cippo E., Postma H., Rhodes N.J., Schooneveld E.M., Van Beveren C., *JINST* **7**, C03009, 2012.
- [7] Schillebeeckx P., Becker B., Danon Y., Guber K., Harada H., Heyse J., Junghans A.R., Kopecky S., Massimi C., Moxon M.C., Otuka N., Sirakov I., Volev K., Nuclear Data Sheets **113**, 3054-3100, 2012.
- [8] Kassianov E., Veron D., J. Quant. Spectrosc. Radiat. Transfer **112**, 566-576, 2011.
- [9] Kopecky S., Siegler P., Moens A., Proc. Int. Conf. Nuclear Data for Science and Techn., Nice, France, April, 2007, pp. 623-626.
- [10] Moxon M.C., Brisland J.B., AEAInTec-0630, AEA Technology, October, 1991.
- [11] Burrus W.R., Report ORNL-2528, Oak Ridge National Laboratory, Jan. 1960.
- [12] Williams M.M.R., "Random Processes in Nuclear Reactors", Pergamon Press Oxford New York Toronto Sydney, 1974.
- [13] Doub W.B., Nucl. Sci. Eng. **10**, 299-307, 1961.
- [14] Randall C.H., Naval Reactor Physics Book, Vol. 1, A. Radkowsky (Ed.), Naval Reactors, Division of Reactor Development, United States Atomic Energy Commission, 1964.
- [15] Williams M.M.R., Ann. Nucl. Energy **35**, 750-757, 2008.
- [16] Levermore C.D., Pomraning G.C., Sanzo D.L., Wong J., J. Math. Phys. **27**, 2526, 1986.
- [17] Vanderhaegen D., J. Quant. Spectrosc. Radiat. Transfer **36**, 557-561, 1986.
- [18] Mazzolo A., Roesslinger B., Monte Carlo Methods and Appl. **10**, 443-454, 2004.
- [19] Talbot J., Schaaf P., Tarjus G., Molecular Physics **72**, 1397-1406, 1991.
- [20] Switzer P., Ann. Math. Stat. **36**, 1859-1863, 1965.
- [21] Lepage T., Delaby L., Malvagi F., Mazzolo A., Nucl. Sci. Tech. **2**, 743-748, 2011.
- [22] W. Mondelaers, P. Schillebeeckx, Notiziario Neutroni e Luce di Sincrotrone **11**, 19 - 25 (2006).

Development of Neutron Resonance Densitometry at the GELINA TOF Facility

P. Schillebeeckx¹, S. Abousahl², B. Becker¹, A. Borella³, F. Emiliani¹, H. Harada⁴, K. Kauwenberghs¹, F. Kitatani⁴, M. Koizumi⁴, S. Kopecky¹, A. Moens¹, M. Moxon⁵, G. Sibbens¹ and H. Tsuchiya⁴

¹ European Commission, Joint Research Centre, Institute for Reference Materials and Measurements, Retieseweg 111, B-2440 Geel, Belgium
E-mail: peter.schillebeeckx@ec.europa.eu

² European Commission, Joint Research Centre, Scientific Policy and Stakeholder Relations, Marsveldstraat 21, B-1050 Brussels, Belgium

³ SCK•CEN - Boeretang 200, B- 2400 Mol, Belgium

⁴ Japan Atomic Energy Agency (JAEA) – Tokai-mura, Naka-gun, Ibaraki 319 – 1195, Japan

⁵ Hyde Copse 3, Marcham, United Kingdom

Abstract:

Neutrons can be used as a tool to study properties of materials and objects. An evolving activity in this field concerns the existence of resonances in neutron induced reaction cross sections. These resonance structures are the basis of two analytical methods which have been developed at the EC – JRC – IRMM: Neutron Resonance Capture Analysis (NRCA) and Neutron Resonance Transmission Analysis (NRTA). They have been applied to determine the elemental composition of archaeological objects and to characterize nuclear reference materials.

A combination of NRTA and NRCA together with Prompt Gamma Neutron Analysis, referred to as Neutron Resonance Densitometry (NRD), is being studied as a non-destructive method to characterize particle-like debris of melted fuel that is formed in severe nuclear accidents such as the one which occurred at the Fukushima Daiichi nuclear power plants. This study is part of a collaboration between JAEA and EC – JRC – IRMM.

In this contribution the basic principles of NRTA and NRCA are explained based on the experience in the use of these methods at the time-of-flight facility GELINA of the EC – JRC – IRMM. Specific problems related to the analysis of samples resulting from melted fuel are discussed. The programme to study and solve these problems is described and results of a first measurement campaign at GELINA are given.

Keywords: non-destructive assay; time-of-flight; resonance analysis; melted fuel; severe accidents; nuclear safeguards; transmission; capture; GELINA

1. Introduction

The probability that a neutron interacts with nuclei strongly depends on the energy of the neutron. This is shown in Fig. 1, which compares the total cross section as a function of the kinetic energy of the interacting neutron for several nuclides. The cross sections reveal the presence of resonance structures. The origin of these structures is well understood. The resonances are related to excited states of the compound nucleus which is formed by the neutron and the target nucleus. The resonance structured cross sections can be parameterized by resonance parameters

based on the R-matrix nuclear reaction formalism [1]. Each resonance is characterized by a set of resonance parameters, in particular the resonance energy and the partial reaction widths. The partial widths (e.g. the neutron, capture and fission width) express the probability for a specific reaction to occur. The smooth part of the total cross section is due to scattering from the nuclear potential and its magnitude depends on the scattering radius. Since resonances are observed at energies which are specific for each nuclide, they can be used as fingerprints to determine the elemental and even isotopic composition of materials and objects [2,3]. The resonance structures in the total and capture cross sections are the basis of Neutron Resonance Transmission (NRTA) and Neutron Resonance Capture Analysis (NRCA), respectively. Both NRCA and NRTA are non-destructive methods, which determine the bulk elemental composition, do not require any sample preparation and result in a negligible residual activation. In this contribution the basic principles of NRTA and NRCA are discussed, with a special emphasis on the use of NRTA as an absolute method to determine the amount of fissile and fertile materials for safeguards applications.

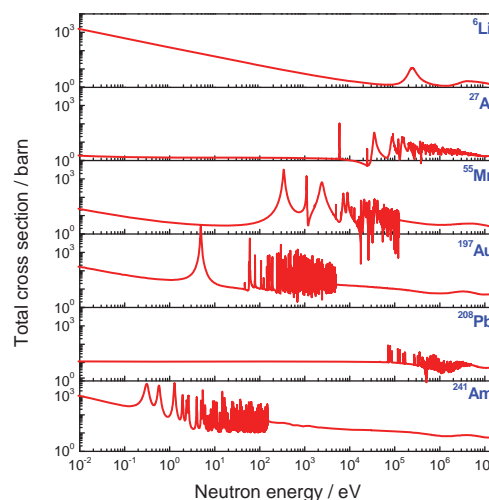


Figure 1: Total cross section as a function of neutron energy for neutron induced reactions in ${}^6\text{Li}$, ${}^{27}\text{Al}$, ${}^{55}\text{Mn}$, ${}^{197}\text{Au}$, ${}^{208}\text{Pb}$ and ${}^{241}\text{Am}$. (Figure inspired from Ref. [4]).

2. Basic principles of NRTA and NRCA

Both NRTA and NRCA are based on the time-of-flight (TOF) technique, which is a standard technique for neutron resonance spectroscopy. They rely on the same principles and

methods as those used for the determination of cross section data in the resonance region. These principles and methods, including the production of full covariance data, have been reviewed recently in Ref. [5]. NRTA is based on the analysis of characteristic dips in a transmission spectrum that can be obtained from a measurement of the attenuation of the neutron beam by a sample [2,3]. These dips are observed at TOF values corresponding to resonance energies. NRCA refers to the analysis of resonance structures in TOF spectra obtained from the detection of prompt γ -rays, which are emitted after a neutron capture reaction in the sample [2,3]. In Ref. [6] a comparison of NRCA and PGAA (Prompt Gamma-ray Activation Analysis), which is also based on the detection of prompt γ -rays, is reported.

2.1 Time-of-flight measurements

A precise knowledge of the energy of the neutron inducing a reaction in the sample is required to make use of the resonance structure in neutron induced reaction cross sections for material analysis. For a quantitative analysis covering a wide range of elements, time-of-flight measurements at an accelerator-based pulsed white neutron source are preferred. Pulsed neutron sources can be realized using electron- and proton-based accelerators. In electron-based accelerators, high-energy electrons generate Bremsstrahlung in a target and neutrons are produced via photoneuclear reactions. High-energy proton accelerators produce neutrons via the spallation process in a target made out of high mass number material. The energy spectrum of neutrons produced by photoneuclear reactions or the spallation process is not directly exploitable for low energy resonance spectroscopy. Therefore, a moderator containing e.g. hydrogen rich material is used to increase the amount of low-energy neutrons and to produce a broad neutron spectrum ranging from thermal energies up to the high energy region.

Experimentally, the time-of-flight t_m is derived from the difference between a stop (T_s) and a start signal (T_o). The start signal is produced by the pulsed charged particle beam. The stop signal in a transmission experiment (NRTA) is provided by the neutron detector. In a capture experiment (NRCA) the arrival time is obtained from the detection of the γ -ray which are emitted in the neutron induced reaction. The time-of-flight t that a neutron needs to travel a distance L can be related to the velocity v of the neutron at the moment it leaves the neutron producing target and enters the detector or sample:

$$v = \frac{L}{t} = \frac{L}{t_m - (t_t + t_d)} \quad (1)$$

where t_t is the time the neutron spends in the neutron producing target and t_d the time spent in the neutron detector or sample. The kinetic energy of the neutron E is given by:

$$E = mc^2(\gamma - 1) \quad (2)$$

where c denotes the speed of light, m the rest mass of the neutron and γ the Lorentz factor.

The resolution Δt is a combination of the broadening due to the finite width of the timing channels and the spread due to the time the neutrons spend in the source and detector. The resolution (ΔE) can be described by the broadening due to both the time-of-flight (Δt) and the distance (ΔL):

$$\frac{\Delta E}{E} = \frac{1}{L} \sqrt{(v\Delta t)^2 + \Delta L^2} \quad (3)$$

Eq. 3 shows that the resolution improves with increasing distance. The use of Eq. 3 supposes that the time and distance follow a Gaussian distribution and that they are not correlated. For the analysis of the data the response function of the TOF-spectrometer is required. This response function is a convolution of different components, which are not all Gaussian distributions [5]. The distance L can be determined by metric measurements with an uncertainty smaller than 1 mm. The contribution Δt due to the time-of-flight depends on the broadening (uncertainty) of T_o, T_s, t_t and t_d . In case of a moderated neutron beam, the broadening in time is dominated by the neutron transport in the target-moderator assembly, i.e. the component t_t . This component is mostly represented by introducing an equivalent distance L_t , as discussed in Ref. [5]. Response functions for TOF measurements at a facility based on a spallation source are broader compared to those for measurements at a photoneuclear source at the same distance as shown in Ref. [3,5]. In addition, a more pronounced tail at long TOF values is observed. This difference is mainly due to the geometry of the target-moderator assembly, which is more compact for a neutron source based on photoneuclear reactions.

Since the neutron flux decreases with increasing distance a compromise between resolution and intensity has to be made.

2.2 NRTA

In a transmission (or NRTA) measurement the observed quantity is the fraction of the neutron beam that traverses the sample without any interaction. For a parallel neutron beam which is perpendicular to a slab of material, this fraction or transmission T is given by:

$$T = e^{-\sum_k n_k \bar{\sigma}_{tot,k}} \quad (4)$$

where $\bar{\sigma}_{tot,k}$ is the Doppler broadened total cross section and n_k is the number of atoms per unit area of nuclide k .

Experimentally the transmission T_{exp} is obtained from the ratio of the counts of a sample-in measurement C_{in} and a

sample-out measurement C_{out} , after subtraction of the background contributions B_{in} and B_{out} , respectively:

$$T_{exp} = \frac{C_{in} - B_{in}}{C_{out} - B_{out}} \quad (5).$$

The spectra in Eq. 5 are corrected for losses due to the dead time of the detector and electronics chain. All spectra are normalized to the same intensity of the neutron beam and TOF-bin width. The background is determined by an analytical expression applying the black resonance technique [5]. For this technique, samples of elements with strong absorption resonances (referred to as black resonance filters) are inserted into the beam. The free parameters in the analytical expression are determined by a least squares fit to saturated resonance dips observed in the TOF spectra, which result from measurements with black resonance filters. To account for the impact of the sample on the background, measurements are carried out with at least one fixed black resonance filter in the beam. A more detailed discussion on the background determination and the analytical expressions can be found in Ref. [5].

Eq. 5 reveals that the experimental transmission is independent of both the detector efficiency and incoming neutron flux. Therefore, a transmission measurement can be considered as an absolute measurement which does not require additional calibration experiments or any reference to a standard cross section [7]. In addition, the experimental observable T_{exp} (Eq. 5) is a direct measure of the theoretical transmission (Eq. 4) if the measurements are performed in a good transmission geometry, which is [5]:

- the sample is perpendicular with respect to a parallel incoming neutron beam;
- all neutrons that are detected have passed through the sample; and
- neutrons scattered by the sample are not detected.

The conditions of an ideal or good transmission geometry can be achieved by a proper collimation of the neutron beam at the sample and detector position. However, it requires a homogeneous sample which does not contain holes. In case of inhomogeneous samples a special procedure is required, as shown in Ref. [5,8].

2.3 NRCA

The observable in a capture (or NRCA) experiment is the fraction of the incident neutron beam undergoing a capture reaction in the sample. The theoretical capture yield Y_γ resulting from a capture reaction can be expressed as a sum of primary $Y_{0,k}$ and multiple interaction events $Y_{m,k}$:

$$Y_\gamma = \sum_k (Y_{0,k} + Y_{m,k}) \quad (6).$$

The latter are due to a capture reaction after at least one neutron scattering event in the sample. For a parallel uniform neutron beam and a homogeneous slab of material

perpendicular to the beam, the primary capture yield $Y_{0,k}$ resulting from a capture reaction by nuclide k is given by:

$$Y_{0,k} = \left(1 - e^{-\sum_j n_j \bar{\sigma}_{tot,j}}\right) \frac{n_k \bar{\sigma}_{\gamma,k}}{\sum_j n_j \bar{\sigma}_{tot,j}} \quad (7)$$

where $\bar{\sigma}_{\gamma,k}$ is the Doppler broadened capture cross section. Only in case of very thin samples and/or small cross sections, the capture yield is directly proportional to the product of the areal density n_k and capture cross section. For relative thick samples, multiple interaction events have a substantial contribution to the yield and complicate the analysis as demonstrated in Refs. [2,3].

In a capture (or NRCA) experiment the prompt γ -rays, which are emitted after a neutron capture reaction in the sample are detected. The experimental quantity, which can be obtained from such an experiment and related to the theoretical capture yield, is the experimental yield Y_{exp} . This yield is derived from:

$$Y_{exp} = \frac{C_\gamma - B_\gamma}{\epsilon \Omega P_\gamma A \Phi} \quad (8)$$

where C_γ and B_γ are the observed dead time corrected sample and background spectra, respectively; Φ is the incident neutron flux; A is the effective area of the sample seen by the neutron beam; P_γ is the probability that the prompt γ -rays escape from the sample; Ω is the solid angle between sample and detector and ϵ is the probability to detect at least one γ -ray created in the capture event. To estimate the background, additional measurements without a sample in the beam and with a pure scattering sample (e.g. a carbon or ^{208}Pb sample, which have a low capture cross section) are performed. A detailed discussion on the background determination is given in Ref. [5].

Eq. 8 reveals that the experimental observable in a NRCA experiment is much more complicated compared to the one obtained from a NRTA experiment. The yield Y_{exp} can only be derived from the observed response once the incoming neutron flux and quantities which are related to the detection of the prompt γ -rays are known. Moreover, in most cases only the solid angle and effective area are independent of the energy of the incident neutron. The energy dependent neutron flux can be determined by measurement of a neutron standard reaction [5,7]. The efficiency to detect at least one γ -ray depends on the technique that is applied to measure the prompt γ -rays. Ideally, a detection system is used with an efficiency that is independent of the γ -ray cascade, i.e. independent of multiplicity and energy spectrum. Such a system can be realized by a total absorption detector with an almost 100% efficiency or by applying the total energy detection principle, so that the detection efficiency becomes proportional to the total γ -ray energy produced in the capture event [9]. More details about such systems can be found in Ref. [5].

2.4 Data analysis

The areal densities of the nuclides present in the sample can be derived by a least squares adjustment, that is by minimizing the expression [5]:

$$\chi^2 = (Z_{exp}(t_m) - Z_M(t_m, \vec{\theta}))^T V_{Z_{exp}}^{-1} (Z_{exp}(t_m) - Z_M(t_m, \vec{\theta})) \quad (9)$$

where $Z_M(t_m, \vec{\theta})$ is a model describing the experimental observable $Z_{exp}(t_m)$. The theoretical estimate is the result of a folding to account for the response function $R(t_m, E)$ of the TOF spectrometer:

$$Z_M(t_m, \vec{\theta}) = \frac{\int R(t_m, E) Z(E, \vec{\theta}) dE}{\int R(t_m, E) dE} \quad (10)$$

The theoretical model $Z_M(t_m, \vec{\theta})$ depends on parameters $\vec{\theta} = (\vec{\eta}, \vec{\kappa})$, which is a combination of resonance parameters and experimental parameters, represented by the vectors $\vec{\eta}$ and $\vec{\kappa}$, respectively. The resonance parameters $\vec{\eta}$ are used to parameterize the cross sections by the R-matrix theory. The experimental parameters $\vec{\kappa}$ include e.g. the detector and sample characteristics including sample temperature and the areal densities of the nuclides present in the sample.

The least squares adjustment can be performed by a resonance shape analysis (RSA) code, such as REFIT [10]. This code, which has been developed to parameterize cross section data in terms of resonance parameters, is based on the Reich-Moore approximation [11] of the R-Matrix formalism. It accounts for various experimental effects such as sample inhomogeneities, self-shielding and multiple interaction events, Doppler broadening, and the response of the TOF spectrometer and detectors. For the analysis of capture data special modules are included to correct for γ -ray attenuation in the sample and for the neutron sensitivity of capture detection systems [5]. Examples of the use of REFIT for NRTA and NRCA are given in Refs. [3,12,13].

3. NRTA and NRCA at GELINA

The Geel Electron LINear Accelerator (GELINA) of the EC-JRC-IRMM offers a pulsed white neutron source with an energy range from 10 meV to 20 MeV. A detailed description of the accelerator and its neutron producing target can be found in Ref. [14]. The main unit is a linear electron accelerator delivering very short electron pulses with energies up to 150 MeV and a maximum repetition frequency of 800 Hz. Electron bunches, with peak currents of 12 A in a 10 ns time interval, are compressed by a post-acceleration compression magnet to a width of less than 1 ns. The high-energy electrons generate Bremsstrahlung in a mercury-cooled rotating uranium target, where neutrons are

produced by (γ, n) and (γ, f) reactions. To produce a neutron spectrum in the low-energy region, neutrons are slowed down in two 4-cm thick Be-containers filled with water and positioned above and below the uranium disk. Using suitable shielding materials in the target room, either the direct (fast) neutron spectrum with good time resolution may be used, or the moderated (slow) neutron spectrum. Most of the NRTA and NRCA measurements at GELINA are performed with a moderated neutron beam. To reduce the γ -ray flash and the fast neutron component a Cu and Pb shadow bar is placed close to the uranium target. The total neutron intensity is monitored by two BF_3 proportional counters located in the concrete ceiling of the target hall.

Transmission experiments in good transmission geometry can be performed at a 25 m and a 50 m measurement station using Li-glass scintillators as neutron detectors. The samples are placed in an automatic sample changer, which is positioned half-way between the detector and neutron producing target. Mostly measurements are performed with the accelerator operated at 800 Hz and a ^{10}B overlap filter is used to eliminate neutrons from a previous burst. At 25 m also measurement with a low operating frequency (100 Hz or 400 Hz) and a Cd overlap filter are carried out to investigate materials using low-energy resonances. At 25 m a NE905 Li-glass scintillator enriched to 95% in ^6Li is used. The scintillator (110.0 mm diameter and 12.7 mm thick) is placed in a thin-walled aluminium can and viewed by EMI9823-QKB photomultipliers (PMT). The detector at the 50 m station is a 6.35-mm thick and 101.6-mm diameter NE912 Li-glass scintillator, which is enriched to 95 % in ^6Li and viewed by one PMT.

Three measurement stations at 12.5 m, 30 m and 60 m distance from the neutron target can be used for the characterization of materials by NRCA. Depending on the elements of interest the accelerator is operated at 100 Hz, 400 Hz and 800 Hz using a Cd or ^{10}B overlap filter. The moderated neutron beam at the stations is collimated to about 75 mm diameter at the sample position. The detection system (i.e. γ -ray detectors, neutron flux detector, electronics and data acquisition system) are similar. The γ -rays are detected by C_6D_6 detectors. The energy dependent neutron spectrum is measured in parallel with a ^{10}B Frisch-gridded ionization chamber placed at about 80 cm before the sample. A double chamber is used with a cathode loaded with two back-to-back layers of ^{10}B . The chambers are operated with a continuous flow of a mixture of argon (90%) and methane (10 %) at atmospheric pressure.

NRTA and NRCA have been applied at GELINA for the characterization of reference samples for neutron induced reaction cross section measurements [12,13] and to study objects of cultural heritage interest [15–18]. Most of the archaeological applications so far are related to copper-alloy artefacts. Apart from Cu, they contain Sn or Zn as other major elements, and As, Ag, Sb, Co, Fe and In as minor or

trace elements. In the course of several years NRCA has been extensively exploited to study various bronze objects of different origin: Etruscan statuettes [15], prehistoric bronze axes [16], Bronze-Age swords [17] and Roman metal objects like parts of water taps [18].

By using a position sensitive neutron detector (PSND) NRTA can be extended to have imaging capabilities. Therefore, a pixelated PSND was developed at the Rutherford Appleton Laboratory (UK) [19]. The PSND consists of 100 Li-glass crystals arranged in a 10 x 10 array. Each pixel is embedded in a support made of boron nitrate and

coupled via a 0.5 mm thick glass disperser to a bundle of four 1-mm diameter acrylic optical fibres which transport the light to a 16-channel PMT. The prototype detector was characterized at GELINA [3,20]. When performing Neutron Resonance Transmission Imaging (NRTI) with a PSND, the ideal transmission geometry can not be fulfilled. Therefore special data reduction procedures have been defined based on measurements at GELINA. They are needed to assess the contribution of neutrons scattered in the sample to the background, as discussed in Ref. [20]. Examples of imaging measurements carried out at the ISIS facility are given in Refs. [3,20].

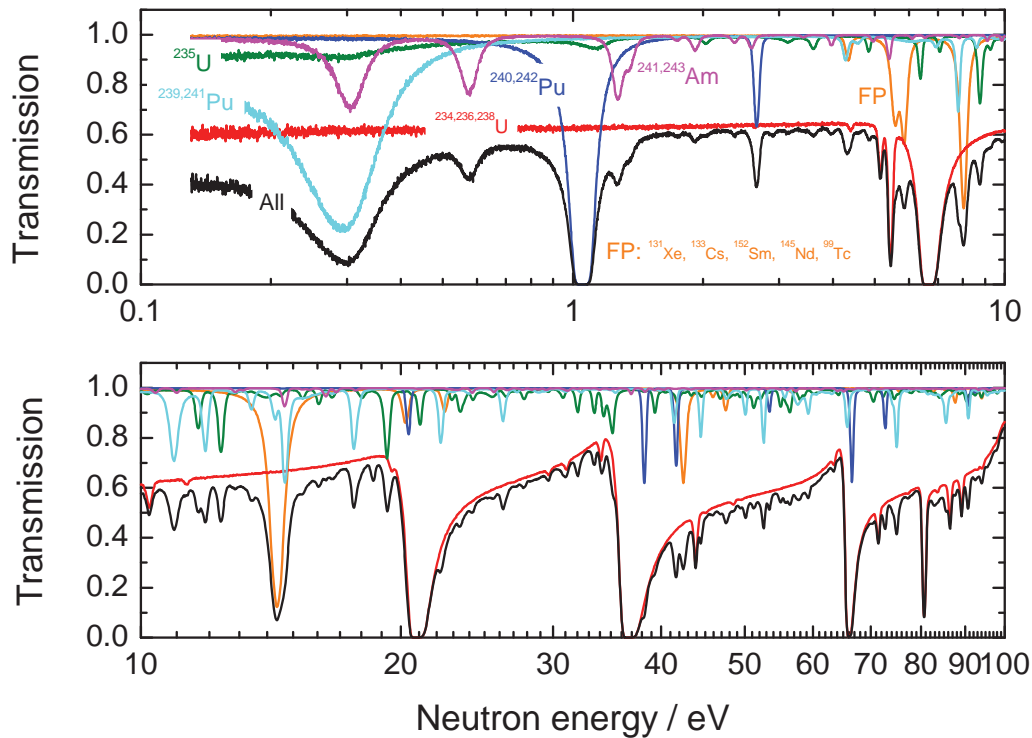


Figure 2: Transmission through a 2.5 cm thick sample with a composition that is similar to spent fuel. The contribution of the different nuclides present is illustrated by plotting separately the transmission due to the presence of only the fission products (FP); $^{241,243}\text{Am}$; $^{234,236,238}\text{U}$; ^{235}U ; $^{240,242}\text{Pu}$; and $^{239,241}\text{Pu}$.

4. Characterization of melted fuel by Neutron Resonance Densitometry

Neutron Resonance Densitometry (NRD) is being investigated as a method to quantify special nuclear material (SNM) in particle-like debris of melted fuel formed in severe nuclear accidents [21]. Characterization of such debris will be required for safeguards material accountancy at the time of removal of melted fuel resulting from the accident at the Fukushima Daiichi nuclear power plants. NRD relies on the use of NRTA together with NRCA combined with PGAA. The quantification of plutonium and uranium will rely on NRTA. NRCA combined with PGAA, using a well-type LaBr_3 detector, will be applied to determine the presence of impurities. In contrast to fresh or spent fuel, information about the elemental and isotopic composition of melted fuel formed after a severe nuclear accident is rather scarce. It is expected that the melted fuel will contain water, boron,

concrete and structural materials. However, the corresponding elemental (and isotopic) composition cannot be predicted. The detection of specific prompt γ -rays can be used to identify the presence of nuclides which do not have resonances in the low-energy region (e.g. ^{10}B , ^{28}Si , ^{56}Fe , ^{53}Cr and ^{58}Ni) and cannot be identified by NRTA.

The potential of NRTA for the characterization of fresh and spent fuel pins has already been demonstrated in Refs. [22, 23]. However, an accurate quantification of the amount of SNM in debris of melted fuel is much more complex. It requires a good understanding of the measurement process such that all components affecting the data are identified. The main sources of systematic effects are related to the specific characteristics of the samples, in particular, the sample inhomogeneity, particle size distribution, presence of neutron absorbing impurities, the total radioactivity and sample temperature. The complexity of the problem is illustrated

in Figures 2-6. For the production of Figures 2-5 the response function of the TOF-spectrometer was approximated by a Gaussian distribution of the equivalent distance with a FWHM of 2.5 cm, independent of the neutron energy.

In Fig. 2 the theoretical transmission as a function of neutron energy through a 2.5-cm thick sample is given. The composition of the sample, which is typical for spent fuel, was taken from Ref. [23]. The transmission is calculated for an ideal transmission geometry with the sample at 400 K and the detector placed at 10 m distance from the source. The contribution of the different nuclides present in the sample is illustrated by plotting separately the transmission due to the presence of only the fission products (i.e. ^{99}Tc , ^{131}Xe , ^{133}Cs , ^{145}Nd , ^{152}Sm); $^{241,243}\text{Am}$; $^{234,236,238}\text{U}$; ^{235}U ; $^{240,242}\text{Pu}$; and $^{239,241}\text{Pu}$. This figure illustrates that the determination of the amount of the fissile material is hampered by overlapping resonances due to the presence of the fission products, Am and the even U- and Pu-isotopes. Hence, the accuracy of the amount of fissile material will depend on the quality of the resonance parameters of the overlapping resonances. The dips corresponding to the strong s-wave resonances of ^{238}U can be used to monitor the background level. However, additional studies are required to verify if the wings of transmission profiles of saturated resonances can be used to extract information about the ^{238}U content.

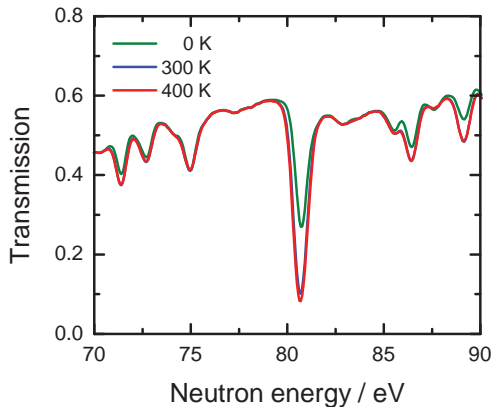


Figure 3: Transmission through a 2.5 cm thick sample with a composition that is similar to spent fuel. The transmission is given for the sample at 0 K, 300 K and 400 K.

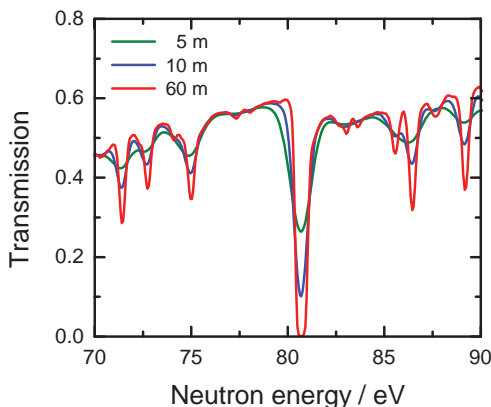


Figure 4: Transmission through a 2.5 cm thick sample with a composition that is similar to spent fuel. The transmission is given for the detector at a distance of 5 m, 10 m and 60 m.

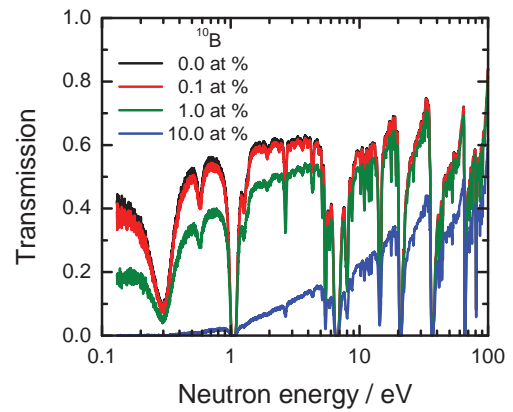


Figure 5: Transmission through a 2.5 cm thick sample with a composition that is similar to spent fuel and with different amounts of ^{10}B (0, 0.1, 1 and 10 wt%).

For a correct quantitative interpretation of the data, the broadening of observed profiles due to both the Doppler effect and the response of the TOF spectrometer has to be taken into account. This is illustrated in Fig. 3 where the transmissions are shown for the sample at 0 K, 300 K and 400 K and in Fig. 4 where the transmissions recorded with a detector at 5 m, 10 m and 60 m distance from the neutron source are compared.

Due to the large absorption cross section of the $^{10}\text{B}(n,\alpha)$ reaction in the low-energy region, the presence of boron will strongly influence the observed transmission. The attenuation of the neutron beam due to the presence of ^{10}B is illustrated in Fig. 5 for different relative amounts of ^{10}B in the sample. This additional attenuation does not only affect the base-line but also the area of the resonance dip. Therefore, it has to be taken into account in the analysis. Unfortunately, light elements such as ^{10}B do not have resonances in the low-energy and special procedures are required to account for the presence of light matrix material.

One of the main difficulties for a correct interpretation of the transmission is the variety in size and shape of the particle-like debris. This can be concluded from results of transmission measurements using a PuO_2 pressed powder sample enriched to 99.93 wt% in ^{242}Pu that was mixed with carbon powder and canned in a copper container [8]. The measurements were performed at GELINA with the sample at 77 K and 300 K. In Fig. 6 the experimental transmissions are shown together with the results of a resonance analysis. In the analysis the areal density was adjusted and the resonance parameters were fixed to those recommended in the JEFF 3.1.2 evaluated data library. The areal density was derived in a fit to the experimental data supposing that the sample was completely homogeneous and by introducing an empirical macroscopic model that accounts for the sample inhomogeneities. This model, proposed by Kopecky et al. [8], includes a log-normal distribution describing the variation in areal density and a parameter reflecting the fraction of holes in the sample. The

results are given in Table 1 and should be compared with the areal density $2.51 \cdot 10^{-5}$ at/b that was derived from weighing and a measurement of the area of the pressed pellet. The data in Table 1 show that there is a strong difference between the areal density which is derived from a fit with and without accounting for the sample inhomogeneities. Supposing a homogeneous sample the areal density resulting from NRTA is biased to lower values. The values at 77 K and 300 K derived by including an areal density and a holes fraction are fully consistent with $2.51 \cdot 10^{-5}$ at/b. In addition, the residuals in Fig. 6 demonstrate that the quality of the fit improves significantly when

the powder grain size and fraction of holes in the sample are included. The improved quality is observed for both the 77 K and 300 K data.

	Areal density ^{242}Pu at/b	
	77 K	300 K
Homogeneous	$1.65 \cdot 10^{-5}$	$1.79 \cdot 10^{-5}$
Inhomogeneous	$2.49 \cdot 10^{-5}$	$2.47 \cdot 10^{-5}$

Table 1: Areal density of ^{242}Pu in a powder determined by NRTA for a homogeneous and inhomogeneous distribution of the areal density (uncertainty due to counting statistics: $4 \cdot 10^{-8}$ at/b)

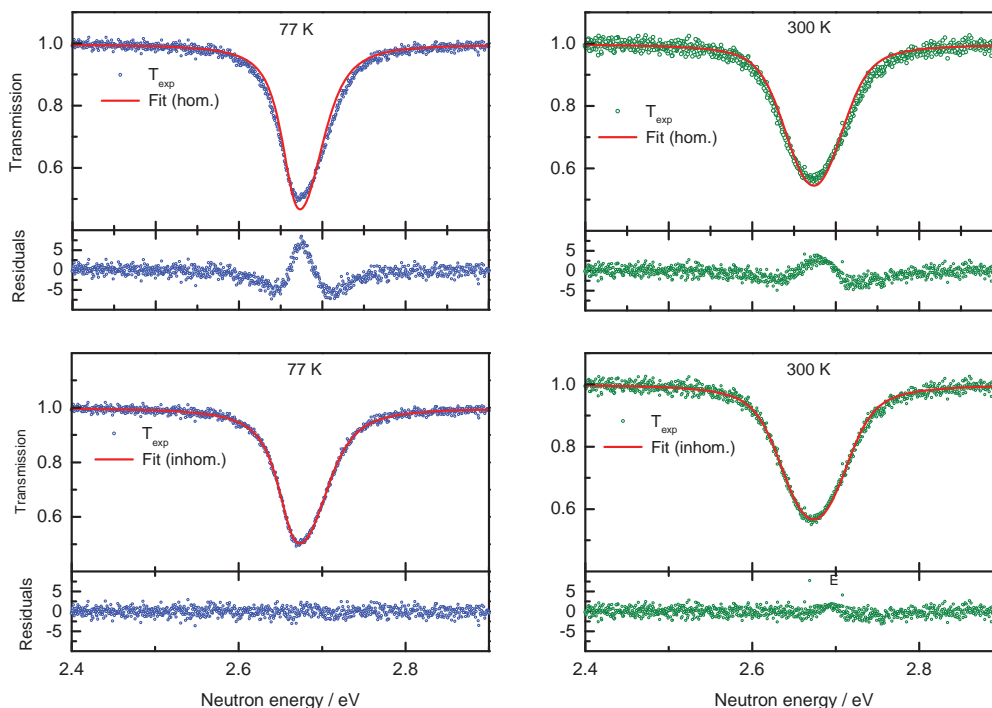


Figure 6: Transmission as a function of neutron energy for a PuO_2 powder sample enriched in ^{242}Pu and mixed with carbon powder. The transmission is given for the sample at 77 K and 300 K. Results of a fit to the data to determine the areal density of ^{242}Pu are given in case of a homogeneous sample and of an inhomogeneous sample.

5. NRD development at GELINA

To study the systematic effects mentioned in section 4, the Japan Atomic Energy Agency (JAEA) and the Joint Research Centre of the European Commission (EC - JRC) started a collaboration. In this collaboration various aspects in the development of NRD, from basic measurement principles up to detector and accelerator development, are included. One of the most important activities is the study of the influence of the sample characteristics in order to improve the analysis procedures and to define target values with realistic uncertainties. This study includes the development of theoretical models to account for sample inhomogeneities and strongly relies on measurements performed at GELINA. The experimental data will be used to validate theoretical models, to improve relevant nuclear data if needed, to determine reference spectra and to define performance values. In addition, the resonance shape

analysis code REFIT [9] will be modified and adapted to the needs of NRD.

Several measurement campaigns are scheduled at GELINA using samples which are dedicated to a specific part of the problem. Measurements on pure Cu metal discs with different thicknesses at the 25 m station will be performed to study the accuracy of NRTA in case of homogeneous samples. The results of these measurements will be used to study the influence of the resonance characteristics (i.e. resonance strength) and to verify if from the wings of transmission profiles of saturated resonance reliable information can be extracted. In addition, measurements with boron and lithium samples added to the Cu discs will be carried out to define a method to account for the presence of matrix material which does not have resonances in the low-energy region. These measurements have already been completed and the analysis of the data is in progress. Parts of the data are shown in Fig. 7 and 8.

In another contribution to the 2013 ESARDA Symposium different models to account for the density variation in powder samples are described [24]. The performance of the models has been compared using results of stochastic numerical simulations as a reference. This comparison will be complemented with experimental data. The data result from transmission measurements using pure metal Cu and W samples and samples made out of Cu and W powder mixed with S powder. The experiments are in progress and will be finished by July 2013.

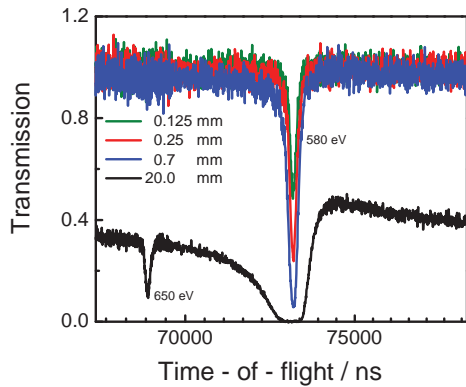


Figure 7: Experimental transmission around the 580 eV resonance through Cu discs with different thickness.

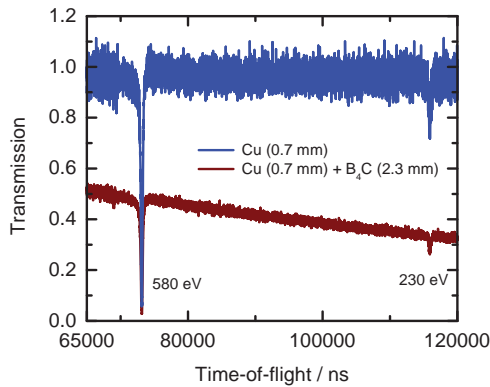


Figure 8: Experimental transmission around the 580 eV and 230 eV resonance through a 0.7 mm thick Cu disc with and without a 2.3 mm thick B₄C disc.

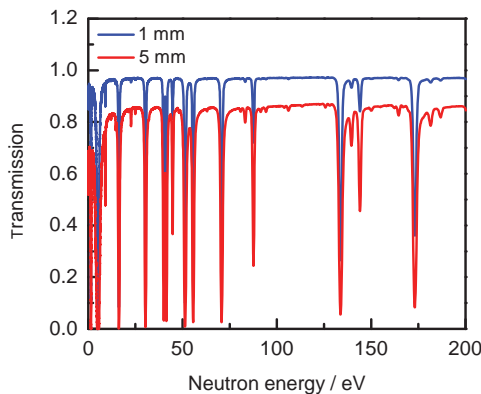


Figure 9: Theoretical transmission through a Ag-In-Zr-Fe-Cr alloy sample (1 mm and 5 mm thick).

Element	at. %	wt. %
Ag	55.0	59.7
Zr	39.9	36.6
In	1.4	1.7
Fe	2.7	1.5
Cr	1.0	0.5

Table 2: Elemental composition of the alloy used as non-radioactive alternative for a melted fuel sample.

For a final validation of the models an alloy consisting of Ag, In, Zr, Fe and Cr has been defined and is being produced. The elemental composition of the alloy is given in Table 2. Considering the resonance characteristics and material properties, Ag and In have been chosen to replace the role of U and Pu, respectively. Two homogeneous discs with a nominal thickness of 1 and 5 mm will be made. In addition, the remaining cast material will be used to produce samples that are similar in shape as the debris of the melted fuel. A simulation of the transmission through the 1 mm and 5 mm homogeneous disc is shown in Fig. 9. The transmission measurements will be performed at different sample temperatures.

6. Summary

A method, referred to as Neutron Resonance Densitometry, has been presented. The method, which relies on the appearance of resonance structures in neutron induced reaction cross section, is being developed for the characterization of melted fuel that is formed after a severe nuclear accident. The basic principles have been explained and special problems related to measurements of particle-like debris have been presented. In addition, the programme to study these problems, to develop dedicated analysis procedures and to assess the performance of NRD has been discussed. This R&D programme, which is part of a collaboration between JAEA and EURATOM, strongly relies on measurements at the time-of-flight facility GELINA installed at the EC-JRC-IRMM.

7. Acknowledgements

This work is part of a collaboration between the Japan Atomic Energy Agency (JAEA) and European Atomic Energy Community (EURATOM) represented by the European Commission in the field of nuclear materials safeguards research and development.

8. References

- [1] Lane A.M., Thomas R.G., Rev. Mod. Phys. **30**, 257-353, 1958.
- [2] Postma H. and Schillebeeckx P., Encyclopedia of Analytical Chemistry (John Wiley & Sons Ltd), 2009; pp. 1-22.

- [3] Schillebeeckx P., Borella A., Emiliani F., Gorini G., Kockelmann W., Kopecky S., Lampoudis C., Moxon M., Perelli Cippo E., Postma H., Rhodes N.J., Schooneveld E.M., Van Beveren C., *JINST* **7**, C03009, 2012.
- [4] Günsing F. and the n_TOF collaboration, Int. Conf. Nuclear Data for Science and Techn., Nice, France, April, 2007, pp. 537 – 542.
- [5] Schillebeeckx P., Becker B., Danon Y., Guber K., Harada H., Heyse J., Junghans A. R., Kopecky S., Massimi C., Moxon M.C., Otuka N., Sirakov I., and Volev K., Nuclear Data Sheets **113**, 3054 - 3100, 2012.
- [6] Postma H., Schillebeeckx P., J. Radioanal. Nucl. Chem. **265**, 297-302, 2005.
- [7] Carlson A.D., Pronyaev V.G., Smith D.L., Larson N.M., Zhenpeng Chen, Hale G.M., Hamsch F.-J., Gai E.V., Soo-Youl Oh, Badikov S.A., Kawano T., Hofmann H.M., Vonach H., Tagesen S., Nuclear Data Sheets **110**, 3215-3324, 2009.
- [8] Kopecky S., Siegler P., Moens A., Proc. Int. Conf. Nuclear Data for Science and Techn., Nice, France, April, 2007, pp. 623-626.
- [9] Borella A., Aerts G., Günsing F., Moxon M., Schillebeeckx P., Wynants R., Nucl. Instr. Meth. **A577**, 626-640, 2007.
- [10] Moxon M.C., Brisland J.B., AEAInTec-0630, AEA Technology, October, 1991.
- [11] Reich C.W., Moore M.S., Phys. Rev. **111**, 929-933, 1958.
- [12] Schillebeeckx P., Borella A., Drohe J.C., Eykens R., Kopecky S., Massimi C., Mihailescu L.C., Moens A., Moxon M., Wynants R., Nucl. Instr. Meth. **A613**, 378-385, 2010.
- [13] Noguere G., Cserpak F., Ingelbrecht C., Plompen A.J.M., Quetel C.R., Schillebeeckx P., Nucl. Instr. Meth. **A575**, 476-488, 2007.
- [14] W. Mondelaers, P. Schillebeeckx, Notiziario Neutroni e Luce di Sincrotrone **11**, 19 – 25 (2006).
- [15] Postma H., Schillebeeckx P., Halbertsma R.B., Archaeometry **46**, 635-646, 2004.
- [16] Postma H., Schillebeeckx P., Kockelmann W., J. Archaeological Sci. **38**, 1810-1817, 2011.
- [17] Postma H., Amkreutz L., Borella A., Clarijs M., Kamermans H., Kockelmann W., Paradowska A., Schillebeeckx P., Visser D., J. Radioanal. Nucl. Chem. **283**, 641-651, 2010.
- [18] Schut P.A.C., Kockelmann W., Postma H., Visser D., Schillebeeckx P., Wynants R., J. Radioanal. Nucl. Chem. **278**, 151-164, 2008.
- [19] Schooneveld E.M., Tardocchi M., Gorini G., Kockelmann W., Nakamura T., Perelli Cippo E., Postma H., Rhodes N., Schillebeeckx P. and the Ancient Charm Collaboration, J. Phys. D: Appl. Phys. **42**, 152003-5, 2009.
- [20] Perelli Cippo E., Borella A., Gorini G., Kockelmann W., Moxon M., Postma H., Rhodes N.J., Schillebeeckx P., Schooneveld E.M., Tardocchi M., Dusz K., Hajnal Z., Biro K., Porcinai S., Andreanii C., Festai G., J. Anal. At. Spectrom., **26**, 992-999, 2011.
- [21] Harada H., Kitatani F., Koizumi M., Tsuchiya H., Takamine J., Kureta M., Iimura H., Seya M., Becker B., Kopecky S., Schillebeeckx P., Proc. of ESAR-DA35 (2013).
- [22] Priesmeyer H.G., Harz U., Atomkernenergie **25**, 109-113, 1975.
- [23] Behrens J.W., Johnson R.G., Schrack R.A., Nuclear Technology **67**, 162-168, 1984.
- [24] Becker B., Harada H., Kauwenberghs K., Kitatani F., Koizumi M., Kopecky S., Moens A., Schillebeeckx P., Sibbens G., Tsuchiya H., ESARDA Bulletin **50**, 2-8 (2013).

Expanding the Capabilities of Neutron Multiplicity Measurements: Conclusions from a Four Year Project

Braden Goddard¹, William Charlton¹, Martyn Swinhoe², Paolo Peerani³

¹ Nuclear Security Science and Policy Institute, Texas A&M University - College Station, Texas, USA

E-mail: goddard.braden@gmail.com, wcharlton@tamu.edu

² Los Alamos National Laboratory, NEN-1, Los Alamos, New Mexico, USA

E-mail: swinhoe@lanl.gov

³ European Commission, EC-JRC-IPSC - Ispra, Italy

E-mail: paolo.peerani@jrc.ec.europa.eu

Abstract:

Neutron multiplicity measurement techniques are a powerful nondestructive assay tool for the quantification of plutonium and uranium. One of the main limitations of this technique is the ability to quantify the content of a sample which contains more than one actinide. The ability of inspection agencies and facility operators to measure powders containing several actinides is increasingly necessary as new reprocessing techniques and fuel forms are being developed. These powders are difficult to measure with current techniques because neutrons emitted from induced and spontaneous fission of different nuclides are very similar. Over the past four years at the Nuclear Security Science and Policy Institute (NSSPI), at Texas A&M University, a neutron multiplicity technique based on first principle methods was developed to measure these powders by exploiting isotope-specific nuclear properties, such as the energy-dependent fission cross sections and the neutron induced fission neutron multiplicity. This technique was tested by three measurement campaigns using the Active Well Coincidence Counter (AWCC) and Epithermal Neutron Multiplicity Counter (ENMC) with various (α,n) sources and measured materials. To complement these measurements, extensive Monte Carlo N Particle eXtended (MCNPX) simulations were performed for each measured sample, as well as for samples which were not available to measure. Four potential applications of this technique have been identified: measurements of U, Np, Pu, and Am materials, mixed oxide (MOX) materials, and uranium materials, as well as weapons verification in arms control agreements. This technique still has several challenges which need to be overcome, the largest of these being the ability to produce results with acceptably small uncertainties.

Keywords: Neutron Multiplicity Counting; Epithermal Neutron Multiplicity Counter (ENMC); Monte Carlo N Particle eXtended (MCNPX); First Principle Methods; Nondestructive Assay

1. Introduction

Neutron multiplicity counting is a well developed technique which is commonly used to quantify nuclear materials. The three primary materials that are measured with this

technique are: plutonium in plutonium samples, plutonium in mixed oxide (MOX) samples, and ^{235}U in uranium samples. Although these materials currently represent the majority of unirradiated nuclear materials which are safeguarded, there is a growing need to develop techniques to measure more complex materials. As new reprocessing methods [1][2] and fuel forms [3-8] are developed, the ability to perform neutron multiplicity measurements on materials which contain other actinides, including neptunium and americium, are becoming increasingly important. In addition to measuring more complex materials, there is an additional need to redevelop the equations and theory of active neutron multiplicity counting to increase the possible applications for this technique. By moving from an active measurement technique which requires known standards of similar composition and geometry to a method which is based on first principles, a wider range of materials can be measured.

2. Theory

Active neutron coincidence counting is currently performed by interrogating the measurement sample with neutrons from an (α,n) source, such as americium-lithium (AmLi) [9]. Because neutrons created from (α,n) reactions are created individually they have a minimal impact on the doubles count rate. Instead of using the detector's correlated count rates to solve for sample related variables, the doubles count rate is often compared to doubles count rates of similar known standards. Through interpolation the mass of the measured sample can be estimated. The main disadvantage of this technique is that it requires known standards of similar composition and geometry, which may not always be available. Methods have been developed, such as the coupling method, to move from a known standards approach to one which incorporates first principle equations, however, these methods still rely on known standards [9][10]. The reason why the point-model equations do not work for active measurements is that with current measurement systems the point-model assumptions are violated. In particular, the assumption that the source of neutrons from the sample can be modelled as a point in space is not rigorously correct. Although neutrons with high energies can penetrate thick actinide materials, thus creating homogeneous

fission rates within them, neutrons which have been slowed down to epithermal energies are absorbed in actinide materials due to capture and fission resonances. These fission resonances cause the majority of fissions to occur on the surface of the measurement sample, [11], thus creating a heterogeneous fission rate and violating the point-model assumptions.

One solution to the problems caused by epithermal neutrons is to prevent them from entering the measurement sample. This can be achieved by surrounding the measurement sample in high content ^{10}B material, such as boron carbide (B_4C). After ensuring that the fission rate in the sample is homogeneous the following first principle equations can be used:

$$(D_{Li} - D_{Passive}) = \frac{F_o^{239}\text{Pu}_{eff_Li} \varepsilon^2 f_d M_L^2 \nu_{Li2}}{2} \left[1 + \frac{(M_L - 1) \nu_{Li1} \nu_{Fis2}}{(\nu_{Fis1} - 1) \nu_{Li2}} \right] \quad (1)$$

where D_{Li} is the doubles count rate from the AmLi measurement, $D_{Passive}$ is the doubles count rate from the passive measurement, $^{239}\text{Pu}_{eff_Li}$ is the effective mass of ^{239}Pu in the sample that would produce the same AmLi doubles count rate as the complete sample, ε is the detector efficiency, f_d is the doubles gate fraction, M_L is the leakage self-multiplication of the item, ν_{Li1} is the first moment of induced fission for neutrons with an AmLi energy spectrum, ν_{Li2} is the second moment of induced fission for neutrons with an AmLi energy spectrum, ν_{Fis1} is the first moment of induced fission for neutrons with a fission energy spectrum, and ν_{Fis2} is the second moment of induced fission for neutrons with a fission energy spectrum. Equation 1 is analogous to spontaneous fission, but acknowledges that the initiating fission source is induced fission from an AmLi neutron source.

Because F_o , the specific fission rate, is based on the induced fission rate and not the spontaneous fission rate, it cannot be treated as a constant. F_o can instead be solved for using:

$$F_o = \frac{\varphi_{Li} \sigma_{f_Li} N_A}{M_{molar}} \quad (2)$$

where φ_{Li} is the neutron flux within the sample during an AmLi measurement, σ_{f_Li} is the average ^{239}Pu microscopic fission cross section for neutrons with an AmLi energy spectrum, N_A is Avogadro's Number, and M_{molar} is the molar mass of the effective mass isotope (approximately 239 amu in this example).

The neutron flux, φ_{Li} , and the average fission cross section, σ_{f_Li} , can be approximated as constants and determined through computer simulations, for a given detector system. Because these values are fairly independent of the sample being measured, a generic geometry and sample composition may be used in the simulations.

Similar to the point-model equations, Eq. (1) is not directly useable. By combining Eq. (1) and (2) and rearranging terms we acquire:

$$^{239}\text{Pu}_{eff_Li} = \frac{2(D_{Li} - D_{Passive}) M_{molar}}{\varphi_{Li} \sigma_{f_Li} N_A \varepsilon^2 f_d M_L^2 \nu_{Li2} \left[1 + \frac{(M_L - 1) \nu_{Li1} \nu_{Fis2}}{(\nu_{Fis1} - 1) \nu_{Li2}} \right]} \quad (3)$$

Analogous to passive neutron coincidence counting, an equation relating the $^{239}\text{Pu}_{eff}$ mass to elemental masses can be created. This equation includes not just those isotopes of plutonium and uranium, but of neptunium and americium as well:

$$\begin{aligned} ^{239}\text{Pu}_{eff_Li} = & C_{U235_Li} m_{U235} + C_{U238_Li} m_{U238} \\ & + C_{Np237_Li} m_{Np237} + C_{Pu238_Li} m_{Pu238} \\ & + C_{Pu239_Li} m_{Pu239} + C_{Pu240_Li} m_{Pu240} \\ & + C_{Pu241_Li} m_{Pu241} + C_{Pu242_Li} m_{Pu242} \\ & + C_{Am241_Li} m_{Am241} + C_{Am243_Li} m_{Am243} \end{aligned} \quad (4)$$

where C_{k_Li} is an equivalent worth constant for a AmLi measurement for isotope k and m_k is the mass of isotope k in the sample.

The constants, C_{k_Li} , can be determined by using a ratio of nuclear properties of the effective isotope [12]:

$$C_{k_Li} = \frac{(\sigma_{f_Li} \nu_{Li2})_k}{(\sigma_{f_Li} \nu_{Li2})_{239}} \left(\frac{M_{molar,239}}{M_{molar,k}} \right) \quad (5)$$

where k represents the isotope of interest.

3. Measurements and simulations

In order to test the first principle measurement method a series of measurement campaigns were conducted at the Joint Research Centre (JRC) in Ispra, Italy and Los Alamos National Laboratory (LANL) in New Mexico, USA. These campaigns included measurements with the Active Well Coincidence Counter (AWCC) [13] and Epithermal Neutron Multiplicity Counter (ENMC) [14][15] in both passive and active modes. Americium-beryllium (AmBe), plutonium-boron (PuB), and AmLi were all considered as (α,n) interrogation sources, with AmBe being rejected due to its significant internal ($n,2n$) reaction rate. A wide variety of nuclear materials were measured including: metals, powders, and ceramics; masses in the range of 5g – 170g; and isotopic compositions ranging from depleted uranium to High Enriched Uranium (HEU) and reactor grade to weapons grade plutonium [16-21]. Each measurement consisted of 60 – 90 cycles at 60 seconds per cycle. The detector response for each measurement was analyzed using the International Atomic Energy Agency (IAEA) International Neutron Coincidence Counting (INCC) software program in rates-only mode to determine the singles, doubles, and triples

count rates with statistical uncertainties [22][23]. Each measurement performed was simulated in Monte Carlo N Particle eXtended (MCNPX) to validate the MCNPX models. The AmBe neutron spectrum used was that of Cody Peebles [24], the PuB spectrum was determined from Sources4C [25], and the AmLi neutron spectrum was that of Geiger and Van der Zwan [26]. The number of histories run in each MCNPX simulation varied from 20 MegaHistories (20 MH or 20 million active histories) to 300 MH, depending on the measurement type being modelled. Both F4 and F8 MCNPX capture gated tallies were used to determine the neutron flux in the measurement sample and the correlated count rates in the ^3He tubes. MCNPX pulse train p-track data was not used for the simulation calculations.

In order to prevent epithermal neutrons from entering the measurement sample, a B_4C cylinder was manufactured with two cylindrical plates for the top and bottom. The B_4C had an inner diameter of 130 mm, inner height of 170 mm, and a thickness of 25 mm on all sides. These dimensions were chosen based on (1) the size of the ENMC measurement cavity, (2) the size of the nuclear standards to be measured, and (3) the epithermal absorption capabilities of the B_4C . The boron isotopic composition was that of natural boron.

Measurements of various plutonium standards, shown in Table 1, were performed using the ENMC in a passive, active AmLi, and active PuB mode. The $^{239}\text{Pu}_{\text{eff}}$ values calculated from Eq. (3) and (4) were determined for the measured, simulated, and declared data.

Item	Pu [g]	^{238}Pu [wt. %]	^{239}Pu [wt. %]	^{240}Pu [wt. %]	^{241}Pu [wt. %]	^{242}Pu [wt. %]	^{241}Am [g]
STDIS03	10.96	0.0053	96.3504	3.5566	0.0328	0.0182	0.010
STDIS09	11.85	0.0175	92.7957	6.8863	0.1216	0.0734	0.036
STDIS12	20.09	0.0481	87.4464	11.8503	0.2787	0.2228	0.158
CBNM-Pu61	5.45	1.0319	65.7930	26.6912	2.0697	4.4143	0.344
STD11	59.74	0.0228	92.7048	6.6156	0.0741	0.5827	0.202
LAO250C10	59.36	0.0470	82.9792	16.3044	0.3318	0.3376	0.621

Table 1: Mass and isotopic composition of the plutonium standards measured at LANL.

The AmLi and PuB results had similar trends, with excellent agreement between the simulated and declared, shown in Figures 1 and 2. This implies that the assay methodology could be both accurate and precise. The results from the measured data are harder to interpret due to the large measurement uncertainties. The large uncertainties come from Eq. (3) in which the passive and active doubles count rates are subtracted from each other. Because these two count rates are of similar magnitude their resultant subtraction is a small value with a large uncertainty. The uncertainties in D_{passive} and D_{Li} were both calculated by INCC which compares mean values for each cycle in the measurement to estimate a 1- σ (68% confidence interval) uncertainty. Performing longer measurements is not an ideal practical solution since this data was acquired with 1 hour measurements of the samples and overnight measurements of the background. A potential solution would be to increase the difference between

these two count rates by increasing the AmLi source strength. Active measurements which have a large background source, such as the spontaneous fission neutrons from plutonium, can benefit from a stronger interrogation source [13]. Simulations were performed to quantify this potential solution. The AmLi source strength was varied over the range of 5×10^3 to 1×10^7 n/s per AmLi source. The AmLi source strength used in the measurements was 5×10^4 n/s for each AmLi source. From the results shown in Table 2, it can be seen that for the larger mass plutonium standards, STD11 and LAO250C10, there is a significant reduction in the expected $^{239}\text{Pu}_{\text{eff, Li}}$ mass uncertainty [27] for active measurements using stronger AmLi interrogation sources. Simulations using a PuB source had similar results. It should be noted that AmLi sources with source strengths larger than 5×10^4 n/s are currently uncommon and sources with strengths in the range of 10^6 n/s may pose operational difficulties.

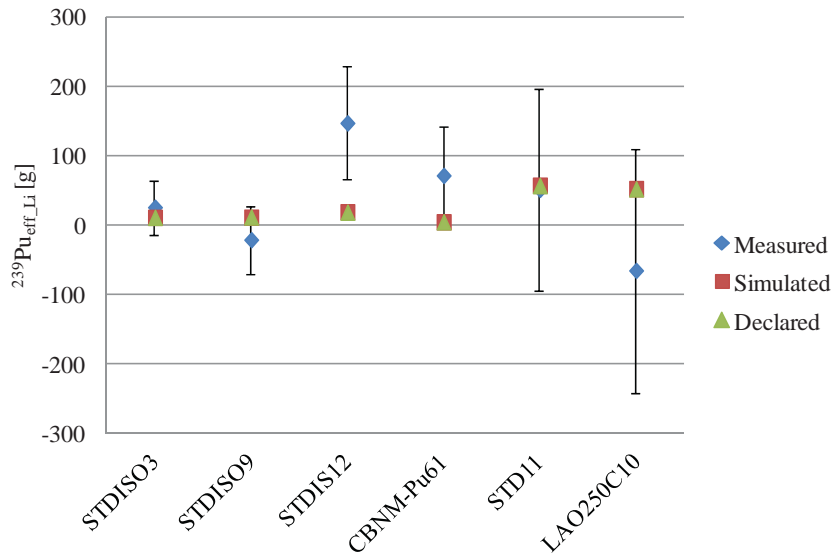


Figure 1: Measured, simulated, and declared $^{239}\text{Pu}_{\text{eff}_L\text{Li}}$ values. Uncertainties stated at the 1- σ (68% confidence interval) level.

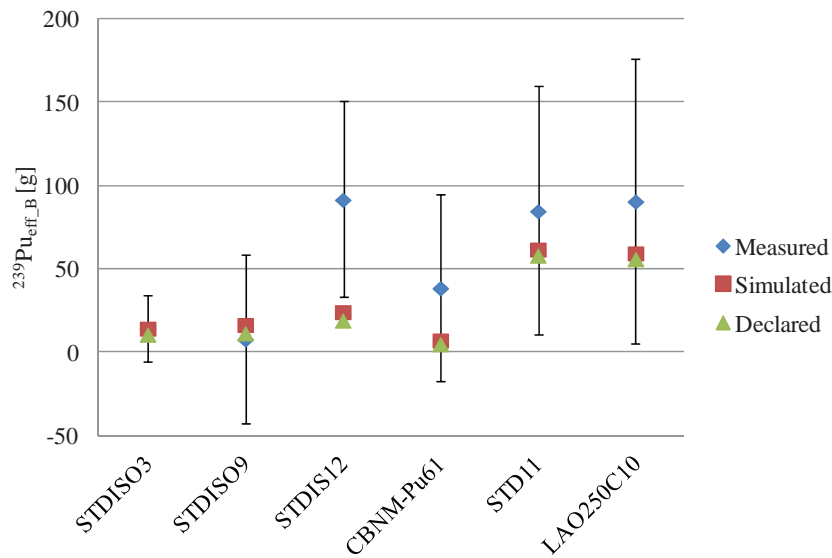


Figure 2: Measured, simulated, and declared $^{239}\text{Pu}_{\text{eff}_B}$ values. Uncertainties stated at the 1- σ (68% confidence interval) level.

Plutonium standards	AmLi strength [n/s each]							
	5×10^3	1×10^4	5×10^4	1×10^5	5×10^5	1×10^6	5×10^6	1×10^7
STDIS03	205	113	50	44	40	40	40	40
STDIS09	337	176	61	49	41	40	40	40
STDIS12	715	365	97	67	45	42	40	40
CBNM-Pu61	637	327	90	63	44	41	40	39
STD11	671	342	84	54	30	28	25	25
LAO250C10	1233	625	142	83	36	31	26	25

Table 2: Source strength optimization for measured plutonium standards using the active configurations of the ENMC. Values shown are expected $^{239}\text{Pu}_{\text{eff}_L\text{Li}}$ [g] uncertainties at the 1- σ (68% confidence interval) level.

4. Results of simulated samples

In order to test the full measurement methodology, simulated samples containing various actinide mixtures were created using the Oak Ridge Isotope Generation and Depletion Automatic Rapid Processing (ORIGEN-ARP) Code and their neutron signatures determined using the ENMC MCNPX model. These samples can be organized into three categories: uranium extraction (UREX) type samples which contain U, Np, Pu, and Am at used fuel isotopic compositions [1]; MOX type samples which contain depleted uranium and weapons grade plutonium [28]; and uranium samples of varying

enrichments. Each sample, seen in Table 3, consisted of 212.5 g of heavy metal mass at a density of 2.5 g/cc in a dioxide matrix. The sample geometry is a cylindrical shape (D=45 mm, H=62.88 mm) located inside a thin aluminium can of thickness 6 mm. The nomenclature on the sample names for the UREX and MOX samples corresponds to their isotopic composition (UREX or MOX) and their non-uranium heavy metal fraction (Np, Pu, and Am). The uranium samples are designated by the letter "U" followed by the ^{235}U isotopic fraction. All the MCNPX simulations were run for 250 MH, with the exception of spontaneous fission simulations which were run for 790 MH.

Sample name	Uranium mass [g]	Neptunium mass [g]	Plutonium mass [g]	Americium mass [g]	^{235}U fraction [%]
UREX1.27	210	0.14	2.46	0.10	0.90
UREX50	106	5.61	96.60	4.04	0.90
UREX10	191	1.12	19.32	0.81	0.90
UREX10_NoNp	191	0.00	20.40	0.85	0.90
MOX50	106	0.00	106.25	0.00	0.25
MOX5	204	0.00	10.22	0.00	0.25
U93	213	0.00	0.00	0.00	93.00
U50	213	0.00	0.00	0.00	50.00
U20	213	0.00	0.00	0.00	20.00
U5	213	0.00	0.00	0.00	5.00
U0.72	213	0.00	0.00	0.00	0.72
U0.25	213	0.00	0.00	0.00	0.25

Table 3: Simulated samples along with their name, actinide masses, and ^{235}U isotopic fraction. The ^{235}U mass fraction is relative to total uranium mass.

4.1 UREX and MOX results

Simulated assayed mass estimates for the plutonium and americium were within $\pm 7\%$ of the stated (exact) values. The ^{235}U and neptunium results, shown in Figures 3 and 4, were less accurate. Although the difference between the assayed and exact values is often good, it is difficult to draw conclusions from the data due to the large uncertainties. In particular, UREX50 has big uncertainties due to the

relatively large amount of reactor grade plutonium in it, which creates a large doubles count rate. It is suspected by the authors that the uncertainty estimates are larger than they statistically should be, although the exact cause of the inflated uncertainties is not yet known. The uncertainties shown are from the $D_{Passive}$ and D_{Li} count rate uncertainties which were then propagated through all the calculation in Eq. (3) and (4).

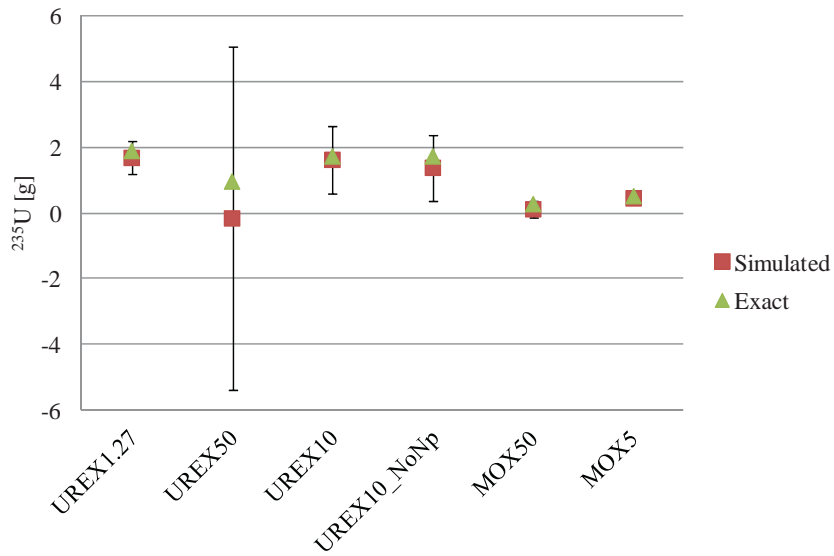


Figure 3: Simulated and exact ^{235}U masses of simulated UREX and MOX samples. The uncertainty shown at $1-\sigma$ (68% confidence interval) is due to statistical uncertainties in the MCNPX results.

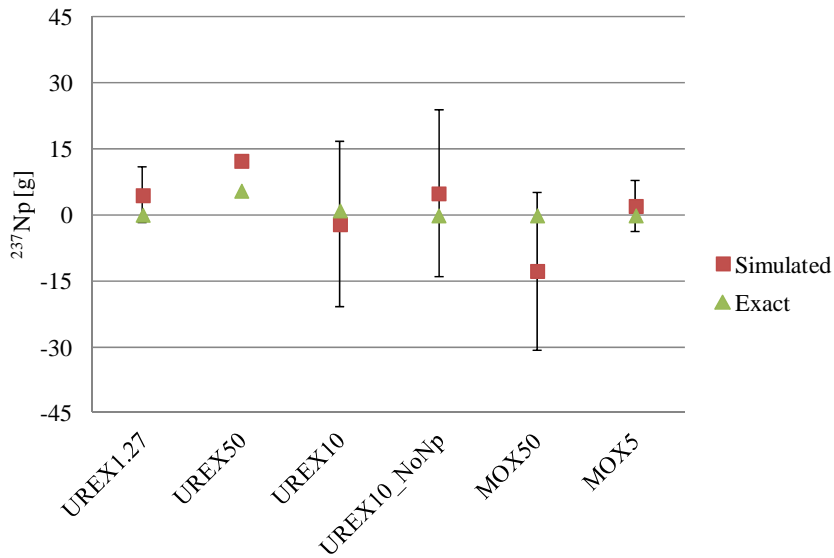


Figure 4: Simulated and exact ^{237}Np masses of simulated UREX and MOX samples. The uncertainty shown at $1-\sigma$ (68% confidence interval) is due to statistical uncertainties in the MCNPX results.

4.2 Uranium results

The ^{235}U assay results, shown in Figure 5, matched very well with the exact values for the uranium samples. The

percent differences are approximately -3% for the HEU samples and more negative for the low enriched uranium (LEU) samples.

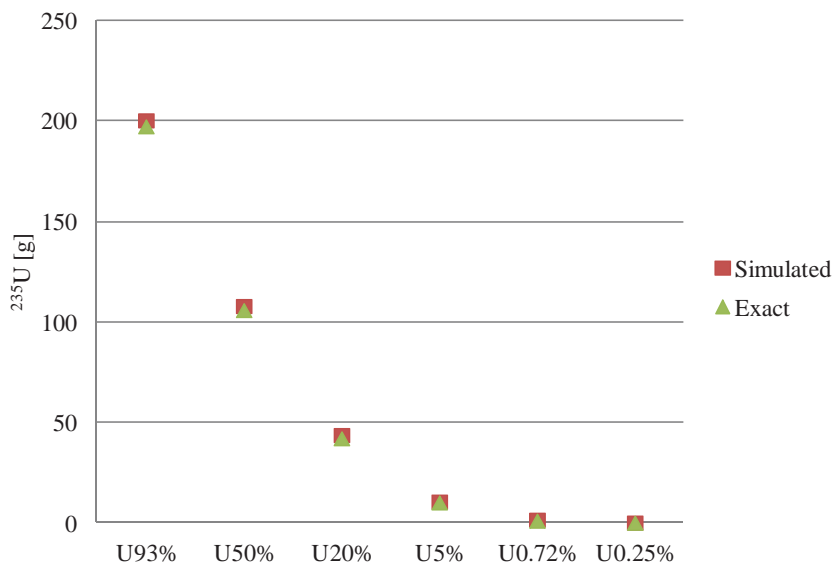


Figure 5: Simulated and exact ^{235}U masses of simulated uranium samples. The uncertainties are too small to be plotted.

5. Discussion and conclusions

Current non-destructive assay (NDA) techniques have been developed to quantify uranium, plutonium, or MOX, but not samples which contain more than these two actinides. There are applications of more complex fuel materials, including neptunium and americium, which are currently being developed. It is important to develop a method of quantitatively measuring these more complex materials before they become commercially common.

The approach taken to quantify a mixture of several actinides was to use a first principle neutron multiplicity counting approach. This technique has the added bonus of being applicable to measurements of shielded or heterogeneous MOX and uranium samples, as well as potentially weapons verification. It is postulated that weapons verification would be possible by analyzing the $^{240}\text{Pu}_{\text{eff}}$ and $^{239}\text{Pu}_{\text{eff}}$ values. These values can distinguish weapons useable materials from fission sources without revealing detailed information about the weapon. The required modifications to existing neutron multiplicity counters to allow for first principle methods to be applied is relatively minor and inexpensive, consisting of a cylindrical can of natural B_4C and a high-energy (α, n) neutron source.

The main challenge of this technique is the ability to make precise measurements. As seen in the measured and simulated data, the slight differences between the passive and active doubles count rates can cause the results using

current detector technology to be statistically irrelevant. Potential solutions to this challenge exist, such as more intense interrogation sources, but they have not been thoroughly tested.

The ability to quantify mixed actinide materials would currently be useful, and in the future may be a necessity. Further research is needed in developing this technique, in particular the ability to reduce uncertainties. Other aspects of this research should be investigated as well, such as results of kilogram sized, non-powder, non-oxide, and varying isotopic composition samples. It is suspected by the authors that this technique's full capabilities can only be utilized with advanced neutron multiplicity detectors, such as future fast neutron detectors.

6. Acknowledgements

The authors would like to acknowledge the Nuclear Nonproliferation International Safeguards Graduate Fellowship Program for supporting Dr. Braden Goddard. ORNL, JRC, and LANL should also be acknowledged for allowing the use of their facilities, equipment, and nuclear materials. The authors would also like to acknowledge Dr. Louise Evans (ORNL) and Mrs. Angela Lousteau (ORNL) for their help in performing the measurements. This research was performed under appointment to the Nuclear Nonproliferation International Safeguards Graduate Fellowship Program sponsored by the National Nuclear Security Administration's Next Generation Safeguards Initiative (NGSI).

7. References

- [1] Goddard, B.; *Development of a Real-Time Detection Strategy for Material Accountancy and Process Monitoring During Nuclear Fuel Reprocessing using the UREX+3a Method*; Thesis; Texas A&M University; College Station, TX; December 2009.
- [2] Leggett, C.; *Development of a Modified TALSPEAK Process to Separate Americium from Curium in Spent Nuclear Fuel*; Proc. Waste Management 2010; Phoenix, AZ; March 7-11, 2010.
- [3] Oigawa, H.; *Perspectives of Partitioning and Transmutation Technology*; Proc. GLOBAL 2011; Makuhari, Japan; December 11-16, 2011.
- [4] Fanghanel, T., Glatz, J., Rondinella, V., and Somers, J.; *Safety of Advanced nuclear Fuel Cycles*; Proc. GLOBAL 2011; Makuhari, Japan; December 11-16, 2011.
- [5] Pillon, S., Somers, J., Grandjean, S., and Lacquement, J.; *Aspects of Fabrication of Curium-Based Fuels and Targets*; Journal of Nuclear Materials; **320**, pp. 36-43, 2003.
- [6] Bays, S., Piet, S., Pope, M., Youinou, G., Dumontier, A., and Hawn, D.; *Transmutation Dynamics: Impacts of Multi-Recycling on Fuel Cycle Performances*; Idaho National Laboratory; INL/EXT-09-16857; September 2009.
- [7] Noyola, H.; *Pin-Wise Loading Optimization and Lattice-to-Core Coupling for Isotopic Management in Light Water Reactors*; Diss.; University of Tennessee; Knoxville, TN; December 2010.
- [8] GEN IV International Form; *Generation IV Systems*; September 3, 2010; <http://www.gen-4.org/>
- [9] Reilly, D., Ensslin, N., Smith, H., and Kreiner, S. (Editors); *Passive Nondestructive Assay of Nuclear Materials Addendum*; Ch. 7; U.S. Nuclear Regulatory Commission; Washington, DC; LA-UR-07-1403; pp. 1-23; 2007.
- [10] Krick, M., Ensslin, N., Ceo, R., and May, P.; *Analysis of Active Neutron Multiplicity Data for Y-12 Skull Oxide Samples*; LA-UR-96-343; Proc. 37th Annual INMM Meeting; Naples, FL; July 28-31, 1996.
- [11] Clarke, S., Pozzi, S., Flaska, M., Oberer, R., Chiang, L., and Gunn, C.; *Monte Carlo Analysis of Gamma-Ray Spectroscopy and AWCC Nondestructive Assay of Uranium-Oxide Samples*; Proc. 53rd Annual INMM Meeting; Orlando, FL; July 15-19, 2012.
- [12] Smith, D., and Jaramillo, G.; *Safeguards and Security Progress Report*; Los Alamos National Laboratory; LA-11356-PR; pp. 18-21; September 1988.
- [13] Menlove, H.; *Description and Operations Manual for the Active Well Coincidence Counter*; Los Alamos Scientific Laboratory; LA-7823-M; May 1979.
- [14] Stewart, J., Menlove, H., Mayo, D., Geist, W., Carrillo, L., and Herrera, G.; *The Epithermal Neutron Multiplicity Counter Design and Performance Manual: More Rapid Plutonium and Uranium Inventory Verifications by Factors of 5-20*; Los Alamos National Laboratory; LA-13743-M; August 2000.
- [15] Menlove, H., Real, C., Kroncke, K., and DeAguiro, K.; *Manual for the Epithermal Neutron Multiplicity Detector (ENMC) for Measurements of Impure MOX and Plutonium Samples*; Los Alamos National Laboratory; LA-14088; May 2004.
- [16] Los Alamos National Laboratory; *53rd Nondestructive Assay Inspector Training Course*; LA-UR-06-5527; August 2011.
- [17] Hsue, W.; *Isotopic Standards from SRP*; Los Alamos National Laboratory; N-1-89-615; July 5th 1989.
- [18] Hsue, S., Stewart, J., Sampson, T., Butler, G., Rudy, C., and Rinard, P.; *Guide to Nondestructive Assay Standards: Preparation Criteria, Availability, and Practical Considerations*; Los Alamos National Laboratory; LA-13340-MS; October 1997.
- [19] Hsue, S., Simmonds, S., Longmire, V., and Long, S.; *Design and Fabrication of SGS plutonium Standards*; LA-UR-91-2646; Proc. American Nuclear Society 4th International Conference on Facility Operations-Safeguards Interface; Albuquerque, NM; September 29 – October 4, 1991.
- [20] Menlove, H., Siebelist R., and Wenz, T.; *Calibration and Performance Testing of the IAEA Aquila Active Well Coincidence Counter (Unite 1)*; Los Alamos National Laboratory; LA-13073-MS; January 1996.
- [21] Geist, W., Stewart, J., and Carrillo, L.; *Results of Uranium Measurements using the ENMC*; Los Alamos National Laboratory; LA-UR-01-0901; 2001.
- [22] Harker, B., Krick, M., Geist, W., and Longo, J.; *INCC Software Users Manual*; Los Alamos National Laboratory; LA-UR-10-6227; March 2009.
- [23] Los Alamos National Laboratory; *International Neutron Coincidence Counting 5.1.2.3*; LA-CC-10-092; September 2010.
- [24] Peeples, C., Mickael, M., and Gardner, R.; *On Replacing Am-Be Neutron Sources in Compensated Porosity Logging Tools*; Applied Radiation and Isotopes; **68**(4-5); pp. 926-931; April-May, 2010.

- [25] Wilson, W., Perry, R., Charlton, W., Parish, T., Estes, G., Brown, T., Arthur, E., Bozoian, M., England, T., Madland, D., and Stewart, J.; *SOURCE-S4A: A Code for Calculating (α,n), Spontaneous Fission, and Delayed Neutron Source and Spectra*; Los Alamos National Laboratory; LA-13639-MS; September 1999.
- [26] Geiger, K. and Van der Zwan, L.; *The Neutron Spectra and the Resulting Fluence–kerma Conversions for $^{241}\text{Am-Li}(\alpha,n)$ and $^{210}\text{Po-Li}(\alpha,n)$ Sources*; *Health Physics*; **21**; pp. 120–123; 1971.
- [27] Croft, S., Swinhoe, M., and Henzl, V.; *A Priori Precision Estimation for Neutron Triples Counting*; Proc. 2nd ANIMMA Conference; Ghent, Belgium; June 6-9, 2011.
- [28] Solodov, A., Charlton, W., Romano, C., and Ehinger, M.; *Evaluation of NDA Techniques for Quantification of the Pu Content in MOX Spent Nuclear Fuel by Destructive Analysis*; Proc. 52nd Annual INMM Meeting; Palm Desert, CA; July 17-21, 2011.

Determination of the half-life and specific thermal power of ^{241}Pu by nuclear calorimetry¹

Stephen Croft

Oak Ridge National Laboratory - PO Box 2008, MS-6166, Oak Ridge, TN 37831-6166 - crofts@ornl.gov

Peter A. Santi

Los Alamos National Laboratory - PO Box 1663, Los Alamos, NM 87545-1663 - psanti@lanl.gov

Robert D. McElroy, Jr.

Oak Ridge National Laboratory - PO Box 2008, MS-6166, Oak Ridge, TN 37831-6166 - mcelroyrd@ornl.gov

Abstract:

^{241}Pu has the shortest half-life of the abundant plutonium isotopes present in reprocessed irradiated nuclear fuel with a value of approximately 14.3 years. It is important to know the half-life of ^{241}Pu with a higher fractional accuracy than that of the other plutonium isotopes because the half-life of ^{241}Pu and its associated uncertainty affects the estimation by decay calculation of both the total amount of separated plutonium in storage and the determination of the total plutonium mass by non-destructive assay. This paper addresses the determination of the ^{241}Pu half-life using nuclear calorimetry by the measurement of the thermal power as ^{241}Pu evolves in time from a sealed plutonium source, ideally initially rich in ^{241}Pu and chemically stripped of ^{241}Am . The absolute accuracy of nuclear calorimeters can be ensured over long periods of time (many years) using long-lived nuclear reference materials and/or traceable electrical heat standards. One can, therefore, expect nuclear calorimetry to offer an accurate way to determine the half-life of ^{241}Pu , which is comparable in quality and independent, yet complementary, to other approaches. Temporal analysis of the power-versus-time data also yields an estimate of the specific power of ^{241}Pu , which other methods do not.

After describing the principle of the method and developing the pertinent mathematical expressions, we outline the approach by drawing on some unpublished notes of Kenneth C. Jordan who carried out such experiments at the Mound Laboratory over 40 years ago. Today, Jordan's work remains possibly the most significant experiment of its type to the ^{241}Pu nuclear data evaluator. However, objectively assigning confidence to his results is problematic because the details of the experiments and data reduction have never been adequately reported. This work goes some way to that end but, without the raw data and first-hand knowledge, cannot provide a complete record. We conclude that a new high-accuracy nuclear calorimetry campaign to re-measure the ^{241}Pu half-life and specific

power is needed as a means to confirm that systematic biases are under control, to support international safeguards, and to improve fundamental metrology and nuclear data – for instance, the mean beta-particle energy emitted by ^{241}Pu and whether the soft beta decay mode rate is influenced by chemical form or other factors.

Keywords: ^{241}Pu ; half-life; specific power; calorimetry; nuclear data

1. Introduction

On the time scale of years to decades, the mass of separated plutonium in storage falls with time primarily as a consequence of the radioactive decay of ^{241}Pu . Therefore, over time, uncertainty in the ^{241}Pu half-life leads initially to a growing apparent uncertainty in the mass of plutonium under safeguards. After many decades, the uncertainty drops again because one can be confident that all the ^{241}Pu has decayed. The predominant decay mechanism of ^{241}Pu is low-energy beta-particle emission leading to an in-growth of the alpha-emitter ^{241}Am . Neither ^{241}Pu nor ^{241}Am exhibits appreciable spontaneous fission, but ^{241}Am has about 2000 times greater specific $\text{O}(\alpha, \text{n})$ yield than ^{241}Pu , about 33 times greater specific heat output than ^{241}Pu , and also contributes more strongly than ^{241}Pu to the surface dose rate for lightly encapsulated materials via its intense 60 keV gamma-ray emission. This affects non-destructive assay measurements by both neutron coincidence counting (adding random background neutrons that contribute to accidental coincidences and increasing the gamma-to-neutron ratio) and calorimetry (introducing an age-dependent item power). As a consequence, the thermal output from ^{241}Pu and its daughter ^{241}Am , changes at a much faster rate (roughly 0.45% per day initially) than any of the other plutonium isotopes, including ^{236}Pu and its daughters. This effect, in turn, changes the thermal power output of storage cans containing plutonium. Confirmatory nuclear safeguards checks of stored items using nuclear calorimetry must, therefore, be corrected for the decay of ^{241}Pu (usually either by calculation or by gamma-ray spectrometry) and compared to a fixed reference time. Again, as the time between measurements increases, the uncertainty in the comparison based on

¹ This manuscript has been authored by UT-Battelle, LLC, under Contract No. DE-AC05-00OR22725 with the US Department of Energy. The United States Government retains and the publisher, by accepting the article for publication, acknowledges that the United States Government retains a non-exclusive, paid-up, irrevocable, world-wide license to publish or reproduce the published form of this manuscript, or allow others to do so, for United States Government purposes.

decay-corrected relative isotopic content grows larger due to the propagation of the uncertainty in the ^{241}Pu half-life. A point will be reached when decay-corrected mass spectrometer values are less well known than gamma-ray spectrometry estimates where they are feasible.

In the 1970's, it was recognized that if a concerted effort was applied to determining the half-life of ^{241}Pu more accurately, the associated uncertainties could be reduced considerably and would essentially no longer be of concern, at least for the application of routine international nuclear safeguards. At that time, strikingly large differences existed in the scientific literature [1]. In fact, until recently, the ^{241}Pu half-life uncertainty was the major source of uncertainty in the calorimetric analysis of aging plutonium sources initially characterized by mass spectrometry, and especially in the long term prediction of ^{238}Pu heat standards used for the direct calibration and quality assurance monitoring of nuclear calorimeters.

To date, the situation has improved dramatically because of the use of the double ratio mass spectrometry technique applied to determine the abundance of ^{241}Pu relative to the long-lived plutonium isotopes, over a roughly three decade period (more than two half-lives), of a homogenized stock of plutonium initially rich in ^{241}Pu [2]. This data provides a robust estimate of the half-life and supports a relatively low (with respect to historic norms) uncertainty [3]. On this basis, a value for the ^{241}Pu half-life of about 14.325 ± 0.015 years can be claimed [2, 3], where the uncertainty is estimated at about the one standard deviation confidence level and is dominated by the challenge of maintaining instrument and procedural consistency over decades. The details are beyond the present scope and the reader is directed to [2, 3].

In the ASTM international consensus standard on nuclear calorimetry [4] reliance has for many years been placed on earlier results (the standard was first documented prior to [2]) and, in particular, great emphasis was placed on the unpublished results of Kenneth C. Jordan of Mound Laboratory. In subsequent sections of this paper we shall review the ASTM recommendations. We can find no trace of Jordan's original work. However, some of Jordan's notes were included in the records transferred from Mound to Los Alamos National Laboratory during the relocation of the calorimetry effort. Although Jordan's notes were clearly not exactly those used by the ASTM and the ANSI [5] committees (prior to ASTM), we shall draw on them here to report on the salient features of Jordan's approach and to establish a sense of the care taken to provide quality measurement results. Additionally, we provide the derivation of the equations needed to interpret the evolution of thermal power from ^{241}Pu rich items.

2. Mathematical framework

The in-growth of ^{241}Am from the decay of ^{241}Pu is governed by the following differential equations:

$$\frac{dN_a}{dt} = -\lambda_a N_a \quad (1)$$

$$\frac{dN_b}{dt} = \beta \lambda_a N_a - \lambda_b N_b \quad (2)$$

where N_a and N_b represent the number of ^{241}Pu and ^{241}Am nuclei present at time t ; λ_a and λ_b are the corresponding nuclear decay constants (the probability that a nucleus will decay per unit time, assumed constant); and β is the branching ratio for beta decay of ^{241}Pu .

Re-arranging the relation for N_b and solving by the well known Integrating Factor method yields the explicit time dependence of the number of ^{241}Am nuclei:

$$N_b(t) = \beta N_a(0) \frac{\lambda_a}{\lambda_a - \lambda_b} [e^{-\lambda_b t} - e^{-\lambda_a t}] + N_b(0) e^{-\lambda_b t} \quad (3)$$

where $N_a(0)$ and $N_b(0)$ are the number of ^{241}Pu and ^{241}Am nuclei, respectively, present at time $t = 0$.

Because $\lambda_a < \lambda_b$ for the $^{241}\text{Pu}/^{241}\text{Am}$ system, as ^{241}Pu decays the amount of ^{241}Am rises to a peak before beginning to drop.

In terms of atomic mass, rather than nuclei number, we have:

$$m_b(t) = \beta \frac{A_b}{A_a} m_a(0) \frac{\lambda_a}{\lambda_a - \lambda_b} [e^{-\lambda_b t} - e^{-\lambda_a t}] + m_b(0) e^{-\lambda_b t} \quad (4)$$

where we have introduced the symbols A_a and A_b to represent the molar masses of ^{241}Pu and ^{241}Am respectively.

The total thermal power, $W(t)$, from a plutonium item, corrected for all other heat contributions other than ^{241}Pu and ^{241}Am (for example ^{238}Pu , if present in an appreciable amount, may be the only other contributor with a significant time dependence over a period of experimental observation of a few years or so) may now be written as the sum of the contributions coming from the decay-corrected initial masses plus the contribution of ^{241}Am in-growth:

$$W(t) = P_a m_a(0) e^{-\lambda_a t} + P_b m_b(0) e^{-\lambda_b t} + P_b \beta \frac{A_b}{A_a} m_a(0) \frac{\lambda_a}{\lambda_a - \lambda_b} [e^{-\lambda_b t} - e^{-\lambda_a t}] \quad (5)$$

where P_a and P_b are the specific thermal powers of ^{241}Pu and ^{241}Am respectively. We are assuming time $t = 0$ is known for the purposes of these expressions and is not measured from some arbitrary moment or from the time of chemical separation, but from the instant $m_a = m_a(0)$ and $m_b = m_b(0)$.

The time dependence is seen to be the sum of two decaying exponential terms. Explicitly, re-arranging the expression for $W(t)$ gives:

$$W(t) = P_b m_a(0) \left[\beta \frac{A_b}{A_a} \frac{\lambda_a}{\lambda_a - \lambda_b} + \frac{m_b(0)}{m_a(0)} \right] e^{-\lambda_b t} - P_b m_a(0) \left[\beta \frac{A_b}{A_a} \frac{\lambda_a}{\lambda_a - \lambda_b} - \frac{P_a}{P_b} \right] e^{-\lambda_a t} \quad (6)$$

which, in a convenient and obvious short-hand notation, we write as:

$$W(t) = C_b e^{-\lambda_b t} - C_a e^{-\lambda_a t} \quad (7)$$

Let us now place these expressions explicitly in the context of the ^{241}Pu - ^{241}Am system. The branching ratio β and the ratio A_a/A_b are both close to unity and so the term $\beta \frac{A_b}{A_a} \frac{\lambda_a}{\lambda_a - \lambda_b}$ is determined mainly by the factor $\frac{\lambda_a}{\lambda_a - \lambda_b} = \frac{1}{1 - \tau_a / \tau_b}$ where we have introduced τ_a and τ_b to denote the half-life of ^{241}Pu and ^{241}Am respectively, and which have values of roughly 14.3 years and 432 years. Thus, the term $\frac{A_b}{A_a} \frac{\lambda_a}{\lambda_a - \lambda_b}$ is close to unity with a value of about 1.03. In the special case of complete chemical stripping of ^{241}Am at time $t = 0$ we have $\frac{m_b(0)}{m_a(0)} = 0$. The ratio of specific thermal powers is in the ratio of the half-lives and the decay energies, that is $\frac{P_a}{P_b} \approx \frac{5.8 \text{ keV} / 14.3 \text{ y}}{5500 \text{ keV} / 432 \text{ y}} \sim 0.032$. Therefore, we expect the term C_b to be about 3% larger than C_a , which we shall later see confirmed in Jordan's calorimetry data. With the stated initial conditions we also have the relation:

$$\frac{P_a}{P_b} = \beta \frac{A_b}{A_a} \frac{\lambda_a}{\lambda_a - \lambda_b} \left(1 - \frac{C_a}{C_b} \right) \quad (8)$$

From this expression, we see that if P_b is well known we can extract P_a given the branching ratio and half-lives combined with the measured ratio of the temporal fitting parameters C_a/C_b . To first order, and as we shall see later, the ratio P_a/P_b is about 0.03.

Another and more direct approach to estimating P_a for calorimetric data over time is to note that at time $t = 0$, $W(t) = W(0) = P_a m_a(0)$ from which we have:

$$P_a = \frac{C_b - C_a}{m_a(0)} \quad (9)$$

The use of this result does not require P_b nor does it need any other nuclear data parameters to be known. The fitting parameters C_a and C_b are, of course, correlated through the fitting procedures and so, in

propagating the experimental uncertainty, we have for the variance $\sigma^2[P_a]$ in P_a the following first order estimator in terms of the contributory standard deviations and covariance:

$$\sigma^2 [P_a] = \left(\frac{\sigma [C_a]}{m_a(0)} \right)^2 + \left(\frac{\sigma [C_b]}{m_a(0)} \right)^2 - \frac{2 \text{cov} [C_a, C_b]}{m_a(0)^2} + \left(P_a \frac{\sigma [m_a(0)]}{m_a(0)} \right)^2 \quad (10)$$

For purposes of illustration only, suppose we start with 1 g of pure ^{241}Pu at time $t = 0$ then, adopting the following values [4, 6]: 1 year = 365.25 days; $\beta = 0.9999755$; $\tau_a = 14.348$ years; $\tau_b = 433.6$ years; $P_a/P_b \approx 0.02988$, $C_b/C_a \approx 1.03185$, we find by numerical calculation that the power output increases almost linearly initially, before peaking (at ~ 95.2 mW) after about 72.3 years. The behavior over a five year period of observation is shown in Figure 1, this puts into context the measurements of Jordan, which will be discussed in the next section. We note that increasing the half-life of ^{241}Pu in this calculation from 14.348 years to 14.448 years results in a power drop of only 0.57% at the end of five years. Although apparently only a relatively small change, nuclear calorimetry is capable of an accuracy (combined precision and bias) of a fraction of 0.1%, and so in principle this change is ten or more standard deviations and is, therefore, a quite significant increment to high accuracy calorimetry measurements.

For the present discussion we focused explicitly only on the heat generated by ^{241}Pu and ^{241}Am , as this is the normal safeguards view point. However, for completeness we have also used decay tables to estimate the decay heat and the temporal evolution of the entire decay chain when one starts with pure ^{241}Pu . We find that the only other nuclide of significance is ^{237}U . In Figure 2 we show that the contribution is small ($< 0.1\%$ after 0.3 years) but, in the context of high accuracy nuclear calorimetry measurements, should not be ignored. We cannot address this problem further with the limited data, which we are about to discuss, but it is something to take note of for future standards work. The impact would be amenable to numerical simulation if the detailed structure of the data set was to become available.

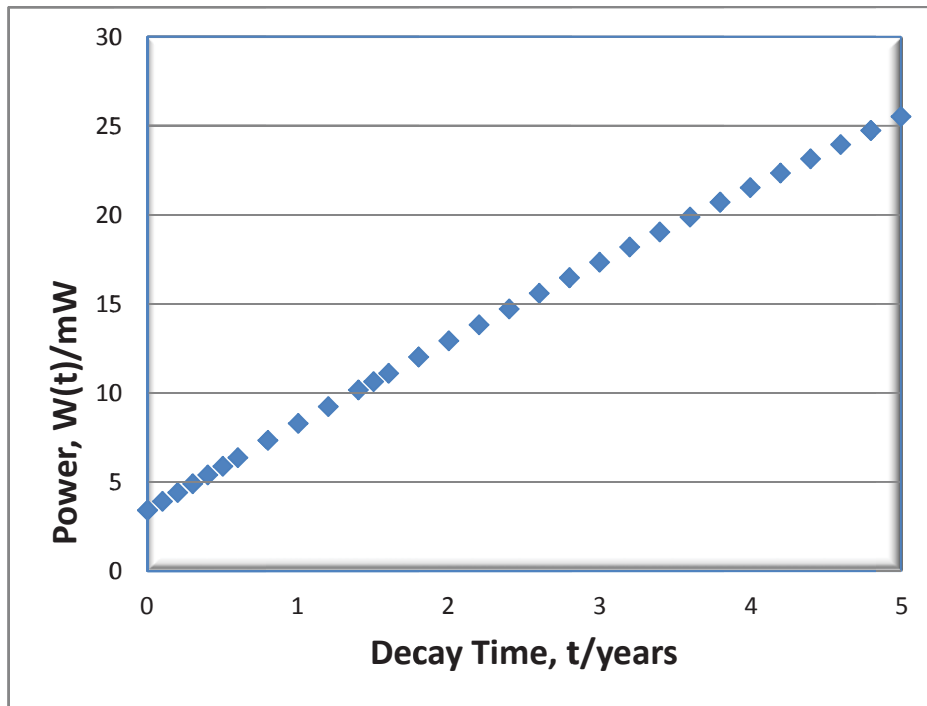


Figure 1: The temporal variation of the total power output for a ^{241}Pu - ^{241}Am system, starting at time $t = 0$ as pure ^{241}Pu , calculated for illustrative purposes using the assumed nuclear data values discussed in the main text.

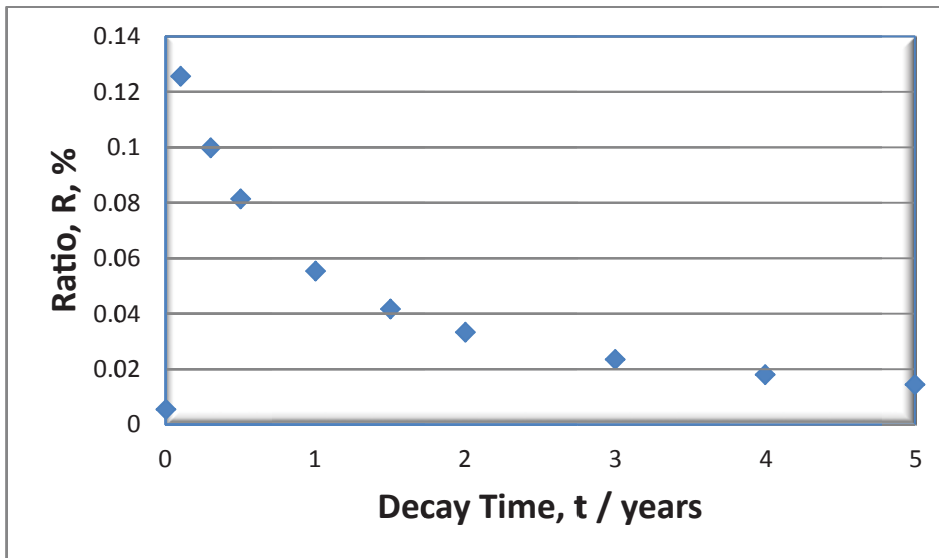


Figure 2: Ratio to the total of the thermal power from nuclides other than ^{241}Pu and ^{241}Am as a function of time starting out with pure ^{241}Pu .

3. Jordan's general approach

In this section, we draw heavily on Jordan's unpublished notes [7] and supporting work [8] to outline his approach to determining the half-life of ^{241}Pu . The period covered is

April 1969 to 24 June 1974. Two items and three calorimeters (designated 58, 91 and 116) were used. Details of the items are listed in Table 1. The second item was loaned from AEC and returned in 1973.

Source	^{241}Pu abundance, %	^{241}Pu mass, g	Separation date
1	84.11	1.511	21 March 1969
2	94.65	13.295	17 June 1969

Table 1: Summary of the ^{241}Pu samples used by Jordan [7].

From each power measurement the thermal power (wattage) of the other isotopes of plutonium were subtracted based on the known total mass of plutonium and isotopic composition. The remainder, which is the sum of the power from ^{241}Pu and ^{241}Am as discussed in the Mathematical Framework section, was fitted by least squares to the sum of two decaying exponentials where C_a , C_b and λ_a are the unknown parameters and λ_b , the decay constant of ^{241}Am was set at 0.0000043738 per day, which is equivalent to a half-life of 433.9 years. The tools and techniques used by Jordan to review and fit his data are not known to us. Data analysis remains a powerful scientific art today, but the scientific literature tells us that uncertainty estimates are often overly optimistic. Workers should be encouraged to archive and report sufficient data to allow data reduction to be revisited. However, as in the historical case we are reviewing here, such information is sadly not always available.

After more than 600 individual power measurements, over a period of more than four years, the results summarized in Table 2 were obtained.

Sample	Calorimeters	Half-life, years
2	116	14.344 ± 0.0023
2	58	14.380 ± 0.010
1	91 & 116	14.356 ± 0.011

Table 2: Summary of the half-life results obtained by Jordan. The uncertainty quoted is the 'internal probable error' (50% confidence limits).

After analyzing the data in many different ways, Jordan concludes that the 'best' half-life supported by the measurements is (14.355 ± 0.005) years, where the uncertainty quoted is the 'probable error' expanded to include some possibility of external (which we take to mean non-random) uncertainty. It is our understanding that the probable error corresponds to a confidence interval of 50%. For a random sample from an infinite normally distributed 'universe' this would correspond to 0.6745 times the standard deviation (68.26% confidence). Jordan comments [7] that even extreme errors of 100% in the mass spectrometry values of the other isotopes (^{238}Pu , ^{239}Pu , ^{240}Pu and ^{242}Pu) have very little impact, only changing the ^{241}Pu half-life extracted by a maximum of 0.003 years. An uncertainty of three years in the assumed value of the half-life of ^{241}Am causes a shift in the ^{241}Pu half-life of only 0.0033 years. At the time of Jordan's work, the half-life of ^{241}Am was well determined from power measurements to be about 432.6 years with an uncertainty of about 0.7 years [9], and so a three year allowance is considered generous. Likewise, the Mound group [10] knew the half-life of ^{238}Pu (87.77 ± 0.02) years, the only other nuclide present with a short period, from studies to evaluate the suitability of various radionuclides for use as heat sources [8], and the group were established masters of applying the nuclear calorimetric method to determine half-life and specific powers.

Based on this discussion, it is clear that the major source of uncertainty in Jordan's determination of the half-life of ^{241}Pu is the calorimetric precision and bias. This is a consequence of the fact that, in a sense, the half-life of ^{241}Pu is determined mainly by the rate of in-growth of ^{241}Am . Furthermore, over a few year time period, this rate of change is affected very little by the other isotopes, which have relatively long half-lives compared to ^{241}Pu . In the case of ^{238}Pu (the next shortest lived) it is also important that it is not very abundant. Another factor is that the method of extracting the half-life of ^{241}Pu does not require the date of separation, nor the degree of separation, to be known.

In addition, from the fitted coefficients C_a and C_b and the weight and isotopic composition of the plutonium items, Jordan was able to calculate the quantities listed in Table 3. These are presented here without justification because adequate detail is not available in Jordan's surviving notes for the uncertainty analysis to be repeated, and unfortunately covariance information is not provided along with the fitted parameters.

Writing in June 1974, after the larger of the two sources had been returned to AEC, Jordan states that the intention was to continue making calorimetric assays of source number 1, the smaller of the two studied, but that no significant reduction in the experimental uncertainty could be expected for several years. We do not know whether this follow-up work was done or not from the records we have access to.

Quantity	Value
^{241}Am half-life	(434.9 ± 0.04) years
Specific thermal power of ^{241}Pu	(3.390 ± 0.002) mW.g ⁻¹
Mean beta energy from ^{241}Pu decay	(5.53 ± 0.04) keV
C_a /mass (with time $t = 0$ being the known time of chemical separation of ^{241}Am)	0.114830 W.g ⁻¹
C_b /mass (with time $t = 0$ being the known time of separation)	0.118220W.g ⁻¹

Table 3: Additional quantities extracted from Jordan's analysis of the ^{241}Pu sample power measurements

4. Review of the ASTM recommendations

The ANSI N15.22-1987 standard on calorimetric assay of Pu-bearing solids is no longer updated and ASTM now maintains the consensus international standard test method on nuclear calorimetry for plutonium, tritium, and ^{241}Am materials. The two data sections are similar. The specific power of ^{241}Pu cannot be calculated accurately and must be measured directly because the mean beta-particle energy is not well known. The value of the specific power of ^{241}Pu adopted in ASTM C1458 is credited to Jordan [unpublished 1982] and is (3.412 ± 0.002) mW.g⁻¹, where the uncertainty is estimated at 1σ . By way of independent verification, the calorimetric result of Oetting [11] can be cited

which makes use of the assigned half-life and is corrected for ^{241}Am . The value adopted by Oetting is $(3.407 \pm 0.034) \text{ mW}\cdot\text{g}^{-1}$. The two values agree, but, because Oetting's uncertainty estimate is 17 times larger, it is inconsequential when forming a weighted mean. Thus, in effect Jordan's value stands alone and unchallenged.

The situation regarding half-life is summarized in Table 4. The adopted value is the un-weighted mean stated to be (14.348 ± 0.022) years. Upon closer inspection, however, we find that the standard deviation is 0.021 years (not 0.022) and what we really require is the 'standard error' (that is the uncertainty on the population mean quoted at the 1σ level) rather than the standard deviation on an individual determination. This is a factor of two smaller at about 0.011 if we assume equal weighing for each of the four measurements. However, to get a (double-sided Gaussian) 68.26% confidence interval we should also apply a coverage factor based on the Student's t-distribution for three degrees of freedom. This is a multiplier of 1.197 which leads to a 1σ estimate of about 0.013. Note for a 95% confidence level the multiplier is about 3.2 compared to about 1.96 when the number of degrees of freedom approaches infinity.

Value (years)	Method	Reference
14.379 ± 0.013	Mass Spectroscopy	LANL: March'80
14.34 ± 0.02	Mass Spectroscopy	NBS: Garner'80
14.328 ± 0.018	Mass Spectroscopy	Geel: DeBievre'81
14.345 ± 0.003	Thermal Power vs. Time	Mound: Jordan'82 (unpublished)
14.348 ± 0.022		Adopted

Table 4: ^{241}Pu half-life data taken from ANSI N15.22-1987 and ASTM C1458.

On the other hand, if we take each entry in Table 4 at face value and apply an inverse variance weighted fit, we obtain a markedly different view because Jordan's value is then very heavily weighted compared to the rest (accounting for about 91% of the fractional weight). In this case, we obtain a half-life estimate of 14.3461 years with an internal standard uncertainty (formed solely from the input (known) variances on each experiment) of 0.0029 years, and an external standard uncertainty (based on the weighted square of the deviations from the weighted mean) of 0.0046 years.

These are two very different conclusions, particularly with regards to the uncertainty statements. This reflects the procedural differences in how the data is being used. Put another way, there is likely a sizable uncertainty in our estimate of the uncertainty. Adopting one rather than another is based on the subjective belief about the relative quality of the measurements and especially on whether the reported uncertainties are actually reasonable and fair. The value of Jordan has by far the lowest reported uncertainty and yet suffers from not being published and open to full scientific scrutiny. In this work we have revisited some of

Jordan's unpublished notes leading to a half-life estimate of (14.355 ± 0.0074) years (uncertainty reported at 1σ) in June 1974. Presumably the 1982 value includes additional data and analysis to account for the shift in value and the reduction in quoted uncertainty – but we do not know. The 1982 value is very close, however, to that reported in Table 2 for item 2 measured using calorimeter 116, but with the uncertainty reported at 68.26% confidence (rather than at the 'probable error' (50% confidence interval)). So it could be that the 1982 choice was simply a selected value. In any case it is long overdue to overhaul the nuclear data parameters included for information in ASTM C1458. The widely used 1996 Table of Isotopes [6] value of (14.35 ± 0.10) years (uncertainty quoted at 1σ) certainly seems conservative in its uncertainty statement compared to experimental capability. The value based on Wellum et al [2, 3], which is approximately (14.325 ± 0.015) years, and that of ASTM (based on the above discussion) which is (14.348 ± 0.013) years are in agreement within the combined uncertainties. But whether reported uncertainties, which are substantially lower, for instance as claimed in Jordan's unpublished work, can be reliably achieved remains open to question. This is important because several well documented measurements of such quality will be needed to convince data evaluators and before we see a substantial reduction in the recommended uncertainty.

5. Conclusions

In recent years, the double-ratio mass spectrometry method has emerged as a powerful and accurate way to determine the ^{241}Pu half-life. The double-ratio technique is believed to be *almost* independent of mass spectrometer instruments, and hence enables measurements to be made on the same batch of homogenized material over a long time period, even though the particular instruments being used may change. It is also clear that the recommended value for the ^{241}Pu half-life in the ASTM standard was never robust and needs revising in the light of currently available and fully documented data [e.g. 2, 3]. Precise half-life determinations with a low bias should also be possible using nuclear calorimetry. In this case, electrical standards or long-lived radionuclide heat sources can be used to maintain absolute power level calibration over many years for a given calorimeter and also between different instruments. However, it is not experimentally established whether nuclear calorimetry is capable of approaching consistent results with a similar overall accuracy to the double-ratio mass spectrometry approach, or, if unrecognized bias in the analysis remains to be discovered (in one or the other or both approaches). We identified the contribution from ^{237}U , which is usually ignored, as an example of a source of possible calorimetric bias. Within the US DOE complex, nuclear calorimetry is primarily used as a routine assay tool. From a radiometry perspective, as our discussion on the ^{241}Pu half-life and specific power

determination has highlighted, calorimetry can also continue to support nuclear data. In particular, to the benefit of both the double-ratio and calorimetry techniques, we suggest an inter-comparison exercise. A batch of plutonium rich in ^{241}Pu should be made, and sealed ^{241}Pu heat sources made for long term (decades) calorimetry. A portion of the same material should be kept and periodically sampled and distributed to various laboratories for mass spectrometry analysis. A program of this kind would also be an important step to maintaining and enhancing vital expertise in these techniques which underpin safeguards measurements. We also see an opportunity to introduce modern curve fitting techniques and approaches to the uncertainty quantification. We strongly urge the community to investigate this possibility with a well-planned international campaign. The same sealed sources can be tracked using high-resolution gamma-ray spectrometry. The nuclear calorimetry data will also yield an estimate of the ^{241}Pu specific power and hence also improve the experimental estimate of the mean energy of the soft beta-ray emitted in the decay, which remains quite poorly known and of interest (along with tritium) to the nuclear physics community, for instance, as a test of nuclear models and as a candidate to study possible variation in specific decay rates to changing environments (chemical, physical, and as the earth moves through space). The full beta-particle spectrum may also be accessible to a suitably designed cryogenic micro-calorimeter (a superconducting, transition-edge, sensor-based, high-resolution spectrometer). The mean energy, power, and half-life are related, so given any two, the third can be calculated.

6. Acknowledgement

This work was supported in part by the U.S. Department of Energy National Nuclear Security Administration, Office of Nonproliferation Research and Development (NA-22).

7. References

- [1] S.K. Aggarwal and H.C. Jain, Half-life of plutonium-241: Past and present, *J. of Radioanalytical and Nucl. Chem., Articles Vol. 109 No.1(1987)183-200.*
- [2] R. Wellum, A. Verbruggen, and R. Kessel, A new evaluation of the half-life of ^{241}Pu , *Journal of Analytical Atomic Spectrometry* 24(2009)801-807.
- [3] S. Croft, T.L. Burr, and A. Favalli, Estimating the half-life of ^{241}Pu and its uncertainty, *Radiation Measurements (In Press)*. Corrected proof of the accepted manuscript is available online: 2-May-2013 DOI information: 10.1016/j.radmeas.2013.04.010. <http://www.sciencedirect.com/science/article/pii/S1350448713002047>
- [4] ASTM C 1458
Standard Test Method for Nondestructive Assay of Plutonium, Tritium and ^{241}Am by Calorimetric Assay, ASTM International, 100 Barr Harbor Drive, West Conshohocken, PA 19428-2959, USA.
- [5] ANSI N15.22-1987, American National Standard for Nuclear Materials ANSI N15.22-1987 (Approved 23 Jan., 1987), Published by the American National Standards Institute, 1430 Broadway, New York, New York 10018.
- [6] R.B. Firestone (Ed.), *Table of Isotopes (8th Edition)*, John Wiley & Sons Inc. (1996). ISBN 0-471-07730-5 (Vol. 1) and ISBN 0-471-14917-9 (Vol. 2).
- [7] Kenneth C. Jordan, Mound Laboratory, Miamisburg, Ohio, USA. Unpublished notes dated 24th June 1974.
- [8] K.C. Jordan, *Calorimetry at Mound Laboratory*, Mound Laboratory report J-121A (1959). Paper presented at the Sixth Tripartite Instrumentation Conference held at Chalk River, Canada, April 20-24, 1959.
- [9] F.L. Oetting and S.R. Gunn, A calorimetric determination of the specific power and half-life of Americium-241, *J. Inorg. Nucl. Chem.* 29(1967)2659-2554.
- [10] W.W. Strohm and K.C. Jordan, Half-lives of the plutonium isotopes and ^{241}Am , *Trans. Am. Nucl. Soc.* (1974)185.
- [11] F.L. Oetting, Average beta energy of plutonium-241 by calorimetry, *Phys. Rev.* 168(4)(1968)1398-1401.

The detection of reactor antineutrinos for reactor core monitoring: an overview

Muriel Fallot

SUBATECH, CNRS/IN2P3, Université de Nantes, Ecole des Mines de Nantes, F-44307 Nantes, France
E-mail: fallot@subatech.in2p3.fr

Abstract:

The field of applied neutrino physics has shown new developments in the last decade. The International Atomic Energy Agency (IAEA) has expressed its interest in the potentialities of antineutrino detection as a new tool for reactor monitoring and has created a dedicated ad-hoc Working Group in late 2010 to follow the associated Research and Development. Several research projects are on-going over the world either to build antineutrino detectors dedicated to reactor monitoring, either to search for and develop innovative detection techniques, or to simulate and study the characteristics of the antineutrino emission of actual and innovative nuclear reactor designs.

The European Safeguards Research and Development Association, ESARDA, has created in late 2010 a group devoted to Novel Approaches and Novel Technologies (NA/NT) allowing to create contacts between the research community and agencies. The ESARDA NA/NT working group has decided one year ago to create a sub-WG dedicated to the detection of antineutrinos. At this 35th ESARDA meeting, we propose to give an overview of the most recent progresses made in the field of antineutrino detection for reactor monitoring, including the actual possibilities and limitations of their detection and the status of various developments towards compact antineutrino detectors for reactor monitoring considered in perspective of the antineutrino emission from various reactor designs. We will then present the objectives of the ESARDA sub-WG devoted to the antineutrino probe.

Keywords: safeguards, non-proliferation, antineutrino detection, nuclear reactors

1. Introduction

The research and Development (R&D) associated to reactor antineutrino detection is very lively. This 35th ESARDA annual meeting has been an opportunity for the antineutrino community to meet in the frame of the NA/NT Working Group (WG) [1]. At this meeting, the proceedings of the last antineutrino detection ad-hoc WG of IAEA (Oct. 2011) has been presented to the attendees, giving the directions that were foreseen by then. After this first part, overview talks focussed on several topics of importance in the field: a

review about each main actual detection technique, a review about reactor simulations, and reviews making the links with other fields strongly connected to the topic: reactor antineutrino detection for fundamental neutrino physics, nuclear physics experiments for reactor antineutrino energy spectra and neutron detection techniques.

In these proceedings we will present the motivations for such a structure of the sub-WG meeting, explaining the context and presenting briefly the different topics of the talks.

Let us first recall briefly the principle of reactor monitoring with antineutrino detection.

Large quantities of antineutrinos are produced in the reactor due to beta decays of the fission products and about 10^{21} antineutrinos/s are emitted by a 1 GWe reactor core. The distribution of fission fragments depends on the fissile isotopes (^{235}U , ^{238}U , ^{239}Pu and ^{241}Pu) and on the energy of the neutrons in the core. The released energy per fission, the average number of emitted antineutrinos and their average energy depend also directly on the fissile isotope that undergoes fission (see Table 1). Consequently, an antineutrino spectrum measured at a reactor will reflect the thermal power emitted by the core and its composition. Adding to these features the intrinsic properties of antineutrinos which are weakly interacting particles, impossible to shield, the antineutrino detection may then become an interesting tool for reactor monitoring.

	^{235}U	^{238}U	^{239}Pu	^{241}Pu
Released energy per fission (MeV)	201.7	205.0	210.0	212.4
Mean energy of antineutrinos (MeV)	1.46	1.56	1.32	1.44
Number of antineutrinos per fission ($E > 1.8$ MeV)	5.58 (1.92)	6.69 (2.38)	5.09 (1.45)	5.89 (1.83)

Table 1: Differences in the ^{235}U , ^{238}U , ^{239}Pu and ^{241}Pu fission properties given in [2] and a calculation of P. Huber and Th. Schwetz [3].

Considering these properties, the IAEA asked to its member states to perform a sensitivity study. The agency organized several meetings between experts and inspectorates since 2003, and created in 2011 an Ad-Hoc Working Group devoted to the antineutrino detection. This WG

meeting was associated to an Antineutrino Applied Physics Workshop [4] and a proceedings was written and circulated [5]. The content of the proceedings has been presented by A. Bernstein for the first time to the R&D community and to ESARDA and IAEA members at our next ESARDA NA/NT WG meeting on May 27. The proceedings give indications of directions for the research to come on the path to use antineutrino detection for reactor monitoring and potentially for safeguards.

An antineutrino detector should be as compact as possible, cheap, safe, unattended and remotely operated and the data analysis should be performed in a nearly automated way in order to be usable by inspectorates. The optimum situation of an antineutrino detector would be above ground just outside a reactor building.

These requirements remain a challenge for physicists. A cubic meter size footprint for an antineutrino detector placed at about 25m from a reactor core is feasible, but one has up to now to add shieldings around the detector in order to get rid of cosmic ray or reactor induced background, and the shielding may enlarge a lot the footprint, though efforts have been made to include passive shielding into a container so as to leave unchanged the overall footprint. At the moment eliminating the shielding seems to be very challenging in the case of a detector located above ground. But as you will see in the following, the on-going developments show promising improvements in background rejection efficiency by an antineutrino target.

2. Main antineutrino detection techniques

The most common interaction used to detect reactor antineutrinos is the inverse beta decay (IBD) process on proton: $\bar{\nu}_e + p \rightarrow e^+ + n$ (threshold: 1.8 MeV). Up to now liquid scintillator targets were used as the standard detection technique, usually doped with Gd in order to capture the emitted neutron. The positron energy is directly related to the antineutrino energy. After a neutron capture, the excited Gd isotope emits a gamma cascade of total energy 8 MeV detected in a delayed coincidence (delayed signal) (in average 30 μ s) with the positron signal (prompt signal). This technique was used extensively by numerous fundamental neutrino physics experiments. The quality of the liquid scintillator doped with Gd has been the object of an important R&D and the new generation reactor experiments Double Chooz, Daya Bay and Reno use this method [6-8]. But one could replace Gd with other nuclei exhibiting large neutron capture cross-sections such as ${}^6\text{Li}$ and ${}^{10}\text{B}$. The advantages of these nuclei is that neutron capture gives birth to heavy nuclei which can be distinguished from gamma rays through Pulse Shape Discrimination techniques (PSD): $n + {}^6\text{Li} \Rightarrow \alpha + {}^3\text{H}$ and $n + {}^{10}\text{B} \Rightarrow {}^7\text{Li} + \alpha$ (6%) and ${}^7\text{Li} + \alpha + 0.48$ MeV (94 %). These neutron captures occur for neutrons less thermalized than in the case of neutron capture on Gd isotopes leading to a shorter

path of the neutron in the detector. This opens the possibility of more compact detectors and maybe to relate with a better accuracy the neutron direction to the impinging antineutrino direction [9]. Unfortunately liquid scintillators doped with ${}^6\text{Li}$ are not yet stable enough and R&D is ongoing to develop new liquids [10]. The actual alternative is to use solid plastic detectors using ${}^6\text{Li}:\text{ZnS}$ layers as we will see in the next section.

In order to comprehend the interests of the various detection media, one has to understand the possible background signals that could blur the antineutrino one. Cosmic rays constitute a recurrent background source, independently of the type of reactor to monitor. Usually fundamental neutrino physics experiments eliminate an important part of this background with underground deployments, allowing large overburdens. Even at shallow depth the hadronic part of the background is eliminated, while remain cosmic muons mainly. These cosmic muons are at the origin of Michel electrons, fast neutrons and cosmogenic nuclei i.e. radioactive nuclei, both created through electromagnetic spallation or muon capture processes in the matter. Let's classify the backgrounds in two categories: the accidental background which mimics the antineutrino signal through random coincidences between for instance gamma rays from natural radioactivity of the rock or materials and fast neutrons arising from the cosmic muons; and the correlated background which mimics the antineutrino signature with a prompt and a delayed signal arising from the same physics event. Fast neutrons can constitute a correlated background if they are moderated in the detection medium on protons which recoil limit the positron energy loss before being captured on the chosen absorbant (Gd or else). Cosmogenic isotopes which are beta-delayed neutron emitters can also be a source of correlated background. With above ground deployments, one has in addition to cope with the hadronic part of the cosmic rays i.e. mainly neutrons.

Different methods can be developed to help distinguishing between the background and antineutrino events. Antineutrino detectors should use low radioactivity materials to minimize accidental background. Lead shielding is also used around the antineutrino target to decrease the gamma ray background, which can be very strong at very short distance of a research reactor. Borated polyethylene shielding is used to decrease the neutron background reaching the target. Then usually the target detectors are complemented with an active cosmic muon veto detector, allowing to tag a muon interaction and preventing to measure events in a definite time window following the muon signal in the veto. In addition Pulse Shape Discrimination technique is used, especially with liquid scintillator targets, with the goal to distinguish neutron from gamma signals. Different target media can also be used to eliminate some background components.

The actual main techniques use these different methods at a different level: liquid scintillator based detectors, solid plastic based detectors and water based detectors [11].

2.1 Liquid scintillator based detectors

The liquid scintillator technique doped with Gd is the most mature detection technique employed for several decades. The properties observed in large detectors designed for fundamental physics are nevertheless hard to transpose to small scale detectors as edge effects combined with a limited number of PMTs affect the energy and spatial resolution one can obtain. The first demonstration of antineutrino detector for reactor monitoring was made by the SONGS experiment [12] with a very simple detector of modest detection efficiency that took data unattended for about one year. Since then, efforts have been concentrated towards an optimization of the detector performance with different designs. According to the simulation work developed to design small scale detectors, the energy resolution can be very good and the detection efficiency as well, depending on the size and number of PMTs used. In order to optimize the background rejection, the use of PSD is mandatory, especially for above ground deployments. Up to now high performance detectors still require shieldings and a cosmic muon veto around the target which increase a lot the detector footprint. There are several on-going efforts worldwide with different goals; SONGS2 (3.6 t detector) at a CANDU reactor in Point Lepreau Canada [11,13], the KASKA prototype first installed at the JOYO fast reactor and now installed above-ground at a PWR (with an on-going PSD R&D) [14], the Nucifer detector at the OSIRIS research reactor in France [15] (with an on-going PSD R&D and the goal of an optimized efficiency).

2.2 Solid plastic based detectors

An alternative to liquid scintillator target detectors is the use of solid scintillators. The use of solid scintillators prevents the safety problems that could arise from the use of liquids of rather low flash points. Another advantage is the possible segmentation of the detector. The segmentation ensures naturally a very good spatial resolution and allows further background elimination thanks to multiplicity cuts. A set of projects develops segmented plastic concepts with Gd layers on slabs, either read by PMTs or MPPCs with fibers: the DANSS (Russia) [11,13], CORMORAD (Italy) [16] and the PANDA (Japan) [11,13] experiments. All three experiments have deployed prototypes at reactors. In these designs, the searched prompt and delayed signals are still produced by photons (use of Gd sheets) and distinguished with an energy cut helped by the topology of the events. If we refer to the DANSS collaboration predictions for their design [11,13], the energy resolution is not as good as in liquid scintillator designs, but the spatial resolution is much better and the detection efficiency could be quite high. No full scale detector has taken data yet, so these figures should be confronted to experimental

measurements before drawing any conclusions. The full scale DANSS detector is under construction and should bring new results in the very next years. Results will be presented at the ESARDA NA/NT meeting in Bruges [11].

Another possibility is the use of solid segmented plastic detectors with ${}^6\text{Li}:\text{ZnS}$ layers instead of Gd sheets. The use of ${}^6\text{Li}$ allows the identification of the neutron through PSD information and the segmentation gives a precise location of the interaction. The neutron is captured after a lower energy loss in ${}^6\text{Li}$ than in Gd, its range is thus shorter. This opens a potentiality for more compact detectors, and direction sensitive measurements.

The Sandia lab. in collaboration with LLNL have already tested a 4-cell prototype with organic scintillator and $\text{ZnS}:\text{Ag}/{}^6\text{LiF}$ screens on outer surface at the San Onofre power station in 2011. The ability of such a design to reduce background thanks to the topology of the events was demonstrated. In Europe, the SOLiD collaboration has developed a different design using fibers for the light collection and MPPCs with electronics inherited from T2K [15,17]. A small prototype is being deployed at the BR2 reactor in Mol (Belgium), and the full scale detector should be built during the upcoming years. These developments will allow to appreciate the real quantitative improvements of this approach which seems to be very promising.

2.3 Water based detectors

Another way to eliminate background is to choose another detection medium, like water detectors in which GdCl_3 is dissolved. In these detectors, the detection reaction is still the IBD process. The prompt signal is provided by the Cerenkov light of the created positron in the water, and the delayed signal by the photons coming from the deexcitation of the Gd isotope after neutron capture. Only the particles generating a Cerenkov signal can be detected. This induces a quite high energy threshold on the reactor antineutrino detection [18] but also allows to eliminate a large part of the fast neutron background as neutrons of energy lower than 500 MeV cannot be detected (because of the recoil proton Cerenkov threshold).

R&D is on-going as there are plans to fill in large detectors for fundamental neutrino physics [18]. Two initiatives of such detectors developed for safeguard purposes exist; the Brazilian project ANGRA and the water detector deployed by LLNL at the San Onofre power station.

The construction of the ANGRA detector is nearly finished and the detector should be deployed above ground before the end of this year [11,13]. The detector of the LLNL is deployed above ground and the data taken are under analysis. The drawback of the water detectors is the impossibility to identify particles and a poor energy resolution. But these detectors are inherently safe thanks to the use of water.

2.4 Comparative properties

One objective of the next antineutrino detection sub-WG group meeting in Brugge is to show the results of these various experiments but also to try to find common ways to quantify the detection properties. We need to agree on common definitions of quantities to qualify the detector performances. This is mandatory to allow comparisons helping leading the further required R&D. This is also mandatory to be able to use the detector performances in the study of diversion scenarios, coupling reactor simulations to detection scenarios. These scenarios can also help leading the R&D by characterizing what are the detection properties to be improved in order to meet the required sensitivity on the fuel composition of various reactor types.

3. Reactor simulation initiatives

Several reactor simulation developments for reactor monitoring with antineutrino detectors are on-going worldwide. The first initiative came from the Double Chooz collaboration with the development of a simulation tool, the MCNP Utility for Reactor Evolution (MURE) code [19] and first scenarios involving PWR and CANDU reactors [20]. Since then several groups study diversion scenarios taking into account reactor physics constraints. The latter point is mandatory because these reactor physics constraints may eliminate de facto some scenarios that would be impossible to realize for safety reasons inherent to the operation of a reactor core. These reactor physics constraints influence also the results of a given scenario as the fission rate variations due to a fissile material diversion may be restricted by constraints on the maximal variation of the multiplication coefficient of the core or the fuel composition may be constrained by the minimum required delayed neutron fraction...

To study whether an antineutrino detector of a footprint of a cubic-meter would reach an accuracy sufficient to detect a "significant" diversion in a "timely" fashion, the studied scenarios usually adopt the following IAEA definitions: a significant quantity would be of 8 kg of plutonium to be detected in the timeliness of 3 months.

IAEA is interested in knowing the response of an antineutrino detector associated to a lot of reactor designs and cases. Among the main ones, are the on-load reactors (CANDU but also Gen-IV Pebble Bed Reactors), the main Gen-IV designs, and the capability to distinguish various fuel compositions, like UO_x vs MOX fuels or innovative fuels (including standard fuel burnt in non thermal reactors).

Several studies are on-going and will be presented at the ESARDA NA/NT WG meeting [21].

A common methodology animates the following studies: first checking the modelled reactor physics using most of the time benchmarks, then check the feasibility of the

considered scenarios under reactor physics constraints and check the interest of the scenario for safeguards (quality, quantity of the diverted materials). The last step is to analyse the probability of detection of the diversion using statistical tests, provided a number of hypotheses on the detector location, size, detection efficiency...

A study is on-going at Georgia-Tech and LLNL to see if antineutrino detection could help monitoring the irradiation of plutonium-based 'MOX' fuel to ensure the material is hard to recover without reprocessing [22]. Two reactor designs are under study, using MCNPX and the CINDER evolution code: a Westinghouse-type PWR with partial MOX loading (most common on the US side) and the Fast reactor BN-600 with partial and full MOX loading (Russian side). The relation between the hypothetical detected antineutrino signal with the burnup is under study. Diversion scenarios of replacement of assemblies by LEU or dummy assemblies are also under study.

Recent results obtained with the MURE code were presented recently [23]. Scenarios for a PBR (Pebble Bed Reactor) and a sodium-cooled FBR (Fast Breeder Reactor) have been studied. These reactors are Gen IV reactors, presenting issues for safeguards purpose: a PBR is an on-load refuelling reactor, easing the withdrawal of plutonium of good quality, while FBR can, by definition, build-up plutonium.

Sophisticated statistical methods inherited from fundamental neutrino physics calculations are also being used to compute the sensitivity of the antineutrino probe to the fuel content [24]. These calculations rely on assumptions made on the detector size, location, performance, but also on the reactor power. They were not yet coupled to realistic reactor simulations but one could imagine to do so in a near future as the statistical tests constitute the ultimate steps of the study of scenarios. One outcome of these studies is the limitation of the sensitivity of the antineutrino probe due to the actual uncertainties associated to the reactor antineutrino spectra [24]. This opens a natural link between our problematics and nuclear physics as the antineutrinos are emitted in the beta decays of the fission products.

4. Links with other physics fields

An important work has been performed recently to investigate the existing methods to compute the antineutrino energy spectra associated to the main isotopes contributing to the fissions in a Pressurized Water Reactor i.e. ^{235}U , ^{239}Pu , ^{238}U and ^{241}Pu . The method developed by Schreckenbach et al. to convert the reference ILL integral beta spectra [25] was revisited leading to a normalisation shift of the newly obtained spectra upward by 3 % [26-28]. In parallel, the method relying on the summation of all the beta decay branches of the fission products was revisited as

well, taking benefit from the huge quantity of nuclear data available nowadays [26, 29], coupled to the MURE code. These works led to new synergies of our problematic with fundamental neutrino research on one hand with new experiments at reactors aiming at evidencing potential sterile neutrinos [30] and with nuclear physics measurements on the other hand to improve our knowledge of the reactor antineutrino spectra [29,31].

4.1 Nuclear Physics

The antineutrino spectrum associated with one of the 4 fissioning isotopes in a moderated reactor can be computed as the sum of the contributions of all fission products thanks to the use of the full information available per nucleus in nuclear databases. This so-called summation method is useful on several aspects. Not only it is the only one adapted to the computation of the antineutrino emission associated to various reactor designs, but also it allows the computation of antineutrino spectra for which no beta spectrum was measured so far. Moreover it is one of the only alternatives to the ILL data whilst takes into account off-equilibrium effects and allows to work with different energy binning of interest for reactor neutrino experiment analyses.

Lately, new summation method calculations of the antineutrino energy spectra arising after the fissions of the four main fissible isotopes $^{235,238}\text{U}$, and $^{239,241}\text{Pu}$ in PWRs were obtained. The new calculations include the recently measured beta decay properties of the $^{102;104;105;106;107}\text{Tc}$, ^{105}Mo , and ^{101}Nb nuclei, that were suspected to suffer from the Pandemonium effect [31]. These beta feeding probabilities, measured using the Total Absorption Technique (TAS) at the JYFL facility of the University of Jyväskylä, have been found to play a major role in the gamma component of the decay heat for ^{239}Pu in the 4-3000 s range [31]. Following the fission product summation method, the calculation was performed using the MURE evolution code coupled to the experimental spectra built from beta decay properties of the fission products taken in evaluated databases. These latest TAS data are found to have a significant effect on the Pu isotope energy spectra and on the energy spectrum of ^{238}U . It has thus been shown that the Pandemonium effect plays a major role in the estimate of the antineutrino spectra [29]. TAS measurements can allow to improve drastically the prediction ability of these spectra. Moreover, independent evaluations of the reactor spectra could provide new constraints on the potential existence of sterile neutrinos but require a complete error calculation associated to the summation method spectra.

4.2 Neutrino Physics

As quoted above, the recent re-computation of the reactor antineutrino spectra has motivated a new search for sterile neutrinos at reactors with short baseline experiments [26-28]. Most of the projects quoted above are mainly

motivated by safeguards, but have added a fundamental physics part to their physics case. Conversely, new projects aiming at measuring sterile neutrinos at reactors could bring new detection and sensitivity information valuable for non-proliferation. In addition to the projects already quoted above, one can quote the following projects: SCRAAM (LLNL US), Neutrino4 (Russia), POSEIDON (Russia), HANARO (Korea), and STEREO (France) [30].

A review will be presented at the ESARDA NA/NT meeting, with emphasis on the possible synergy with reactor monitoring using antineutrino detection [21].

In addition to these projects, large detectors deployed at power plants measuring the θ_{13} mixing angle, Double Chooz, Daya Bay and Reno, can bring new results regarding the antineutrino probe. First the R&D performed in the frame of these fundamental physics experiments triggered some of the R&D made for neutrino applied physics.

Secondly, their near detector measurements will provide sensitivity limits for probing the fuel content of a power reactor core when combined with the associated reactor simulation and operation parameters. In this frame, a detailed full-core simulation of the Chooz PWRs, the most common reactor design in the world, has been successfully developed last year with the MURE code in order to compute their antineutrino emission for the Double Chooz experiment [6, 32]. These simulations will be compared during the second phase of the Double Chooz experiment with the near-detector data, giving a limit to the sensitivity on the fuel composition and reactor power that antineutrino detection could bring. A careful estimate of the fission rate systematics has been done and could allow to maintain the error associated to the antineutrino prediction as low as 1.7% [32]. This simulation is the first realistic simulation of a reactor core performed in the frame of a reactor antineutrino experiment. This constitutes a key step of the studies of the detection of antineutrinos for non proliferation purpose as it will enable us to evaluate the sensitivity of this probe thanks to its accuracy. This validation is all the more important as we are moving toward an integrated tool (detector + simulation) for our non proliferation effort. Thirdly, the near detector measurements may constrain the value of the weak magnetism term entering in the antineutrino spectrum calculation. This term is subject to large uncertainties akin to affect the normalisation of the antineutrino spectra [27].

4.3 Neutron Detection

As we have seen in the first sections of these proceedings, the detection of a reactor antineutrino is signed by a delayed coincidence between the signals created by a positron and a neutron. There is thus obviously strong synergies between antineutrino detector and neutron detector R&D. For instance some segmented plastic detector designs quoted above have led to detectors that

could possibly replace ^3He counters. The STUK develops a design of neutron detector combining plastic scintillator and ^{10}B . We can also quote the scintilla project which aims, among other objectives, at developing alternative techniques to ^3He counters to detect low energy neutrons [33]. We thus have to create bridges between the two research communities which should allow to improve neutron and antineutrino detection efficiencies and share ideas [21].

5. Conclusions and outlooks

In these proceedings, we have attempted to review briefly the main experimental projects on-going for near-field reactor monitoring. Several complementary techniques are employed to reject backgrounds while preserving the antineutrino detection efficiency, either based on different detection media either based on geometrical properties. This large variety of designs is accompanied by a large variety of deployment sites and a lot of results can be expected in the coming two years.

All these research axes are the object of discussions and exchanges between nuclear facility operators, safeguard authorities and researchers in the frame of the sub-working group (WG) devoted to the antineutrino probe of the European Safeguards R&D Association (ESARDA [1]). This sub-WG is part of the NA/NT WG created in 2010 by the ESARDA. The goal of the sub-WG is to establish a roadmap for the development and performances of antineutrino detectors for reactor monitoring. Regular meetings are organized and the last one was held at the occasion of the ESARDA annual meeting in Brugge (Belgium) on May 27, 2013 [1] and is the object of these proceedings. Very interesting discussions were held at this occasion, presenting the proceedings of the first Ad-Hoc WG meeting at IAEA [5, 22], review talks on the on-going studies, but also on the synergies with other physics areas [21]... This material should help the community to draw the roadmap bringing the antineutrino detection on the next level of the Technology Readiness scale [34].

6. Acknowledgements

The author would like to acknowledge Harri Toivonen and Julian Whichello for their support, which makes possible the organization of the next meeting of the antineutrino sub-WG in the frame of the ESARDA NA/NT WG. The author would like to thank in addition all the speakers and all the participants for their participation.

[1] ESARDA NA/NT Working Group Meeting, May 2012, http://esarda2.jrc.it/events/esarda_meetings/luxembourg-2012/index.html. See also the ESARDA BULLETIN, No. 46, December 2011 for the creation of the sub-Working Group devoted to stand-off detection of antineutrinos.

- [2] Kopeikin V. I., Mikaelyan L. A., and Sinev V. V., 1997. *Spectrum of electronic reactor anti-neutrinos*. Phys. Atom. Nucl. **60** (1997) 172.
- [3] Huber P. & Schwetz Th., *Precision spectroscopy with reactor antineutrinos*, Phys. Rev. D **70**, 053011 (2004).
- [4] *Antineutrino Applied Physics Workshop 2011*, Vienna, <http://aap2011.in2p3.fr/Home.html>.
- [5] IAEA Report, *Proceedings of the first meeting of the Ad Hoc Working Group on Safeguards Applications utilizing Antineutrino Detection and Monitoring*, SG-EQGNRL-RP-0002 (2012).
- [6] Abe Y. et al. (Double Chooz collaboration), *Indication for the disappearance of reactor electron antineutrinos in the Double Chooz experiment*, Phys. Rev.Lett. **108**, 131801, (2012).
- [7] An F. P. et al., (Daya Bay collaboration) *Observation of electron-antineutrino disappearance at Daya Bay*, Phys. Rev. Lett. **108** (2012) 171803.
- [8] Ahn J. K. et al. (RENO collaboration), *Observation of Reactor Electron Antineutrinos Disappearance in the RENO Experiment*, Phys. Rev. Lett. **108** (2012) 191802.
- [9] Apollonio M. et al., Phys.Rev. D**61**, 012001, (2000).
- [10] See Kim Y.'s contribution to the Nuclear Data 2013 conference in New York.
- [11] See the review talks at the ESARDA NA/NT WG meeting in Brugge: Lhuillier D. and Furuta H. for liquid scintillator detectors, Vacheret A. and Egorov V. for plastic detectors, Bernstein A. and Anjos J. for water Cerenkov detectors.
- [12] Bowden N. et al., *Experimental Results from an Antineutrino Detector for Cooperative monitoring of Nuclear Reactors*, Nucl. Instrum. Meth. A, vol.572, 2007, p 985-998.
- [13] See the contributions to the *Antineutrino Applied Physics Workshop 2012*, Hawaii, <http://www.phys:hawaii.edu/jgl/AAP/AAP2012.html>.
- [14] Furuta H. et al., Nucl. Inst. and Meth. A **662** (2012) 90-100.
- [15] Cucoanes A.' contribution to the Nuclear Data 2013 conference in New York, *The Nucifer Experiment*, proceedings to be published.
- [16] Battaglieri M. et al., Nucl. Inst. and Meth. A **617** (2010) 209-213.
- [17] Vacheret A. et al., SOLiD experiment proposal to the Institut Laue Langevin PAC, 2013.

- [18] Beacom and Vagins, Phys. Rev. Lett., 93:171101, 2004. See also for instance T. Yano's contribution at the 36th International Conference on High Energy Physics 2012.
- [19] MEPLAN O. et al., MURE: MCNP Utility for Reactor Evolution, ENC Proceedings, Versailles (2005). <http://www.oecd-nea.org/tools/abstract/detail/nea-1845>.
- [20] Fallot M. et al. *Estimated sensitivity of the antineutrino probe for future reactor monitoring*, Proc. Of the INMM's 53rd annual meeting, Orlando, Florida (2012).
- [21] See the review talks at the ESARDA NA/NT WG meeting in Bruges: A. Erickson and M. Fallot for reactor simulations, Algora A. and Fallot M. for the link with nuclear data, P. Huber and A. Cucoanes for the link with fundamental neutrino physics and Toivonen H. for the synergy with neutron detection.
- [22] See Bernstein A.'s contribution at AAP 2012 and Erickson A.'s contribution at this NA/NT meeting.
- [23] See Cormon S.'s contribution to the Nuclear Data 2013 conference in New York, *Determination of the Sensitivity of the Antineutrino Probe for Reactor Core Monitoring*, proceedings to be published.
- [24] See Huber P.'s contribution to the Nuclear Data 2013 conference in New York, *Nuclear Data in the theta13 measurement by the Daya Bay experiment*, proceedings to be published.
- [25] Hahn A. A. et al., *Antineutrino Spectra From ^{241}Pu and ^{239}Pu Thermal Neutron Fission Products*, Phys. Lett. B218, 365 (1989) and references therein.
- [26] Mueller Th. A. et al., *Improved Predictions of Reactor Antineutrino Spectra*, Phys.Rev. C 83, (2011) 054615.
- [27] Huber P., *Determination of antineutrino spectra from nuclear reactors*, Phys. Rev. C 84, 024617 (2011) and erratum [Phys. Rev. C 84, 024617 (2011)].
- [28] Mention G. et al., *Reactor antineutrino anomaly*, Phys. Rev. D83, 073006 (2011).
- [29] Fallot M., Cormon S., Estienne M. et al., *New Antineutrino Energy Spectra Predictions from the Summation of Beta Decay Branches of the Fission Products*, Phys. Rev. Lett. 109:202504,(2012). See also Estienne M.'s contribution to the Nuclear Data 2013 conference in New York, *Contribution of recently measured nuclear data to reactor antineutrino energy spectra predictions*, proceedings to be published.
- [30] Abazajian K. N. et al., *Light Sterile Neutrinos: A White Paper*, <http://arxiv.org/abs/1204.5379>.
- [31] Algora A. et al., *Reactor Decay Heat in ^{239}Pu : Solving the γ Discrepancy in the 4–3000-s Cooling Period*, Phys. Rev. Lett. 105, 202501 (2010). See also Algora A.'s contribution to the Nuclear Data 2013 conference in New York, *Total Absorption Study of Beta Decays Relevant for Nuclear Applications and Nuclear Structure*, proceedings to be published.
- [32] Onillon A.'s contribution to the Nuclear Data 2013 conference in New York, *Reactor and antineutrino spectrum calculations for the Double Chooz first phase results*, proceedings to be published.
- [33] The Scintilla European Project, <http://www.scintilla-project.eu/>.
- [34] Toivonen H., *New and Novel Technologies for CTBT Radionuclide Measurement and Analysis*, CTBT Science and Technology 2011, Vienna, June 2011.

Burnup monitoring of VVER-440 spent fuel assemblies

I. Almási, C.T. Nguyen, Z. Hlavathy, J. Zsigrai¹, L. Lakosi and P. Nagy

Centre for Energy Research - Hungarian Academy of Sciences, 29-33 Konkoly-Thege M. u., Budapest, 1121 Hungary
E-mail: istvan.almasi@energia.mta.hu, laszlo.lakosi@energia.mta.hu

¹ Present address: EC, JRC, Institute of Transuranium Elements, Karlsruhe, Germany

Abstract:

This paper reports on the results of the experiments performed on spent VVER-440 fuel assemblies at the Paks Nuclear Power Plant (NPP), Hungary. The fuel assemblies submerged in the service pit were examined by high-resolution gamma spectrometry (HRGS). The assemblies were moved to the front of a collimator tube built in the concrete wall of the pit in the reactor block at the NPP, and lifted down and up under water for scanning by the refueling machine. The HPGe detector was placed behind the collimator in an outside staircase. The measurements involved scanning of the assemblies along their length of all the 6 sides, at 5-12 measurement positions side by side. Axial and azimuthal burnup profiles were taken in this way. Assembly groups for measurements were selected according to their burnup (10–50 GWd/tU) and special positions (e. g. control assembly, neighbour of control assembly). Burnup differences were well observable between assembly sides looking towards the center of the core and opposite directions. Also, burnup profiles were different for control assemblies and normal (working) fuel assemblies. The ratio of the measured activities of Cs-134 and Cs-137 was evaluated by relative efficiency (intrinsic) calibration. Measurement uncertainty is around 3 %. Taking into account irradiation history and cooling time (i. e. the time elapsed since the discharge of the assembly out of the core), the activity ratio Cs-134/Cs-137 shows good correlation with the declared burnup.

Keywords: Cs-134/Cs-137 ratio; high resolution gamma spectrometry; non-destructive assay; spent fuel verification

1. Introduction

Safeguarding spent fuel includes independent verification of fuel parameters such as burnup, cooling time, and fission material contents. Burnup is usually calculated and declared by the operator. Improving the accuracy of the calculation code has a great importance. The objective of this project is to support burnup calculation of spent VVER-440 type fuel assemblies at Paks Nuclear Power Plant (NPP) by an independent experimental method. Most often nondestructive methods are used employing gamma and neutron techniques [1, 2].

On the other hand, burnup data are useful for the assessment of fuel performance in the core as well as for reactor safety and fuel economy considerations. The burnup limit is provided by the supplier of the fuel. For safety reason, this value is to be reduced by the uncertainty of the burnup determination. The limit obtained in this way should be observed during reactor operation. Thus, effective exploitation of the nuclear fuel is limited by the uncertainty of the burnup calculation code. If the uncertainty of calculation were less, the safety margin could be decreased, thus fuel burnup could be raised for more effective fuel use (in addition to introduction of new assembly types and longer refueling period). Producing more power involves burnup increase, otherwise the amount of fuel should be raised thereby worsening the economy.

For verifying burnup calculated from reactor parameters, high resolution gamma spectrometric (HRGS) experiments have started at our institute for assessing the uncertainty of the burnup code used at the NPP. This paper presents a comparison of the measured and simulated values of a quantity found to be in correlation with the burnup; namely the activity ratio of the fission products Cs-134 and Cs-137. Improving the burnup calculation code based on the data presented here will ensue later.

This paper is split up into three parts reporting the experiments. The first section describes the technique used in the experiment, followed by evaluation and results. Finally some conclusions are drawn in context with enhancing the precision of the measurements and its role in refining the correlation between burnup and the activity ratio Cs-134/Cs-137.

2. Experimental

The fuel assemblies were transferred under water to the service pit for measurement. The experimental setup, shown in Fig. 1, was the same as described in an earlier paper [3]. The assemblies were moved to the front of a lead collimator built into the concrete wall of the pit in the reactor block, and moved down and up under water by the refueling machine. The 120 cm long collimator tube was shut on the water side by a 5 mm thick steel plate. Translation and rotation of the assemblies were performed for a full scanning. The distance of the assemblies from the closing plate of the collimator was from 30 to 60 cm in water depending on the activity of

assembly. Gamma spectra were taken by a 46 cm³ coaxial HPGe detector placed behind the collimator in an outside staircase. The collimator enabled the detector to see the whole cross section of the assemblies, in 1 cm height. The remote controlling of a laptop computer was done from the

measurement stand in the reactor hall by another laptop PC controlling the multichannel analyzer in the staircase through a local area network. Measurements were performed at 5-12 measurement positions along each of the 6 sides of the hexahedral prism shape assemblies.

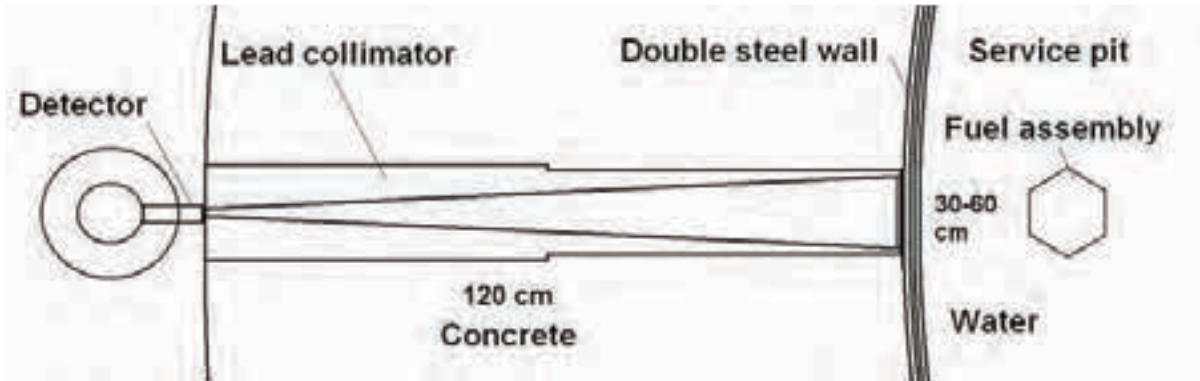


Fig. 1: Scheme of the experimental setup

A direct fission product ¹³⁷Cs is widely considered as the best isotope for burnup verification. It has a measurable penetrating gamma energy of 662 keV, and similar yield comes from both U and Pu fission, where neutron absorption is negligible, and has a long half life of 30 yrs. This latter also explains its insensitivity to changes of the irradiation history. The activity of Cs-137 is proportional to the burnup (see, e. g., [4]). The

measured Cs-137 intensity depends on the geometry as well. The correlation between burnup and the count rate of ¹³⁷Cs measured at half-height of the assemblies is shown in Fig. 2.

A typical axial distribution of the count rate of the 662 keV gamma rays of Cs-137 and the calculated burnup profile are plotted in Fig. 3.

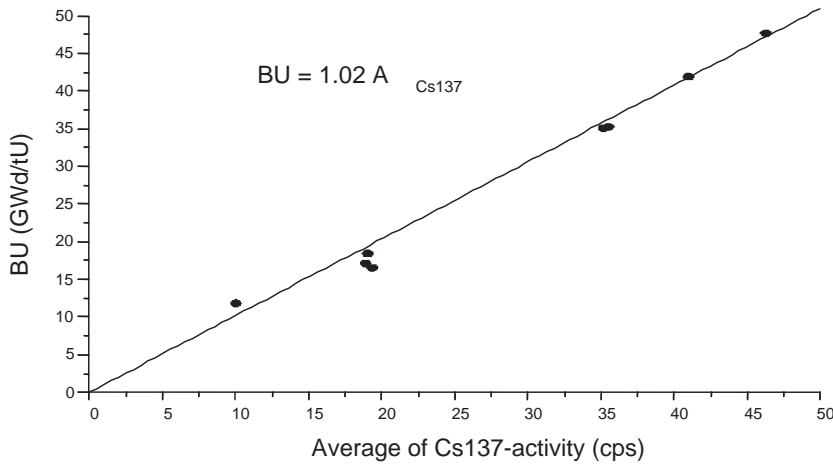


Fig.2: Correlation between burnup and the count rate of ¹³⁷Cs measured at half-height of the assemblies. The line fit corresponds to the equation for the operator-declared burnup BU = 1.02 A_{Cs137}.

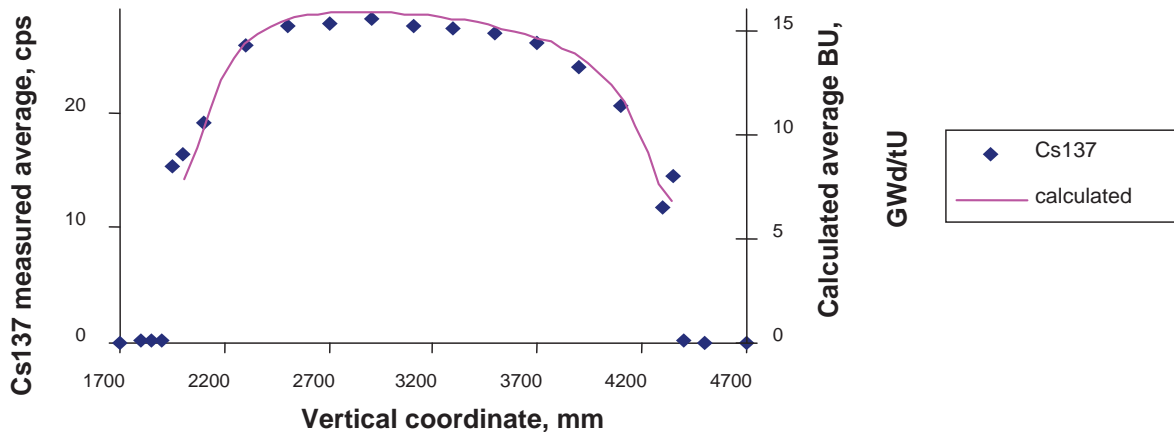


Fig. 3: A typical measured axial Cs-137 activity profile and the burnup profile calculated by the operator. Vertical coordinate is indicated on the refuelling machine

Whereas the intensity profile along the length of an assembly follows the *axial* burnup profile, intensity values, however, depend on the measurement geometry, the absorption of gamma-rays, and the detector applied. Furthermore, incorrect assembly positioning is much more likely during assembly rotation than during axial scanning. Since experimental conditions did not allow arranging the geometry precisely enough, Cs-137 activity alone is not suitable for examining the *azimuthal* burnup profile, for which the activity ratio Cs-134/Cs-137 is more suitable. As Cs-134 is not a direct fission product, but is formed by neutron

capture on the fission product Cs-133, its abundance is approximately proportional to the square of the burn-up. The activity ratio of Cs-134 to Cs-137 (Cs ratio) is therefore approximately proportional to the burnup again [1, 5]. Unlike the count rate of a given peak, the activity ratio is independent of the geometry, the absorption, and the detector. For illustration, an assembly was measured at different distances from the collimator. The dependence of the Cs ratio on the distance is shown in Fig. 4. As seen, the measured ratio remains unchanged within to 1% at the assembly movement of more than 20 cm.

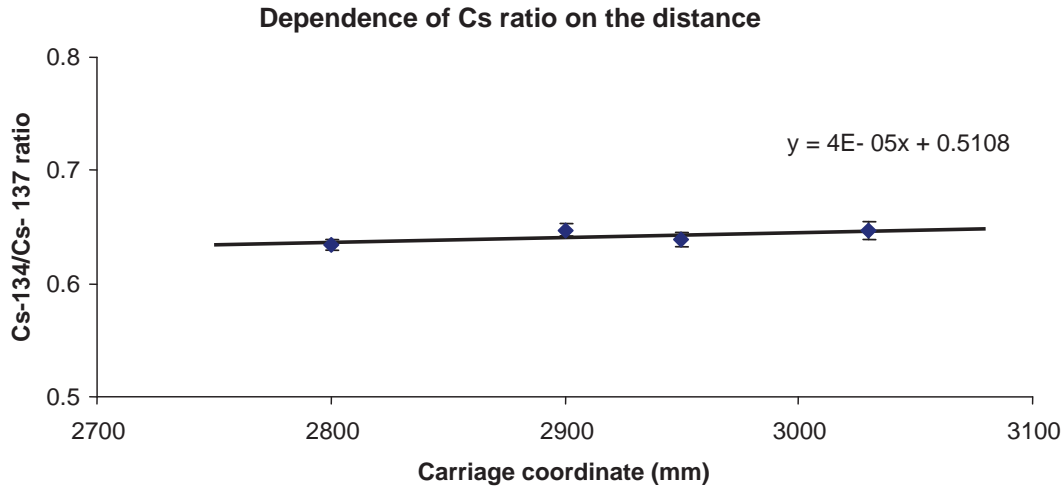


Fig. 4: The activity ratio Cs-134/Cs-137 plotted as a function of collimator window-to-assembly horizontal distance. The coordinate 2800 corresponds to 335 mm water layer

A total of 28 spent fuel assemblies were measured at 5-12 fixed height positions, from all six sides. Table 1 shows the main characteristics of the assemblies assayed. Four assembly groups were selected, six assemblies in each, as the core was divided into six sectors. From all sectors, assemblies of similar positions and histories were chosen. Their burnup and

cooling time varied between 10 – 45 GWd/tU and between 0.7 – 5.7 years, respectively. Follower parts of two control assemblies and their neighbours were also assayed. The intensities of the 605 and 796 keV peaks of Cs-134 as well as the 662 keV peak of Cs-137 were measured for 300 – 600 s in each position.

Table 1: Main data of the assemblies measured. Each group contains 6 assemblies of the same initial enrichment, burnup and irradiation history. Besides total burnup, yearly data are also given. Measurements were carried out at the end of the last campaign. Accumulated (over the campaigns) cooling times are indicated.

main				BU / Campaign			
group	enr. %	BU tot.	cooling time years	1	2	3	4
1	3.8	44.34	0.7	9.59	12.67	11.24	10.84
2	1.6	10.26	5.7	10.26			
3	3.8	39.49	1.6	10.37	12.75	12.20	4.18
4	2.4	26.44	2.6	8.57	9.90	4.16	3.82
follower	2.4	20.87	1.6	10.75	10.13		
follower	3.8	32.43	0.7	9.73	12.17	10.53	
neighbour	3.8	40.91	0.7	11.56	13.45	11.66	4.23
neighbour	3.8	40.91	0.7	11.56	13.45	11.66	4.23

The measurement campaign lasted for 5 weeks. About 1200 spectra were evaluated by dedicated software developed at the institute. Statistical uncertainty of peak areas was around 1%. Cs ratios were extrapolated to a common

date of the beginning of the measurements, due to the relatively short half-life (2.06 y) of Cs-134, and were determined for each measurement point. The extrapolated Cs activity ratios varied between 0.1 and 1.5.

3. Evaluation and results

Activity ratios were determined using the main gamma lines of Cs-134 (605, 795 keV) and the 662 keV line of Cs-137 by the relative efficiency (intrinsic) calibration method [5]-[7], which utilizes the fact that activities calculated from different gamma lines of the same isotope must be equal. Cs-137 activity and the activity ratio were evaluated at every measurement point.

A relative efficiency curve was constructed by using the two gamma lines of Cs-134 mentioned above. For energies above ~300 keV, the efficiency curve of HPGe detectors can be approximated with a linear function on a log-log scale. In the short interval between 605 and 796 keV, however, the linear approximation gives acceptable accuracy. For real spectra, the statistical uncertainty of the peaks other than those at 605 and 796 keV is quite high, thus only the peaks at 605 and 796 keV were used for constructing the relative efficiency curve. Using only two points on the linear scale simplifies the calculations, and provides an efficiency curve which might be the cause for small systematic biases in the measured Cs-ratio, but is free from random uncertainties which would emerge from using more gamma energies and a more complicated functional form for the efficiency. The eventual systematic bias is expected to be well below the uncertainty which is aimed at the present stage of the project. Using the γ -energies 605, 662, and 796 keV, a Monte Carlo simulation provided a difference below 2% from the linear approximation in the relevant energy interval. The γ -rays of the three energies coming from various pins were taken into account in the model, and the ratios of the corresponding count rates were examined after intensity summing, considering various radii of the water cylinder the assembly being immersed.

The relative efficiency $\epsilon_{Cs134}(E)$ as a function of the gamma-ray energy E can be given as

$$\epsilon_{Cs134}(E) = \frac{(I_{796} / B_{796} - I_{605} / B_{605})}{(796 - 605)keV} \times E(keV) + \frac{(I_{605} / B_{605}) \times 796keV - (I_{796} / B_{796}) \times 605keV}{(796 - 605)keV} \quad (1)$$

Then the activity ratio $^{134}Cs/^{137}Cs$ can be determined as

$$\frac{A_{134}}{A_{137}} = \frac{\epsilon_{Cs134}(662keV)}{I_{662} / B_{662}} \quad (2)$$

Here I_{605} and I_{796} are the measured peak areas of the 605 and 796 keV γ -lines of ^{134}Cs , I_{662} is that of the 662 keV γ -line of ^{137}Cs , whereas B_{605} , B_{796} , and B_{662} are the corresponding emission probabilities.

The measured and calculated burnup profile of an assembly in terms of the Cs ratio is shown in Fig. 5. The calculation was carried out by the operator [8]. Production and decay of the Cs isotopes was followed by the C-PORCA code [9]. This model was developed with the help of the burn-up calculation procedure of the HELIOS 2D transport code [10]. The necessary fission yields, decay constants, cross section data and number densities arose from the data library of HELIOS code which was based on the ENDF/B-VI data files [11] in this case. The system of the differential equations was solved by the method of fourth order Runge-Kutta as part of the C-PORCA code. The results of calculations represent the burn-up and the concentrations of Cs isotopes in individual pins of an assembly at axial nodes of 6 cm height. This means that calculated burn-up and concentrations for an assembly comprise a dataset of 41 values for each of the 126 pins. Burnup asymmetries throughout the core were revealed and interpreted. Four groups of assemblies were measured with various burn-up and cooling time. Differences of uniform burnup assemblies were observable between assembly sides looking at the center of the reactor core and opposite directions.

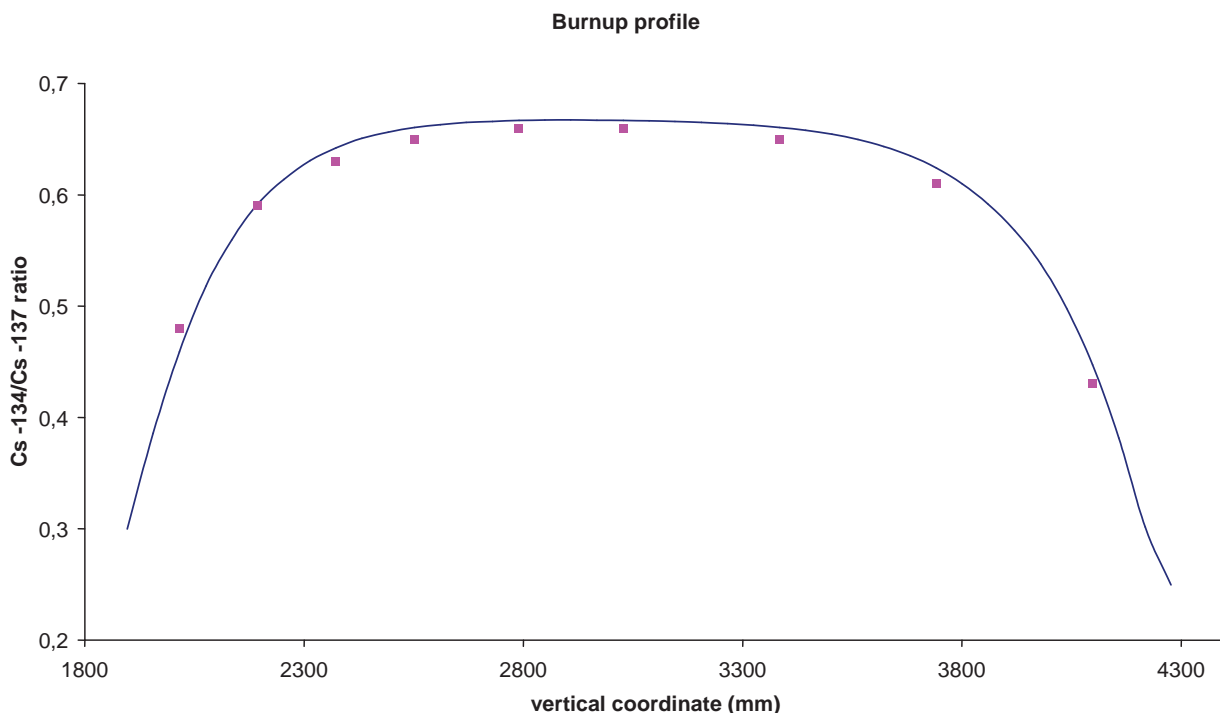


Fig. 5: A typical Cs ratio profile with experimental points and theoretical curve

This is illustrated on a polar diagram in Fig. 6 by a graphical representation of the Cs ratio measured in a group of six assemblies symmetrically positioned around the core during reactor operation. The burnup of the assemblies was uniformly 26 GWd/tU, whereas they were measured with 2.6 years cooling. It was shown that Cs ratios (in blue) are higher on the assembly sides looking at the core centre (the values plotted at the vertices of the hexagons correspond to those at faces of the assemblies). In this case

Cs ratio is varying between 0.47 – 0.66, reaching the higher value on the side nearer the core centre and the lower value on the opposite side.

For example, Cs ratios measured on the 6 sides of the assembly on the top of the figure are as follows: on the side looking straight down (direction core centre), it is around 0.66, whereas on the side looking straight up, around 0.47.

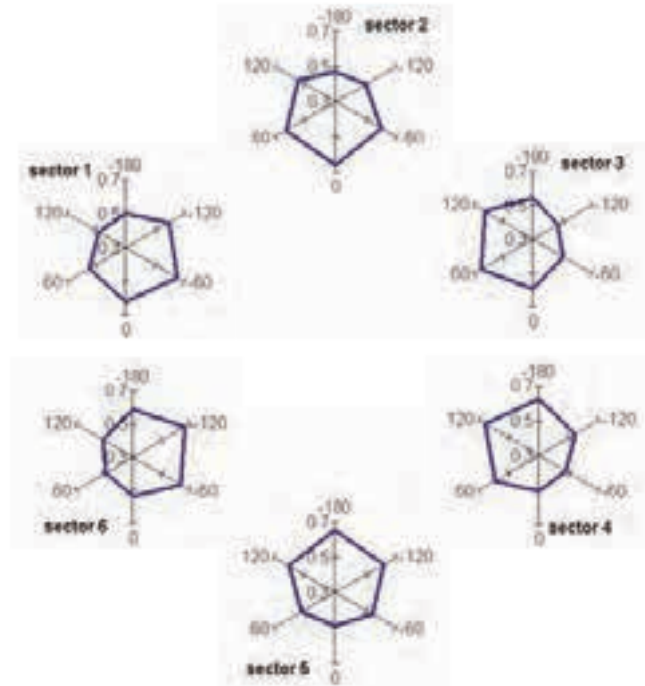


Fig. 6: Measured azimuthal Cs-ratio profiles at half-height of pins of the 26 GWd/tU burn-up assembly group around the core

Certain groups of assemblies show strong burnup asymmetries depending on the position of their sides with respect to the centre of the core, referring to “anomalies” in temperature or neutron flux in the core. Burnup profiles of the working assemblies and of the followers also differ from each other, in accordance with the measurements.

Measured axial profiles (in terms of Cs ratio) of a working assembly are plotted in Fig. 7, whereas those of a control assembly are in Fig. 8, at various angles of assembly rotation. Control assemblies consist of absorber and follower parts, the latter contain fuel pins like working assemblies.

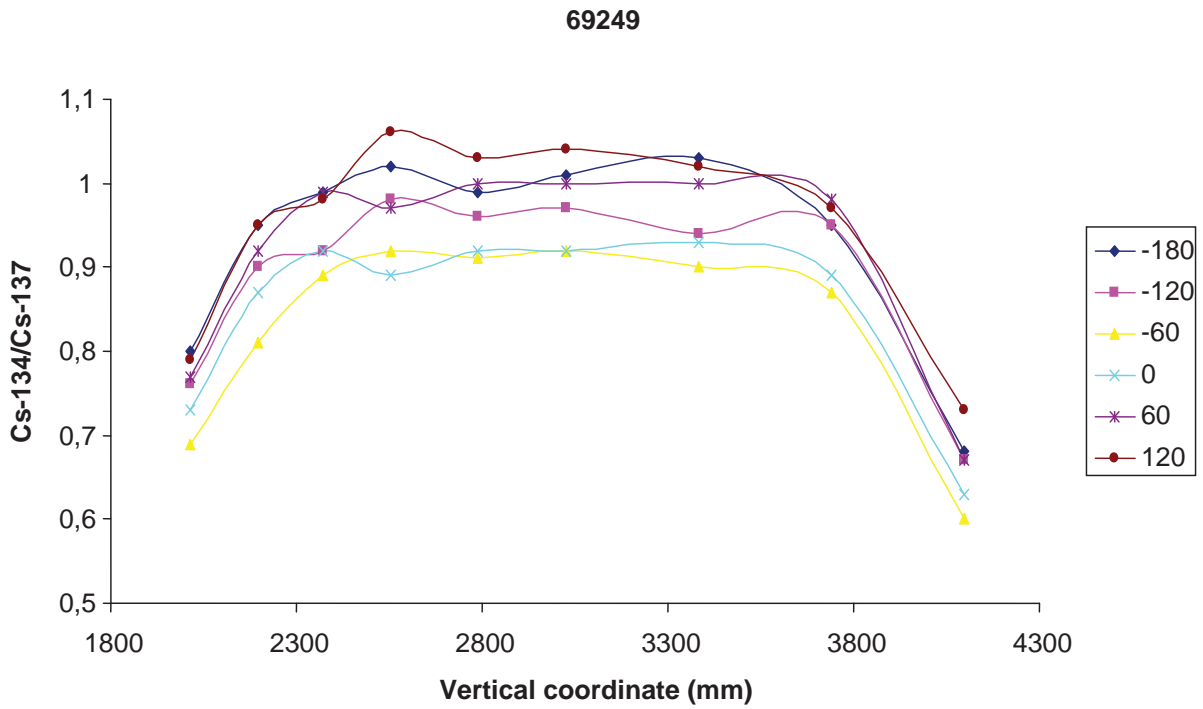


Fig 7: Measured axial burnup profiles of a working assembly plotted at various angles. Experimental points are connected with continuous curves for guiding the eye

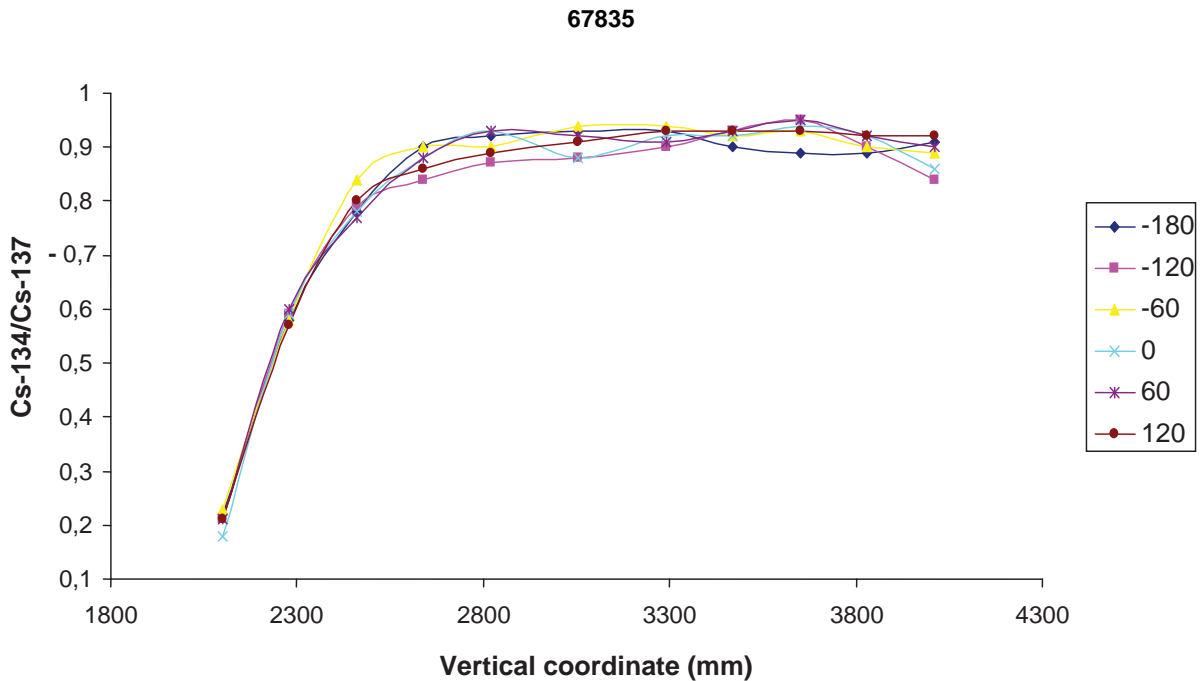


Fig. 8: Measured axial burnup profiles of the follower part of a control assembly plotted at various angles. Experimental points are connected with continuous curves for guiding the eye

Further experiments are required to refine the agreement between experiment and calculation, thus further decrease the uncertainty of both the measurements and the calculation.

4. Conclusions

Both the axial and azimuthal burnup profile of spent fuel assemblies can very precisely be followed using the results from non-destructive HRGS measurements.

Considering the statistical error (1%) and the linear approximation of the efficiency, uncertainty of the measured data is about 3 %. This can be improved by longer measurements and a more accurate treatment of the efficiency. We would eventually like to reach 1 % accuracy at least.

It is expected in this initial state of the project that the currently assumed 13 % (3σ) uncertainty of burnup calculation can be decreased by utilizing the data of the experimental results. This facilitates observing safety limits more

accurately in planning of the loading pattern of the core and during reactor operation.

Measurement of additional assemblies is needed to refine the agreement between experiment and calculations.

It is foreseen that the experimental results will be used for improving the accuracy of the burnup calculation code, thus enabling more efficient use of the nuclear fuel. However, the connection between the uncertainty of the burnup value and the Cs activity ratio needs to be investigated for different operational parameters and cooling times.

5. Acknowledgements

The authors would like to acknowledge the sponsorship of Paks NPP and its personnel for assisting at the measurements as well as Messr. T. Parkó and I. Pócs of the NPP for performing Cs ratio and burnup calculations for the measured assemblies. Also, the project was partly supported by the Hungarian Atomic Energy Authority. The authors are greatly indebted to Mr. J. Huszti for developing the dedicated software package.

6. References

- [1] Bibichev BA, Majorov VP, Protesenko YM, Fedotov PI, Sunchugashev MA, *The problem of determining fuel burnup from the Cs-134/Cs-137 activity ratio* (in Russian). In: *Nuclear Safeguards Technology, Vol. 1*. International Atomic Energy Agency, Vienna, 1979, p 387-394.
- [2] Tarvainen M, Riihonen M, *Spent fuel measurements at Loviisa Nuclear Power Station, May 1982 STUK-A49*, Finnish Centre for Radiation and Nuclear Safety, Helsinki, February 1984.
- [3] Lakosi L, Sáfár J, Józsa I, *Spent fuel measurements at NPP Paks, ESARDA Bulletin*, ed. L. Stanchi, JRC Ispra, No. 13, Oct. 1987, p 31-32.
- [4] Phillips JR, *Irradiated Fuel Measurements*. In: *Passive Nondestructive Assay of Nuclear Materials. NUREG/CR-5550, LA-UR/90-732*, D. Reilly, N. Ensslin, and H. Smith, Eds., Los Alamos National Laboratory, 1991, p 539-541.
- [5] Dragnev TN, *Intrinsic self-calibration of nondestructive gamma-ray spectrometric measurements*, *J. Radioanal. Chem.* 36, 1977, p 491-508.
- [6] Hsue ST, *Methods for the non-destructive assay of irradiated nuclear fuels for safeguards*, *Atomic Energy Review* 16, 1978, p 89-128.
- [7] Parker JL, *General Topics in Passive Gamma-Ray Assay*. In: *Passive Nondestructive Assay of Nuclear Materials. NUREG/CR-5550, LA-UR/90-732*, D. Reilly, N. Ensslin, and H. Smith, Eds., Los Alamos National Laboratory, 1991, p 155.
- [8] Parkó T, Pócs I, private communication
- [9] Pócs I, Parkó T, Patai Szabó S, *Application of discontinuity factors in C-PORCA 7 code, 20th Symposium of AER on VVER Reactor Physics and Reactor Safety*, Espoo, Finland, 20-24 Sep 2010.
- [10] Studsvik Scandpower *HELIOS 1.10 Documentation*, 2008.
- [11] Rose PF and Dunford CL, *ENDF-102 Data Formats and Procedures for the Evaluated Nuclear Data File ENDF-6, BNL-NCS-4495*, Brookhaven National Laboratory, Upton, New York, 1990.

Development of a reference spent fuel library of 17x17 PWR fuel assemblies

Riccardo Rossa^{1,2}, Alessandro Borella¹, Klaas van der Meer¹

¹ Studiecentrum voor kernenergie - Centre d'étude de l'énergie nucléaire (SCK•CEN)

² Université libre de Bruxelles (ULB)

Emails: rossa@sckcen.be, aborella@sckcen.be, kvdmeer@sckcen.be

Abstract:

One of the most common ways to investigate new Non-Destructive Assays (NDA) for the spent fuel assemblies are Monte Carlo simulations. In order to build realistic models the user must define in an accurate way the material compositions and the source terms in the system.

This information can be obtained using burnup codes such as ORIGEN-ARP and ALEPH2.2, developed at SCK•CEN. These software applications allow the user to select the irradiation history of the fuel assembly and to calculate the corresponding isotopic composition and neutron/gamma emissions as a function of time.

In the framework of the development of an innovative NDA for spent fuel verifications, SCK•CEN built an extensive fuel library for 17x17 PWR assemblies, using both ORIGEN-ARP and ALEPH2.2. The parameters considered in the calculations were initial enrichment, discharge burnup, and cooling time. The combination of these variables allows to obtain more than 1500 test cases.

Considering the broad range of the parameters, the fuel library can be used for other purposes apart from spent fuel verifications, for instance for the direct disposal in geological repositories.

In addition to the isotopic composition of the spent fuel, the neutron and photon emissions were also calculated and compared between the two codes. The comparison of the isotopic composition showed a good agreement between the codes for most of the relevant isotopes in the spent fuel. However, specific isotopes as well as neutron and gamma spectra still need to be investigated in detail.

Keywords: Spent Fuel; PWR; ORIGEN-ARP; ALEPH2.2

1. Introduction

Spent fuel is characterized by a very high neutron and gamma emission due to the spontaneous fission of heavy nuclides and radioactive decay of fission products that have been produced during irradiation. The irradiation in the reactor produces numerous fission products and actinides that make the resulting isotopic composition and associated gamma spectra particularly complex [1]. Considering the

high neutron and gamma field together with the significant heat coming from the decay of the fission products and actinides, the spent fuel is generally stored under water in a spent fuel pool and it is not directly accessible by the safeguards inspectors. Given the characteristics listed above, the spent fuel can be considered as one of the most difficult materials to verify during an inspection.

Non-destructive assays (NDA) are one of the possible methods to verify the spent fuel and several research projects are trying to improve their current capabilities [2],[3]. One of the ways to investigate new NDA for the spent fuel assemblies are Monte Carlo simulations. In order to build realistic models the user must define in an accurate way the material compositions and the source terms in the system. Therefore an effort was made to define a spent fuel library that serves as reference to benchmark the performances of the measurements methods under investigations.

The goals of this preliminary work are therefore twofold. The first one is to understand how the irradiation history of the fuel influences its isotopic composition (and consequently its neutron and gamma source strength). The second one is to generate automatically several input cards compatible with the MCNPX [4],[5] code that will be used in the study of innovative NDA techniques. To achieve both goals the spent fuel needs to be characterized in terms of isotopic composition, neutron and gamma emission (both source intensity and energy spectrum).

Section 2 of this paper describes the main features of ORIGEN-ARP and ALEPH2.2, the two codes used for the simulations, together with a brief explanation on the models that have been incorporated in both codes.

The third section gives an overview of the main structure of the spent fuel library and of the range of the parameters used to create it (initial enrichment, burnup, and cooling time). This section contains the main results obtained with the ORIGEN-ARP simulations. The neutron emissions are separated into the two main components (α ,n reactions and spontaneous fissions) and the total values are plotted against initial enrichment (IE), burnup (BU) and cooling time (CT). In addition, the role of individual isotope is studied to understand how the composition of the spent fuel influences the neutron emissions.

A comparison between the results obtained with ORIGEN-ARP and ALEPH2.2 is carried out in section 4. Both the

neutron emissions and nuclide concentrations calculated by the two codes are evaluated as a function of the burn-up and cooling time.

Section 5 considers some parameters (e.g. boron concentration in the water) that have an impact on the final results of the simulations. The impact is estimated both in terms of neutron emissions and nuclide concentration. This chapter is based on the results of ALEPH2.2 simulations, since with this code the user can completely define the geometry and material composition of the system.

The libraries built with the two codes are compared in section 6 with the spent fuel reference library developed by the Los Alamos National Laboratory (LANL). This comparison considered the data of the total neutron emission and of four neutron emitters (two Cm isotopes and two Pu isotopes) of three corresponding cases (i.e. simulations with the same IE, BU, and CT).

The conclusions at the end of the document summarize the main results coming from the simulations, highlighting the main factors behind the change in the neutron and gamma emission and isotopic composition of the spent fuel.

2. Computational models used for the calculations

The study of the time evolution of the nuclear fuel generally requires the combination of computer codes to model the neutron transport in the reactor and to predict the fuel composition due to the radioactive decay of its isotopes.

Two different codes have been used to perform the simulations: ORIGEN-ARP and ALEPH2.2.

The first code uses a set of pre-compiled averaged cross section values (called ORIGEN-ARP cross section library) as input to the depletion calculation. This procedure avoids the time consuming neutron transport and therefore leads to the strong reduction in the computational time required for the simulations.

The second code uses a statistical approach (Monte Carlo method) for the calculation of the neutron transport and then performs the fuel depletion. By using the Monte Carlo code MCNP(X), ALEPH2.2 retains the great flexibility in the definition of the system (geometry, materials) and in the nuclear data used in the simulation. As a drawback the computational time can be significantly longer than in the case of ORIGEN-ARP.

The simulations with ORIGEN-ARP generally took less than one minute to complete with a regular portable PC. Most of the time was spent by the user in the selection of the input parameters.

The computational time required by the simulations with ALEPH-2.2 strongly depends on the statistics requested by the user (i.e. the parameters of the kcode used as

source term) and by the burnup of the assembly. By using a cluster with 16 cpus, the fastest case was the one of 5 GWd/tU and took about 2 hours to complete, whereas the case with 70 GWd/tU took almost 5 days.

2.1 ORIGEN-ARP

The first code used to generate the fuel library is ORIGEN-ARP [6] and it is part of the SCALE package [7] that is developed by Oak Ridge National Laboratory (ORNL).

ORIGEN-ARP employs a graphical user interface (GUI) to select several characteristics of the fuel assembly. The PWR 17x17 (w17x17) case has been chosen considering its worldwide use in the nuclear power plants. The GUI is composed of several menus that are shown subsequently when all parameters in one window have been introduced and validated by the user.

Apart from the type of fuel geometry, the first window (“Express”) contains other parameters as follows:

- all results are normalized to 1 ton of uranium;
- the average power is set to 40 MW/tU. This value is taken from [8] and results in a burnup of 14.4 GWd/tU for a cycle of 360 days;
- the moderator density is the default value of 0.723 g/cm³.

The next section is the “Composition” window:

- the abundances of the uranium isotopes are the default values proposed by ORIGEN-ARP depending on the initial enrichment selected in the previous section;
- oxygen was added to the list of isotopes in the fresh fuel in order to model the UO₂ material in the fuel pin. The natural isotopic composition was selected with a concentration of 134500 g/t.

The section “Neutron” allows selecting the energy-group structure for the neutron source spectra. The “238-group ENDF5” is the option chosen in the calculation. This group structure extends from 10⁻⁵ eV up to 20 MeV. This section determines only the division of the energy groups and does not select the data library used by the code for the nuclear data.

At the same way, the photon emissions are treated according to a 74-group library defined by the user. The group structure extends from 10 keV up to 10 MeV.

The most extensive section in the ORIGEN-ARP interface is the “Cases” windows, where the user selects the characteristics of the irradiation history. All simulations for the fuel library consider irradiation cycles of maximum 360 days, after which the fuel assembly undergoes a decay period of 30 days. The duration of the last irradiation cycle is adapted to reach the desired level of burnup at the discharge. Following this procedure, the fuel assembly is exposed to the same power level during all cycles in the reactor. After the final unloading from the reactor (i.e. the last irradiation cycle is completed), the ORIGEN-ARP calculation considers 30 cooling

times to compute the isotopic composition and both neutron and gamma emissions.

Other options selected in ORIGEN-ARP are:

- no cutoff is selected for the composition so all the isotopes are reported in the output file;
- output precision is 6 digits for the values of the mass concentrations;
- output precision is 4 digits for the neutron and gamma emission;
- the fuel matrix for the (α ,n) evaluation is the UO_2 ;
- bremsstrahlung is not considered in the model.

2.2 ALEPH2.2

ALEPH is the Monte-Carlo burn-up code being developed by SCK•CEN since 2004 [9]. The code belongs to the category of shells coupling Monte Carlo particle transport codes and deterministic depletion algorithms.

The fuel assembly model considered in ALEPH2.2 tries to be identical to the case considered with ORIGEN-ARP. The geometry is the same as the PWR 17x17 fuel assembly modelled in ORIGEN-ARP (Table D1.A.3 of [6]), with the exception that the active length is reduced to 1 meter. It has been supposed that there is no water gap between neighbouring assemblies and this has been simulated placing reflecting surfaces around the fuel assembly.

The irradiation history is defined in terms of irradiation power (MW), length of the irradiation step (days), and length of the decay step (days, years). All these parameters are chosen to have the same conditions as those used for the ORIGEN-ARP simulations.

Other parameters in the input files are:

- the geometry of the fuel assembly (pin radius and pitch) and the initial composition of the fuel is the same as the ORIGEN-ARP simulations;

- the fuel temperature is 900 K;
- the cladding temperature is 620 K;
- the moderator temperature is 575 K (with a density of 0.723 g/cm^3);
- the water contains 630 ppm of Boron (according to abundances of ^{10}B and ^{11}B). This is the average Boron concentration reported in ORIGEN-ARP (Table D1.A.3 in Ref. [6]); this value is kept constant during the irradiation simulations in ALEPH2.2.
- each irradiation step runs a kcode with 5000 particles and an initial value for $k_{\text{eff}}=1.16$. The k_{eff} of the assembly is calculated taking the average value of 100 cycles, neglecting the first one from the calculations;
- the neutron source is modeled as a Watt fission spectrum with the parameters of the neutron-induced fission of ^{235}U [4].

3. Main characteristics of the fuel library

The reference spent fuel library has been developed using three variables to take into account the most representative irradiation histories of the spent fuel. In particular:

- Initial enrichment (IE): 4 values from 3.5% to 5.0%, with increments of 0.5%
- Discharge burnup (BU): 14 values from 5 up to 70 GWd/tU, with increments of 5 GWd/tU
- Cooling time (CT): 30 values ranging from immediate discharge up to 3 million years

The combination of these parameters allows to obtain 1680 different compositions and source terms.

This fuel library does not consider the element history in the reactor core (location, different length of outages, different power level during irradiation). Future work will refine the results obtained at this stage and investigate these factors.

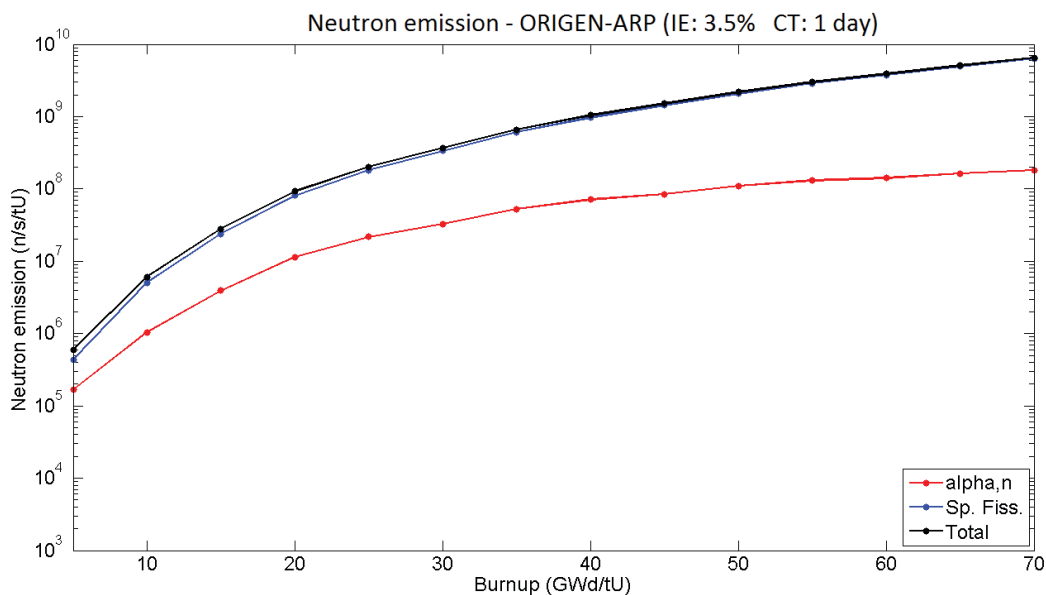


Figure 1: Neutron emission as a function of the burnup for a 17x17 PWR spent fuel assembly with initial enrichment of 3.5% and cooling time of 1 day. The contributions due to (α ,n) and spontaneous fission reactions as well as the total neutron emission are shown.

Figure 1 shows the neutron emissions as a function of the burnup. The data have been calculated with ORIGEN-ARP, with a fuel of 3.5% initial enrichment and after a cooling time of 1 day. The plot reveals that the spontaneous fission is the main source for the neutron emission after a short cooling time. This fact needs to be evaluated also with higher cooling times.

In order to do so, Figure 2 shows the neutron emission as a function of cooling time for the burnup value of 10 GWd/tU.

The contribution from (α,n) reactions is generally one order of magnitude lower than the term due to spontaneous

fission. The only exception is for burnup of 10 GWd/tU with cooling times between 30 and 300 years (Figure 2). For these combinations the two contributions are similar, with cases where the (α,n) reactions have the dominant role on the neutron emission.

Looking at Figure 2, there is a clear increase of the (α,n) contribution around 100 years of cooling time. This is due to the build-up of ^{241}Am from ^{241}Pu (half-life of 14.4 years). The same effect is present also at higher burnup, but it is not visible due to the higher neutron emission that conceals this contribution.

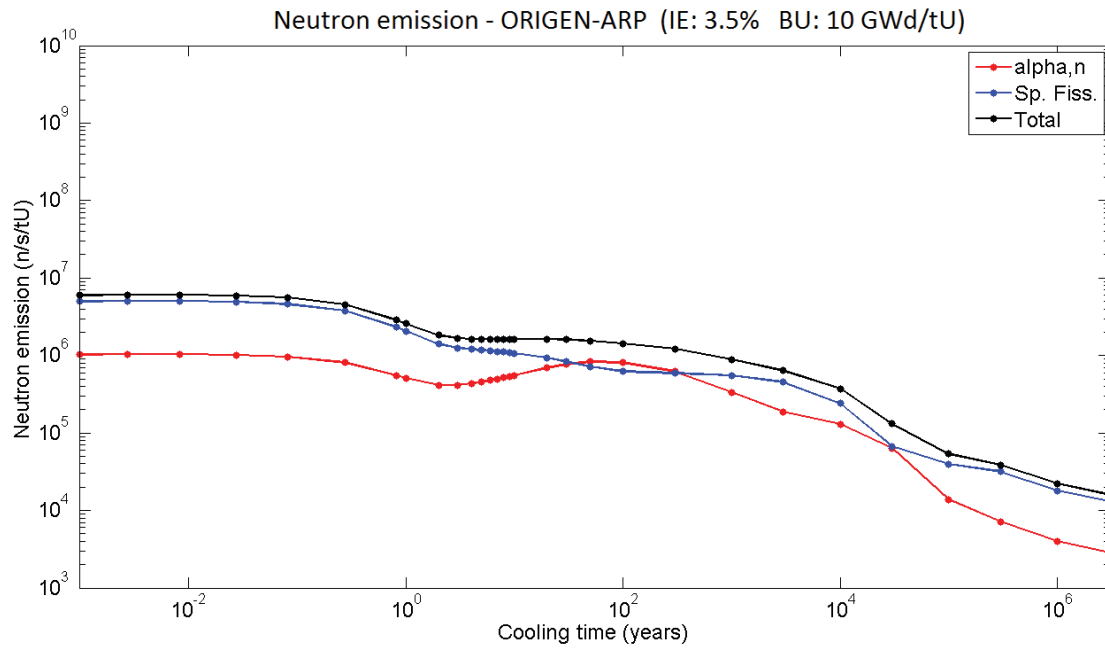


Figure 2: Neutron emission as a function of the cooling time for a 17x17 PWR spent fuel assembly with initial enrichment of 3.5% and discharge burnup of 10 GWd/tU. The contributions due to (α,n) and spontaneous fission reactions as well as the total neutron emission are shown.

In order to refine the study it is important to understand the role of each isotope in the total neutron emission.

Figures 3 and 4 show the percentage of the total neutron emission due to each isotope as a function of cooling time.

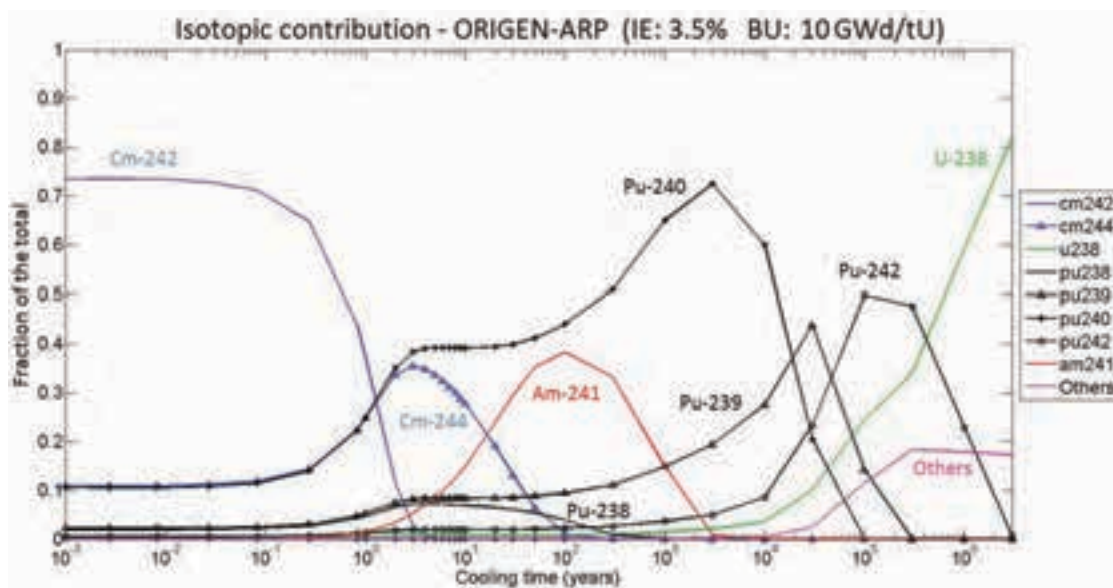


Figure 3: Fraction of the total neutron emission due to a set of isotopes as a function of the burnup for a 17x17 PWR spent fuel assembly with initial enrichment of 3.5% and discharge burnup of 10 GWd/tU. The contributions due to specific isotopes and the sum of all remaining isotopes ('Others') are shown.

Both for Figure 3 and 4 there are 11 isotopes that are responsible for about 99% of the total neutron emission (the value 'Others' is relevant only for cooling times higher than 10000 years).

At low burnup the ^{242}Cm is the main responsible for the neutron emission up to 100 days, a role that is taken then by ^{244}Cm and several plutonium isotopes. Another relevant contribution comes from ^{241}Am (as it has been suggested from the peak in Figure 2). Other curium isotopes are not present at low burnup values because the short irradiation time did not allow the build-up of these high-Z isotopes.

With a burnup of 35 GWd/tU (Figure 4) two isotopes of curium (^{242}Cm and ^{244}Cm) are responsible for basically all neutron emissions up to a few years of cooling time, but opposite to Figure 3 now ^{244}Cm is the main actor. Increasing the cooling time another Cm isotope (^{246}Cm) has an

impact on the total neutron emission because the other previous isotopes have short half-lives. Other contributions come from ^{241}Am , ^{240}Pu , and ^{242}Pu .

The latter isotope is the main responsible for the neutron emission in the long term, together with ^{238}U , and a list of other isotopes (indicated as 'Others'). One must bear in mind that the magnitude of the emission for high cooling times is very low compared to the value at the discharge and this is the reason why many isotopes have a non-negligible role for long cooling times.

Increasing the burnup to 60 GWd/tU there are small differences to the case of 35 GWd/tU. ^{244}Cm takes an even higher contribution for the short cooling times, as well as ^{246}Cm for intermediate values. At very high cooling time ^{248}Cm appears to be important along with ^{242}Pu and ^{238}U .

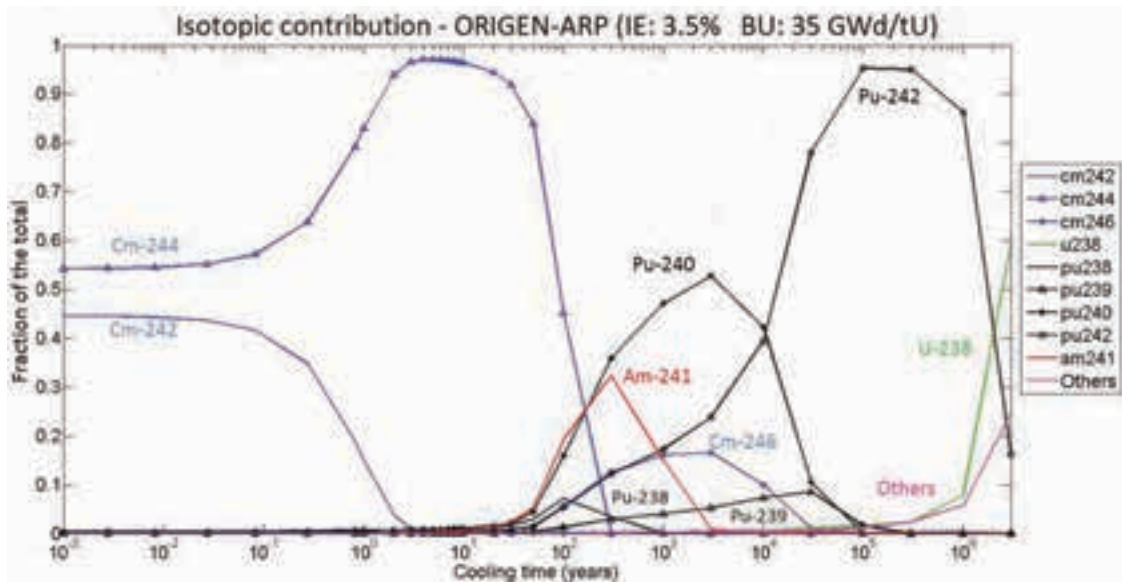


Figure 4: Fraction of the total neutron emission due to single isotopes as a function of the burnup for a 17x17 PWR spent fuel assembly with initial enrichment of 3.5% and discharge burnup of 35 GWd/tU. The contributions due to specific isotopes and the sum of all remaining isotopes ('Others') are shown.

The analysis so far focused on the influence of burnup (BU) and cooling time (CT) on the neutron emissions. Since the initial enrichment (IE) plays also a role, the next part investigates this variable. Figure 5 shows the ratios of the total neutron emission as a function of the burnup for the enrichments considered in the simulations.

By looking at the magnitude of the difference between the enrichment values, it seems that this variable plays a minor role in the determination of the neutron emission compared to burnup and cooling time. In fact, while by changing the burnup the neutron flux value varies of more than one order of magnitude, the maximum difference with the initial enrichment is of less than a factor 3.

The origin of the peak observed in Figure 5 can be explained by looking at Figure 6. This plot shows the ratio of the total neutron emissions after a cooling time of 10 years. In addition to the curve 'Total' (that is the same of the curve '3.5/5.0' of Figure 5) also the ratios for specific isotopes are added. The curve related to the single isotopes is calculated taking the ratio between the neutron emission due to this isotope at 3.5% initial enrichment and the total neutron emission at 5.0%

It is clear that the shape of the curve 'Total' is determined by the one of ^{244}Cm at burnup higher than 30 GWd/tU, while at lower burnup mainly ^{239}Pu , ^{240}Pu , and ^{241}Am determine the shape of the curve.

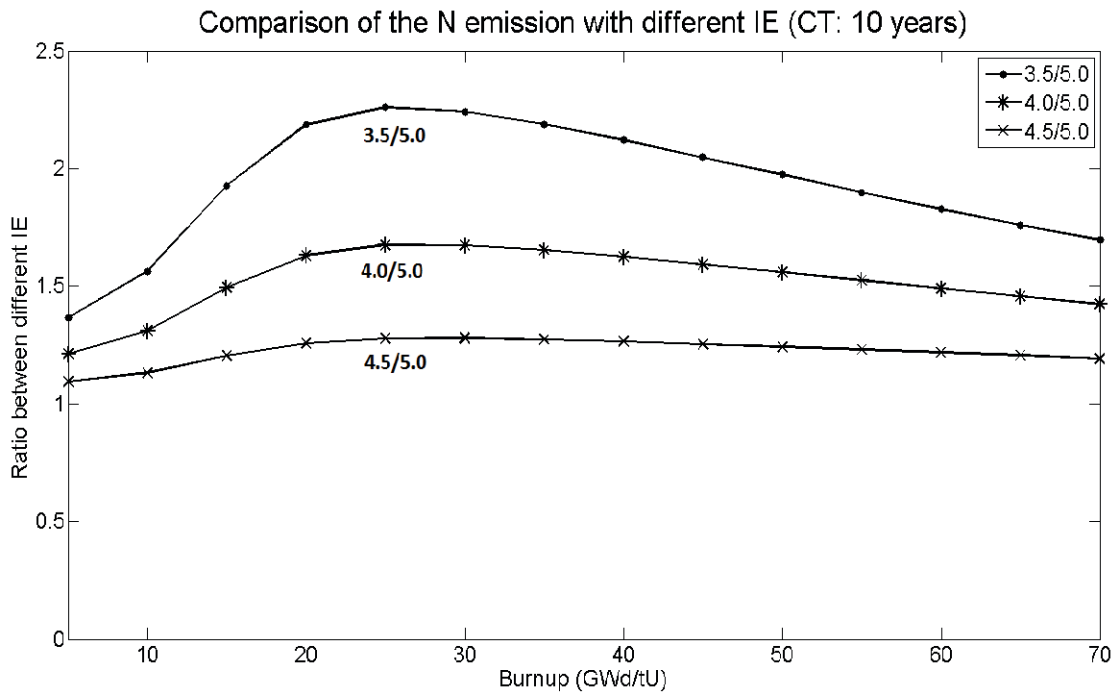


Figure 5: Ratio of total neutron emissions for different enrichments as a function of the burnup for a 17x17 PWR spent fuel assembly with cooling time of 10 years. The initial enrichments used for the ratio are indicated close to the corresponding curve.

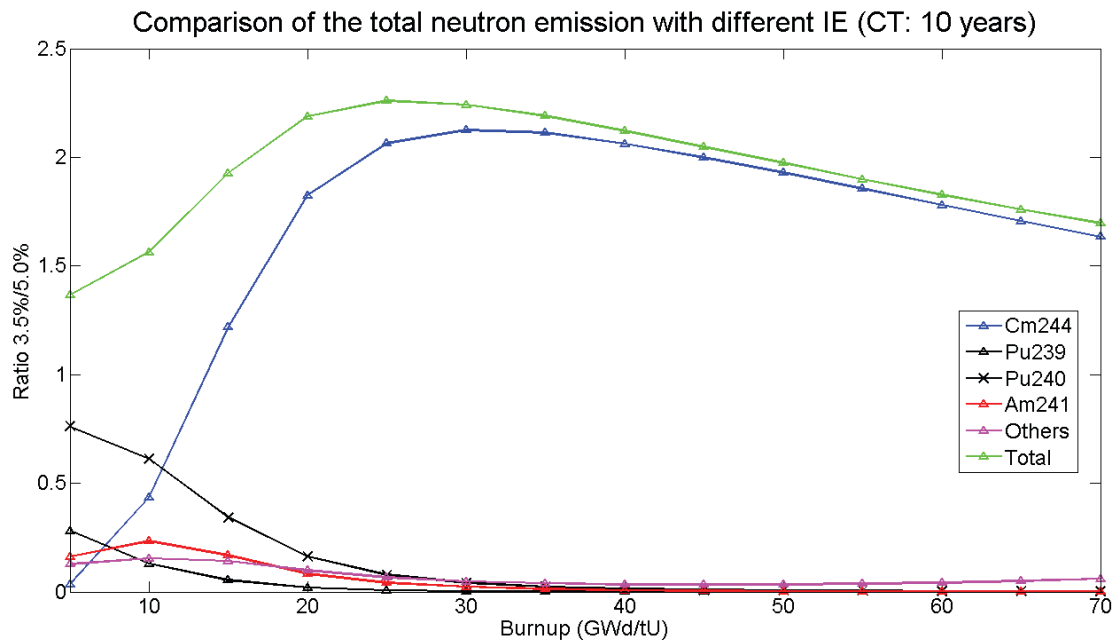


Figure 6: Total neutron emission with different initial enrichments – role of selected isotopes (CT: 10 years). The green curve ('Total') is the same of Figure 5 ('3.5/5.0'). The curves relative to single isotopes are calculated taking the ratio between the neutron emission due to the specific isotopes in the case of fuel with 3.5% initial enrichment and the total neutron emission at 5.0% initial enrichment.

4. Comparison of the two codes

The next step is to compare the two codes used to generate the spent fuel library. The set of simulations in the codes used the same values of:

- IE, BU, and CT;
- average power during irradiation;
- radius of the fuel pin, cladding, and pitch between neighbouring pins;

- boron concentration in the water.

The impact of the boron concentration, the water gap between the assemblies, and the data library on the final results will be investigated in the next section.

Each code applies a different normalization unit for the calculated data (t_U for ORIGEN-ARP and cm^3 for ALEPH2.2). In order to compare the two codes it is necessary to renormalize one of the two to have the same measurement unit in all simulations.

Figure 7 compares the results of ORIGEN-ARP and the ones coming from ALEPH2.2 in relative terms. The fuel used in these simulations had an initial enrichment of 3.5%. ORIGEN-ARP always yields a lower value of emissions compared to ALEPH2.2. The ratio of the

values coming from the two codes remains rather constant around 0.95 with the burnup. The only exception is at 100 years of cooling time, where there seems to be a decreasing trend for burnup higher than 40 GWd/tU.

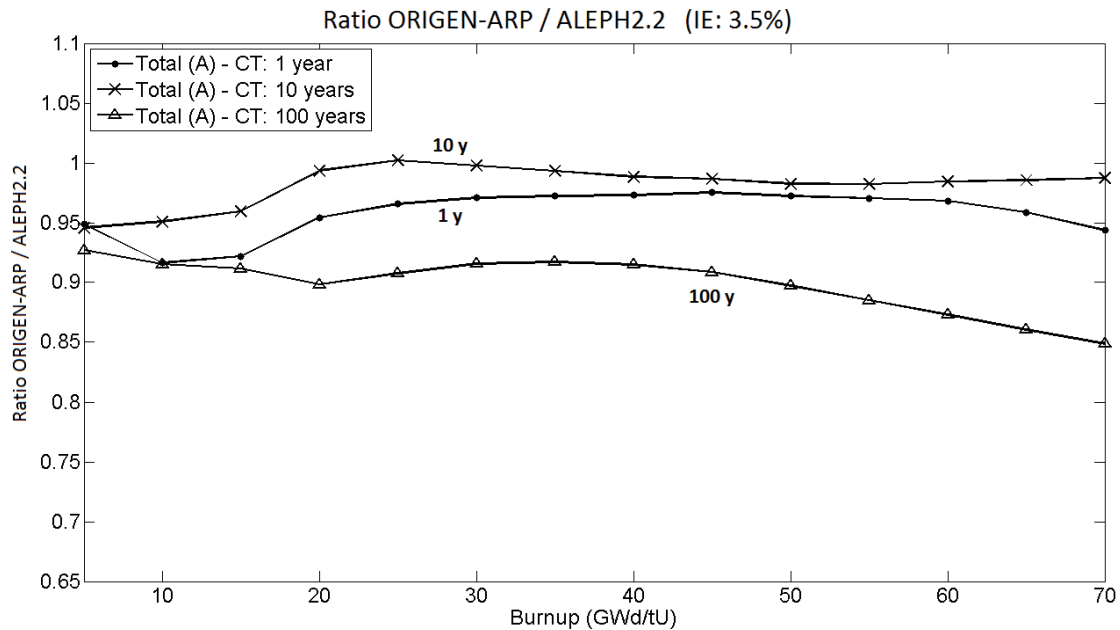


Figure 7: Ratio of the total neutron emission as a function of the burnup. The plot shows the ratio between the total neutron emission calculated by ORIGEN-ARP and ALEPH2.2 for fuel with a 3.5% initial enrichment and 1, 10, and 100 years of cooling time.

A comparison of the nuclides concentrations obtained by the two codes has been made in order to understand the reason of the difference in the neutron emissions. The following table shows the ratio between the concentrations of selected nuclides as a function of the burnup. The isotopic compositions are calculated at direct discharge.

Table 1 shows that the mass concentrations of the main neutron emitters calculated by ORIGEN-ARP are

usually lower compared to the results obtained with ALEPH2.2.

The fact that ²⁴²Cm and ²⁴⁴Cm are responsible for over 90% of the neutron emission up to few years of cooling time, explains the lower neutron emission calculated with ORIGEN-ARP. The values in the table follow the same trend independently from the initial enrichment of the fuel.

Isotope BU (GWd/tU)	cm242	cm244	cm246	cm248	u235	u238	pu238	pu239	pu240	pu241	pu242	am241
5	0.862	1.126	0.875	0.870	0.996	1.000	1.101	1.012	1.024	1.046	1.091	1.052
10	0.828	1.005	0.740	0.697	0.991	1.000	1.046	1.000	0.997	1.063	1.071	1.049
15	0.840	0.978	0.698	0.645	0.987	1.001	1.023	0.995	0.976	1.068	1.079	1.079
20	0.857	1.007	0.732	0.669	0.981	1.001	1.004	1.000	0.990	0.993	1.054	1.076
25	0.845	1.007	0.737	0.693	0.976	1.001	0.985	1.001	0.991	0.990	1.018	1.057
30	0.838	0.998	0.724	0.696	0.970	1.002	0.966	1.004	0.988	0.991	1.003	1.054
35	0.841	0.990	0.720	0.685	0.965	1.002	0.949	1.005	0.995	0.969	0.996	1.073
40	0.845	0.982	0.704	0.683	0.960	1.002	0.932	1.006	0.995	0.971	0.983	1.080
45	0.846	0.979	0.690	0.675	0.956	1.003	0.916	1.009	0.994	0.970	0.976	1.082
50	0.851	0.973	0.682	0.662	0.954	1.004	0.901	1.008	0.997	0.961	0.973	1.106
55	0.858	0.971	0.672	0.653	0.953	1.004	0.885	1.009	0.998	0.963	0.965	1.118
60	0.861	0.972	0.663	0.646	0.954	1.005	0.871	1.014	0.995	0.965	0.961	1.120
65	0.866	0.972	0.657	0.637	0.958	1.006	0.857	1.013	0.998	0.963	0.958	1.145
70	0.873	0.973	0.650	0.628	0.963	1.006	0.844	1.015	0.999	0.965	0.955	1.160

Table 1: Ratio between the nuclide concentrations obtained with ORIGEN-ARP and ALEPH2.2 as a function of the burnup. The fuel had 3.5 % initial enrichment and the concentrations were taken at direct discharge from the reactor.

5. Impact of other parameters on the results

5.1 Boron concentration

Simulations with ALEPH2.2 considered cases with water without boron and with a boron concentration of 630 ppm (the same as the ORIGEN-ARP cases). In this section the impact of boron on the neutron emissions is discussed.

The neutron emissions as a function of the burnup obtained with and without boron follow the same trend as in Figure 1. The trend of the curves is very similar, but the neutron emissions are higher when boron is present. The magnitude of the boron impact can be seen in Figure 8 where the ratio between corresponding values of burnup is shown. By looking at the ratio, one can estimate that the influence of boron is within 10% of the total neutron emission.

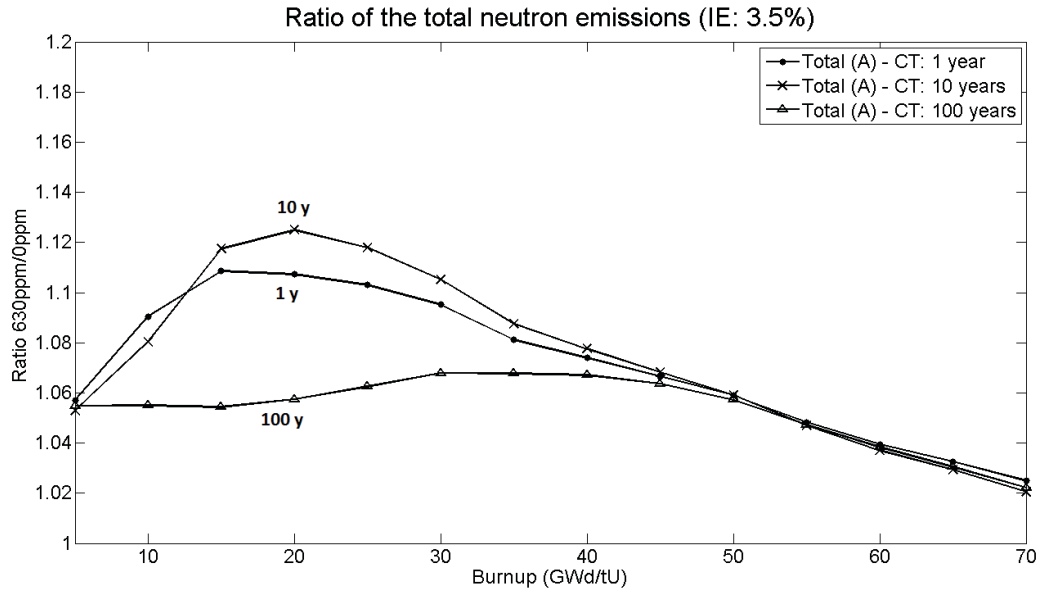


Figure 8: Influence of the boron concentration as a function of the burnup – ratio of the neutron emission. The fuel had 3.5 % initial enrichment and the ratio has been calculated for 1, 10, and 100 years of cooling time.

The presence of boron modifies the energy spectrum of the neutron flux during irradiation in the reactor. This is because boron is an absorber of thermal neutrons and therefore the contribution of epithermal neutrons to the spectrum becomes higher when boron is present in the moderator.

This induces an increase of the resonance captures and a higher production of actinides. Figure 9 shows the ratio

between the mass concentration of ^{242}Cm , ^{244}Cm , and ^{240}Pu calculated with and without boron. The fuel had an initial enrichment of 3.5% and a cooling time of 10 years. Considering that the isotopes in Figure 9 are the main neutron emitters, this explains the higher neutron emission observed in the simulations with 630 ppm of boron.

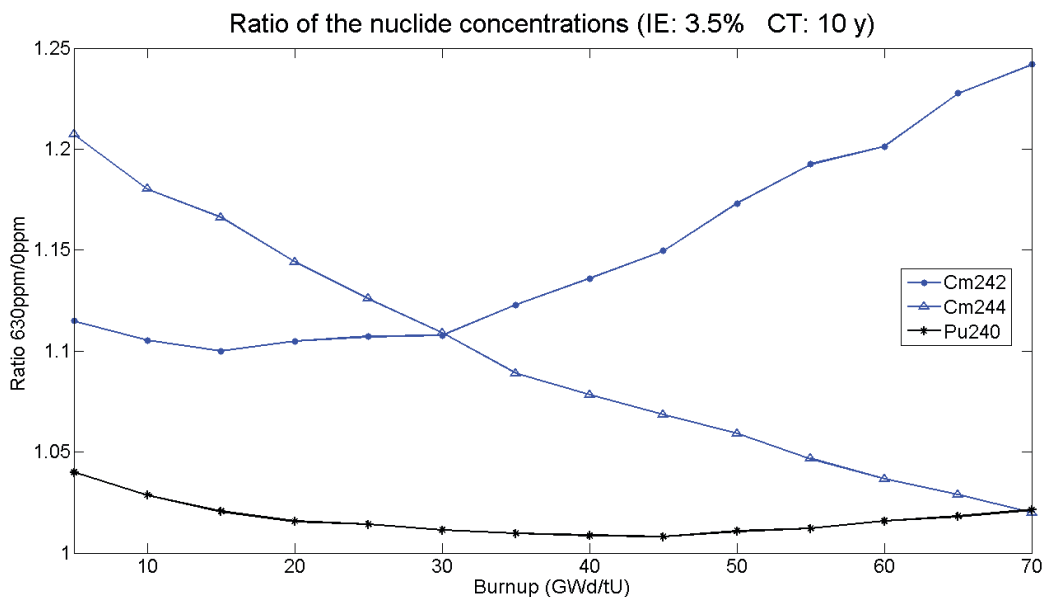


Figure 9: Influence of the boron concentration as a function of the burnup. The plot shows the ratio of the nuclide concentrations calculated with ALEPH2.2 considering fuel with 3.5% initial enrichment and 10 years of cooling time.

5.2 Water spacing between fuel assemblies

One important characteristic about the geometry of the fuel assembly is the distance between two neighbouring fuel assemblies during the irradiation in the reactor. This parameter depends on the type of fuel assembly and likely also on the particular configuration of the reactor (e.g. number of fuel assemblies in the core).

A set of simulations has been run to quantify the impact of the spacing between fuel assemblies on the concentration of the nuclides and consequently on the neutron and gamma emissions from the spent fuel. The only parameter changing in the simulations was the water

spacing between the fuel assemblies (from 0 up to 10 mm). Other characteristics were:

- The initial enrichment of the fuel was 3.5%
- The discharge burnups were 10, 35, and 60 GWd/tU
- The water in the reactor had a constant boron concentration of 630 ppm.

Figure 10 shows the total neutron emission as a function of the water spacing and discharge burnup. The ratio has been calculated normalizing all values to the neutron flux without water gap between the assemblies. From the plot it is evident that the water around the assembly influences significantly the neutron emissions. Already with a water gap of 4 mm (i.e. 2 mm for each side) the total emission is altered by 5%. However, this difference decreases with increasing burnup.

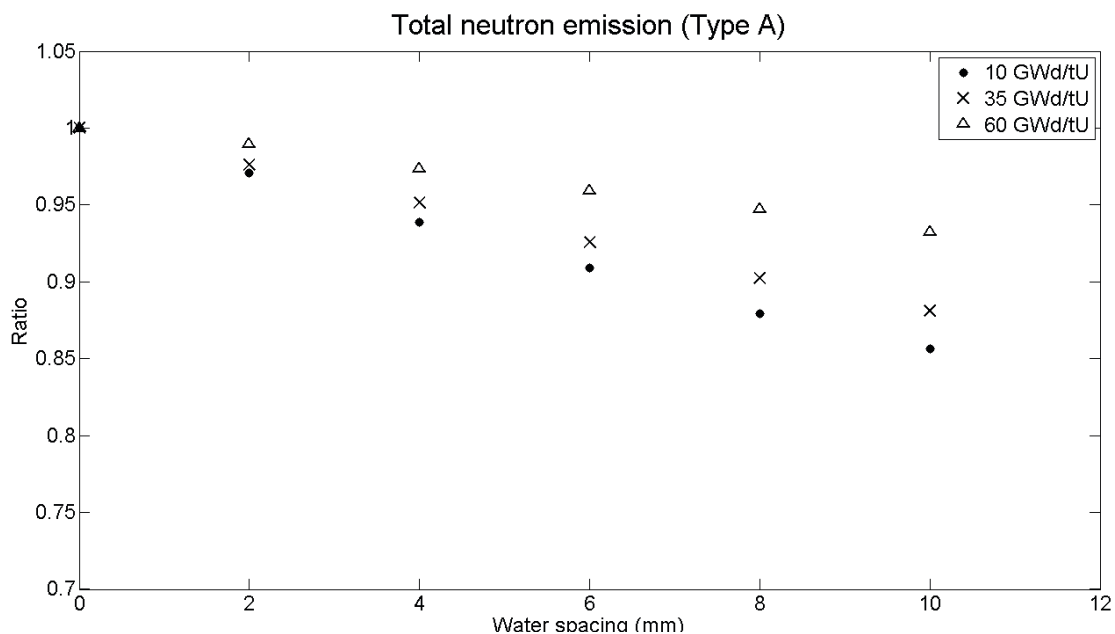


Figure 10: Total neutron emission as a function of the water spacing. The values are normalized to the case without gap between the assemblies. The fuel had 3.5% initial enrichment and the values refer to direct discharge from the reactor.

No water gap has been placed in the default simulations and this is motivated by the fact that operators try to keep uniform conditions over the whole core cross section. Therefore the pitch between outer rows of neighbouring fuel assemblies should be similar (if not equal) to the pitch of the rods within one single assembly.

5.3 Nuclear data library used in the codes

Another important parameter in the simulations is the set of data library that is used. The data libraries available in ALEPH2.2 are the ENDF/B-VII.1 [10] and JEFF-3.1.2 [11] libraries. Both libraries contain full data sets which include neutron transport data (cross sections and secondary particle emission data), radioactive decay data (which are used by the depletion module for the neutron source calculation), and fission product yields data (which are also used by the depletion module). The choice of the library influences the results because of the different values for the

evaluated nuclear data (e.g. nuclides cross sections) adopted in each data set.

Figure 11 shows the ratio of the neutron emissions at discharge calculated using the different libraries as a function of the burnup. The difference in the results is within 10%, with the simulations using the ENDF data library always overestimating the neutron emission compared to the calculations with the JEFF library.

ALEPH2.2 calculates the spontaneous fission neutron source in two ways: the first one generates the Watt fission spectrum of the neutrons for nuclides undergoing spontaneous fission, with the parameters taken from ORIGEN-S [9] ('Type A' curve in Figure 11); the second one calculates the source using the information stored in radioactive decay data library (ENDF/B or JEFF, 'Type B' curve in Figure 11). Usually, the two methods give close results, but a trend is observed for high burnup with the 'Type B'

calculations. The trend observed with the calculations arises because ALEPH2.2 recognizes a different set of isotopes contributing to the neutron emission from spontaneous fissions depending on the data library that is used in the calculation. The impact of the nuclides that are missing according to some data library (e.g. ²⁵²Cf is not used if the

data library is ENDF/B-VII.1) is not negligible and it is the reason of the trend shown in Figure 11.

It is important to mention that ALEPH is still in the development phase and there are interactions with the development team to investigate this issue.

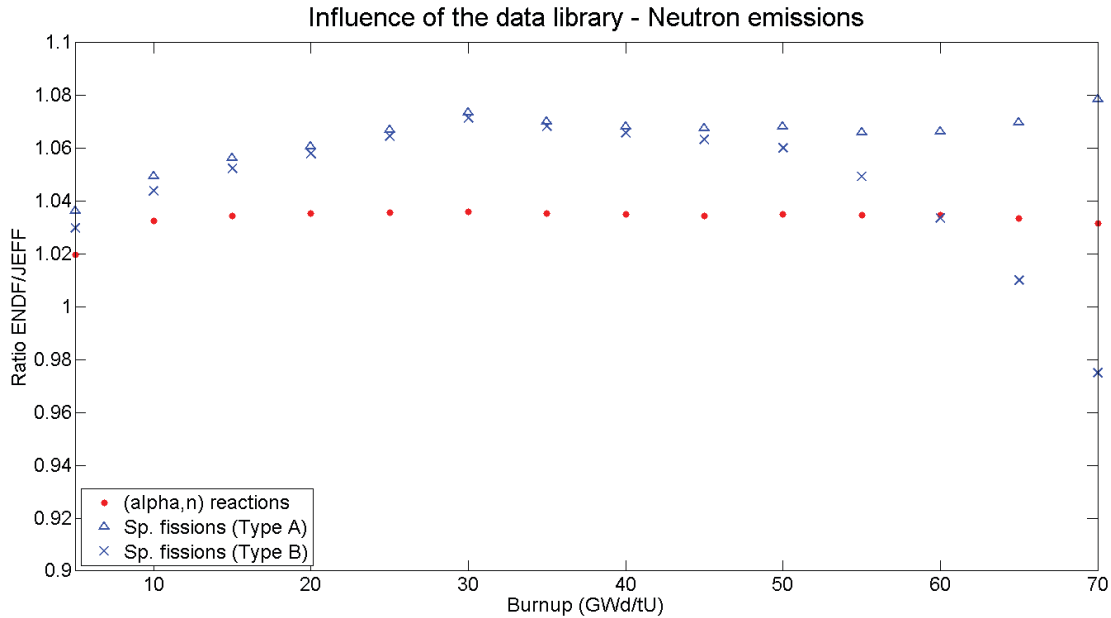


Figure 11: Ratio of the neutron emission calculated with ALEPH2.2 using different nuclear data libraries. The fuel had 3.5% initial enrichment and the values refer to direct discharge from the reactor. The contributions due to (α,n) reactions and spontaneous fission are shown.

Table 2 shows the ratio between the nuclide concentrations calculated with the two libraries available in ALEPH2.2. The values refer to the fuel with initial enrichment of 3.5% and directly after discharge.

As shown in the comparison between the two codes, also in the case of different data libraries the highest

discrepancy is found for curium isotopes (²⁴⁴Cm and ²⁴⁶Cm). The selection of the data library influences most of isotopic concentration within 5% but also for ²³⁸Pu the disagreement is higher and it increases with the burnup.

Isotope BU (GWd/tU)	cm242	cm244	cm246	u235	u238	pu238	pu239	pu240	pu241	pu242	am241
5	1.053	1.195	1.179	1.000	1.000	1.018	1.006	1.013	1.020	1.025	1.031
10	1.042	1.159	1.172	1.000	1.000	1.017	1.001	1.007	1.015	1.016	1.020
15	1.037	1.147	1.166	1.000	0.999	1.021	1.001	1.004	1.011	1.011	1.017
20	1.036	1.138	1.156	1.000	0.999	1.025	1.002	0.998	1.013	1.012	1.018
25	1.035	1.130	1.155	1.001	0.999	1.033	1.001	0.996	1.011	1.010	1.018
30	1.034	1.124	1.159	1.001	0.999	1.041	1.000	0.995	1.008	1.010	1.017
35	1.032	1.108	1.156	1.001	0.998	1.050	0.999	0.993	1.007	1.010	1.016
40	1.031	1.097	1.154	1.001	0.998	1.059	0.998	0.991	1.008	1.009	1.015
45	1.029	1.089	1.153	1.001	0.998	1.069	0.998	0.988	1.006	1.008	1.015
50	1.029	1.084	1.145	1.002	0.997	1.080	0.998	0.985	1.009	1.007	1.015
55	1.028	1.074	1.138	1.002	0.997	1.092	0.997	0.983	1.007	1.008	1.015
60	1.027	1.066	1.134	1.001	0.997	1.104	0.994	0.985	1.000	1.008	1.012
65	1.026	1.058	1.128	1.000	0.996	1.117	0.992	0.984	0.997	1.007	1.010
70	1.023	1.051	1.123	0.999	0.996	1.130	0.990	0.983	0.996	1.005	1.006

Table 2: Ratio between the nuclide concentrations obtained with the two libraries (ENDF/JEFF) as a function of the burnup. The fuel had 3.5% initial enrichment and the values refer to direct discharge from the reactor.

6. Comparison with the LANL reference spent fuel library

In the framework of the Next Generation Safeguards Initiative (NGSI), the Los Alamos National Laboratory developed several reference spent fuel libraries [12], [13].

Since the geometry of the fuel assembly is the same as the one chosen for our case, it is possible to compare the results of the neutron emissions obtained with their calculations. However, of all the libraries developed by LANL, only the first one is relevant for the comparison since it assumed a uniform composition and irradiation conditions for the complete fuel assembly.

There are three combinations of initial enrichment, burnup, and cooling time that are coincident between our library and their case:

- Case 1 - IE: 4% BU: 30 GWd/tU CT: 5 years
- Case 2 - IE: 4% BU: 45 GWd/tU CT: 5 years
- Case 3 - IE: 5% BU: 60 GWd/tU CT: 5 years

The comparison focused on the neutron emissions of the main contributors and on the total neutron emissions.

The next table shows the ratio between the values calculated by Los Alamos (LA) and with ALEPH2.2 (ALE) or ORIGEN-ARP (ORI). They contain also the ratio between the values obtained with ORIGEN-ARP and ALEPH2.2 (column ORI/ALE).

IE:	4.00%	BU:	30 GWD/tU	CT:	5 years				
Nuclide	ORI/ALE			LA/ALE			LA/ORI		
	(α,n)	Sp. Fiss.	Total	(α,n)	Sp. Fiss.	Total	(α,n)	Sp. Fiss.	Total
pu238	0.8101	0.9642	0.8314	0.8098	0.9483	0.8290	0.9996	0.9835	0.9970
pu239	0.8288	0.9720	0.8289	0.8473	0.9737	0.8474	1.0223	1.0017	1.0223
pu240	0.8150	0.9963	0.9704	0.8350	1.0020	0.9781	1.0245	1.0057	1.0080
pu242	0.8628	1.0182	1.0180	0.8776	1.0163	1.0161	1.0171	0.9981	0.9981
am241	0.8039	0.9981	0.8040	0.8374	1.0191	0.8375	1.0417	1.0210	1.0417
cm242	0.8193	1.0119	0.9751	0.8377	1.0142	0.9805	1.0224	1.0022	1.0055
cm244	0.8556	1.0044	1.0032	1.1653	1.3454	1.3439	1.3619	1.3394	1.3396
cm246	-	0.7414	0.7414	-	1.5552	1.5552	2.1419	2.0976	2.0976
Total	0.8202	1.0036	0.9968	0.8954	1.3368	1.3205	1.0918	1.3320	1.3247

IE:	4.00%	BU:	45 GWD/tU	CT:	5 years				
Nuclide	ORI/ALE			LA/ALE			LA/ORI		
	(α,n)	Sp. Fiss.	Total	(α,n)	Sp. Fiss.	Total	(α,n)	Sp. Fiss.	Total
pu238	0.7745	0.9219	0.7949	0.8058	0.9347	0.8236	1.0404	1.0138	1.0361
pu239	0.8317	0.9753	0.8317	0.8553	0.9740	0.8554	1.0284	0.9987	1.0284
pu240	0.8218	1.0044	0.9783	0.8390	0.9971	0.9745	1.0209	0.9927	0.9961
pu242	0.8377	0.9886	0.9884	0.8738	1.0023	1.0022	1.0432	1.0139	1.0139
am241	0.7897	0.9803	0.7898	0.8422	1.0152	0.8423	1.0665	1.0356	1.0664
cm242	0.7987	0.9864	0.9505	0.8768	1.0511	1.0178	1.0978	1.0657	1.0708
cm244	0.8387	0.9845	0.9833	1.1283	1.2898	1.2885	1.3454	1.3100	1.3103
cm246	0.5935	0.7145	0.7145	1.2754	1.4891	1.4891	2.1489	2.0843	2.0843
Total	0.8077	0.9826	0.9795	0.9546	1.2880	1.2819	1.1819	1.3108	1.3088

IE:	4.00%	BU:	45 GWD/tU	CT:	5 years				
Nuclide	ORI/ALE			LA/ALE			LA/ORI		
	(α,n)	Sp. Fiss.	Total	(α,n)	Sp. Fiss.	Total	(α,n)	Sp. Fiss.	Total
pu238	0.7619	0.9071	0.7820	0.8037	0.9239	0.8203	1.0549	1.0186	1.0491
pu239	0.8314	0.9750	0.8315	0.8595	0.9699	0.8595	1.0337	0.9948	1.0337
pu240	0.8230	1.0059	0.9798	5.9134	0.0000	0.8451	7.1853	0.0000	0.8625
pu242	0.8308	0.9805	0.9803	0.8767	0.9969	0.9968	1.0552	1.0168	1.0168
am241	0.7887	0.9788	0.7888	0.8472	1.0117	0.8472	1.0741	1.0336	1.0741
cm242	0.8020	0.9905	0.9545	0.8840	1.0508	1.0189	1.1023	1.0609	1.0675
cm244	0.8375	0.9833	0.9820	1.1116	1.2598	1.2585	1.3273	1.2812	1.2816
cm246	0.5893	0.7095	0.7095	1.2601	1.4586	1.4585	2.1382	2.0557	2.0557
Total	0.8049	0.9798	0.9771	0.9659	1.2569	1.2523	1.2000	1.2828	1.2818

Table 3: Comparison between the neutron emission due to specific isotopes (as well as the total values) reported in the LANL reference spent fuel library, and the ones calculated with ALEPH2.2 (LA/ALE) and ORIGEN-ARP (LA/ORI). The data from the comparison between ORIGEN-ARP and ALEPH are also reported (ORI/ALE). The values of initial enrichment, burnup, and cooling time are shown at the top of each table.

The agreement with the LANL fuel library is very good for ^{240}Pu and ^{242}Pu (all values within 5%), while there are different results with the other isotopes. The LANL fuel library generally has higher values ($\approx 15\text{--}30\%$) compared to the ones calculated with ORIGEN-ARP and ALEPH2.2 and this induces higher total neutron emissions as well.

From information available on the report on the LANL spent fuel library we can highlight some similarities and differences that can explain in part the discrepancy in the results:

- The boron concentration in the water was 660 ppm for the LANL simulations whereas we used a concentration of 630 ppm.
- The fuel, moderator, and cladding temperatures are the same for both libraries.
- The only geometric parameters that change are the length (365.76 cm for LANL, 100 cm for ALEPH cases) and the pellet radius (0.41 cm for LANL, 0.4025 cm for ALEPH).
- There are four radial subdivisions for the fuel pellet modelled by LANL.
- The average power during irradiation is 38 MW/tU instead of 40 MW/tU used in our cases.
- The simulations done by LANL considered irradiation cycles of 420.3 days, apart from the last irradiation cycle that is reduced to 312.3 days.
- Each irradiation cycle of the LANL library determines an additional burnup of about 15 GWd/tU to the fuel assembly.
- The nuclear data library used by the LANL cases was the ENDF/B-VII.0, whereas the ORIGEN-ARP cases used data from ENDF/B-VI.2 and the ALEPH simulations from the ENDF/B-VII.1 data set.

Apart from the factors included in the previous list, the difference in the results can be determined also by other characteristics that are not contained in the LANL report.

7. Conclusions

A reference spent fuel library has been built using the software ORIGEN-ARP and ALEPH2.2 to provide some insights of the different isotopes relevant for neutron emission. A comparison of the two codes has been performed to check their consistency and the reasons of possible discrepancies.

The neutron emission increases with increasing burnup, whereas there is an opposite trend with initial enrichment and cooling time. Apart from very low burnup values, the spontaneous fissions are the main contribution to the total neutron emission, with (α, n) reactions accounting for the remaining.

By looking at the role played by individual isotopes, it is clear that the main contributors are the curium isotopes

(^{242}Cm and ^{244}Cm are very important up to 100 years of cooling time, while ^{246}Cm and ^{248}Cm arise at high burnup). At low burnup and also at high cooling times there are significant contributions from plutonium isotopes (especially ^{240}Pu and ^{242}Pu). As a general consideration, there are always less than 10 isotopes that combined are responsible for about 99% of the total neutron emissions. Only for cooling times higher than 10000 years more isotopes have relevant contributions.

The build-up of several actinides (such as the Cm isotopes) explains the trend of the neutron emission with initial enrichment, burnup, and cooling time of the spent fuel. In fact, decreasing the initial enrichment or increasing the burnup will lead to a higher fluence level, a higher production of actinides and therefore to a higher neutron emission.

Comparing the two codes used in the simulations, the general agreement is rather satisfactory since the total neutron emission values are within 15%. This is due to a different concentration of actinides calculated by the two codes and possibly also to approximations applied in both models.

The boron added to the water during irradiation in the reactor core is also playing a role, although reduced compared to the main variables associated to the irradiation of the spent fuel (IE, BU, CT).

The presence of boron determines the hardening of the neutron energy spectrum during the irradiation in the reactor. This induces an increase of the resonance captures and a higher production of actinides. The results show that the addition of 630ppm of boron increases the total neutron emission of about 10%. Other important parameters that affect the calculated composition of the spent fuel are the water spacing between neighbouring fuel assemblies during the irradiation in the reactor (decrease of the total neutron emission of roughly 1% for each mm of gap) and the nuclear data library that is used in the calculations (10% on the total neutron emission).

The library has been compared with one reference spent fuel library made by LANL. There are three comparable cases (i.e. same IE, BU, and CT) and the comparison showed good agreement (difference lower than 5%) for some plutonium isotopes, but a larger discrepancy for the curium isotopes ($\approx 30\%$).

8. Acknowledgements

This work is sponsored by GDF SUEZ in the framework of the cooperation agreement CO-90-07-2124 between SCK•CEN and GDF SUEZ.

9. References

- [1] International Atomic Energy Agency (IAEA), “*Spent Fuel Reprocessing Options*”. IAEA-TECDOC-1587. August 2008
- [2] International Atomic Energy Agency (IAEA), “*Addressing Verification Challenges. Proceedings of an International Safeguards Symposium*”. Vienna, 16-20 October 2006
- [3] S. J. Tobin et al., “*Next Generation Safeguards Initiative research to determine the Pu mass in spent fuel assemblies: Purpose, approach, constraints, implementation, and calibration*”. Nuclear Instruments and Methods in Physics Research A 652 (2011) 73-75. September 2010
- [4] Oak Ridge National Laboratory (ORNL), “*RSICC COMPUTER CODE COLLECTION – MCNP5/MCNPX*”. CCC-740. June 2011
- [5] D.B. Pelowitz et al., “*MCNPX User’s Manual, Version 2.7.0*”. LA-CP-11-00438. April 2011
- [6] I. Gauld, S. Bowman, J. Horwedel. “*Origen-ARP: automatic rapid processing for spent fuel depletion, decay, and source term analysis*.” ORNL/TM-2005/39. January 2009
- [7] Oak Ridge National Laboratory (ORNL), “*SCALE: A Modular Code System for Performing Standardized Computer Analyses for Licensing Evaluation*”. ORNL/TM-2005/39. January 2009
- [8] A. Borella et al., “*Spent Fuel Measurements with the Fork Detector at the Nuclear Power Plant of Doel*”, 33rd ESARDA Symposium, Budapest, May 2011
- [9] A. Stankovskiy, G. van den Eynde. “*ALEPH 2.2 A Monte Carlo Burn-up Code*”. SCK•CEN-R-5267. September 2012
- [10] M.B. Chadwick et al., “*ENDF/B-VII.1 Nuclear Data for Science and Technology: Cross Sections, Covariances, Fission Product Yields and Decay Data*”, Nuclear Data Sheets Volume 112, Issue 12. December 2011
- [11] Nuclear Energy Agency (NEA), “*The JEFF-3.1.1 Nuclear Data Library*”, JEFF Report 22, OECD/NEA, Paris (2009), and “*The JEFF-3.1 Nuclear Data Library*”, JEFF Report 21, OECD/NEA, Paris (2006)
- [12] J. Richard, “*Summary of Summer Work: Analysis of the Neutron Source Term of a Spent Fuel Assembly*”, LA-UR-10-00075. September 2009
- [13] H. R. Trellue et al., “*Description of the Spent Nuclear Fuel Used in the Next Generation Safeguards Initiative to Determine Plutonium Mass in Spent Fuel*”, LA-UR-11-00300. December 2010

Seismic monitoring of an Underground Repository in Salt - Results of the measurements at the Gorleben Exploratory mine

Jürgen Altmann

Experimentelle Physik III, Technische Universität Dortmund, 44221 Dortmund, Germany

Abstract:

We have measured seismic and acoustic signals from various mining activities in the Gorleben exploratory mine in Germany, underground at -840 m and at the surface, tasked by the German Support Programme to the IAEA, in order to provide basic knowledge on the detectability of undeclared activities. During 7 weeks total nearly all sources of sound and vibration available in the mine were covered, with sensors at several positions and sources at several sites, sometimes with background signals from on-going exploration elsewhere.

The peak-to-peak values of vibration velocity, referred to 100 m distance, range from tenths of micrometres/second for a hand-held chain saw via few $\mu\text{m/s}$ to tens of $\mu\text{m/s}$ for other tools such as picking, for vehicles, drilling and sledge-hammer blows. A grader with compactor plates produces hundreds, and a blast shot around one hundred thousand $\mu\text{m/s}$. The last two sources could be detected at the surface, too, at about 1.1 km slant distance; blasts were even seen at 5-6 km distance. The signal strengths vary by a factor 2 to 5 for similar conditions. Fitted by a power law, the decrease with distance is with an exponent mostly between -2 and -1.

Spectra of seismic signals from periodic sources (such as percussion drilling or vehicle engines) show harmonic series. Rock removal, e.g. by drilling, produces broad-band excitation up to several kilohertz. Acoustic-seismic coupling is relevant.

Monitoring could be done with an underground geophone "fence" around the repository, e.g. 500 m from the salt-dome margin and possibly in the salt 1 km off the repository. With that excavation by drilling and blasting could be detected by a simple amplitude criterion. Under which conditions excavation by tunnel boring machine or road header machine and other weaker activities could be detected needs to be studied.

Keywords: final repository, salt, seismic monitoring, mining, Gorleben

1. Introduction

In the case of direct disposal spent nuclear fuel contains plutonium, thus such material should remain under IAEA

safeguards even after emplacement in an underground final repository. Underground final disposal of nuclear waste presents a new challenge for safeguards and has led to proposals of using geophysical techniques and methods for monitoring [e.g. 1, 2, 3]. During operation, the tasks would include monitoring for creation of undeclared cavities and surveillance of those parts of the mine already filled with refuse for undeclared re-opening. After the emplacement phase, when drifts and shafts will have been closed, and the above-ground parts of the final repository will have been cleared for other uses, the IAEA needs the capability of long-term monitoring for covert access to the mine.

Mining and other underground operations produce seismic vibrations directly as well as via acoustic noise. Seismic excitation propagates through the ambient medium and can thus be used to detect activities remotely. The main question with seismic monitoring is whether signals from undeclared activities can be detected, that is separated from signals from different sources and from other background noise. In the operational phase of the repository most noise stems from normal activity (mining, transport, filling, etc.), and sensors can be deployed at many sites in the mine. After closure, no sensors and cables can remain in the mine; in this phase sensors will be located at considerable distance from the repository, deep underground and maybe also near the surface. Seismic background will be much lower, produced no longer by activities in the mine; the remaining sources at the surface are traffic, industry, agriculture and weather, plus seismicity proper (near and far earthquakes and underground explosions). For answering the question about detection and discrimination, the first task is to determine the characteristics of the signals from various mining activities and of their propagation to potential sensor locations. This was the goal of the measurement project described here.

Seismic monitoring of underground final repositories has been studied only rarely. In Yucca mountain, formerly planned as a repository for the US, where the rock is tuff, vibration caused by a tunnel-boring machine was measured at the surface [4]. A study of the issues for detecting undeclared excavation discussed many basic questions, dealing mainly with granite [2]. The Canadian Safeguards

Support Program had a theoretical investigation done based on experiences with microseismic monitoring systems in working mines where events such as blasts and excavation-induced seismicity are classified and localized [5]. A local seismic network has been monitoring the excavations at the Onkalo planned repository in Finland for many years [6]. With its focus on the localisation of blasts it could follow the tunnel advance well, but raise boring and other continuous activities have not been studied systematically yet.

One potential repository site in Germany is the Gorleben salt dome; it has been explored for its usability since 1986 under contract to the Federal Office for Radiation Protection (BfS) by the firm Deutsche Gesellschaft zum Bau und Betrieb von Endlagern für Abfallstoffe mbH (DBE). It extends from 3.2 to 0.3 km depth (Figure 1).

Not much is known about seismic signals from mining activities in salt – neither at close range within salt nor after propagation through the surrounding sediment layers. Some seismic measurements had been done on the Gorleben site in the 1990s during sinking of the first shaft, using a temporary geophone network. These measurements were mainly directed at propagation velocities [8]. A

network of borehole seismometers around the site (with 5 to 15 km distance) is operated continuously, also by the Federal Institute for Geosciences and Natural Resources (BGR), but this concentrates on the earthquake-safety aspect [e.g. 9].

In order to gain information on the properties of seismic signals from mining activities, a dedicated measurement project was carried out at Gorleben, tasked by the German Support Programme to the IAEA. The objective was to measure and characterise all sources of vibration available in the exploratory mine at Gorleben. Because seismic signals are also produced by acoustic ones, microphones were deployed, too. Sensors were placed underground and near the surface, at different positions and source distances. Signals from typical mining activities as well as background noise were recorded by geophones, low-frequency accelerometers and microphones. The presentation here focuses on the geophone measurements. (High-frequency recordings were made in parallel by the Fraunhofer Institute for Non-Destructive Testing Dresden; these are not treated here but are part of the common JOPAG report published by the German Support Programme to the IAEA [10].)

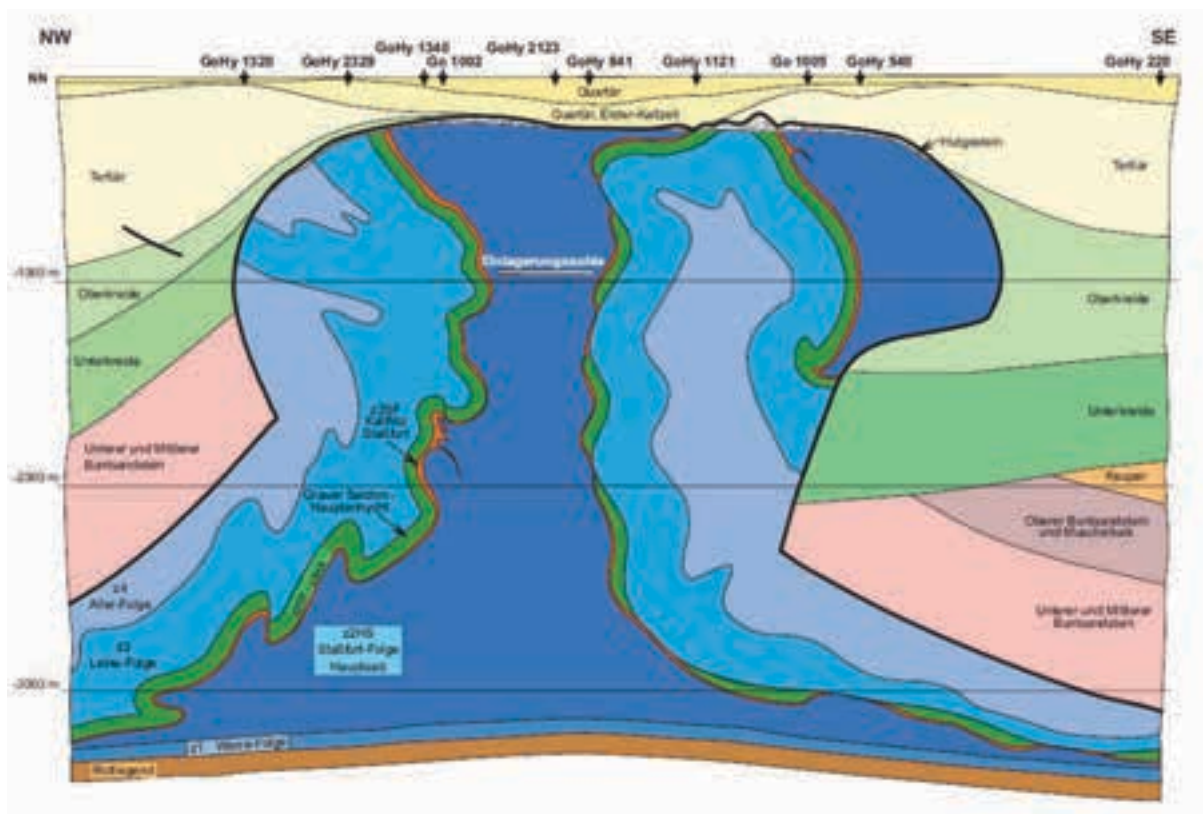


Figure 1: Simplified geological cross section through the Gorleben salt dome. Indicated is a possible repository level at about 930 m depth. The main exploration tunnels are at 840 m. (From [7], © Federal Institute for Geosciences and Natural Resources (BGR), Hannover, reproduced by permission)

2. Measurements

The main measurement systems were deployed in the drift system at 840 m depth (Figure 2). Here nearly all activities took place as well. (Spent fuel would be stored somewhat more deeply.) In addition a measurement system was deployed at the surface. The sampling rate was 10 kHz throughout, with 16+8 analogue channels recorded underground and 8 at the surface. The underground sensors (geophones sensing vibration velocity, some three-dimensionally, others vertically sensitive only) were bolted to the salt-rock wall. At the surface geophones were buried about 0.2 m deep; in addition one plus three of the old on-site BGR geophones in about 7 m deep wells were used. The recorded-signal bandwidth was a few hertz to 4.5 kilohertz. All stations were synchronised by pulses derived from GPS signals.

After a test experiment of one week in April 2011 the main measurements were done during three weeks each in June/July 2011 and in November/December 2011. Nearly all sources of vibration and sound available in the mine could be measured somehow, but not all of them under good conditions – the use of equipment at certain locations was decided by the operational needs of the mine. In some cases sources were too far away to yield useful signals, in others more than one source was active at the same time near the sensors so that one source masked the other. The following main categories were measured: blast shots, vibrating compactor plate, transport installations/activities, drilling rigs, scaler, roof cutter, heavy to light vehicles and hand tools. To produce impulse-type signals a sledge hammer was used for excitation of seismic waves and balloon blasts for acoustic ones.

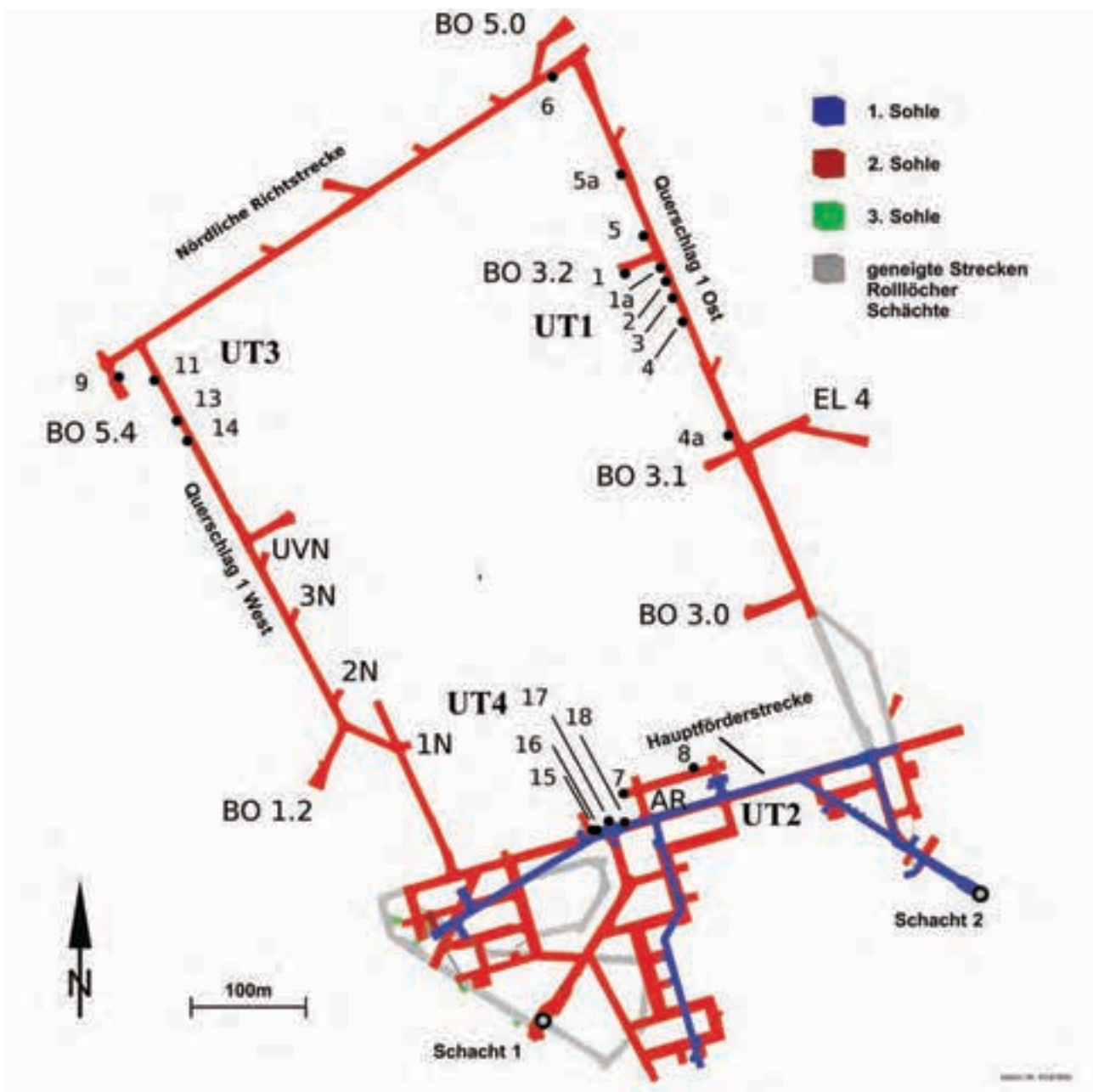


Figure 2: Gorleben exploratory mine, main drift system at 840 m depth, consisting of the “Hauptförderstrecke”, “Querschlag 1 Ost”, “Nördliche Richtstrecke” and “Querschlag 1 West”. Two shafts (“Schacht 1/2”) provide access. Indicated are the Dortmund underground measurement stations (UT1, UT2, UT3, UT4) and sensor positions (numbers); not all were used at the same time. Abbreviations for particular locations: AR: “Arbeitsraum”, BO “Bohrort” (BO), N niche. (Based on figure provided by DBE)

3. Some results

Here the most important results are given.¹ Full detail is contained in the JOPAG report [10]. The signal strength is measured mostly by the peak-to-peak value because the root-mean-square value is only sensible for continuous sources. These values show considerable variation with source and sensor positions even if the mutual distance is similar. A statistical evaluation of exactly the same propagation paths was done only for one source (Section 3.2). The variability shows up as scatter in the graphs of strength versus distance, and the trends derived have considerable uncertainties.

3.1 Wave speeds

Of fundamental importance are the wave speeds because they determine the arrival times of signals and the reflection and refraction at media boundaries. They depend on the elastic constants and the density of the material. For seismic waves (that is waves in an elastic solid) the fastest wave is the compressional or longitudinal one where the particle motion is in the direction of propagation. Shear or transversal waves are slower, here the motion is orthogonal to the propagation direction. The speeds of these primary (P) and secondary (S) waves are [e.g. 11: 238-243]

$$c_p = [(\lambda + 2\mu)/\rho]^{1/2} \quad \text{and} \quad c_s = [\mu/\rho]^{1/2},$$

respectively. Here λ and μ are the Lamé constants describing the relation between strain and stress of an isotropic elastic medium, and ρ is the density. (Waves along a surface are somewhat slower than S waves.) The first equation also applies to fluids where shear waves do not exist ($\mu = 0$).

Hammer blows were applied to various positions along a drift and recorded by several geophones. From the onsets of the primary (P) and the secondary (S) waves the seismic speeds in the central salt were determined by linear fits to be (4.52 ± 0.06) km/s for the P wave and $(2.590.04)$ km/s for the S wave (95% confidence intervals assuming normal distribution). The ratio is equal to the theoretical value of $\sqrt{3}$ for a medium where the Lamé constants λ and μ are equal.

Similarly, onset times of the sound wave from balloon blasts resulted in a sound speed of (351 ± 5) m/s, fitting well to the theoretical value for dry air at 30°C temperature.

3.2 Seismic-background amplitudes

The simplest way of seismic detection of a certain activity is by the amplitude rising above some threshold. For a high detection range the threshold needs to be low, but this has its limit by the background noise; to avoid too many false alarms the threshold is usually set at some

factor above 1 times the background amplitude. The seismic background is thus another important characteristic.

The seismic background was determined at relatively quiet periods, however with some machinery such as ventilators and the shaft haulage running at distant positions. The peak-to-peak values of wall velocity underground, in the main drift system at 840 m depth, varied between positions considerably, from a few tenths of a $\mu\text{m/s}$ to several $\mu\text{m/s}$, for the vertical as well as horizontal components. However, at one position in a drift (Pos. 2 in Figure 2) there was much higher excitation with strong temporal variation (time scale of a second) between a few $\mu\text{m/s}$ and nearly 100 $\mu\text{m/s}$, different from two other positions (Pos. 1a and 5) only 20-30 m away; the reason is unclear. The background peak-to-peak values when the mine was active were in the same range, between 0.6 and 10 $\mu\text{m/s}$, during a certain period, as can be derived by multiplying the comparison root-mean-square values of Figure 7 below by a factor eight.

For the post-operational phase it is important to know the background at positions at several hundred metres depth without any activity in the mine. Such conditions did not exist during the measurements. Obviously the lowest value observed is an upper bound. It seems plausible that the background peak-to-peak value (with a bandwidth from a few hertz to a few kilohertz) is around 0.1 $\mu\text{m/s}$.

At the surface the background during quiet periods was between 1.5 and 3 $\mu\text{m/s}$ peak to peak for the geophones at 0.2 m depth and 1-2 $\mu\text{m/s}$ at 7 m depth. During a period of heavy rain the general background increased to about 15 $\mu\text{m/s}$ in 0.2 m and to 3-5 $\mu\text{m/s}$ in 7 m depth, with individual pulses – probably from single big raindrops – between 70 and 150 $\mu\text{m/s}$ in 0.2 m depth.

Similar values would probably hold during the operational phase should Gorleben be selected. The background at the surface from human activity thereafter will depend on the land use; for weather-produced background no change is expected. Its relatively high values argue against relying mainly on sensors at or close to the surface.

3.3 Variability between sensor positions

Variation between the seismic-signal strengths with position was not only observed with the background, but also with the sources observed. Systematic evaluation was done with signals from picking by an electropneumatic pick hammer (breaker, Hilti TE 1000-AVR) at one site, recorded after travelling from the western to the eastern drift through about 430 m of salt. Because the picking-caused amplitudes did not dominate the signals, the latter were high-pass filtered with 500 Hz corner frequency; spectral analysis had shown that most of the power from picking was between 500 Hz and over 3 kHz. Figure 3 shows the

¹ With slight corrections and modifications of the presentation at the ESARDA 2013 Symposium.

peak-to-peak values of the filtered signals during picking after subtraction of the ones before/after picking at different sensor positions of approximately equal distance, with their respective standard deviations resulting from 5 to 8 usable picking events each. At sensor Positions 1, 1a, 3, 5 and 6 the variation among the events is reasonably low, with standard deviations between 10 and 20%, and the mean values agree among the positions. The higher values at Position 5a are consistent, as are the very low values (around $0.3 \mu\text{m/s}$) measured at Position 2. The latter seem to have nothing to do with the very strong low-frequency background at this position. Since all

geophones were mounted at the same height (1 m) by holders of the same type, the most plausible reason for the variation is the rock structure.

One can conclude that the seismic-signal strength of the same event measured at various positions of approximately equal distance can vary considerably, here by a factor 0.3 to 1.5. This variability should be taken into account for example when estimating detection ranges. As a consequence signal strengths are mostly presented in logarithmic scale, and decrease with distance needs two or more orders of magnitude to be taken as valid.

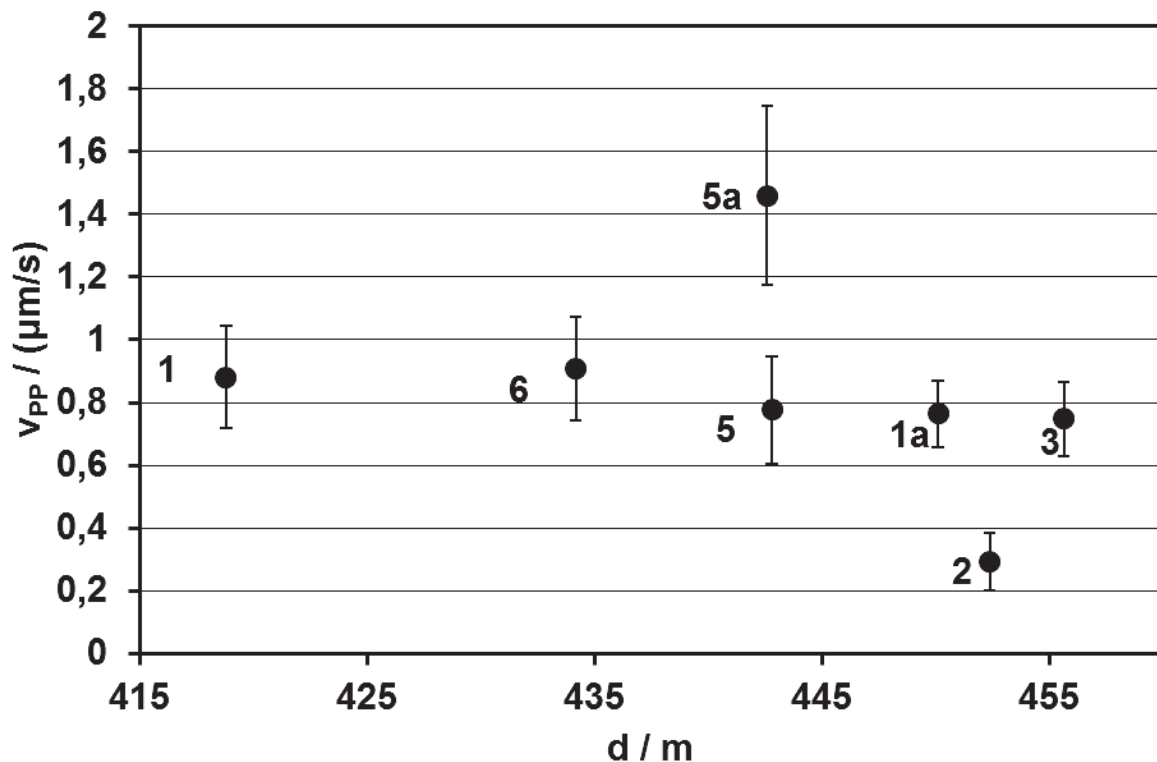


Figure 3: Peak-to-peak value of vertical wall velocity at various sensor positions (indicated by the numbers) of Dortmund station UT1 during eight picking events at the same position (northern corner of “Querschlag 1 West”, length coordinate 510 m), versus sensor distance, determined by high-pass filtering with 500 Hz corner frequency and subtraction of the peak-to-peak values before/after picking, in linear scale. Shown are the mean values plus/minus the standard deviations ($N = 7$ mostly, $N = 8$ twice, $N = 6$ and $N = 5$ once each).

3.4 Amplitude decrease with distance

Because of the strong signal-strength variation only changes above 30-50% are relevant, and the graphics use logarithmic scale. For a seismic volume wave propagating from a point source spherically into a homogeneous medium, due to energy conservation and geometrical expansion, one expects a decrease of intensity (power per area) with distance r in proportion to $1/r^2$. Since intensity is proportional to amplitude squared, the amplitude decreases in proportion to the inverse of the distance, that is, according to a power law with exponent -1. Often the wave energy is reduced by absorption and scattering. This is described by an additional factor that decreases exponentially with distance; the attenuation coefficient often increases linearly with frequency.

The present case is much more complicated. The medium is inhomogeneous with reflection and refraction, several wave types may be excited, shafts and drifts can block a direct seismic path but present an acoustic waveguide with weaker decrease of sound amplitude with distance than the r^{-1} dependence valid for free space. Sound impinging on shaft and drift walls can cause them to vibrate; acoustic resonances in the cavities may further complicate the picture. The sources may be extended with a complicated spatial and temporal dependence, they may be driven with different force in varying directions.

To roughly catch the losses due to geometric expansion, if needed refraction and reflection at media boundaries, and attenuation, a simple model is used: the empirical

decrease of peak-to-peak value of wall vibration velocity v_{PP} with distance d is described by a power law

$$v_{PP}(d) = v_{PP}(d_0) \left[\frac{d}{d_0} \right]^a$$

where the exponent a and the value at the arbitrary reference distance d_0 are gained from a fit to an appropriately selected sub-set of the observed data pairs, analogously for the rms value. (The scatter in the measured data generally is too big to separately determine the exponential attenuation.) Plotted in double-logarithmic scale a power law gives a line, its slope is the exponent a . The empirical power-law exponent of distance thus derived is normally lower than the simple theoretical one of -1. Due to the variation of the signal strengths the exponent is questionable if the strength values span less than two orders of magnitude.

3.4.1 Blast shots

Figure 4 shows three underground signals from a blast at "Bohrort 5.0", using 130 kg of explosive in 24 drill holes of 5 m length. As best seen in the centre trace, there were 12 individual shots with 0.25 s delay. The signal is 4 orders of magnitude above the noise at about 30 m and 2-3 orders at about 200 m. Figure 5 shows the signals at the

surface after propagation through about 800 m of salt and 300 m of overlying sediment; here the individual shots are no longer discernible, but the signal is still 1-2 orders of magnitude above the noise. Blast shots were even visible at 5-6 km distance at the seismometers in 300 m deep boreholes (with accordingly less background noise), here the signal-to-noise ratio (at much lower bandwidth) had decreased to 1-3.

Systematic amplitude evaluations were done with the blast of 1 December 2011 (several shots distributed over about 2 seconds) and a contour blasting of 6 December 2011 (one single shot only). Figure 6 shows the maximum peak-to-peak values of vertical wall or ground velocity. A clear trend can be seen from 140 to 1100 m, here the power-law exponents are -2.3 ± 0.6 and -2.1 ± 0.5 (95% confidence intervals assuming normal distribution), respectively, much below the theoretical value of -1. Combining both sets gives -2.2 ± 0.3 . The closest and the farthest distances are excluded from the fit. The sensor at 45 m distance is at the opposite wall of the adjoining drift, so that it was located in the seismic shadow of the drift. The signals from the BGR seismometers at 5 and 6 km have much narrower bandwidth (their sampling rate is 100 Hz), so they fall outside of the trend, too.

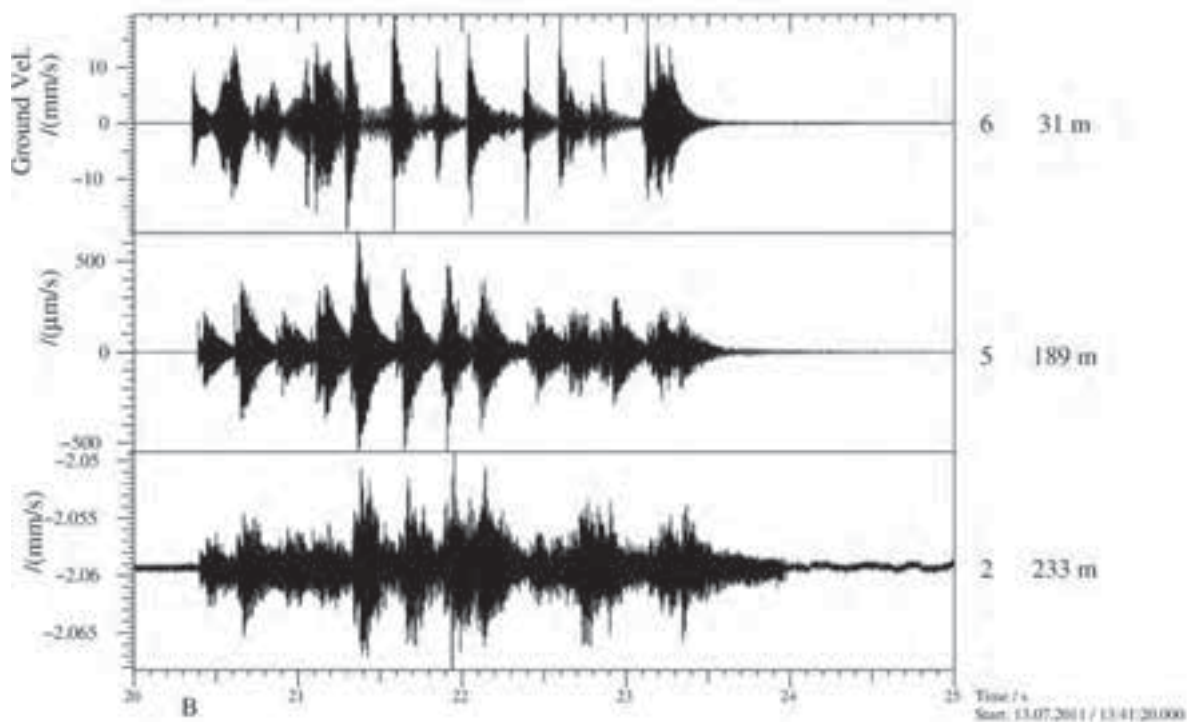


Figure 4: Signals of vertically sensitive underground geophones near site "Bohrort 3.2" during the blast at site "Bohrort 5.0" of 13 July 2011; the blast occurred at 13:41:36.25 CEST ("B"). Positions and slant source-sensor distances are indicated at the right. At Position 2 (bottom) the amplitude is uncertain due to the high DC offset. The 12 individual shots are best seen in the trace of Position 5 (centre). (The PC time at the axis is 15.91 s too low.)

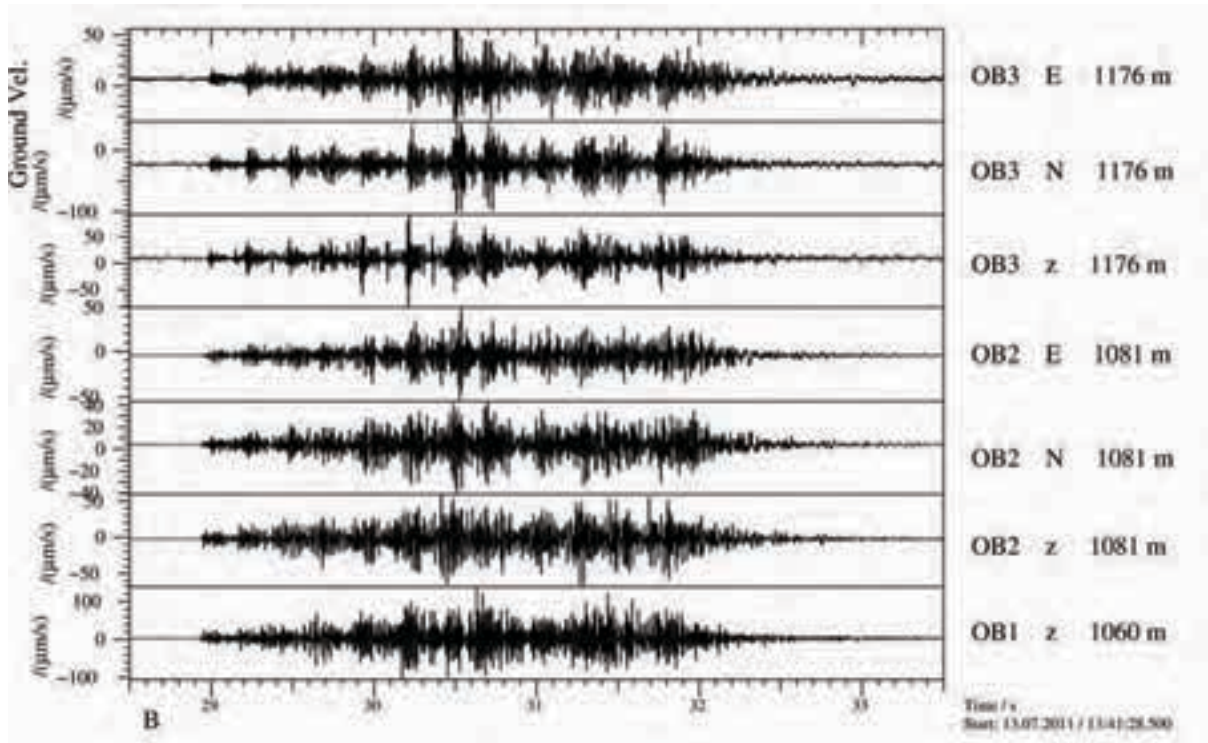


Figure 5: Geophone signals at the Dortmund surface station from the blast shot at site “Bohrort 5.0” of 13 July 2011. The blast occurred at 13:41:36.25 CEST (“B”). Positions, geophone directions (z vertical, N north, E east) and slant source-sensor distances are indicated at the right. At Positions OB1 and OB2 there were old BGR geophones in about 7 m depth, at Position OB3 Dortmund geophones were buried at 0.2 m. (The PC time at the axis is 7.63 s too low.)

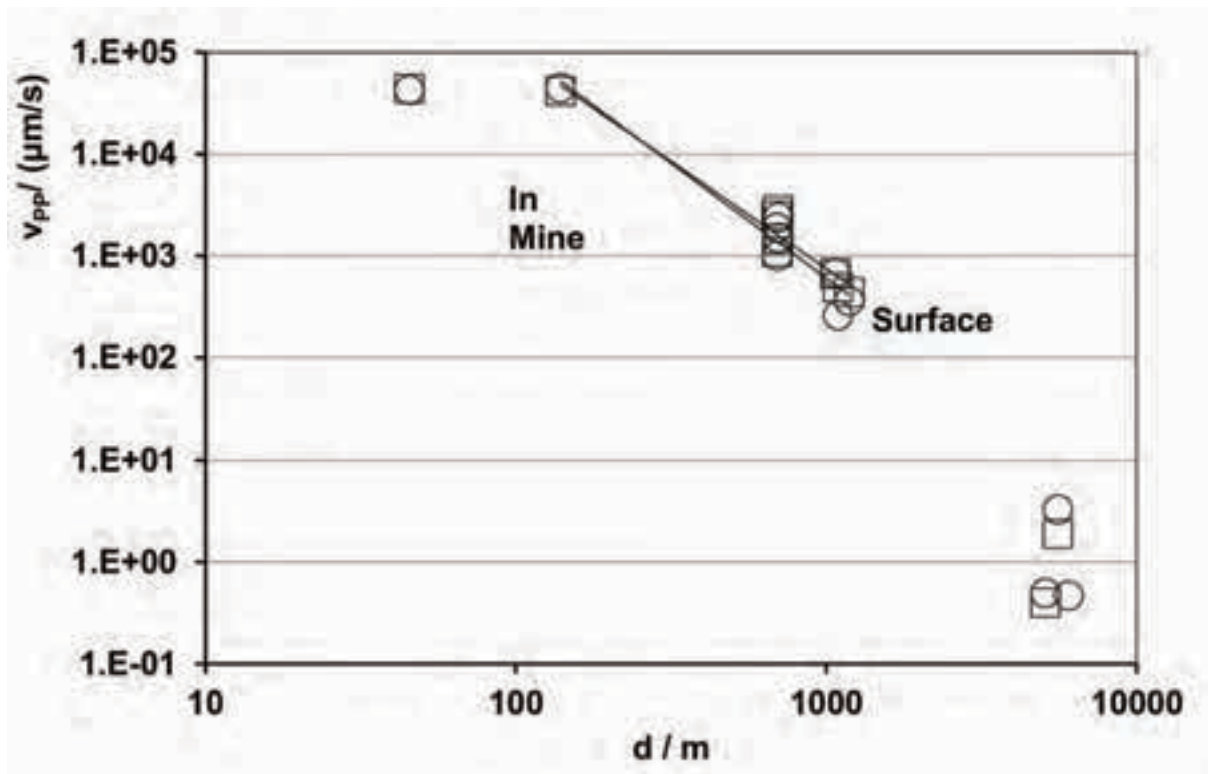


Figure 6: maximum peak-to-peak value of vertical wall/ground velocity from blasting versus distance for the events of 1 December (several shots, circles) and 6 December (single shot, squares) 2011, double-logarithmic scale. The sensors from 45 m to about 700 m distance were deployed underground in the mine, the ones at about 1100 m were at the surface. The geophone at 45 m is in the seismic shadow of the drift. The BGR seismometers at 5-6 km are in 300 m deep holes, here recording is done with much lower bandwidth. The power-law trend lines from 140 to 1100 m have exponents of -2.3 ± 0.6 and -2.1 ± 0.5 , respectively.

3.4.2 Grader with vibrating compactor plates

The grader vehicle at its front carries a plate compactor of three plates (Stehr SBV 55 H3). Each plate contains two counter-rotating eccentric masses driven hydraulically that cause a vertical vibrating force to the ground (amplitude 60 kN per plate, frequency 60 Hz). This was the second-strongest seismic source, 2.5 orders of magnitude below the blasts. On spectrograms it was also seen at the surface, at 1.1 km slant distance (0.8 km through salt plus 0.3 km through the overlying sediment); after removing machinery noise by high-pass filtering with 90 Hz corner frequency it became even visible in the signal amplitude. For this source root-mean-square (rms) values of vertical seismic velocity underground were evaluated over 20 seconds each while the plate compactors were vibrating, and over about the same time period while they were inactive for comparison. The latter values differed considerably between the positions, probably because

different machinery (for example for ventilation) was running at different distances from the sensors. Figure 7 shows the rms values of vertical wall velocity versus slant distance from the respective grader position to the respective sensor. (The corresponding peak-to-peak values are higher by about a factor eight.) Also shown are some of the comparison rms values, the variation between positions is evident.

The general decrease of seismic rms value with distance r follows a power law with exponent -1.9 ± 0.2 (95% confidence). Extrapolating the trend one sees that clear detection of compacting by amplitude only should be possible to around 1 km distance for the lower range of background rms values, but only to 500 or 200 m for the higher-background positions. Obviously for achieving maximum detection distance one should use sensor positions with the lowest-possible background signal.

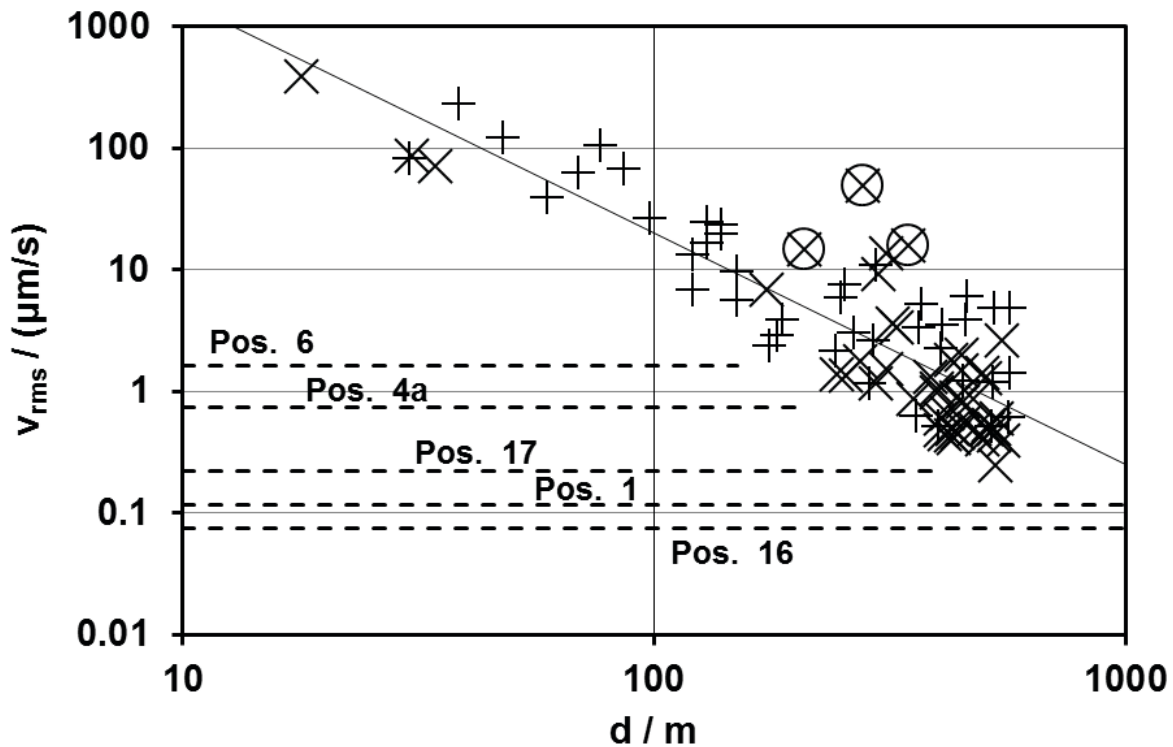


Figure 7: Rms values of vertical wall velocity during plate-compactor activity versus slant distance from source to sensor in double-logarithmic scale (x: measured at the main Dortmund station UT1 in “Bohrt 3.2”, +: measured at the smaller Dortmund station UT4 in the “Hauptförderstrecke”, near shaft 1). The power-law trend line has a slope of -1.9 ± 0.2 . (Additional circles mark the signals at Position 6 in the “Nördliche Richtstrecke” from the three sites in the same drift.) The dashed horizontal lines indicate the comparison rms values at several sensor positions when the plate compactors were inactive.

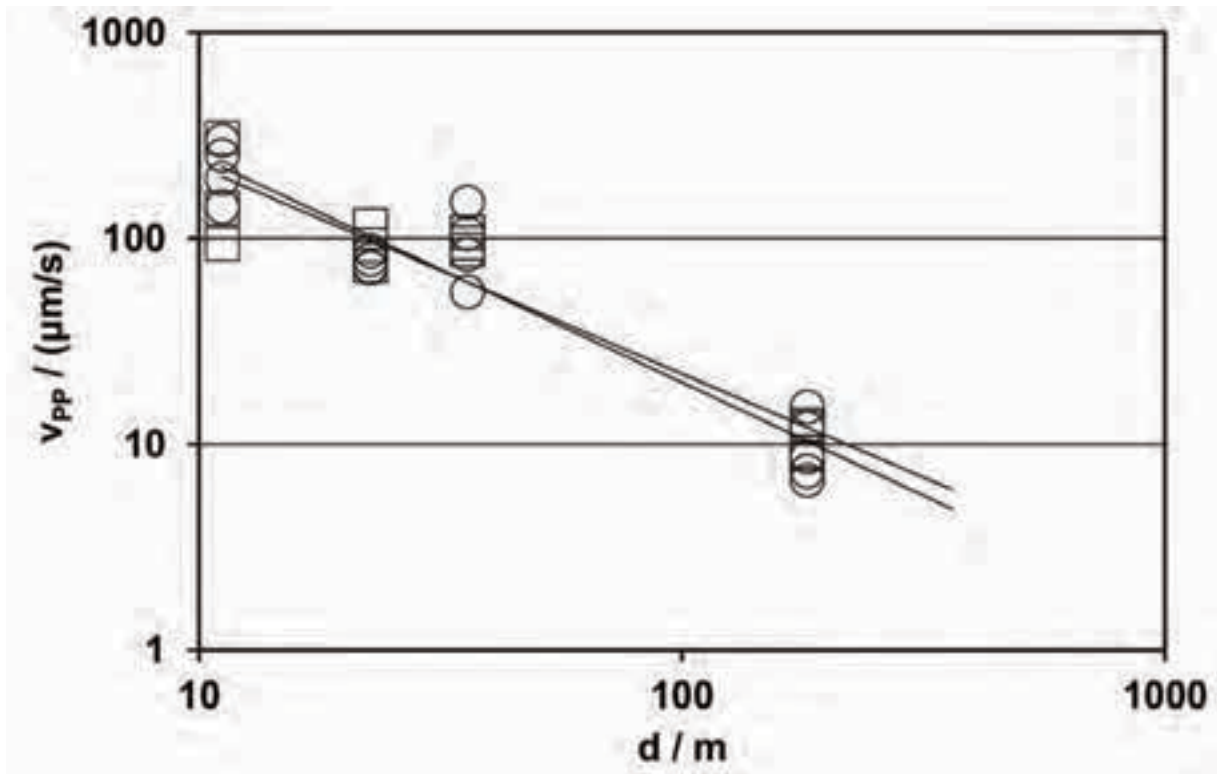


Figure 8: maximum peak-to-peak values of vertical wall velocity from the scaler versus distance, double-logarithmic scale. Circles: during scaling, squares: in between. For the shortest distance 11 m was used while in fact it varied between about 5 and 15 m by vehicle movement. The power-law trend lines have exponents of -1.1 ± 0.2 and -1.0 ± 0.2 , respectively.

3.4.3 Scaler

The scaler (Proxima C1 BF AKR) is a heavy vehicle with a strong hydraulic arm. At its end there are steel cutting edges at three sides (left, top, right). These edges are moved forcefully along the side walls or roof of a drift to remove salt that has become loose. It is interesting that often the seismic amplitude was higher between the periods of scaling, caused by the engine rotating faster for moving the vehicle or for moving the arm, probably from coupling of acoustic to seismic excitation (see also Figure 12 below).

Figure 8 shows the maximum peak-to-peak values of vertical wall velocity from the scaler versus distance during periods of scaling as well as in between, that is including the high values from engine rotation between scaling. The maxima show considerable variation. The power-law trend lines have exponents of -1.1 ± 0.2 and -1.0 ± 0.2 (95%)

for scaling and in between, respectively. Whether these values – differing from the exponent around -2 determined for several other sources – are a consequence of the primary source being acoustic remains to be investigated.

3.4.4 Picking

The hand-held electropneumatic pick hammer (breaker) Hilti TE 1000-AVR applies repeated blows to the material via a chisel. For breaking into and removal of salt the chisel angle is varied from time to time by the operator. In order to determine the maximum peak-to-peak values at distances above 8 m, a 500-Hz high-pass filter was applied as for Figure 3. Figure 9 shows the results versus distance. The decrease can be approximated by a power law with exponent -1.3 ± 0.3 (95%), closer to the theoretical one of -1.0 for a seismic body wave without attenuation than the value -2 found with other sources.

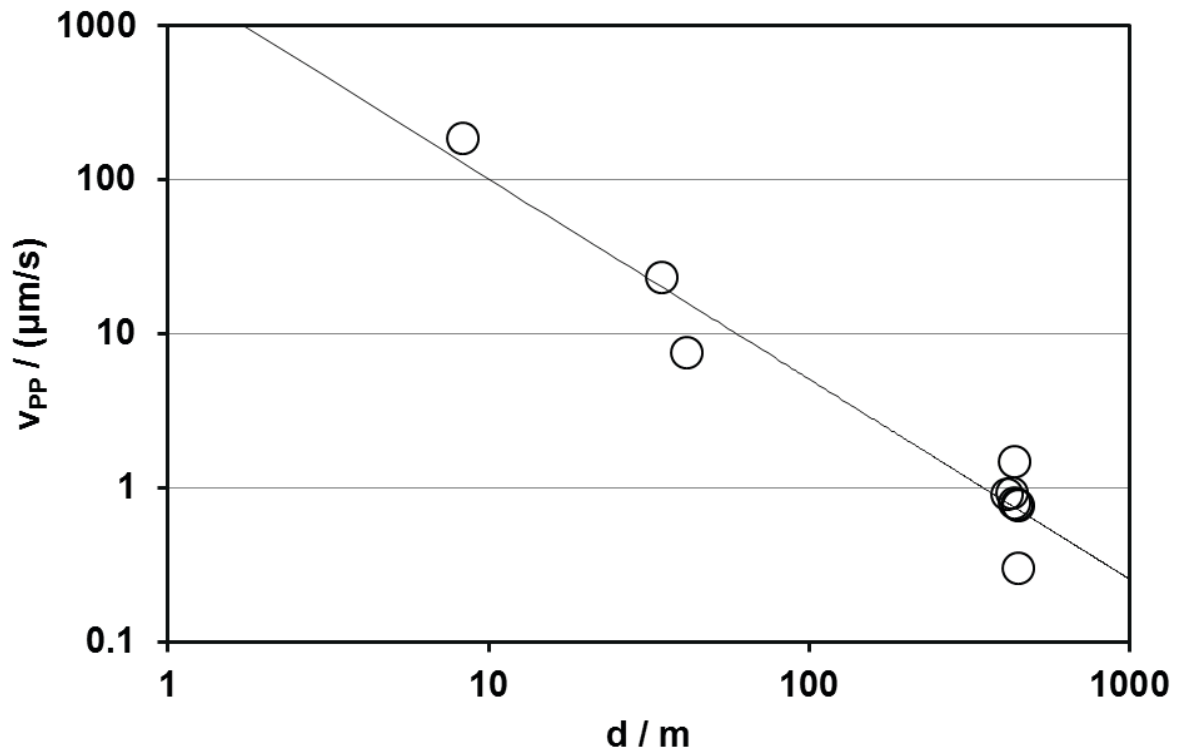


Figure 9: maximum peak-to-peak value of vertical wall velocity during picking versus sensor distance, double-logarithmic scale. At the lowest distance the signal was evaluated directly, elsewhere it was high-pass filtered with 500 Hz first. The values around 450 m are the mean values shown in Figure 3. The power-law trend line has an exponent of -1.3 ± 0.3 .

3.4.5 Chain saw

The hand-held chain saw (Spitznas no. 5 1029 0010, power 3.0 kW, rotation rate to 6500 min^{-1}) is driven pneumatically by compressed air, its blade length is 0.43 m. This turned out to be the weakest seismic source. It was used at two sites in the “Arbeitsraum”; at the farthest, only one sensor showed a signal discernible from the background. Because of masking by different sources (probably a vehicle among them), the recordings were filtered with a high pass of 1 kHz corner frequency, retaining most of the chain-saw-related contributions.

Figure 10 shows the distance dependence of the peak-to-peak as well as the rms values of the chain saw. Trends can only be computed for the closer excitation site, the power-law exponents are -2.0 ± 1.0 (peak-to-peak) and -2.1 ± 0.8 (rms). These values fit to the -2 found for several other sources, but are less reliable because here the distances extend over half an order of magnitude only. Figure 10 also demonstrates the typical ratio of 8 between peak-to-peak and rms values.

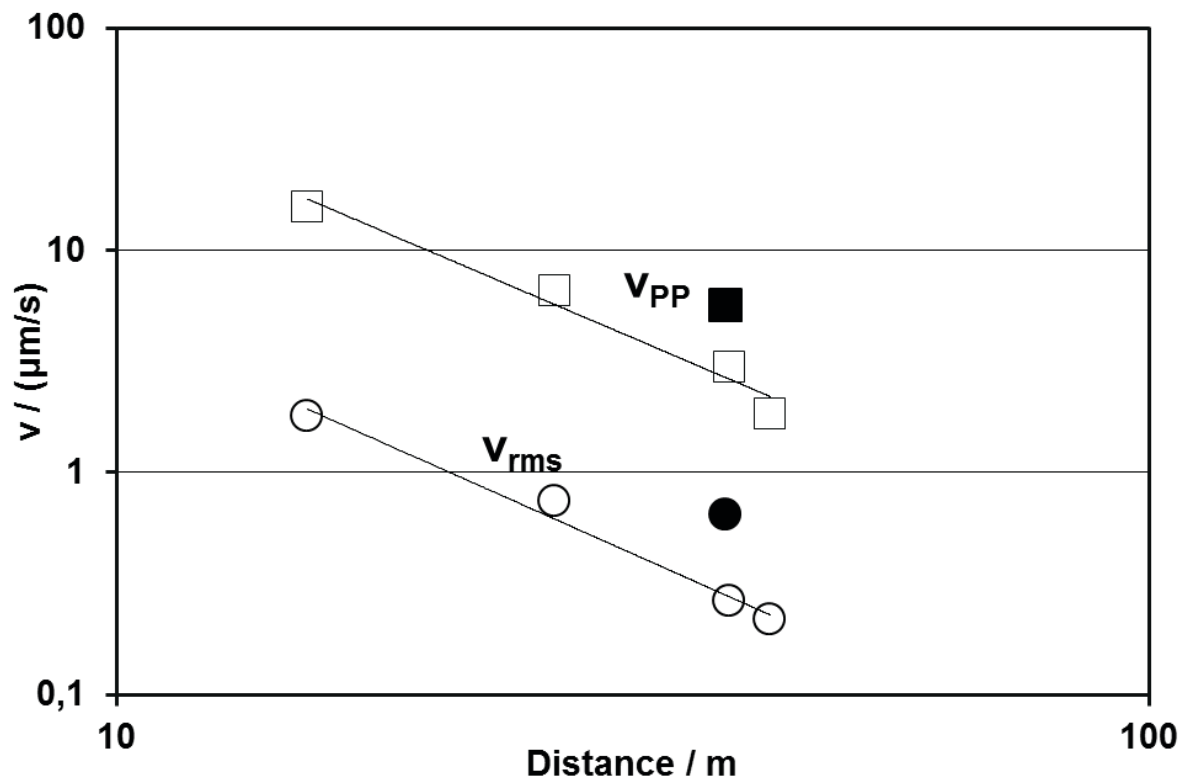


Figure 10: Peak-to-peak and rms values of vertical wall velocity when the chain saw was used, high-pass-filtered with 1 kHz, versus distance, in double-logarithmic scale. Open symbols: sawing at the western wall of the “Arbeitsraum” at closer distances. Solid symbols: sawing at the northern wall with generally larger distances and the drift in the direct path, only visible at the closest sensors; the relatively high excitation raises the suspicion that it was rather caused by a different source. The power-law trend lines for the closer sawing position (open symbols) have exponents of -2.0 ± 1.0 (peak-to-peak) and -2.1 ± 0.8 (rms).

3.5 Comparison of seismic strengths for various sources

From the power-law trend found for a source rough estimates of the peak-to-peak values of vertical seismic velocity at any distance can be gained. In doing so one should keep in mind the variability in signal strength by a factor two to five and more (see Section 3.3).

Power-law trends were computed for 14 representative sources, using the reference distance $d_0 = 1$ m. From this the nominal peak-to-peak value at 100 m distance was computed. This value and the exponent with its

confidence interval are given in Table 1, together with the range of distances over which the trend was determined. The exponents have confidence intervals (95% for normal distribution) of ± 0.2 to ± 1.6 . Not unexpectedly the uncertainty is higher when the range for the trend computation ends markedly below 100 m. In these cases the 100-m values are particularly uncertain, more than the factor 2 or so holding for the other sources. more reliable values would need a better understanding of the sources and the propagation. Table 1 also contains the general signal properties: pulse, broadband noise or harmonics.

Table 1: Power-law trend data for the representative sources: distance range from which the trend was gained, exponent with 95%-confidence interval, ensuing theoretical peak-to-peak value of vertical seismic velocity at 100 m distance (ranked by this value), general properties of signal. When the trend range ends markedly below 100 m (source in *italics*), the value should be taken with caution.

Source	Range for trend / m	Exponent	Value at 100 m / ($\mu\text{m/s}$)	Remarks	Signal properties
Blast	139-1184	-2.2 \pm 0.3	1.0 \cdot 10 ⁵	a	Pulse, repeated
Grader compacting	18-569	-1.9 \pm 0.2	1.6 \cdot 10 ²	b	Broadband
<i>Heavy loader</i>	13-45	-0.6 \pm 0.6	7.1 \cdot 10 ¹	c, d, e	Broadband, engine harmonics
5-kg sledge hammer	7.1-178	-1.5 \pm 0.3	6.7 \cdot 10 ¹	f	Pulse
Scaler					
engine only	11-182	-1.1 \pm 0.2	2.0 \cdot 10 ¹		Engine harmonics
scaling	11-182	-1.0 \pm 0.2	2.2 \cdot 10 ¹		broadband
Large-hole drilling rig	18-99	-0.8 \pm 1.2	1.8 \cdot 10 ¹	g	Broadband
<i>Core drilling</i>	27-58	-1.9	1.6 \cdot 10 ¹	a, d, h	Broadband
Hoist platform	18-173	-1.7 \pm 0.4	1.2 \cdot 10 ¹	i	Engine harmonics, broadband
<i>Roof cutter</i>					
engine only	16	-	about 3 \cdot 10 ⁰	d, j	Broadband
cutting	16-49	-1.4 \pm 0.3	1.0 \cdot 10 ¹	d	Broadband
<i>Salt through drop hole</i>	24-42	-1.3 \pm 0.5	6.3 \cdot 10 ⁰	d	Broadband
Picking	8.4-460	-1.3 \pm 0.3	5.1 \cdot 10 ⁰		Broadband, chisel harmonics
<i>Stud driving</i>	4.6-42	-1.6 \pm 0.5	3.6 \cdot 10 ⁰	d	Pulse
<i>Percussion drilling</i>	4.6-42	-1.3 \pm 1.6	3.0 \cdot 10 ⁰	d	Broadband, percussion harmonics
<i>Chain saw</i>	15-43	-2.0 \pm 1.0	4.1 \cdot 10 ⁻¹	d	Broadband

Remarks:

- a The closest position was in the seismic shadow of a drift; this value – markedly below the trend – was excluded.
- b Peak-to-peak values estimated as 8 * rms values.
- c 2 distances below 10 m excluded because they are in the range of the vehicle size.
- d 100 m is markedly beyond the range for the trend.
- e When passing 3 positions (in front of “Bohrort 3.2”, 23 m south and 19 m north of it), 2 passes.
- f Averages from 4 blows at “Bohrort 3.2”. The values from hammer blows at “Bohrort 3.1”, distance 167-210 m, are clearly lower.
- g The closest point at 18 m is at the opposite wall of the hall, but was included.
- h Only two points were used for the trend, no confidence interval can be computed.
- i When passing in front of “Bohrort 3.2”, one pass each in 2nd, 3rd and 4th gear.
- j Too few points for trend were available, but an estimate for 100 m was possible.

The nominal 100-m values are depicted in Figure 11. Assuming a background-noise value one can deduce detection ranges simply from amplitude by defining a detection-threshold signal-to-noise ratio S/N_{det} . Somewhat generously requiring $S/N_{\text{det}} = 2$, for example with a background peak-to-peak value around 10 $\mu\text{m/s}$ as found during the plate-compacto measurements at Position 6 (8 times the rms value of about 1.2 $\mu\text{m/s}$, see Figure 7), one concludes that the scaler and stronger sources could be detected at 100 m whereas the large-hole drilling rig and weaker sources would be below the detection threshold. Assuming on the other hand a background peak-to-peak value of 0.6 $\mu\text{m/s}$ as at Position 16 during the grader measurements (the rms value in Figure 7 is about 0.08 $\mu\text{m/s}$), all sources except the chain saw would be detectable at 100 m.

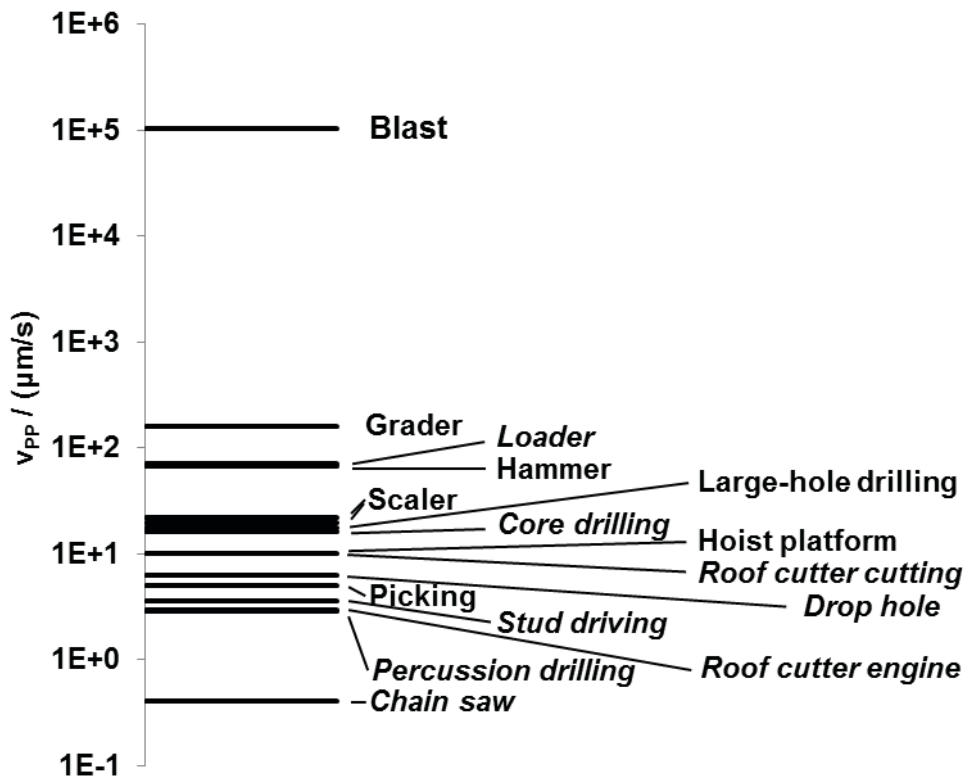


Figure 11: Nominal peak-to-peak value of vertical wall velocity in 100 m distance from various sources, logarithmic scale. These values are uncertain by a factor 2, and more if the distance interval used for the trend ends markedly below 100 m (italics).

For monitoring after repository closure seismic sensors would be deployed at distances on the order of 1 km. With a quiet mine and sensors at several hundred metres depth a background peak-to-peak value of 0.1 to 0.2 $\mu\text{m/s}$ seems achievable. Summarily assuming a power-law decrease from 100 m to 1000 m with an exponent of -2 as observed with the blasts the values at 1 km are lower than at 100 m by a factor 1/100. With a threshold of $2 \times 0.2 \mu\text{m/s}$ the four sources from blasts down to the hammer would be detectable, with $2 \times 0.1 \mu\text{m/s}$ the set of detectable sources would expand by the scaler and possibly the large-hole drilling rig. If the signal strength decreases more slowly, for example with a power-law exponent of -1.5, as found for hammer blows, the reduction factor from 100 m to 1000 m is about 1/30. In this case core drilling, the hoist platform, the roof cutter cutting and salt falling through a drop hole, maybe also picking, would be detectable and the stronger sources would reach out correspondingly farther. more exact statements require looking at the amplitude decrease with distance for each source specifically.

Of course, the amplitude crossing a detection threshold is a simple criterion and not the only one available; looking at spectra or using other more sophisticated detection procedures one can find signals masked by noise.

For seismic monitoring during the emplacement phase – for example to support information provided by surveillance cameras by a second, redundant signal – the background noise will be markedly higher, probably similar to the values measured under different conditions in the present project (see Section 3.2), resulting in lower detection ranges. On the other hand, sensors could be deployed much more densely, close enough to the potential sources that their amplitude is higher than the background under normal conditions. Here the problem of masking one source by another, stronger one close-by has to be tackled.

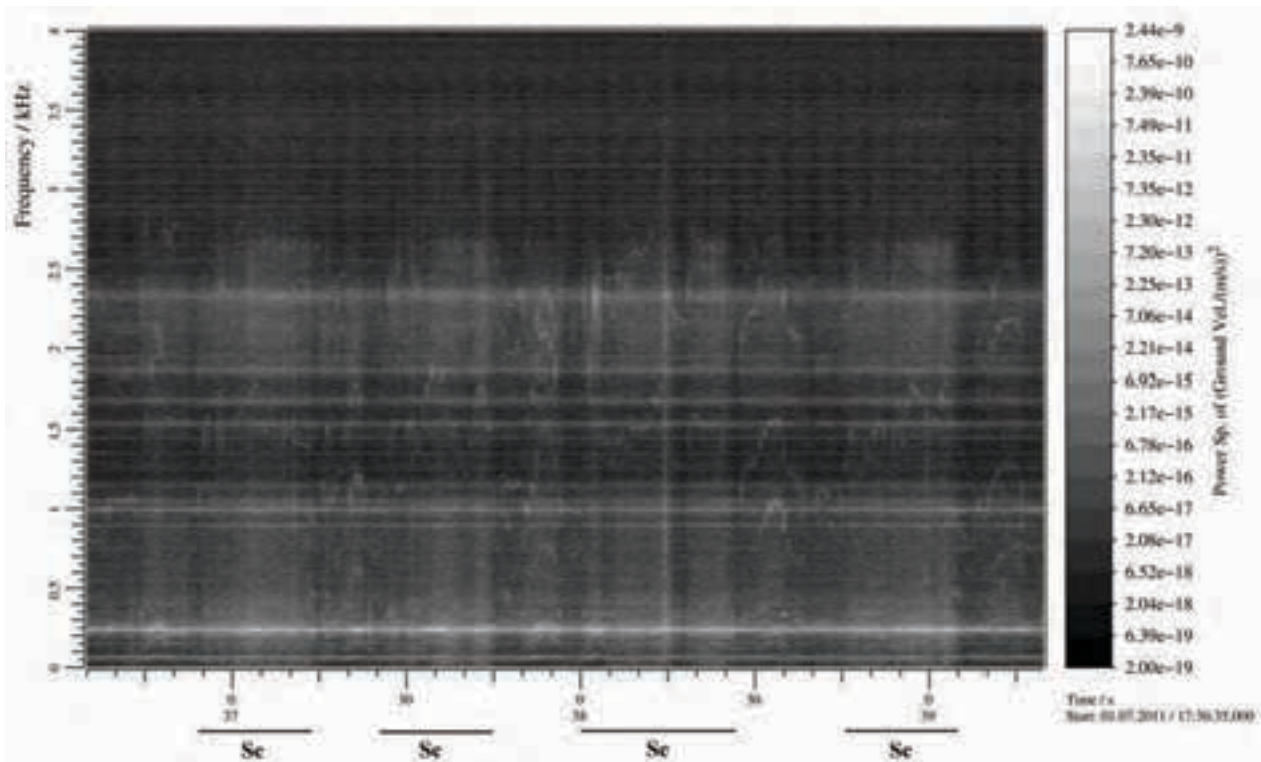


Figure 12: Spectrogram of vertical wall velocity at Position 1 of station UT1 (in the niche “Bohrt 3.2”) when the scaler (Proxima C1 BF AKR) worked in the adjacent drift. Grey value: spectral power in logarithmic scale. Periods of scaling are indicated by “Sc”, they are characterised by broad-band power from 0 to 2.7 kHz. In between the frequencies of the engine harmonics show up as curves at discrete frequencies, increasing strongly and decreasing again, e.g. with peaks at 1.0 and 1.5 kHz around 17:38:33. The constant-frequency lines are probably due to holder vibration.

3.6 Seismic spectra

Spectra show how components with different frequencies contribute to the total signal. If two signals with different frequency content are superposed this can be seen in spectra. In particular, since the background spectrum is known, an additional activity with a different spectrum shows up even if the amplitude is not increased significantly by it; this can be used as a more sophisticated detection criterion than just amplitude. Based on spectra one can design filters suppressing certain frequencies for improved detection. Spectra at different distances from a source may allow one to determine frequency-dependent properties of propagation. Periodic signals (for instance from machinery) show up as peaks at the fundamental frequency (the inverse of the period) plus at integer multiples of it (harmonics); the signal form is reflected in the relative strength and phase of these peaks. Change of spectra over time can indicate motion or other variation of a source. This is visualised by a spectrogram where the abscissa denotes time, the ordinate frequency, and the spectral power (or amplitude) is coded in grey value or colour. Here only a few example spectrograms are presented, with grey value in logarithmic scale.

Figure 12 is a spectrogram of the scaler operating in about 25 m distance. During scaling broadband excitation

extends to 2.7 kHz. In the periods in between the frequencies of the engine harmonics increase and decrease again with the engine rotation rate as the hydraulic arm is moved and the vehicle drives to the next scaling position. Acoustic-seismic coupling from the greatly increased engine noise can explain the strong seismic signals in these periods (see Section 3.4.3).

Figure 13 is a spectrogram from a pass of the heavy loader with 3-4 m/s speed, fully loaded with about 9 t of salt. There is a harmonic series of lines typical of the periodic signals from a reciprocating engine, probably produced by acoustic coupling. The frequencies follow the variation of the engine rotation rate, jumps can be explained by gear switching. It is notable that there is considerable broadband excitation up to the Nyquist frequency of 5 kHz (half the 10-kHz sampling rate). Its power increases and decreases in parallel to the engine rotation rate.

Figure 14 is a spectrogram from picking, percussion drilling and stud driving at close range. All three activities produce spectral power nearly up to the Nyquist frequency of 5 kHz. Due to their periodic blows to the salt rock, picking and drilling show harmonics of a fundamental frequency. This is about constant at 44 Hz for picking, while it decreases with growing friction from about 57 to about 37 Hz for drilling as the drill hole gets deeper.

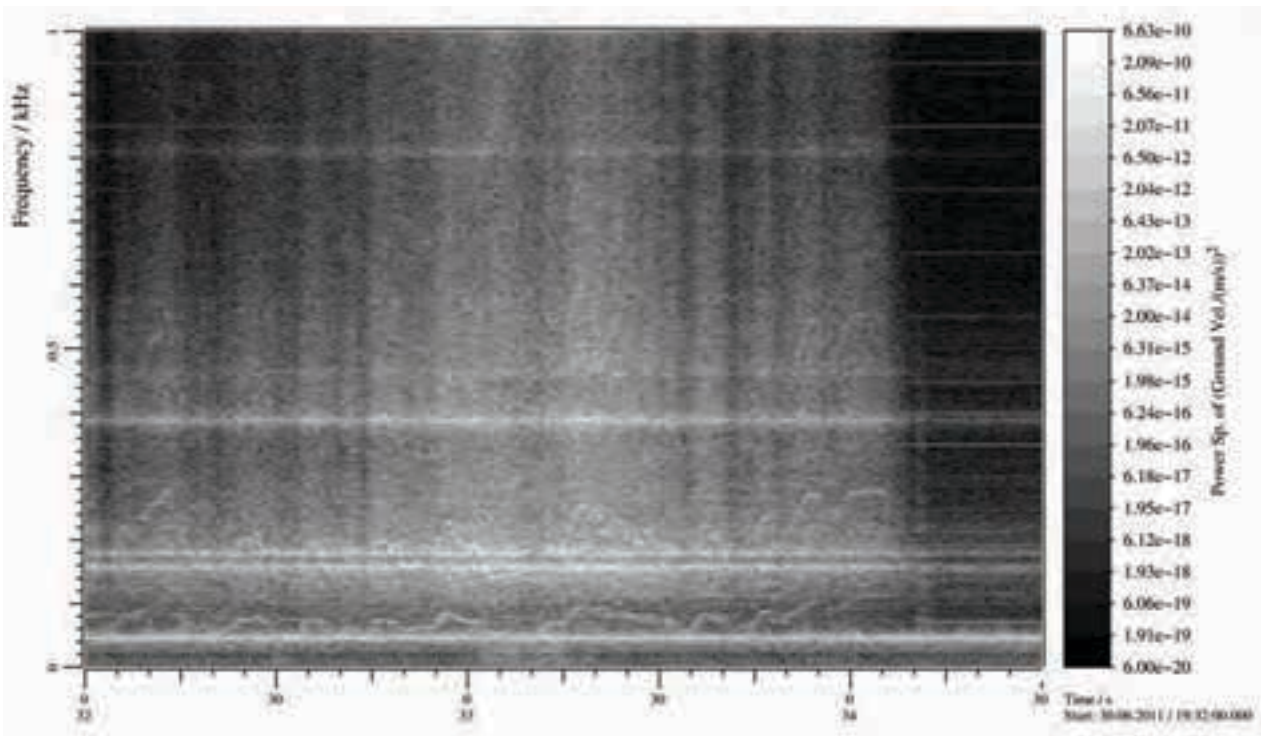


Figure 13: Spectrogram of vertical wall velocity at Position 2 (at the drift wall) during a pass of the heavy loader (Centauri I HFL 00 K R), fully loaded, with speed 3-4 m/s. Grey value: spectral power in logarithmic scale. The sensor was passed at about 19:33:05 (brightest region 19:32:55 to 19:33:30, with variations in parallel to engine rotation rate). The curves of varying frequency are harmonics of the engine, probably from acoustic-seismic coupling. In addition broadband power exists up to 5 kHz.

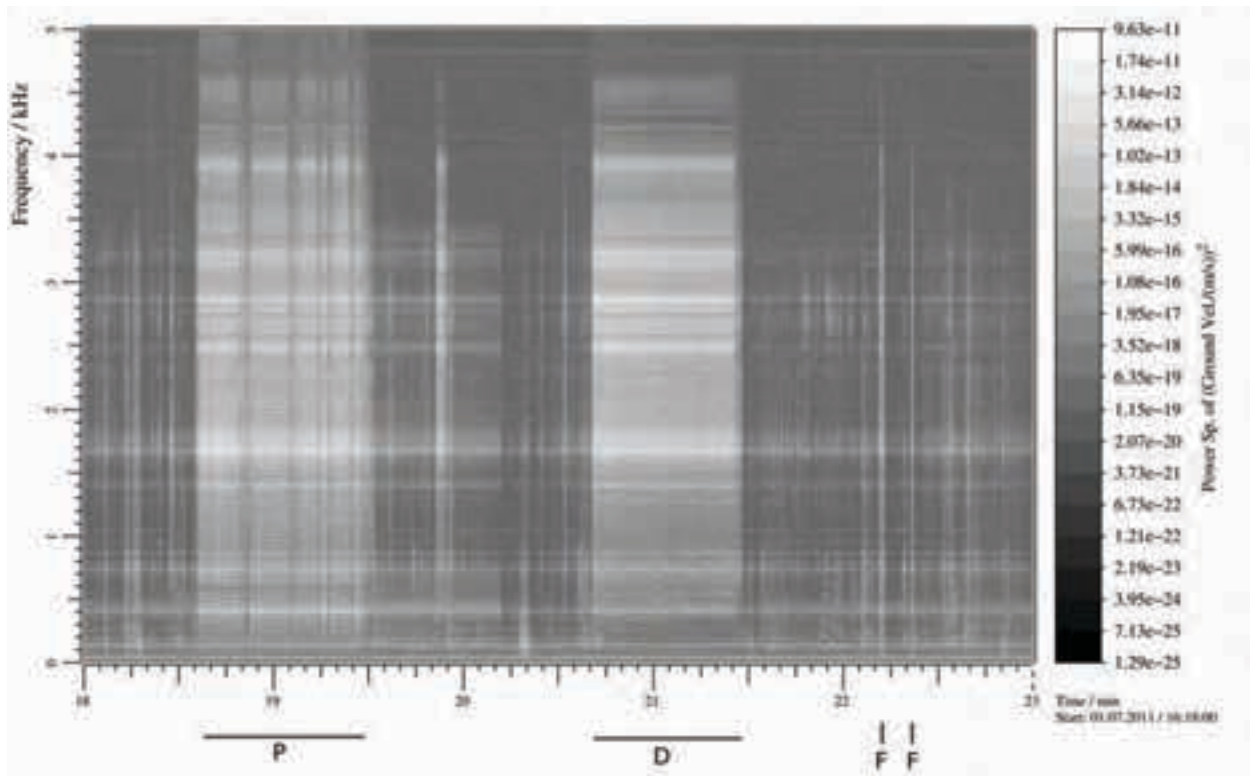


Figure 14: Spectrogram of vertical wall velocity 8.4 m from a site where picking (P) (Hilti TE 1000-AVR), percussion drilling (D) (Hilti TE 6A36) and stud driving (F) (Hilti DX 460 KIT) were done. Grey value: spectral power in logarithmic scale. Picking and drilling produce harmonic and broadband features over the duration of the activity, the harmonics are best visible between 0.3 and 1.5 kHz. The impulses from stud driving make broadband power contained only in one 0.8-s spectrum (or two neighbouring ones) each. Several weaker events are visible, too.

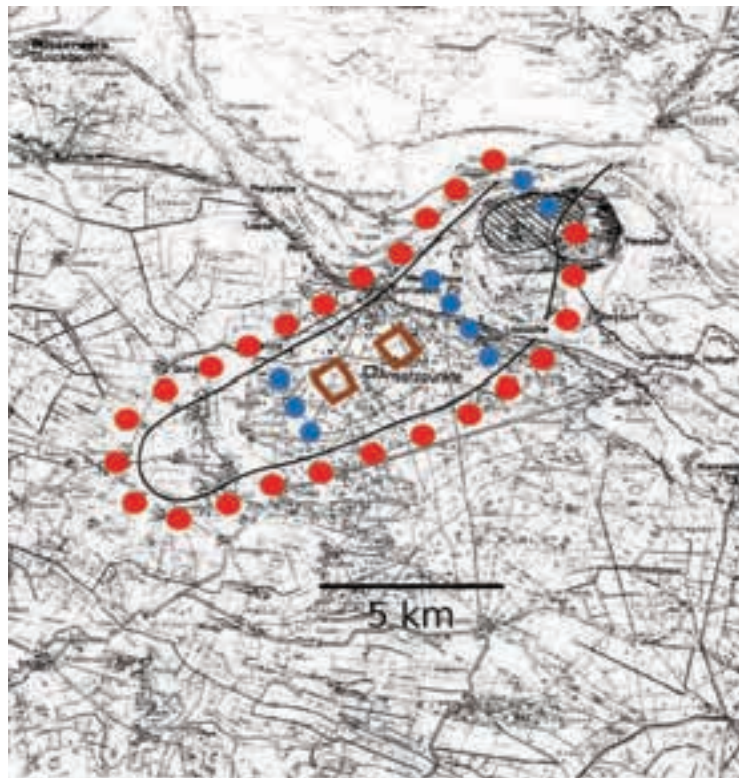


Figure 15: Notional possibilities for placement of seismic sensors after a possible emplacement phase in Gorleben, avoiding the repository volume in the salt-dome centre (brown/light-grey quadrangles). Blue/light grey: in the salt dome, red/dark grey: surrounding it. Additional sensors could be placed in the overburden above the dome. (Based on map from Federal Office for Radiation Protection (BfS), used by permission)

4. Conclusions

On a general level several findings are relevant:

- Removing rock by drilling or cutting produces broad-band vibration.
- Different from drilling the signals from the scaler, but also the roof cutter are irregular, as rock is hit or not during movement of the respective arm.
- Periodically working machinery produces harmonic signals in addition.
- In the underground cavities significant coupling from acoustic to seismic excitation takes place. This is most relevant with the engine noise from heavy vehicles.
- Seismic excitation in the salt rock extends to very high frequencies (tens of kilohertz, not shown here), and geophone signals contain frequencies up to several kilohertz. In future monitoring at least within the salt dome the high frequencies should not be neglected, in particular for localisation.
- After propagation through the overburden of sand, silt and clay to the surface, kilohertz frequencies have vanished by attenuation, only frequencies up to several 100 hertz remain (not shown here).
- Not shown here likewise: Very low frequencies (below a few hertz) are not excited to a relevant extent, so that specific sensors covering these are not needed.

With a view towards seismic detection of mining activities the following can be stated:

- Seismic-signal strength shows considerable variability, peak-to-peak values from the same source at the same distance can vary by a factor 2 to 5.
- Power-law fits to signal strength versus distance give exponents in the range -2.2 to -0.6; if credible values from distances of 100 m and more exist, the range is -2.2 to -0.8, with confidence intervals of ± 0.2 to ± 1.2 .
- Detection ranges by amplitude alone are many kilometres for blasts, many hundreds of metres for heavy vehicles and, depending on background noise, 100 m to a few times this value, for weaker sources.

The shorter detection ranges are relevant mostly for the emplacement phase when the mine is open and active, and seismic sensors could be deployed along shafts and drifts with relatively close spacing, for example 50 m or 100 m. Their signals would be evaluated and processed continuously, mostly in an automatic mode. The results could complement the information gained from video cameras and other traditional safeguards sensors.

After closure of the repository sensors and cables must not remain in it. monitoring for undeclared activities, that is for excavation in the former mine or close to it, would

rely on sensors far from the repository, also active continuously, forming a “fence” in the surrounding sediment, maybe with parts in the salt dome (Figure 15). Keeping 500 m distance from the salt margin and 1 km from the repository in the salt, relevant distances from the repository would be 1-3 km, without sensors in the dome up to 5-8 km. With the mine closed a much lower background will hold. Assuming deployment in boreholes of several 100 m depth, a value of 0.1-0.2 $\mu\text{m/s}$ is plausible. With a power-law exponent of -2, the sources down to the scaler and possibly large-hole drilling could be detected at 1 km distance. This is a very rough estimate – with an exponent of -1.5 instead of -2 the signals at 1 km would be 3-fold higher. Additional sensors could be placed above the dome in the sand/silt/clay overburden, at, for example, 150-200 m depth. Here the distances from the repository would be 0.7 to 1.5 km, with about the same conditions for detection.

Excavation could be done by two major methods: drilling and blasting, or by cutting machines (tunnel boring machines or smaller road-header machines) (principally, salt could also be removed by water dissolution; if deemed relevant this scenario should be investigated separately). In the first method blasts would provide a very strong and clear signal, even if drilling could not be detected. Removal of rock by cutting machines would set much higher requirements on detection – a road header should be similar to the roof cutter, not a strong vibration source, see Figure 11. But with a road header advance would be relatively slow. A tunnel boring machine that would proceed faster should produce stronger signals with a larger detection range. Such a machine was not available in the Gorleben mine; for this problem at least some estimates should be made. machine activity would also be needed for removing debris. If a vehicle were used, the signal strength would probably be somewhere between the loader and the hoist platform, with corresponding conditions for detection.

In terms of monitoring prospects it can be stated that excavation by drilling and blasting can be detected by the sketched concept with virtual certainty. Whether removal of salt by tunnel boring machine or road header machine can be detected at sensor positions far enough away from the repository, and what the requirements on sensors and sensor density would be, needs to be studied. Scenarios should also consider other methods of reducing seismic excitation.

Most relevant is the investigation of the propagation of seismic waves from sources in the salt dome to longer distances in the salt dome and in particular to the surrounding and overlying sediment. This can be done at first by detailed seismic modelling, taking into account the properties of the various underground media and all boundaries between them. Such a project has begun at TU

Dortmund. Some validation of its results will be possible using data gained in the measurements described here, including from the surface. If seismic modelling gives a reasonably positive outcome, then a subsequent project can validate the results at other positions using sensors in a few exemplary boreholes.

The results found will generally hold also for a different salt dome, with variations due to different geometry and internal as well as external structure. Concerning a repository in another medium (for example granite or clay, both alternative media are under research in Finland and France, respectively, and are being discussed in Germany), there is no reason to assume that seismic monitoring would be markedly less suitable than with salt. But there will be considerable differences for several reasons. For example, rock of different hardness can lead to different source strength for drilling. Acoustic-seismic coupling can differ. Propagation will be affected by different wave speeds and attenuation. Quantitative statements such as the ones made here will require a study with measurements for each potential site.

5. Acknowledgements

I want to express my thanks to DBE and DBE Technology, and to all their personnel involved, for the support in the preparation and in particular the carrying out of the measurements. Thanks go also to Felix Gorschlüter (TU Dortmund) who helped greatly with programming and measuring. I am grateful to the Federal Institute for Geosciences and Natural Resources (BGR) for providing data from its seismic monitoring network and to the Federal Office for Radiation Protection (BfS) for allowing access to the data, and to both institutions for permissions to use figures. Finally I want to thank two anonymous reviewers for valuable comments.

This work was funded under task C1611 of the German Support Programme to the IAEA.

6. References

- [1] Peterson, P.F., Long-term safeguards for plutonium in geologic repositories, *Science & Global Security* **6** (1), 1-29, 1996.
- [2] Peterson, P.F., Issues for Detecting Undeclared Post-Closure Excavation at Geologic Repositories, *Science and Global Security*, **9** (1), 1-39, 1999.
- [3] International Atomic Energy Agency, *Technological Implications of International Safeguards for Geological Disposal of Spent Fuel and Radioactive Waste*, IAEA Nuclear Energy Series No. NW-T-1.21, Vienna: IAEA, 2010, http://www-pub.iaea.org/MTCD/publications/PDF/Pub1414_web.pdf.

- [4] Garbin, H.D., Herrington, P.B., Kromer, R.P., A Study on the Feasibility of monitoring Sealed Geological Repositories Using Seismic Sensors, *38th INMM meeting*, Phoenix AZ, 1997.
- [5] Canadian Safeguards Support Program, *The Feasibility of using Passive Seismic monitoring To Safeguard a Geological Repository*, Ottawa: Canadian Nuclear Safety Commission, 2002.
- [6] Saari, J., malm, m., *Local Seismic Network at the Olkiluoto Site - Annual Report for 2012*, Working Report 2013-21, Olkiluoto: Posiva, 2013, http://www.posiva.fi/files/3157/WR_2013-21.pdf.
- [7] Bornemann, O. et al., *Standortbeschreibung Gorleben Teil 3 – Ergebnisse der über- und untertägigen geologischen Erkundung des Salinars*, Geologisches Jahrbuch C73, Hannover/Stuttgart: BGR/Schweizerbart, 2008 (English version via http://www.bgr.bund.de/DE/Themen/Endlagerung/Aktuelles/2011_04_20_aktuelles_gorleben_engl_Part1bis3.html).
- [8] Alheid, H.-J.; *Felsdynamische Untersuchungen im schachtnahen Bereich – Abschlußbericht zur Teilaufgabe des AP 9 G 41 34 00* (unpublished); Hannover: Bundesamt für Geowissenschaften und Rohstoffe; 1999.
- [9] Alheid, H.-J., Leydecker, G., Lüdeling, R., Richter, B., Eilers, G., Kranz, H.; *Seismological monitoring of the Gorleben Site and its Vicinity*, Joint Programme on the Technical Development and Further Improvement of IAEA Safeguards between the Government of the Federal Republic of Germany and the International Atomic Energy Agency, Task A.14/C197; Jülich: Forschungszentrum Jülich; Oct. 1998.
- [10] Altmann, J., Kühnicke, H.; *Acoustic and Seismic measurements at the Gorleben Exploratory mine – Research for Safeguards at a Potential Underground Repository for Spent Nuclear Fuel*, JOPAG Report, Joint Programme on the Technical Development and Further Improvement of IAEA Safeguards between the Government of the Federal Republic of Germany and the International Atomic Energy Agency, Jülich: Forschungszentrum Jülich; 2013 (submitted).
- [11] Lai, W.M., Rubin, D., Krempl, E., *Introduction to Continuum mechanics*, Oxford etc., Butterworth-Heinemann, 1996.

Intrinsic fingerprints inspection for identification of dry fuel storage casks

Dmitry Demyanuk¹, Michael Kroening¹, Andrey Lider¹, Dmitry Chumak², Dmitry Sednev¹

¹ National Research Tomsk Polytechnic University, Lenin Avenue, 30, Tomsk, 634050, Russia

² Odessa National I.I. Mechnikov University, Dvoryanskaya str., 2, Odessa, 65082, Ukraine

E-mail: sednev@tpu.ru

Abstract:

The paper describes the practical implementation of the idea of 3S: safety, security and safeguards synergy, which was widely discussed at the relevant forums, in particular at the Seoul summit. The idea was aimed at improving the efficiency of the cooperation between these elements, which have relatively large number of common points, but at the same time have their proper features. Careful consideration has showed that the sphere of non-destructive testing is the most appropriate one to start 3S synergy implementation. Non-destructive testing methods and devices are widely applied in each S-element and could quite often be retargeted. The prototype of closure weld seam was inspected by the means of standard ultrasonic echo-pulse method. However, the collected data was processed with developed mathematical algorithm, that allows to use this information for security and safeguard purposes as tagging instrument. The main challenges for industrial application were defined.

Keywords: Intrinsic fingerprints; spent nuclear fuel; accounting; dry fuel storage; ultrasonic inspections.

1. Background

The International Atomic Energy Agency (IAEA) Director General Yukiya Amano, in his statement to the Fifty-Sixth Regular Session of the IAEA General Conference in 2012, emphasized that "...Eighteen months after the accident [Fukushima Daiichi accident], it is clear that nuclear energy will remain an important option for many countries. Our latest projections show a steady rise in the number of nuclear power plants in the world in the next 20 years"[1]. It means further dissemination of nuclear energy for peaceful use among new countries and in the new regions as well as improving existing capabilities.

Nuclear energy technology is complex and sophisticated and requires high level of scientific development, but at the same time poses potential hazards for humanity and requires the most advanced and well-thought actions. Despite the worldwide robust experience in operating nuclear facilities and related infrastructure, the Fukushima accident showed that the use of nuclear energy still can lead to disastrous consequences. Thus the system of nuclear energy

utilization requires new and innovative ideas to improve the level of nuclear safety, nuclear security and nuclear safeguards. It is clear, that each of S has its particular duties and peculiarities, but together these elements create a stable system for the peaceful use of nuclear energy.

Within "2012 Seoul Nuclear Security Summit", which was held in Seoul in March 2012, as one year past after Fukushima Daiichi accident, synergy between safety and security was one of the main topics of discussion. On the official Seoul Summit Communiqué highlighted: "Acknowledging that safety measures and security measures have in common the aim of protecting human life and health and the environment, we affirm that nuclear security and nuclear safety measures should be designed, implemented and managed in nuclear facilities in a coherent and synergistic manner" [2]. Additionally to this statement, in the context of protecting human life and health and the environment, safeguard measures (non-proliferation) also needs to be taken into account. Thus, today, the key challenge for scientists, politicians, diplomats is to seek options for preventing any situation which can undermine the reliability of peaceful use of nuclear energy. One of the ways of resolving this problem is to enhance the synergies between nuclear safety, security and safeguards.

Careful consideration has showed that the non-destructive testing (NDT) is one of the most appropriate options to start 3S synergy implementation. NDT methods and devices are widely applied in each S-element and quite often could be retargeted. [3] To understand what we should choose as the very first object for synergy implementation we need to screen for the most vulnerable stages in the nuclear fuel cycle. According to the official Russian ROSATOM guidelines, the following challenge exists for applying sealing technologies: "...there is no official data concerning sealing systems that could not be faked..." [4].

Within 3S initiative Tomsk Open Laboratory for Material Inspections of National Research Tomsk polytechnic university has launched the project on NDT methods application for fingerprinting by intrinsic features of dry intermediate storage (DIS) casks with spent nuclear fuel (SNF). Nowadays, NDT is mainly focused on safety purposes, but it seems possible to apply those methods for providing national and IAEA safeguards. [5] The containment of spent fuel in

storage casks and vaults at DIS could be dramatically improved in case of development of so-called “smart” spent fuel storage and transfer casks. Such casks would have tamper indicating and monitoring/tracking features integrated directly into the cask design. These features could be an add-on package or be integrated into the cask construction. The microstructure of the containers material as well as of the dedicated weld seam applied to the lid and the cask body provides a unique fingerprint of the full container, which can be reproducibly scanned by using an appropriate technique. Reproducing of a unique fingerprint can be achieved due to the following factors: 1) DIS cask design – it is based on defence in depth principle in order to prevent harmful influence from stored SNF (neutron radiation and any kind of corrosion); 2) ultrasonic techniques allow to choose area of control quite precisely what helps to avoid influence of external factors (wedges, coupling, scratches etc.). Additionally, this paper contains description of the weld seams investigation performed by ultrasonic backscattering technique for providing those fingerprints

2. Overview of a dry cask storage design

The energy content of SNF is significant and thus becomes the incentive to keep the option of future use of SNF. The historical vision towards the future of the nuclear fuel cycle was determined by key idea that LWR SNF is a valuable resource. Plutonium from LWR SNF was to be recovered and fabricated into fuel for the start-up of fast reactors. Such a system could increase

the available energy from uranium by more than an order of magnitude. [6]

The technologies currently available for spent fuel storage fall into two categories, wet and dry, distinguished in compliance with the cooling medium used. In wet storages the fuel cooling is performed by water and in dry it is performed by air, accordingly. Whereas wet storage option has been used for spent fuel storage and cooling at reactor sites and in some off-site storage facilities around the world. A variety of technical methods for dry storage has been developed since then and is available in the international market.

Intact fuel storage, which is the most prevalent dry storage method, refers to storage of fuel assemblies with no attempts to pre-compact them or alter them by destructive methods prior to storage. A variety of storage systems have been developed to meet specific requirements of different reactor fuels and a number of designs based on these generic technologies is now available for dry storage for the spent fuel containers (also called casks) or vaults (horizontal, vertical etc). The general examples of storage types are highlighted in Table 1. The technology continues to evolve keeping up with the design optimization and new materials. One of the driving forces of the trend towards dry storage options (especially those of casks) is the inherent technical flexibility linked to economics. Compared to the pool facilities, which need to be built at full capacity initially, the modular type dry facilities can be added as needed with the advantage of minimizing capital outlays. [7]

Item	Type of Storage	Containment & Shielding	Features	Notes
1	Independent Spent Fuel Storage Pool (Wet Storage of Spent Fuel)	Water in a deep stainless steel lined concrete pool within an enclosed structure	Traditionally used for expanded storage of spent fuel. Many examples worldwide	Current trends are for dry rather than wet storage, for reasons of reduced maintenance (water management) and improved safety and security.
2	Vertical Dual-Purpose Spent Fuel Dry Storage/Transfer Cask	Heavily shielded steel cask with spent fuel sealed in inner steel canister (i.e. double lidded)	Vertical, dual purpose, dry spent fuel storage and transfer cask	Examples: CASTOR, TN NAC-ST/STC BGN Solutions
3	Vertical Concrete Dry Spent Fuel Storage Cask/Silo	Heavily shielded concrete cask/silo with spent fuel sealed in an inner steel canister	Vertical, dry spent fuel storage cask/silo	Examples: CONSTOR HI-STORM
4	Horizontal Modular Concrete Dry Spent Fuel Storage	Heavily shielded modular concrete storage with spent fuel sealed in an inner steel canister	Horizontal, modular dry spent fuel storage vault	Examples: NUHOHMS NAC-MPC/UMS MAGNASTOR
5	Concrete Dry Storage Vault with Thimble Tube Storage Wells	Heavily shielded concrete vault with thimble tube storage wells for spent fuel	Vertical, dry spent fuel or vitrified waste storage vault with thimble tube storage wells	Examples: MVDS MACSTOR
6	Dry Geologic Storage (Tunnel or Mine)	Dry gas-filled spent fuel canisters emplaced in an isolated deep tunnel or mine and backfilled with earth	Dry spent fuel storage in tunnel or mine; vertical or horizontal fuel orientation	Example: Olkiluoto NPP Spent Fuel Repository (Onkalo)

Table 1: Storage options for away-from-reactor storage of spent fuel [8]

Several variations of these fuel storage concepts, often by combination of existing dry storage technologies, have been developed with prospective applications in the future. Cask is currently the most popular option that can be purchased or leased from the competitive market for expedited installation, on the assumption that the necessary license can be obtained and any other obstacles such as opposition on behalf of the affected local community have been or could be resolved. Inheriting the technology initially developed for large-scale transportation of spent fuel from storage to re-processing operations, several large size casks are now being marketed for storage services. Concrete modules have also become popular as a competitive option, with more designs licensed and implemented over the years. Markets for concrete modules are merging with those for vaults as a compact storage system, in terms of advantages when land availability is an issue. Multi-purpose technologies (i.e. a single canister package for storage, transportation and disposal) have also been developed, for instance in the US. Within this paper we will focus on Vertical Dual-Purpose Spent Fuel Dry Storage/Transfer Cask as the most popular type of DIS cask in Russia.

3. Ultrasound inspection

The echo-sounder technique is most commonly used method for material inspection. The ultrasonic pulse called transmitter pulse is usually generated by piezo-electric conversion. The pulse propagates through the material that is supposed to be isotropic. Part of the acoustic wave is scattered back to the transducer and converted again by the reciprocal piezo-effect. The received pulse is A-scan. The amplitudes of the A-scan indicate the intensity of reflection correlates with the reflector dimension. The arrival time of reflector amplitudes is used for their localization and providing straight propagation along the central line of the wave field intensity profile.

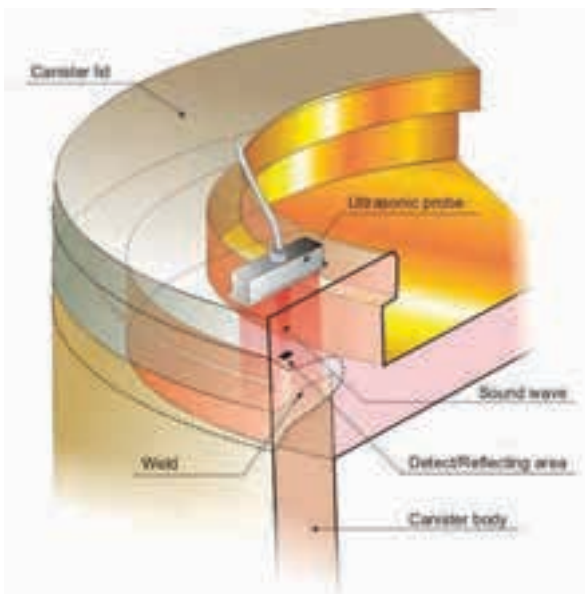


Figure 1: Typical UT inspection of cask weld

Figure 1 represents the scheme of Vertical Dual-Purpose Spent Fuel Dry Storage/Transfer Cask UT inspection for safety reason. For the detection of structural features, especially planar, normal incidence of the wave field to receive the backscattered reflection is required. Depending on possible critical flaw geometries and a risk classification of the inspected component the inspection procedure requires various angles of sound wave incidence.

The required angle of incidence is realized by plastic wedges of different sound velocity and low attenuation. Snell's law [9] can be used for the wedge design of the specified angle of sound incidence as long as the beam is directed. A typical angle beam transducer design is shown in Figure 2.

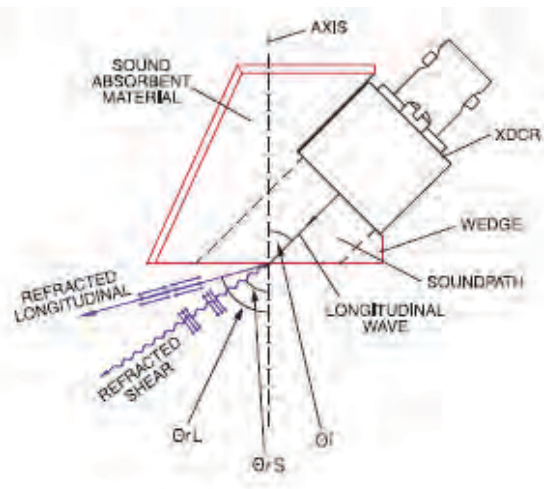


Figure 2: Typical design of an angular beam transducer [10]

Both the longitudinal mode ($c_L = 5920$ mm/sec in steel) and the slower shear mode ($c_s = 3250$ mm/sec in steel) can be realized by the appropriate wedge design. Above the first critical angle of 90° refracted longitudinal mode and only shear waves are transmitted into the sample. We use acoustic noise, reflected from material's artefacts, received from both modes while travelling through controlled material; and the purpose of it is to obtain structural fingerprinting. Raleigh scattering forms most of the acoustic noise and usually not evaluated for flaw detection and assessment. However, we assume that the acoustic noise depends on the microstructure what specifies the position. Geometric extended reflectors are by far more position related and may be evaluated for position data and position changes. However, in high quality steels which are used for structures extended material flaws or material inhomogeneity are quite rare. It is worth mentioning, that only point reflectors will provide accurate data as required. Back-wall reflection is independent of the transducer position. Compound reflector geometries, such as crack faces, require careful analysis of the radio frequency (RF) A-scans to separate individual and interfering scatter centres [11].

The number of experiments was conducted during the investigation. The main goal of experiments was the

development of methodology for structural fingerprints identification. Experimental set-up was developed to achieve the goal. Russian universal industrial ultrasonic flaw detector USD 60 was chosen as basis for the installation. (Fig.3) Transducer by Olympus Panametrics 2,5 MHz,

70° beam angle and standard laptop with software included in the set-up, also. Software package consisting of signal receiving utility provided with flaw detector, freeware digitizing module and Origin Lab. All specific algorithms were realised by means of C#.



Figure 3: Experimental installation

Three steel plates with dimension 100x100 mm and different thickness (8, 10, 12 mm) were welded and used as samples dedicated to be equivalent of cask weld seam. (Fig.4) The thickness of the samples was recommended by our Russian industrial partner – customer of DIS casks. Weld seams at each sample were cut off for 40 mm from the edge.

For the investigation were chosen nine points of interest in order to provide required statistics. (Fig. 5) 50 measurements were done in each point. Around 100 measurements were done to investigate the main factors that influence the results, such as position inaccuracy, coupling problem etc.



Figure 4: The sample example – 8 mm thickness

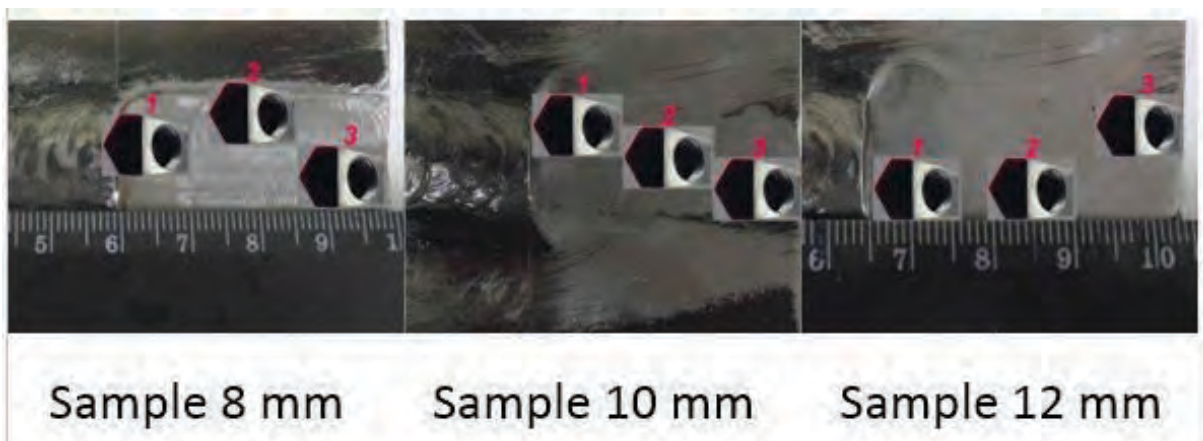


Figure 5: The sample example – 8 mm thickness

So-called “Area of interest” is used in order to prevent internal or external influence on material structure, within frameworks of the experiment. It is internal

volume that is placed for 2 mm above internal surface of the sample. (Fig.6)

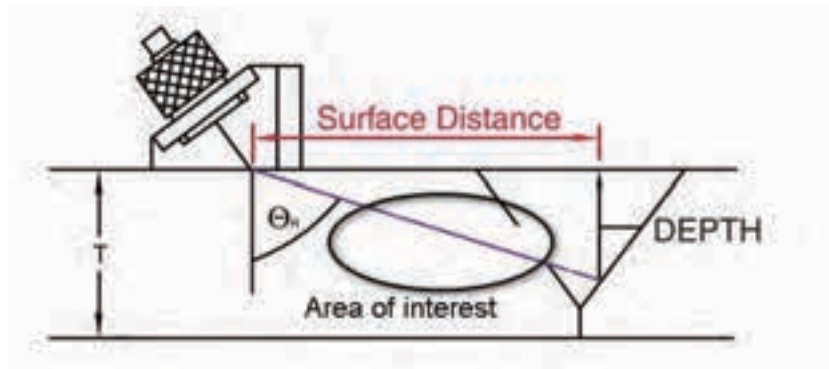


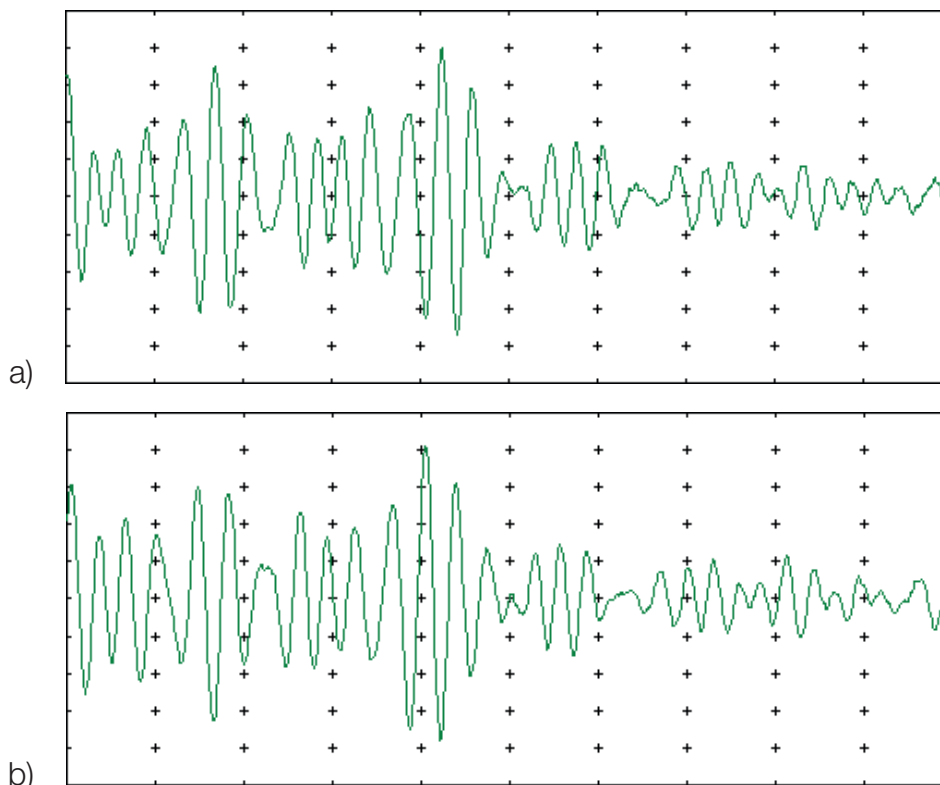
Figure 6: Scheme of sound distribution

During the investigation, we used standard software for data acquiring and processing. The development of data processing model is based on biometric system as the most reliable. Fingerprinting systems are used as reference technology. In these systems matching threshold is defined by equation 1.

$$k = \frac{D^2}{p \times q}, \quad (1)$$

where k – required correlation rate; D – quantity of defined features; p , q – amplitudes of features in reference and measured signal respectively. [12] In this case, a correlation threshold for a valid result is 65 percent. This threshold was taken for development and testing of the data processing system.

Ultrasound equipment allows to use different types of signals.. Radio frequency A-scan was chosen for the investigation to present data in real scale. During ultrasonic testing procedure, reference signature (Fig. 7a) was obtained. Further fingerprint images the system digitizes and analyses the input data. Then the most distinctive point should be picked from a digitized image, on the basis of those points system creates a pattern for reference signature. The same steps are taken for authentication process, the last one will be matching points of patterns. The correct signature (Fig. 7b) was obtained and more than 65% of points met with each other. identity of signatures is proven and the controlled item is considered not the object of malicious acts. [13] In case when inherent microstructure of closure weld is corrupted and correlation rate is below than the threshold, a poor signature as result of the inspection is obtained. (Fig.7 c)



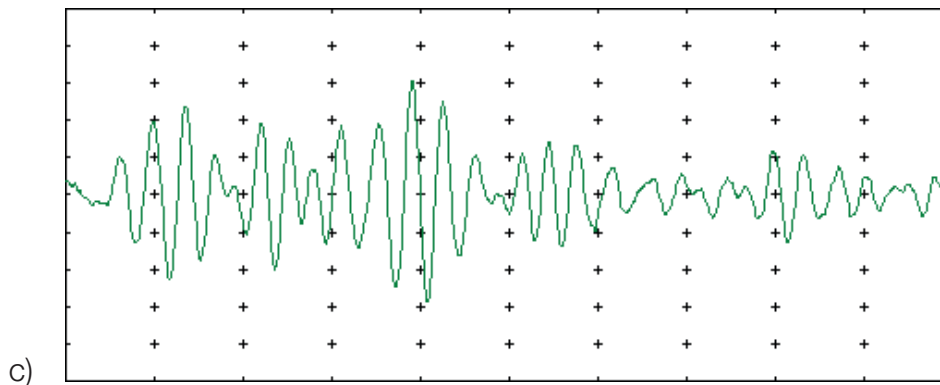


Figure 7: a) Reference signature; b) Corrected signature; c) Poor signature

50 portable network graphics (png) images of the RF signal were acquired for each of nine points. Comparative data analysis proved the uniqueness of the acoustic noise image.

Further data processing was performed whereby the initial signals were digitised and represented in the shape of data arrays thus representing them by a set of X and Y coordinates. The error minimization problem was solved by averaging the X and Y values for each signal,

after which an optimal number of peaks was defined and found to vary between 38 and 43. Noteworthy, due to the fact that a sufficient number of points is required in order to form a pattern the correlation rate decreased when the number of peaks was less than 38. However, a number of peaks higher than 43 will also result in the correlation rate decreasing due to the presence of peaks artificially created by the hardware. Thus, in the present study the optimal number of peaks was chosen to be equal to 40 (Fig.8).

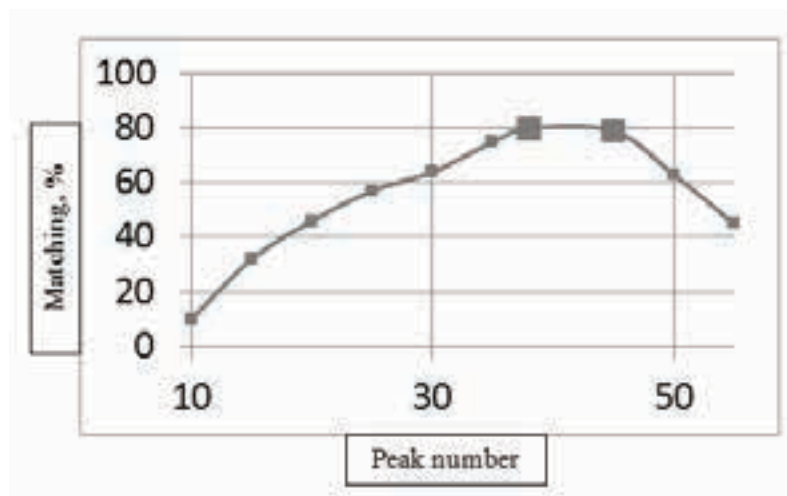


Figure 8: Data quantity optimizing

The peaks obtained create a pattern for the chosen measurement point described by a suitable function using OriginPro Lab 8.0. These data will be used for authentication.

During an inspection it is necessary to perform control measurements at some points chosen by the inspector, the results of which are compared to the patterns originally

assigned to the measurements at the same positions. In order to evaluate the data obtained, the confidence interval is defined taking into account the maximal number of peaks to minimize false data. Exceeding the confidence gate by 0.4 point leads to a significant increase in false data (Fig.9) and this is taken into consideration. The reference signal amplitude is taken as 1 and the gate is within the range [0.8 to 1.2].

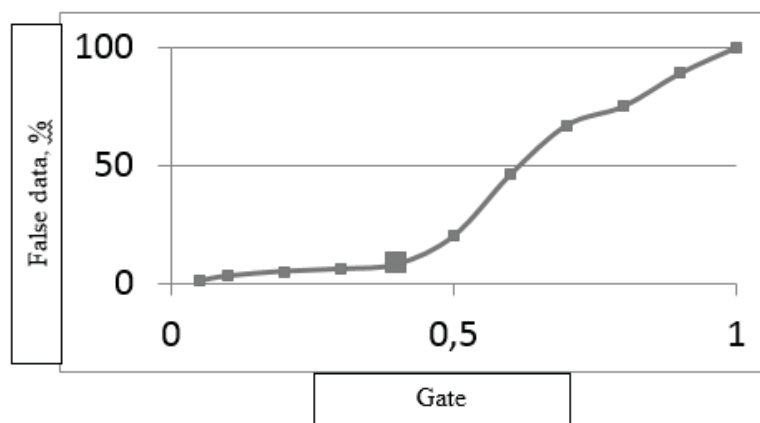


Figure 9: Confidence interval gate

Experiments have shown that in case of the successful authentication the match accuracy reaches from 72,5% to 87,5%. The divergences with the pattern are more often seen at the initial and final values of the data array. The Poor authentication case simulation demonstrates the match accuracy within the interval 12,5% to 45% that is considerably less the Successful authentication range.

4. Conclusion

Obtained results during the experiment have verified the consistency of the chosen combination of the control method and structural fingerprint appliance. The successful authentication demonstrates the levels of the feature points' compliance exceeding the given threshold on 65% which differs considerably from the percentage of the concurred points during authentication from other points. Since reproduction or doubling of the proposed unique identification characteristics is impossible at the current state science and technology, application of this technique is considered to identify the interference into the nuclear materials displacement with high accuracy.

Obtained results revealed the fact, that information for all 3S can be gathered by applying single measurement. Ultrasonic inspection of DIS cask closure weld has approved the following useful applications: for safety reasons - possible cracks and flaws for evaluating degradation of material; for security - intrinsic features of weld – natural fingerprint of material can be used as non-tamperable seal for controlling and accounting purposes; and for safeguards - automatic data acquisition and processing facilitates creation of the data storage in order to make verification process easy and robust.

5. Legal matters

I agree that ESARDA may print my name/contact data/ photograph/article in the ESARDA Bulletin/Symposium

proceedings or any other ESARDA publications and when necessary for any other purposes connected with ESARDA activities.

6. Acknowledgement

The reported study was partially funded by Federal Program "Science", No. 0.1146.2013.

7. References

- [1] Statement to Fifty-Sixth Regular Session of IAEA General Conference 2012 by IAEA Director General Yukiya Amano // www.iaea.org/newscenter/statements/2012/amsp2012n012.html
- [2] Seoul Nuclear Security Summit Communiqué // www.un.org/disarmament/content/spotlight/docs/Seoul_Communique.pdf
- [3] Kroening H.M., Sednev D.A., Chumak D.V. Non-destructive Testing at Nuclear Facilities as Basis for The 3S Synergy Implementation // Vol.2. – 2012. – p. 194-197. – 7th International Forum on Strategic Technology
- [4] ROSATOM guidelines to applying of sealing technologies for control and accounting purposes. <http://www.vniia.ru>
- [5] Safeguards Techniques and Equipment. – IAEA, Printed in Austria, 2003. – 82 p.
- [6] MIT Study on The Future of the Nuclear Fuel cycle - Massachusetts Institute of Technology, 2009. – 14 p.
- [7] Selection of Away-From-Reactor Facilities for Spent Fuel Storage - IAEA-TECDOC-1558 – IAEA, Vienna, 2007 – 8 p.
- [8] Safeguards-by-Design: Guidance for Independent Spent Fuel Dry Storage Installations – National

- Nuclear Security Administration Defense Nuclear Nonproliferation, 2012 – 29 p.
- [9] Snell's law. http://en.wikipedia.org/wiki/Snell's_law.
- [10] Olympus. 2011. Olympus Technical Notes - Ultrasonic Transducers. s.l. : Olympus, 2011.
- [11] Yastrebova, O., Kröning, M., Bulavinov, A. 2008. Real-time Measurement of Relative Sensor Position Changes using Ultrasonic Signal Evaluation. Stuttgart : 34. MPA-Seminar, 2008.
- [12] I.L. Erosh, M.B. Sergeev, N.V. Solovyov Image processing and recognition in security systems – Handbook – St. Peterburg, 2005 – 154 p.
- [13] Kroening H.M., Demyanyuk D.G., Sednev D.A., Lider A.M. Structural Fingerprints Of Containers With Nuclear Materials For Material Control And Accounting Purposes // Vol.2. – 2012. – P. 190-193. – 7th International Forum on Strategic Technology
- [14] Workman, G. L., Kishoni, D., Moore P.O. Ultrasonic Testing. American Society for Nondestructive Testing, 2007. – 329 p.
- [15] Yastrebova, O., Kröning, M., Bulavinov, A. Real-time Measurement of Relative Sensor Position Changes using Ultrasonic Signal Evaluation. –Stuttgart : 34. MPA-Seminar, 2008. – 23-29 p.
- [16] Achenbach, J. D. 2000. Quantitative nondestructive evaluation. International Journal of Solids and Structures. 2000, Bd. Vol. 37, Issues 1-2.
- [17] The interface between safety and security at nuclear power plants: a report by the International Nuclear Safety Group. – Vienna : International Atomic Energy Agency, 2010.
- [18] M. Suzuki, Y. Izumi, T. Kimoto, Y. Naoi, T. Inoue, B. Hoffheins “Investigating 3S Synergies to Support Infrastructure Development and Risk-Informed Methodologies for 3S by Design” Nuclear Nonproliferation Science and Technology Center, Japan Atomic Energy Agency 2-4 Shirane, Shirakata, Tokai-mura, Nakagun 319-1195 Japan
- [19] The Interface Between Safety and security at nuclear Power plants: a Report by The International Nuclear Safety Group. - Vienna: International Atomic Energy Agency, 2010.

State Regulatory Authority (SRA) Coordination of Safety, Security, and Safeguards of Nuclear Facilities: A Framework for Analysis

Stephen Mladineo[1], Sarah Frazar[1], Andrew Kurzrok[1]; Elina Martikka[2], Tapani Hack[2], Timo Wiander[2]

[1] Pacific Northwest National Laboratory - P.O. Box 999, Richland, Washington 99352 USA

Email: Steve.Mladineo@pnnl.gov

[2] Radiation and Nuclear Safety Authority, STUK, Finland

Abstract:

In November 2012 the International Atomic Energy Agency (IAEA) sponsored a Technical Meeting on the Interfaces and Synergies in Safety, Security, and Safeguards for the Development of a Nuclear Power Program. The goal of the meeting was to explore whether and how safeguards, safety, and security systems could be coordinated or integrated to support more effective and efficient nonproliferation infrastructures. While no clear consensus emerged, participants identified practical challenges to and opportunities for integrating the three disciplines' regulations and implementation activities. Simultaneously, participants also recognized that independent implementation of safeguards, safety, and security systems may be more effective or efficient at times. This paper will explore the development of a framework for conducting an assessment of safety-security-safeguards integration within a State. The goal is to examine State regulatory structures to identify conflicts and gaps that hinder management of the three disciplines at nuclear facilities. Such an analysis could be performed by a State Regulatory Authority (SRA) to provide a self-assessment or as part of technical cooperation either with a newcomer State, or to a State with a fully developed SRA.

Keywords: 3S; facility operations; regulatory development

1. Introduction

It has been long recognized that there are organizational and technical incompatibilities and at the same time overlaps among Safety-Security-Safeguards (3S)¹ requirements in nuclear facilities. In 2008, led by Japan, the G8 countries agreed to support the concept of 3S. The objective was to set up nuclear energy infrastructures in countries that were beginning nuclear programs. The idea was to help countries to integrate their approach to implementing safety, security, and safeguards measures so that they all receive appropriate attention, and through regulatory development, training. This approach would enable countries to take advantage of the synergies among the 3S components, while recognizing the differences.

Subsequently there has been much discussion about the concept of 3S. ESARDA and INMM meetings have devoted sessions to various elements of the topic, such as 3S by design and 3S culture. A special session at the 2013 INMM meeting in Palm Desert, California, focused on 3S including discussions of regulatory oversight, implementation at a spent fuel facility, and 3S by design [1]. International Meetings on Next Generation Safeguards have also addressed the topic [2]. In November 2012 the IAEA conducted a Technical Meeting in Vienna on Safety, Security and Safeguards: Interfaces and Synergies for the Development of a Nuclear Power Programme, which noted several interfaces and synergies between nuclear safety, security, and safeguards [3].

These discussions about 3S are typically conducted at a high level and rarely examine specific examples of when safeguards, safety and security measures intersect. In these cases, the reviews – while moving the literature forward – are typically limited to one element of 3S such as non-destructive testing [4], probabilistic risk analysis [5], or operator organizational structure [6]. Consequently, these discussions do not examine thoroughly whether such intersections reinforce or undermine the objectives of each discipline. Indeed, existing literature on the topic of 3S appears to echo the assumption that these intersections are inherently beneficial to the operator. The literature often continues to argue for greater coordination and integration of the three disciplines, particularly during the nuclear infrastructure development process.

The assumption that 3S is inherently beneficial does not encourage consideration of fundamental questions: Is there really a need for greater coordination and integration among the disciplines? Are there really many conflicts among the disciplines? Would greater coordination and integration have a measureable impact on facility operations or reduce perceived vulnerabilities or risks?

When we looked for examples that required a coordinated 3S intervention, we found a few, but each seemed to have reasonably simple solutions. The classic example has to do with emergency exits. You need to let people exit the facility in a fire emergency, but there is also a need to subsequently corral them for security reasons. There are also safeguards components to this example to ensure that no

¹ Acknowledging that there is no IAEA definition for 3S, we use the term in this paper as shorthand for Safety-Security-Safeguards.

one is exiting illegally while possessing nuclear material. Security can help, but the circumstances may require a physical inventory verification prior to letting people back into the facility. This well-known example seems to persuade people that there is something important about 3S, but more examples are needed to warrant promotion of the concept. Some other areas ripe for research and development include access control, facility design, and computer security risks.

Without a thorough examination of the intersections among the three disciplines, nuclear plant operators and regulators are limited in their conclusions about whether and in what contexts greater coordination among the disciplines would truly generate beneficial results. The purpose of this paper is to propose a framework for analysis of the concept, and then suggest how various entities might employ the framework. Officials from Finland's nuclear regulatory body, STUK, provide specific examples from their experience enforcing safeguards, safety and security regulations in Finland.

2. Framework

As part of the effort to develop a framework, we sought to record in a table intersections of safeguards, safety and security through the identification of discrete events that trigger interactions among the three disciplines.

Working from left to right, the table's four columns specify areas of impact ("Intersection Area"), the specific instigator of a possible 3S conflict ("Event"), the risk(s) posed by that event to one or more of the 3S disciplines ("Event Impact"), and potential ways to address these risks by restoring the equilibrium among the three disciplines ("Risk Mitigations").

(The order of the blocks in the table is arbitrary). By investigating each element of the framework individually, while focusing on the discrete events where the disciplines intersect, regulators, designers, operators and staff may be able to better identify who can take best advantage of or reinforce the 3S concept.

The event impacts described in the table and the risk mitigations proposed are illustrative. Further, the set of intersection areas may not be comprehensive. As recommended in the conclusion, stakeholders will need to further develop the content of this framework.

The table requires two prefatory notes:

When describing 3S intersections, risks and opportunities are two sides of the same coin. A situation can either be characterized as a risk that requires mitigation or an opportunity that overcomes a challenge. For example, the table could be structured to say either that "separate nuclear laws create conflicts and regulators should integrate them" or "an integrated nuclear law allows regulators to avoid conflicts that can arise". We have chosen for consistency to structure the table as risks that require 3S mitigation.

Further, it is important to note that this framework focuses on 3S impacts. As described in Suzuki et. al. [5], interactions between the three disciplines can include one or more of the three discipline pairs (safety-security; safety-safeguards; and security-safeguards) or impact all three disciplines. Table 1 is limited to the narrow set of interactions that force an intersection among all three disciplines, but future work could expand the table to capture additional events that only affect one or more of the discipline pairs.

Intersection Area	Event	Event Impact	Risk Mitigations
Nuclear laws and regulations	Development of a national nuclear law	Legislation with multiple compliance- or performance-based regulatory requirements for each of the three disciplines may create conflicts for operators	An integrated law can reduce the risk of conflicts among the requirements imposed by each of the three disciplines. Further, regular self-assessments, benchmarking with other nations' laws and cross-training can mitigate risk of inconsistent or conflicting regulations.
	Creation of regulatory organization(s) and authority(ies)	Regulators (or offices within a single regulator) may experience friction over jurisdiction and prioritization.	With appropriate management attention, an integrated nuclear regulatory authority can minimize friction points and provide processes to resolve conflicts. The operator only has to answer to one authority.
	Design of storage vaults	Opening the vault for inspection can create environmental dynamics that pose safety risks and weaken the security posture.	Tags/seals and unattended remote monitoring systems can maintain continuity of knowledge to meet safeguards needs while mitigating safety/security risks because the door remains closed.
Facility design	Design of data center(s)	Three independent data storage systems can lead to waste on certain shared needs (e.g., back-up power generation, access control) and can introduce risk through inconsistency of information.	Jointly housing data could optimize facility usage; provide savings on installation, facility space, and security; and minimize inconsistencies. Computer security [13] including data backup is essential to avoid single point failures.
	Risk Assessment [5]	Risk assessment methodologies within each discipline that do not consider the impact on other disciplines can create design conflicts and introduce risk.	Ensuring that risk assessment is harmonized across the three disciplines encourages optimized design choices. Special attention should be paid to the interfaces as these could pose significant risks, as experts from one discipline might assume that certain events are taken care of by the other domains
	Design of nuclear safety containment system [6]	A narrowly-focused nuclear safety containment design can create security or safeguards risks.	3S-cognizant nuclear safety containment design simultaneously reduces risks from accidents, theft, or diversion.
Inspections	Definition of physical protection system requirements [6]	Physical protection requirements impact radiation protection, loss avoidance, and safeguardability.	Developing facilities with 3S in mind reduces the risk of design conflicts and allows designers to optimize resource usage.
	State Regulatory Authority Inspection	Inspections focused on single disciplines might suggest recommendations that are detrimental to the other disciplines. Multiple inspections increase the burden on operators.	Cross training of inspectors. Participation in other domain inspections. Joint missions.
	Evacuation emergency (e.g. fire, criticality) at a facility that requires rapid egress	Personnel safety takes priority, potentially undermining security of the plant or of nuclear material, and risks loss of containment/surveillance continuity of knowledge about the material.	Security layers (e.g. secure evacuation points inside and outside the facility or operations on emergency exits). Physical inventory taking prior to return to normal exercises to identify and address possible weaknesses.
Information networks (computer security)	Computer-enabled attack on facility infrastructure that threatens security systems or plant operational systems (e.g. control room)	Confidentiality, integrity, and availability of security, safety systems and safeguards information are all at risk.	Note that network segregation is not adequate control alone, as Stuxnet has proven. Joint 3S vulnerability assessments of computer systems, potentially including penetration testing, fuzz testing, or exploiting data from one discipline to attack another can reveal potential points of attack and response solutions. Design principles and plans should be adequately protected against malevolent use.
	Physical attack on facility's information network that allows unauthorized access to facility's information systems	Confidentiality, integrity, and availability of security, safety systems and safeguards information are all at risk.	Joint 3S vulnerability assessments of computer systems can reveal potential points of attack and response solutions. Adequate backup solutions should include procedures for response if communication networks are lost.
	Development of facility IT platform(s) [7]	Data stored for each discipline independently can become stove-piped, or be not readily comparable.	Virtual consolidation of data on one secure supervisory software IT platform may yield savings on IT infrastructure while potentially making it more reliable and resilient.
	Communications protocols development [7]	Multiple protocols for similar tasks across the three disciplines (e.g., reports, alarms) can unnecessarily burden resources.	Implementation of standard communications protocols can yield savings on IT infrastructure, recognizing that as described by Stein et al. [7], standard communications protocols would have separate authentication and encryption schemes for each user role.

Training	Inspector training, curriculum design	As a starting point skills requirements should be defined and monitored. Inspectors trained to narrowly focus on their own discipline may miss seeing and reporting potential risks or vulnerabilities.	Cross-trained inspectors are more likely to identify potential risks or vulnerabilities in operational practices or regulation implementation; continual training helps keep all inspectors aware of new threats and points of consideration. Training records should be kept and analyzed against requirements.
Nuclear Operations	Diversion of nuclear material	An unauthorized diversion may create security and safety risks in addition to safeguards noncompliance.	IAEA safeguards inspections could trigger a safety or security alarm through a report of an anomaly.
	Inventory of nuclear material in storage	Conducting inventory can place safety (e.g., minimizing dose) in tension with safeguards and security (minimizing time that material is subject to theft or diversion).	Technical solutions could mitigate safety and security risks (e.g. remote verification, or containment and surveillance).
	Surveillance and assessment camera installation [6]	Independent safety, security, and safeguards cameras may be redundant and can strain resources.	Thoughtful placement of some cameras (with effective encryption and authentication for safeguards) could increase the facility's flexibility to respond to events in a defense-in-depth manner while reducing costs. It may be necessary to retain some non-networked cameras.
	Facility management process development [8]	The effectiveness of operations in each discipline can suffer from weak management.	Implementing advanced management concepts such as quality assurance, root cause analysis, equipment preventative maintenance, risk assessment, configuration management, design control, change control, document control, and records management reduce the risk of poor management oversight. Corporate governance policies, segregation of duties, identifying dangerous work combinations and good communications all play a significant role. Poor management can be a result of not knowing the big picture.
	Establishment of material accounting areas [6]	Gaps or overlaps in material accounting areas can introduce diversion opportunities and force duplicative equipment procurements.	Design accounting areas to avoid duplication of equipment and IT tracking conflicts.
	Facility design verification [6]	Facility as-constructed must meet safety, security, and safeguards design criteria, but developing verification procedures independently may waste resources or overlook vulnerabilities.	Planning validation and verification procedures to proceed with 3S in mind can resolve potential conflicts and save resources.

Table 1: 3S Events, Impacts, and Risk Mitigations

3. Preliminary Conclusions

From our preliminary findings suggested in the table, we can assert that there is value in the concept of 3S, and that a framework can be developed to support thoughtful analysis about how the three disciplines interact at a facility. Moreover, there are instances where safeguards, safety and security measures could be better coordinated, integrated or considered holistically by regulators, operators, designers and staff to improve facility operations. Recognizing that our framework and approach are not complete, we provide recommendations for various users to advance discussion on this topic. More research will be needed to validate our preliminary conclusions.

4. Implications

4.1 Regulators

Each State will choose its own approach to handling the coordination or integration of the three disciplines. Responsibilities for each discipline may reside in one or more organizations. In a nuclear newcomer state, it may be important to keep all of the issues under one organization to ensure that none of them is ignored. In a state with an advanced nuclear energy infrastructure, the disciplines may need to be managed separately. A regulatory authority with responsibility for all the disciplines may be most cost effective. A State with more than one regulatory authority will need to closely coordinate among these authorities to avoid conflicts or gaps. Either approach can ensure that regulators are able to see possible contradictions among requirements for operators. As a starting point there should be a joint risk assessment, including possible use of DBT, and risk management program among the 3S participants. The regulators for each of the three disciplines should be cognizant of the requirements of the other disciplines. With cross training of inspectors, they will be able to recognize conflicts when inspecting for any of the three disciplines. This would ensure that harmonization of regulations will prevent conflicts among requirements for each discipline.

In Finland, STUK is the 3S regulator. STUK experience has been that simply locating the responsibility in one organization is not enough. Regulations should reflect the possible synergies, interfaces and conflicts among the disciplines. And good practices to strengthen cooperation among the different sections include good coordination, assertive management, common informative meetings, and combined inspections by inspectors from each of the three disciplines.

4.2 Operators

In an operating facility, nuclear safety can eclipse nuclear security and safeguards due to its direct impact on worker safety and health and facility operations. Because of its

overriding priority, safety will often drive the budget, limiting the amount of money dedicated to safeguards and security measures. There are consequences to allowing this to happen. Reducing security measures can leave vulnerabilities. Limiting resources for safeguards implementation can lead to inaccurate or incomplete reporting to the International Atomic Energy Agency, which could generate suspicions that there has been a diversion. These suspicions may require greater IAEA scrutiny and intrusion into facility operations. A rigorous assessment by the operator of how the three disciplines benefit most from harmonization, or how they are likely to generate vulnerabilities would help inform resource allocation for a facility.

From a Finnish perspective, it is essential that the operator incorporate safeguards and security into the bidding process to achieve more functional nuclear plants and save costs. This is not strictly a design issue, as all the relevant parties developing new plants should understand the basic criteria on safeguards and security. This requires informative meetings among the operator, the State Regulatory Authority, and designers with the IAEA or the regional safeguards authority. This will facilitate safeguards measures with the needed equipment and cabling being implemented in a harmonized way, integrated with safety and security requirements.

4.3 Designers

For nuclear facility design engineers, safety has been the overriding paradigm. Accidents at Three Mile Island, Chernobyl, and Fukushima have reinforced that concern. Industrial safety, criticality safety, radiation safety, electrical safety, high pressure safety, and other areas of safety are likely to be second nature to the designers. In the past, security was left to the security professionals, and therefore was often an add-on to the facility design and computer systems. International Safeguards has had even less emphasis in the design community, and has had to be developed as an afterthought. Clear requirements and guidance are needed for developers.

One example is the first final-disposal facility for spent nuclear fuel, currently under licensing review and partially under construction in Finland. The facility will consist of an encapsulation plant and a geological repository for spent nuclear fuel. The safety of final disposal is a fundamental issue. The current process and plans for the encapsulation plant and geological repository have been designed primarily with safety in mind. The implementation of security and safeguards must not compromise safety. However, challenges appear from the security point of view. These include the identification of vital and inner areas; creation of a new design basis threat (DBT); identification of interfaces, synergies and challenges between safety, security and safeguards, and handling classified information throughout the lifecycle of the facility.

The safeguards concerns of final disposal are unprecedented. Traditional safeguards measures for the spent fuel will be impossible once the fuel is stored and tunnels are backfilled. The whole process must provide sufficient assurance that the fuel has been stored and emplaced according to declarations and that no diversion has been possible. Several safeguards decisions are part of broader 3S considerations. For example:

- The calibration of the equipment used for verifying spent fuel before encapsulation involves both computer security and safeguards aspects,
- Continuity of knowledge from the first verification of spent fuel to the last one before encapsulation is an issue that involves safety, security and safeguards.
- Once the capsules are moved from the encapsulation plant to the final disposal storage underground verification is no longer possible. This movement involves safety, security and safeguards.

Some challenges have occurred in the design of the facility, underscoring the importance of recognizing the safeguards requirements early in the design phase. An analogy is designing a house without considering electricity, and it is only once construction is done that you realize that you forgot to include cabling. In a nuclear facility, particularly one where the operating duration is measured in centuries, including safeguards in the design phase would prevent such problems. Further, during the life of the facility some parts may be storing nuclear material while other parts will still be under construction. Therefore, it is necessary that safeguards be designed into the facility along with safety and security to manage these activities.

The international community has started to meet this challenge. The International Atomic Energy Agency published guidance on safeguards by design principles in 2013 [9], and US National Nuclear Security Administration's Next Generation Safeguards Initiative has sponsored development of a series of Safeguards by Design guidance documents to be used for reference by designers [10]. In January 2012, the IAEA issued a new Safety Requirements document that includes the requirement that safety measures, nuclear security measures and arrangements for the State system of accounting for, and control of, nuclear material for a nuclear power plant shall be designed and implemented in an integrated manner so that they do not compromise one another [14].

Consideration of all three disciplines during the design phase may lead to operational efficiencies but more research is needed in this area.

4.4 Staff

In previous articles some of the current authors have discussed the culture of the three disciplines (safety-security-safeguards) using an organizational culture construct [11].

We argued that safety culture was the best developed of the three, with nuclear security still catching up since the attacks of September 11, 2001. Safeguards culture is the least developed of the three, partly because there is no natural analogue to international safeguards in daily life. Additionally, safeguards culture does not benefit from having an internationally agreed-upon definition as do safety culture and nuclear security culture. Even less developed is the concept of a 3S culture. We have argued elsewhere that an international agreed-upon definition of safeguards culture should be a next step prior to consideration of 3S culture. [12] The framework developed in this paper suggests there are specific actions staff may be able to take to reinforce 3S objectives and communicate the importance of all three disciplines in an organization. A closer examination of these actions could lead to more productive development of the 3S concept.

5. Conclusions

We have proposed a framework for analysis, but have not performed the rigorous analysis that we argue needs to be done. Rather than continuing to talk about 3S in the abstract, we propose a focused research project that brings together experts from each of the disciplines to give the nuclear community a better understanding of the range of specific conflicts that 3S integration could help resolve. Once understood, communities of regulators, operators, and designers can begin to discuss best practice. By taking actionable steps to scope and implement 3S, the international community can take advantage of the potential benefits of 3S activities.

6. References

- [1] *Proceedings of the Institute of Nuclear Materials Management; 54th Annual Meeting*, July 2013.
- [2] "NNSA Completes Fourth International Meeting on Next Generation Nuclear Safeguards"; Press Release; July 12 2012; accessed October 7, 2013; <http://www.nnsa.energy.gov/mediaroom/pressreleases/safeguards071212>.
- [3] Martikka E; Hack T; *Chairperson's Summary; Technical Meeting (TM) on Safety, Security and Safeguards: Interfaces and Synergies for the Development of a Nuclear Power Programme*; Vienna, Austria; 2012.
- [4] Kroening M; Sednev D; Chumak D; *Nondestructive Testing At Nuclear Facilities As A Basis For The 3S Synergy Implementation; 7th International Forum on Strategic Technology*; IEEE; 2012.
- [5] Suzuki M; Izumi Y; Kimoto T; Naoi Y; Inoue T; Hoffheins B; *Investigating 3S Synergies to Support Infrastructure Development and Risk-Informed*

- Methodologies for 3S by Design; IAEA-CN-184/64; Safeguards Symposium: Preparing for Future Verification Challenges; International Atomic Energy Agency; 2010.*
- [6] Al Hashmi W; Al Remeithi R; Qasem M; Al Darmaki S; Al Katheeri N; Al-Madhloum AM; Schuller M; Williams AD; *One Path to Integrating Nuclear Safety, Security and Safeguards Systems: Perspectives of GNEII Alumni; 53rd Annual Meeting of the Institute of Nuclear Materials Management; Orlando, FL; 2012.*
- [7] Stein M; Morichi M; Van Den Durpel L; *Safeguards by Design—An Industrial View; 51st Annual Meeting of the Institute of Nuclear Materials Management; Baltimore, MD; 2010.*
- [8] Kovacic DN; Raffo-Caiado A; McClelland-Kerr J; Van Sickle M; Bissani M; Apt K; *Nuclear Safeguards Infrastructure Development and Integration with Safety and Security; 50th Annual Meeting of the Institute of Nuclear Materials Management; Tucson, AZ; 2009.*
- [9] International Atomic Energy Agency; *International Safeguards in Nuclear Facility Design and Construction; IAEA Nuclear Energy Series; No. NP-T-2.8; Vienna, Austria; 2013.*
- [10] NGSi Safeguards by Design; National Nuclear Security Administration; accessed April 26, 2013; <http://nnsa.energy.gov/aboutus/ourprograms/nonproliferation/programoffices/officenonproliferationinternationalsecurity-0-0>.
- [11] Frazar S; Mladineo S; *Safeguards Culture: Lessons Learned; ESARDA Bulletin; Vol. 44. June 2010.*
- [12] Frazar S; Mladineo S; *Safety, Security, and Safeguards (3S) Culture; Proceedings of the 7th Joint ESARDA/INMM Workshop; Aix en Provence, France; October 16-20, 2011.*
- [13] IAEA Nuclear Security Series No. 17. Computer Security at Nuclear Facilities. Available at: http://www-pub.iaea.org/MTCD/Publications/PDF/Pub1527_web.pdf (Referenced 8 Oct. 2013).
- [14] IAEA Safety Standards: Safety of Nuclear Power Plants: Design for protecting people and the environment No. SSR-2/1 Specific Safety Requirements January 2012 STI/PUB/1534

Collection and Analysis of Open Source News for Information Awareness and Early Warning in Nuclear Safeguards

Giacomo G.M. Cojazzi, Erik van Der Goot, Marco Verile, Erik Wolfart

Joint Research Centre, European Commission - Via Fermi, Ispra 21020 (VA) Italy

Marcy Rutan Fowler, Yana Feldman, William Hammond, John Schweighardt, Matthew Ferguson

International Atomic Energy Agency - Wagramerstrasse 5, P.O. Box 100, 1400 Vienna, Austria

Abstract:

Acquisition and analysis of open source information plays an increasingly important role in the IAEA's move towards safeguards implementation based on all safeguards relevant information known about a State. The growing volume of open source information requires the development of technology and tools capable of effectively collecting relevant information, filtering out "noise", organizing valuable information in a clear and accessible manner, and assessing its relevance.

In this context, the IAEA's Division of Information Management (SGIM) and the EC's Joint Research Centre (JRC) are currently implementing a joint project to advance the effectiveness and efficiency of the IAEA's workflow for open source information collection and analysis. The objective is to provide tools to support SGIM in the production of the SGIM Open Source Highlights, which is a daily news brief consisting of the most pertinent news stories relevant to safeguards and non-proliferation. The process involves the review and selection of hundreds of articles from a wide array of specifically selected sources.

The joint activity exploits the JRC's Europe Media Monitor (EMM) and NewsDesk applications: EMM automatically collects and analyses news articles from a pre-defined list of websites, and NewsDesk allows an analyst to manually select the most relevant articles from the EMM stream for further processing.

The paper discusses the IAEA's workflow for the production of SGIM Open Source Highlights and describes the capabilities of EMM and NewsDesk. It then provides an overview of the joint activities since the project started in 2011, which were focused i) on setting up a separate EMM installation dedicated to the nuclear safeguards and security domain (Nuclear Security Media Monitor, NSMM) and ii) on evaluating the NSMM/NewsDesk for meeting the IAEA's needs. Finally, it presents the current use NSMM/NewsDesk at the IAEA and proposes options for further integration with the IAEA workflow.

Keywords: open source information, information collection and analysis, media monitoring, non-proliferation, nuclear safeguards

1. Introduction

The Agency collects and processes safeguards relevant information about a State from a wide range of sources: information provided by the State itself (e.g. declarations and reports); safeguards activities conducted by the Agency in the field and at Headquarters (e.g. inspections, design information verification, material balance evaluations); and other relevant information (e.g. from open sources and third parties) [1].

Open source information is defined as any information that is neither classified nor proprietary. It includes but is not limited to: media sources, government and non-governmental reports and analyses, commercial data, and scientific/technical literature. The Agency conducts ongoing reviews of all safeguards relevant information and evaluates its consistency with the State's declarations about its nuclear programme.

The growing volume of open source information, the diverse forms of information available (text, audio, visual), and the technical competence required to evaluate this information poses significant challenges to effective information collection and analysis. Meeting these challenges requires the development of technology and tools capable of effectively collecting relevant information, filtering out "noise", organizing valuable information in a clear and accessible manner, and aiding in the assessment of the information's relevance.

To improve the IAEA's ability to utilize open source information, a joint project is currently underway as part of the European Commission's (EC) support to the IAEA Department of Safeguards (task EC-D-1880) to optimise existing processes involved in the daily collection of open source information by the Global Monitoring Team (GMT) and production of SGIM Open Source Highlights (OSHL) [2]. The project utilizes the Europe Media Monitor EMM/NewsDesk application, developed by the EC's Joint Research Centre (JRC).

This paper describes the continuation of a project which was previously reported on at the Institute of Nuclear Materials Management (INMM) Annual Meeting in 2011 [3]. Section 2 describes the workflow for the daily collection of open source information by the SGIM GMT and for the

production of SGIM Open Source Highlights (as it existed prior to the start of the joint project). Section 3 discusses the EMM family of tools and provides an overview of the main functionalities and underlying technologies.

Section 4 describes the work that has been carried out in order to customise EMM to IAEA's needs with the goal of optimizing IAEA's Open Source Collection process: it discusses the testing that took place in the pre-launch phase (coverage tests), and the deployment and outcomes of the Phase 1 launch of the application (usability tests). Section 5 details the ongoing joint activities to streamline the production of the OSHL and proposes efforts to enable a more effective and efficient mining of open source information to enhance state evaluation through continuous monitoring. Section 6 draws some conclusion.

2. Open Source Information at IAEA

Acquisition and analysis of safeguards-relevant open source information plays an important role in the understanding of a State's nuclear fuel cycle and activities. All safeguards relevant information available to the IAEA is used not only to support the drawing of safeguards conclusions, but also to plan the optimal set of safeguards verification activities to be conducted in a State. The evaluation of all information is an ongoing and iterative process, in which knowledge about a State will continue to expand and improve. This allows the Agency to draw safeguards conclusions in the most effective and efficient way [4].

The Department of Safeguards uses open sources in several ways in support of the State evaluation process, including: i) daily review of open source information by the GMT to maintain current awareness and serve as early warning for safeguards-significant events; ii) as part of continuous monitoring of safeguards-relevant activities within a State, which contributes to State evaluation; iii) for focused research to support in-field verification activities such as complementary access; and iv) for special investigations related to a specific State, entity, fuel cycle step, or technology.

The IAEA's focal point for the collection and analysis of open source information is the Division of Information Management (SGIM) within the IAEA's Department of Safeguards. As part of its mandate for reviewing and analysing open source information to maintain current awareness and provide early warning for safeguards-significant events, SGIM produces a daily news briefing, called SGIM Open Source Highlights (OSHL), which covers safeguards-relevant news and analyses items, as well

as relevant developments in nuclear non-proliferation, disarmament, arms control, and the nuclear fuel cycle. OSHL generally consists of four to eight news stories daily, and has a distribution list of nearly 600 staff members within the Department of Safeguards and other IAEA staff. A typical snapshot of SGIM Open Source Highlights is shown in Figure 1.

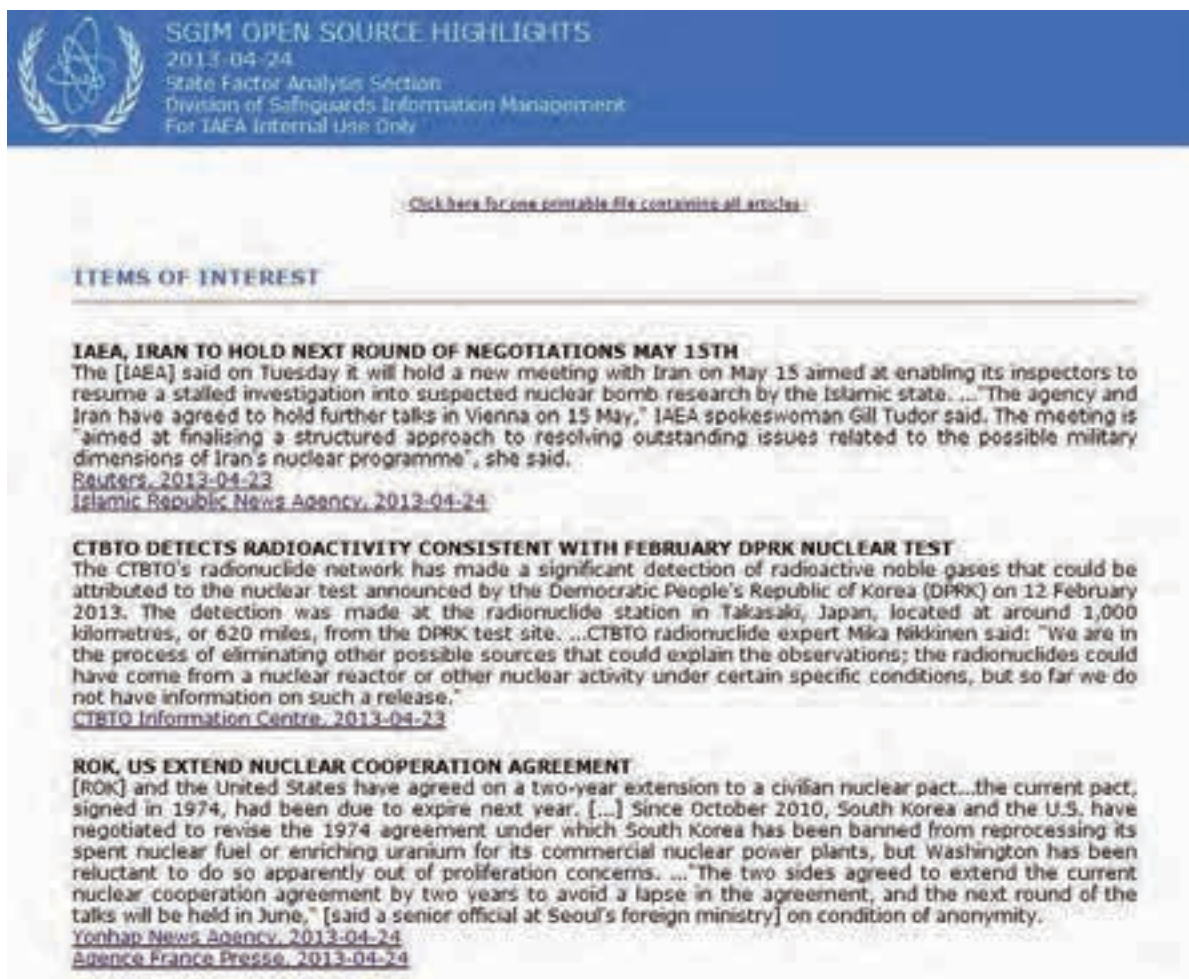
Periodically, the IAEA conducts a user survey of SGIM Open Source Highlights readers. In the most recent survey conducted, over 90% of those who responded considered Highlights important in their work. The majority of staff use Highlights to stay informed of safeguards-related news around the world, and, to a lesser degree, to track country-specific issues and to learn of relevant commentary and analysis on safeguards and non-proliferation issues. Three-quarters of respondents read Highlights every day, and over 95% read Highlights the same day it comes out. 90% of respondents prefer to receive Highlights with abstracts. Overwhelmingly, the Highlights' readership finds the breadth of issue coverage and sources used appropriate and satisfactory. 99% of respondents are satisfied or highly satisfied with the product.

2.1 Daily Review Procedures

The production of OSHL begins with a coordinated daily review by the Global Monitoring Team (GMT) of news repositories and websites. Sources of information include subscription-based news databases and aggregators, general news media sites, blogs, non-governmental organizations (NGOs), universities and research institutes, and government agency websites.

The daily monitoring consists of a preliminary manual review by the GMT of approximately 1500 news items on average. Prior to the Phase 1 NewsDesk deployment (see section 3.1), the daily monitoring consisted of three streams of information: i) a subscription-based news database, ii) website-tracking software set up to monitor over 100 news and analysis sites not covered by the database, and iii) a set of websites composed of nuclear-focused news aggregators, internal sources, and subscription-based publications.

Approximately 100 articles are selected for secondary review by the OSHL editorial team, which then selects articles either for inclusion in OSHL or for further back end processing ensuring the long-term availability of the information. Following these previous procedures, the preliminary review required approximately three staff-hours, followed by the secondary review by the OSHL editorial team of approximately one staff-hour.



SGIM OPEN SOURCE HIGHLIGHTS
2013-04-24
State Factor Analysis Section
Division of Safeguards Information Management
For IAEA Internal Use Only

[Click here for one portable file containing all articles.](#)

ITEMS OF INTEREST

IAEA, IRAN TO HOLD NEXT ROUND OF NEGOTIATIONS MAY 15TH
The [IAEA] said on Tuesday it will hold a new meeting with Iran on May 15 aimed at enabling its inspectors to resume a stalled investigation into suspected nuclear bomb research by the Islamic state. ... The agency and Iran have agreed to hold further talks in Vienna on 15 May," IAEA spokeswoman Gill Tudor said. The meeting is "aimed at finalising a structured approach to resolving outstanding issues related to the possible military dimensions of Iran's nuclear programme", she said.
[Reuters, 2013-04-23](#)
[Islamic Republic News Agency, 2013-04-24](#)

CTBTO DETECTS RADIOACTIVITY CONSISTENT WITH FEBRUARY DPRK NUCLEAR TEST
The CTBTO's radionuclide network has made a significant detection of radioactive noble gases that could be attributed to the nuclear test announced by the Democratic People's Republic of Korea (DPRK) on 12 February 2013. The detection was made at the radionuclide station in Takasaki, Japan, located at around 1,000 kilometres, or 620 miles, from the DPRK test site. ... CTBTO radionuclide expert Mika Nikkinen said: "We are in the process of eliminating other possible sources that could explain the observations; the radionuclides could have come from a nuclear reactor or other nuclear activity under certain specific conditions, but so far we do not have information on such a release."
[CTBTO Information Centre, 2013-04-23](#)

ROK, US EXTEND NUCLEAR COOPERATION AGREEMENT
[ROK] and the United States have agreed on a two-year extension to a civilian nuclear pact...the current pact, signed in 1974, had been due to expire next year. [...] Since October 2010, South Korea and the U.S. have negotiated to revise the 1974 agreement under which South Korea has been banned from reprocessing its spent nuclear fuel or enriching uranium for its commercial nuclear power plants, but Washington has been reluctant to do so apparently out of proliferation concerns. ... "The two sides agreed to extend the current nuclear cooperation agreement by two years to avoid a lapse in the agreement, and the next round of the talks will be held in June," [said a senior official at Seoul's foreign ministry] on condition of anonymity.
[Yonhap News Agency, 2013-04-24](#)
[Agence France Presse, 2013-04-24](#)

Figure 1: Snapshot of SGIM Open Source Highlights. News stories are presented in order of importance to safeguards activities.

2.2 Production and Distribution of SGIM Open Source Highlights

Once news stories are selected for inclusion in OSHL, they are distributed to the OSHL editorial team. Editors research the stories, and create an abstract of the issue of approximately 3-5 sentences, pulling together several sources as necessary. The abstracts are posted as drafts in a blog format on a SharePoint intranet portal called the IAEA Safeguards Portal. The abstracts are then reviewed by an editor and published on the Safeguards Portal. Each abstract includes a link to a PDF of the full-text article(s) that is saved for archival purposes.

Once abstracts of all news stories for the day are completed, they are also distributed in an email newsletter to nearly 600 IAEA staff members. Production of the OSHL takes approximately an additional four to six staff-hours a day, depending on the volume of news and the complexity of the issues.

2.3 Back End Processing

Because of the dynamic nature of information contained in websites, the daily monitoring of open source information also serves to build an IAEA internal knowledge base. This

ensures that information that is identified as relevant by the GMT is available to the Agency in the future. Selected articles are manually processed to add metadata and then transferred to the internal repository. This process takes approximately one staff-hour per day. The resulting repository is used as a starting point for subsequent analysis work related to State evaluations and other safeguards verification activities.

3. Europe Media Monitor Platform and Tools

The Europe Media Monitor (EMM), developed by JRC [5], is a web-based multilingual news aggregation system that collects over 170 000 news articles per day in about 50 languages from more than 4000 web news sources. The sources are mainly general news sites with a world-wide coverage, but also include some specialist websites and twenty commercial news providers. The system employs text mining techniques to provide a picture of the present situation in the world as conveyed in the media. These techniques include automatic multilingual categorization, entity extraction, geo-location, quote extraction and sentiment analysis. In addition, an algorithm for detecting breaking news automatically clusters all collected news articles every ten minutes and displays the ten largest

clusters per language by plotting them on a time-by-size graph. It also provides all the necessary hyperlinks to navigate through the clusters and to go to the source for a detailed exploration. Furthermore it applies some deeper semantic information analysis techniques, for example, to automatically detect violent events, derive reported social networks and analyze media impact [6].

EMM creates a searchable full-text index of all articles that flow through the system. For each article, it stores meta-information including title, description, source, category, language, and original URL (Uniform Resource Locator). However, it does not store the original article itself.

At the core of the EMM system is a processing chain of lightweight extensible processes each independently running and chained together using a very basic but reliable in-house developed web service architecture. Articles flow through the processing chain as thin RSS (Really Simple Syndication) items that grow as meta-data gets added at each stage of the processing chain. The first process in this chain is a Scraper. This process periodically checks all web sites of interest and generates a simple RSS feed containing a list of the current items published on the site. The next system in the chain, Grabber, is then notified with the resulting RSS feed. Grabber detects the new articles published and using a text extraction process determines the main content of the new articles. Grabber produces a new RSS feed for each site, containing title, link, description and text for all new articles detected, which is then passed on to the next process in the chain, the automated language detection process. The automatic language detection process uses word frequency tables to automatically detect the language of the RSS content in the title and description. Next the Entity Recognition process detects people and organizations in the article from a home grown information base of entities and organizations which is populated by an automated (offline) entity recognition system [7]. Homonyms are detected and disambiguated using a multilingual, classified geospatial information base of place names, provinces, regions and countries. The disambiguation module also uses the meta-information of previously recognized entities, in order to perform geo-tagging. Then, the classification system works on two levels, first it classifies articles on Boolean combinations of multilingual keywords, second it classifies on Boolean combinations of previously discovered classes and other metadata. A near-duplicate detection system identifies and flags duplicate articles, even if they contain small variations. It uses character trigram feature vectors and performs a simple cosine distance calculation. Finally a tonality module assigns tonality to the RSS item using a similar keyword based approach as the classification system. All of these processes that implement basic information extraction rely on the use of highly efficient finite state machine pattern matchers.

The articles then flow into the Clustering and Story Tracking Cache. Every 10 minutes the last 4 hours of articles are

hierarchically clustered in every language individually. Initially each news article is considered to be a cluster, the process is agglomerative and employs average group linkage to determine the distance between the clusters using a simple cosine measure. The clustering process continues until the maximum cosine distance falls below a certain set threshold. The article feature vectors are simple word count vectors, constructed using a simple bag of words approach, with some additional ad-hoc rules like: ignore top 100 frequent words, ignore words of 2 characters. A cluster only remains if it has at least 2 articles that are not duplicates from at least 2 different news stories. The system also tracks the evolution of stories over time. It is represented as the evolution of a news cluster as it grows or shrinks in time.

Several EMM installations have been set-up providing varying thematic focus and user accessibility. The main EMM installation monitors generic news media with little coverage of specialised thematic areas and serves as a general media monitor and demonstrator of EMM capabilities. Its front page – the EMM Newsbrief [8] – provides a user interface to all this information and is visited on a regular basis by some 25 000 users, and gets some 1.5 million hits per day. A snapshot of the EMM website is shown in Figure 2. Other EMM installations are targeted at specific thematic areas and/or customers. For example, MedISys is specialized in medical and health-related topics [9].

3.1 NewsDesk

EMM is a powerful tool for automatically aggregating and analysing open source information from the Internet. However, if the information needs to be disseminated further or fed into an existing information analysis workflow, the generated news stream has to go through a review and selection process carried out by a domain expert. For this purpose, the JRC developed the NewsDesk application (see Figure 3).

NewsDesk allows for manual review and selection of the most relevant articles with an easy-to-use drag-and-drop interface. It also supports the rapid production of newsletters which can be disseminated to interested user groups. The articles selected in NewsDesk including the meta-information extracted by EMM can be posted to existing third-party IT systems, for example, to ingest the information into a back end archive or to publish the selected news on a web portal.

NewsDesk is conceived as a collaborative environment, i.e. users are organised in virtual groups where they can work as a team on the news articles review and newsletter production. It is a web application, which uses RSS feeds as information input – typically generated by EMM. However, it is also possible to ingest feeds from third-party applications. NewsDesk allows users to send notifications via SMS or e-mail; it also integrates an automated notification system to alert personnel on duty during holidays or out of office hours.



Figure 2: Partial view of the EMM Newsbrief page showing details of the main functional areas: the graph at the top shows the development of the ten top stories over the last twelve hours; details of the top stories and the links to the related articles are listed below the graph. The top stories are across all thematic areas. The navigation bar on the left provides access to sub pages that filter articles – based on EMM's classification system - according to thematic or geographic areas of interest. The part of the page that allows filtering the articles according to language is omitted for improved readability.

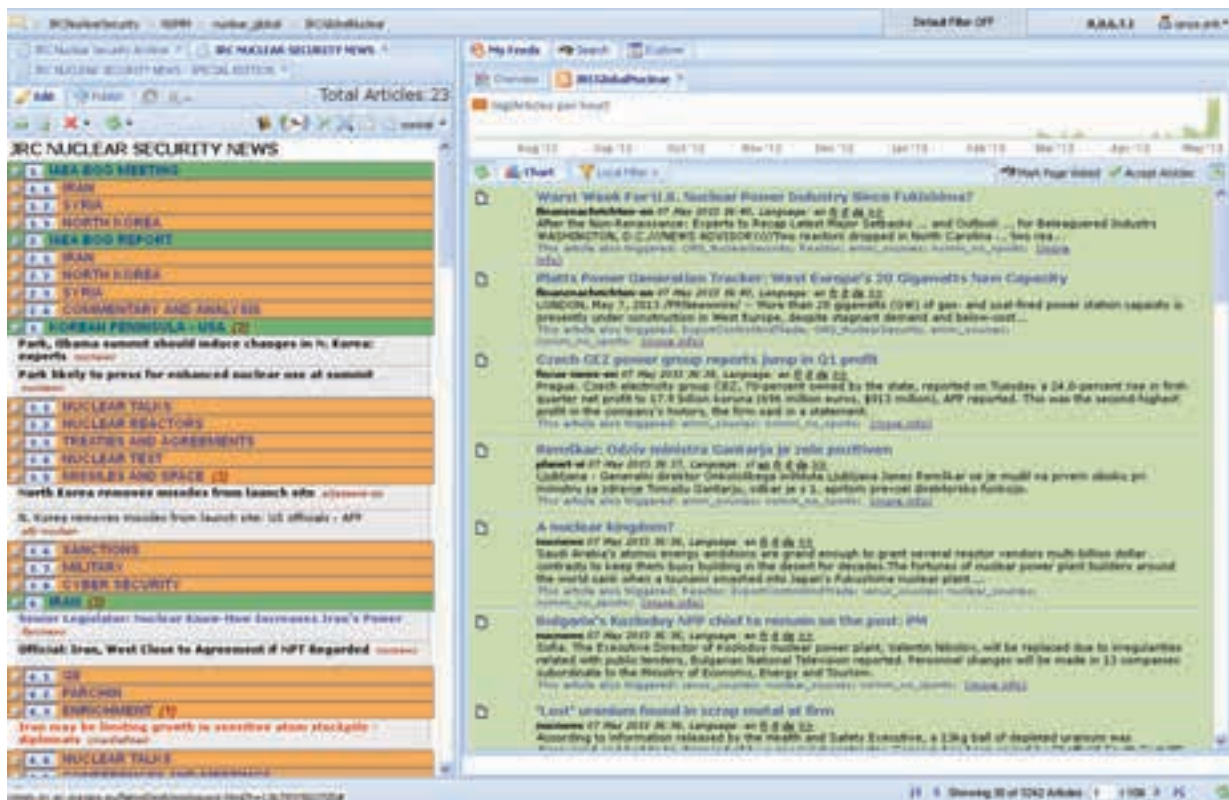


Figure 3: Screenshot of the NewsDesk workspace. The news feed generated by EMM is displayed in the right column. The analyst reviews the information, selects relevant articles and drags them to the newsletter area in the left column. Selected articles can be edited and then published using a customisable newsletter template.

3.2 Other EMM Tools

Besides NewsBrief web site and NewsDesk moderation tool, the EMM platform provides additional tools including:

- *Category Editor*: 'Categories' are a fundamental part of the EMM system, as they allow generating automatic alerts and filters according to thematic or geographic areas of interest, thus significantly reducing the information overload. The Category Editor is a web-based application that enables users to create and maintain the category definitions, which can be based on complex keyword or meta-data combinations. A description of the category mechanism and results for applying it to the medical and health domain is given in [10].
- *Media Impact* is a media analysis tool that, starting from a dataset (typically news articles selected via a search in NewsDesk), allows media analysts to further tag and aggregate articles in order to produce statistics and reports. The primary purpose is to analyse how specific events are reported in the world-wide media and to examine their media impact according to country, media type or other criteria. The tool exploits the meta-information automatically extracted by EMM together with manually added metadata.
- *EMM Mobile Apps* for both iOS and Android platforms addresses the need of a personalized access to the EMM content and functionality. The web site content

selection is fully automated and its ergonomics offers a common navigation through the daily news. NewsDesk and Media Impact are meant for human-moderated news selection where final clients receive a product conceived and structured by analysts; EMM Mobile Apps ultimately gives end-users direct control on content selection and visualization in order to render their own view of the daily news [11].

4. Optimizing IAEA's Open Source Collection Process

The IAEA intends to increase the efficiency of its open source information monitoring process and OSHL production workflow and therefore is interested in using EMM/NewsDesk. IAEA and JRC are engaged in a joint project to evaluate EMM/NewsDesk for IAEA needs and to analyse how the applications can be integrated in the existing IAEA workflows and systems.

The IAEA has a well-established workflow for the open source information collection and SGIM Open Source Highlights production, which is constrained by various boundary conditions including legacy IT systems, confidentiality considerations and time and human resource availability. The IAEA/JRC collaboration on the project aims to analyse EMM/NewsDesk compatibility with respect to i) source coverage ii) interoperability with existing

IAEA back end IT systems and iii) NewsDesk functionality and compatibility with IAEA workflow. It is anticipated that at a minimum EMM/NewsDesk will be used to process the information sources that IAEA currently monitors manually. Potentially, it can cover the entire workflow including the review of all sources, the production and dissemination of OSHL and back end processing.

The remainder of this section illustrates the issues that have been addressed since the start of the project in order to introduce EMM/NewsDesk to the IAEA workflow and describes the current status of the activities.

4.1 Nuclear Security Media Monitor (NSMM): Extending Source Coverage

The public version of EMM monitors pre-selected websites targeting mainly general news media with little coverage of specialised thematic areas. Typically, important news stories are duplicated across many media sites, thus generating some redundancy in the system. Consequently, the system tolerates a certain degree of undetected articles, meaning that not all relevant articles of all targeted sites need to be retrieved.

The IAEA, however, also needs to monitor a set of specific nuclear safeguards-related websites, including NGOs, blogs and sites of national and international authorities. Hence, IAEA provided a list of more than 140 nuclear-specific

websites, which it would like to be added to the EMM source list (hereafter referred to as nuclear websites).

In order to fine-tune EMM to IAEA needs without interfering with the public EMM website, it was decided to set-up a separate EMM installation dedicated to the nuclear safeguards and security domain, hereafter referred to as Nuclear Security Media Monitor (NSMM). The types of websites of potential interest to the IAEA and therefore monitored by NSMM include: nuclear-focused news agencies and aggregators; regional, national and local government and intergovernmental organisations whose domain covers nuclear issues; NGOs, academic sources and blogs providing analyses on safeguards-relevant topics; general news sources and aggregators; technical publications on the nuclear fuel cycle, etc. A classification of the sources monitored by NSMM is given in Table 1 and a snapshot of the NSMM NewsBrief page is given in Figure 4.

Some technical challenges still needed to be resolved as the nuclear websites differ from the general news media typically targeted by EMM in several aspects: i) the nuclear websites often publish unique information, thus a high reliability in the detection of new articles is required, ii) the nuclear websites are more static, i.e. the frequency of new articles/reports is much lower and iii) some of the nuclear sites require authentication.

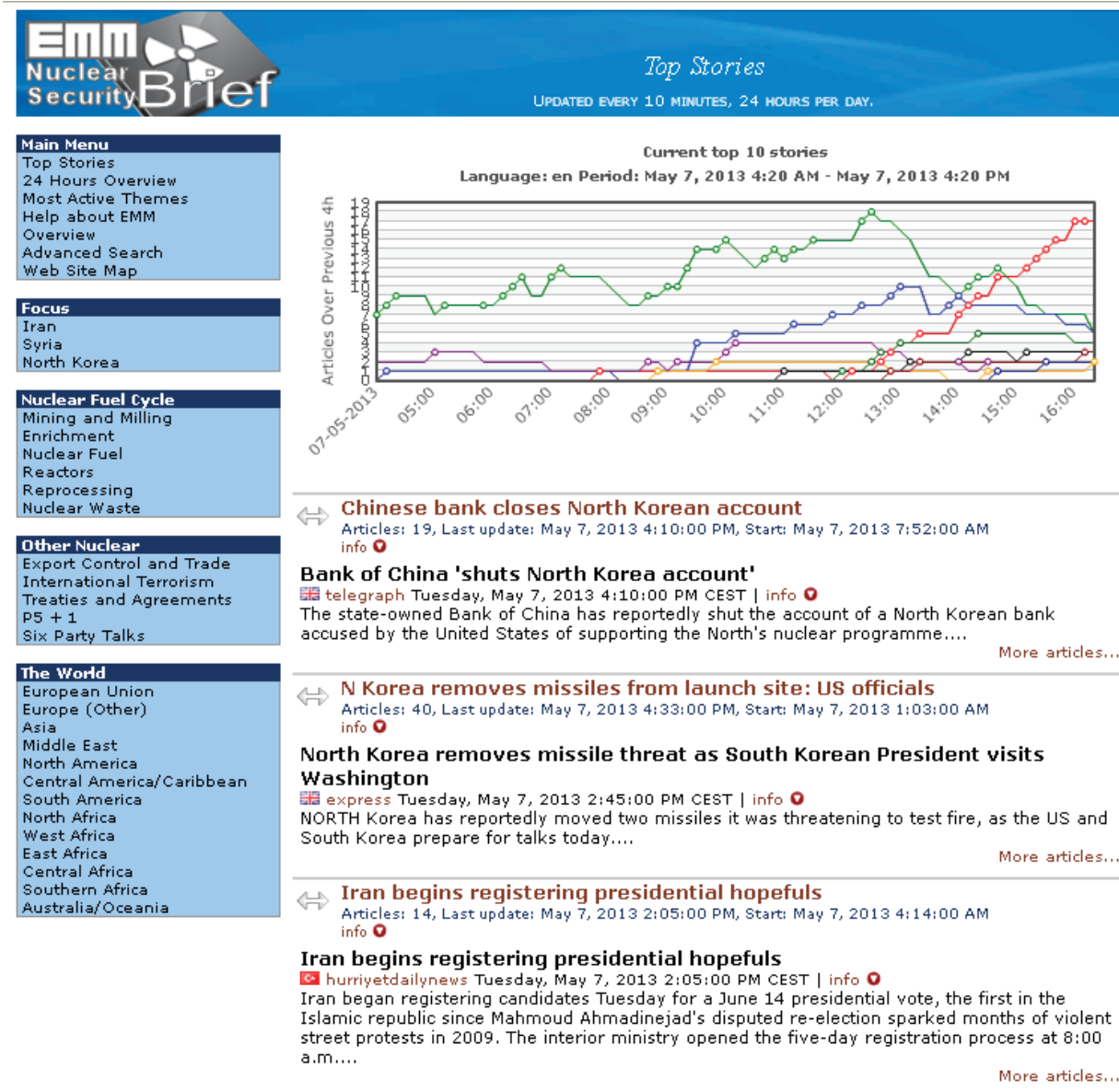


Figure 4: Partial view of the NSMM NewsBrief page. Structure and functionality of the page correspond to the generic EMM NewsBrief page as detailed in Figure 3; however, both the automatically generated top stories and the thematic areas of interest relate to nuclear security and safeguards issues.

Category Name	Content	Frequency
General News and Aggregators	Directly-accessed news sources, news aggregators, and "fee-based" comprehensive news archive with collection of newspapers, periodicals, and news wires, filtered by user defined keywords.	Very High
Nuclear News Aggregators	Articles from news agencies and news aggregators that customarily or primarily report on issues related to nuclear industry and safeguards.	High
NGO & Academic	Non-governmental organization or university providing detailed reports and added value assessments concerning State's nuclear programmes and activities, and general nuclear nonproliferation issues.	Medium
Blogs	Interactive websites with commentaries on nuclear issues.	Medium
Government & Intergovernmental	Information from relevant intergovernmental organizations and competent authorities at national level are a unique source of authoritative information on nuclear safeguards and nuclear industry issues.	Low / Medium
Nuclear Industry	Information on companies including location(s), products, capabilities, activities, number of employees, main customers, exports of nuclear related items.	Low / Medium

Table 1: Classification of sources monitored by NSMM

Considerable effort was made to configure and test the monitoring of the nuclear websites: for each site, the relevant RSS feeds and/or HTML pages were selected and inserted into an EMM configuration file. The monitoring results are validated to ensure that all relevant articles are collected successfully. The maintenance of the nuclear sources is a continuous task: some of the source definitions have been optimized or updated following changes on the site or the source URL and additional sources have been added to the system on IAEA's request.

4.2 Interoperability with Existing IAEA Back End IT Systems

It is important that all information which is selected during the daily review within the EMM/NewsDesk operating environment are permanently transferred to the IAEA back end systems. The efficient archiving of information selected in NewsDesk into a back end system is essential for compatibility with IAEA workflows. As NewsDesk does not directly provide this functionality, the project aims to identify possible mechanisms for transferring the EMM/NewsDesk output (i.e. the list of selected articles including the meta-information) to the IAEA repository.

4.3 Testing and Deployment

4.3.1 Pre-launch Coverage Testing

In order to evaluate NSMM/NewsDesk performance with respect to the nuclear sources, several trials were carried out by simultaneous manual monitoring of the websites and review of articles processed in NewsDesk. Search results were then compared in number and relevance to identify the coverage of retrieved articles and required resources. The trials confirmed that the articles collected with the existing tools and workflows, could also be captured with NSMM/NewsDesk and that at a minimum the coverage provided by NewsDesk adequately replicates the coverage from the previous monitoring method.

4.3.2 Phase 1 Launch

After the coverage test results were found to be satisfactory, the IAEA carried out a number of usability tests to assess the efficiency of the new process in comparison with the previous method. Following weeks of intensive usability testing, the NewsDesk application was deployed in Phase 1--utilized for information review and collection. During Phase 1, web sources previously monitored manually or via a website tracker were consolidated into one source stream in the NewsDesk. Certain sources from this set remain outside the NewsDesk and continue to be reviewed manually. The consolidation affected nearly two-thirds of the search effort involved in daily monitoring, and was found to raise the overall efficiency of the GMT.

From 11-29 March 2013 SGIM GMT conducted a usability survey of NewsDesk that documented total articles

reviewed, total number of relevant articles selected for review by the SGIM Open Source Highlights editor, and the total amount of search time. In this three week period, the GMT reviewed a total of 5800 documents using NewsDesk, and passed on 236 (roughly 5%) of these to the OSHL editorial team for further review.

Prior to the Phase 1 introduction of the NewsDesk application into daily operations, GMT staff members conducted searches from a set of websites and information repositories, with a collective effort of approximately three staff-hours daily. Consolidating hundreds of sources of varying structure and style into one format in the NewsDesk application that also permits a degree of de-duplication, has streamlined the daily review, reducing the effort to two-staff hours per day. The survey also found that the average length of time required to conduct the review with the help of NewsDesk was approximately one hour¹. This represents approximately a 33% time savings in daily search and collection effort, with no loss in coverage or quality of results (see Table 2).

Table 2: Overall daily effort for GMT and OSHL (in staff-hours)

	Collection ²	Editor review and OSHL Production	Back end processing	Total daily time requirements
Pre-NewsDesk launch	3 hours	5-7 hours	1 hour	9-11 hours
NewsDesk Phase 1	2 hours	5-7 hours	1 hour	8-10 hours

5. Future Developments

After the successful introduction of NSMM/NewsDesk into IAEA's Open Source monitoring workflow, IAEA's initial focus is to gain operational experience with the system and to evaluate different possibilities to fully benefit from the NSMM/NewsDesk capabilities. The options that are currently under consideration are listed hereafter.

5.1 NewsDesk for Article Collection and OSHL Production

In the next phases it is foreseen that all sources currently monitored manually should be included in the NewsDesk application, such as news aggregators, internal sources, and subscription-based websites.

In subsequent phases, the project anticipates the use of NewsDesk for the production of Open Source Highlights newsletter, which will be predicated on further integration of the NewsDesk application with SGIM workflow and infrastructure. A critical element of the process is the ability to automate the back end processing of the newsletter

¹ This includes the manual review of select news aggregators, internal websites and subscription-based websites.
² Includes total collection time for all three source streams (see Section 2 above)

information, which is expected to result in additional savings of one to two staff-hours per day.

5.2 NSMM for Real-time Information Awareness

Under the current scope of the project, NSMM is intended as an information source for SGIM Open Source Highlights production. A further step could be the broader distribution and use of the NSMM NewsBrief page within IAEA Safeguards. The nuclear-specific categories which automatically filter the incoming information could be further refined and thus allow the users to access the articles according to areas of interest, such as a geographic region, the different stages of the nuclear fuel cycle, or event types such as illicit trafficking of nuclear material, export control violations or dual-use equipment transfers.

The NSMM could allow an IAEA safeguards inspector or analyst involved in State evaluation to set up filters for their assigned States or facilities to ensure access to relevant open source information on a near real-time continuous basis. This passive continuous monitoring would free up (human) resources that could be re-allocated for tasks requiring more in-depth active searching. A schematic overview of a potential future setup based on NSMM and NewsDesk is illustrated in Figure 5. The user base could also be enlarged beyond SGIM; depending on the selected deployment architecture (e.g. if deployed on JRC servers), the system might even be opened as a public service to the general nuclear security community.

5.3 NSMM/NewsDesk for Country-Specific Monitoring

As well as the daily news monitoring and OSHL production, SGIM analysts also carry out country-specific monitoring and searches, which typically involves monitoring additional national sources and generates more state-specific information. Following the positive experience in the general daily monitoring, SGIM analysts are considering

using NSMM/NewsDesk for country-specific monitoring. For initial trials, country-specific 'targets' i.e. separate containers where the collected information is located in NewsDesk, will be setup. State-specific daily monitoring using NSMM/NewsDesk has the potential to enhance the effectiveness and efficiency of the continuous monitoring and evaluation of states.

Plans for developing and implementing processes and technologies for the collection, analysis, dissemination and management of open source information within the Department of Safeguards are described in the IAEA's biennial Development and Implementation Support (D&IS) Programme for Nuclear Verification 2012-2013. The purpose of this programme is to assist the Department of Safeguards meet its short term development objectives and to support the implementation of its verification activities in a manner which is effective, efficient and encourages innovation and excellence. It has been produced in accordance with the Departmental Long-Term Strategic Plan, 2012–2023, the IAEA Medium-Term Strategy, 2012–2017, and the Long-Term R&D Plan, 2012–2023.

In order to support the long-term direction, activities are initiated, continued and/or finalized during the biennium and are structured under the following key objectives: 1. Optimize information utilization, 2. Expand and Diversify Sources and 3. Enhance Information Evaluation and Analysis. Funding for most of the described D&IS activities is foreseen to be provided by Member State Support Programmes (MSSP) which will continue to play a major role in achieving the stated project objectives. By facilitating the use of EMM and NewsDesk to the IAEA, the JRC continues to support the first key objective, enhancing information collection by introducing new data collection methodologies which is contributing to streamlining open source information handling within the Department of Safeguards [12].

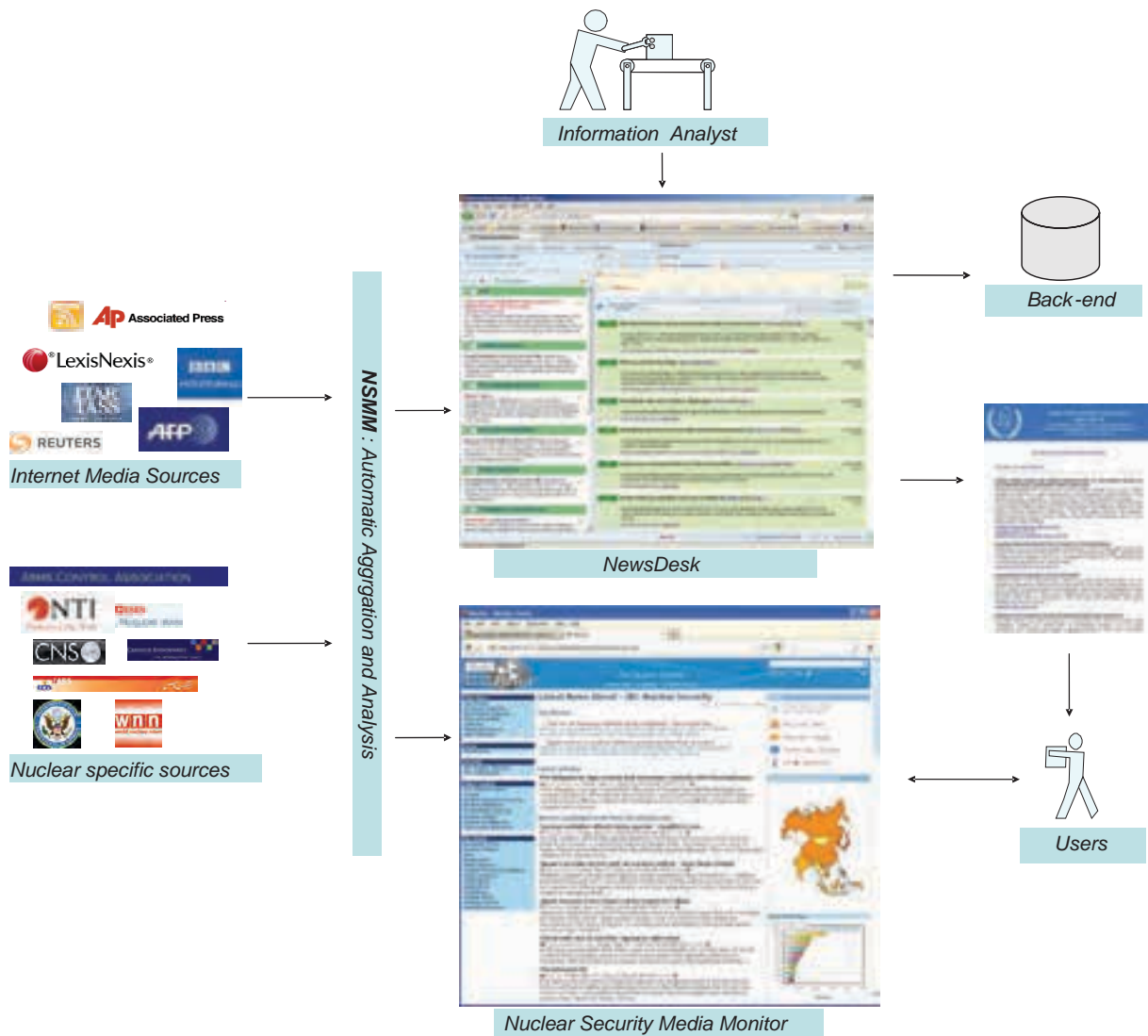


Figure 5: Schematic overview of information flow in a possible future setup for open source information collection and analysis based on NSMM and NewsDesk.

6. Conclusions

The IAEA possesses robust open source capabilities. However, the growing volume of information and variety in the number of available sources has made it imperative for the IAEA to continue to increase the effectiveness and efficiency of its collection, analysis, and dissemination processes. A clear priority for the Department of Safeguards is to streamline the acquisition and analysis of open source information and move away from the current labour intensive information collection/newsletter production process to a more efficient system.

NSMM/NewsDesk is a powerful tool developed by JRC for automatically aggregating and analysing open source information from the internet focusing on the nuclear security and safeguards domain. After extensive testing showed that utilizing NSMM/NewsDesk improves the efficiency of IAEA's open source collection process, the IAEA has started using the system in its daily workflow. Currently, the IAEA is gaining operational experience with the system and intends to further integrate NSMM/

NewsDesk into IAEA's workflow in order to fully exploit the system capabilities.

As safeguards implementation evolves to make better use of all safeguards relevant information available to the IAEA new effective and efficient approaches for open source information collection and analysis are required [13]. The utilisation of tools such as NSMM/NewsDesk together is one example of how new technologies and tools can support this process.

7. Acknowledgements

The work here presented has been carried out within the European Commission (EC) Support Programme to the IAEA, task on Collection, Analysis and Dissemination of Open Sources.

8. References

- [1] IAEA, *The Conceptualization and Development of Safeguards Implementation at the State Level*, GOV/2013/38, Date: 12 August 2013

- [2] IAEA, *Development and Implementation Support Programme for Nuclear Verification 2012-2013 (STR-371)*, Vienna, 2012.
- [3] Giacomo G.M. Cojazzi, Flavio Fuart, Erik van Der Goot, Erik Wolfart, Zoe Gastelum, Yana Feldman, William Hammond, Ryszard Zarucki, Matthew Ferguson, "Collection, Analysis and Dissemination of Open Source Safeguards-Relevant News Using Web Based Applications", *INMM 52nd Annual Meeting*, Palm Desert, CA, USA, July 2011.
- [4] Michael Barletta, Ahmed El Gebaly, William Hammond, Thomas Lorenz, Stephen Robb, Nicholas Zarimpas, Ryszard Zarucki. "Open Source Information Acquisition and Analysis in the IAEA Department of Safeguards", *ESARDA Annual Meeting*, Budapest, Hungary, May 2011.
- [5] Martin Atkinson, Erik van der Goot, "Near real-time information mining in multilingual news". In: *Proceedings of the 18th International World Wide Web Conference (WWW 2009)*, Madrid, Spain, pp. 1153–1154, April 2009.
- [6] Ralph Steinberger, Bruno Pouliquen, Erik van der Goot, "An introduction to the Europe media monitor family of applications". In: Gey, F., Kando, N., Karlgren, J. (eds.) *Proceeding of the SIGIR Workshop on Information Access in a Multilingual World (SIGIR-CLIR2009)*, Boston, USA, July 2009.
- [7] Ralf Steinberger, Bruno Pouliquen, "Cross-lingual Named Entity Recognition". *Journal Linguisticae Investigationes*, Special Issue on Named Entity Recognition and Categorisation LI 30:1 (2007) John Benjamins Publishing Company. ISSN 0378-4169. 135-162, 2007
- [8] <http://emm.newsbrief.eu>
- [9] <http://medisys.newsbrief.eu>
- [10] Ralf Steinberger, Flavio Fuart, Erik van der Goot, Clive Best, Peter von Etter & Roman Yangarber, "Text Mining from the Web for Medical Intelligence". In: Fogelman-Soulié Françoise, Domenico Perrotta, Jakub Piskorski & Ralf Steinberger (eds.) *Mining Massive Data Sets for Security*, pp. 295-310, IOS Press, Amsterdam, The Netherlands, 2008.
- [11] <http://ecurl.eu/emm-mobile>
- [12] *Development and Implementation Support Programme for Nuclear Verification 2012–2013. STR-371.*
- [13] IAEA, *IAEA Department of Safeguards Long-Term R&D Plan, 2012-2023 (STR-375)*, Vienna, 2013

New Approaches and New Technologies for the Verification of Nuclear Disarmament

David Keir

Verification Research, Training and Information Centre (VERTIC), Development House, 56-64 Leonard Street, London EC2A 4LT, United Kingdom david.keir@vertic.org

Abstract:

ESARDA's New Approaches/Novel Technologies Working group has recently begun to take a great interest in technology for use in arms control verification, in parallel with a focus on Nuclear Safeguards technology. A topic-based meeting of members of the NA/NT Subgroup was hosted at Joint Research Centre (JRC), ITU-Nuclear Security Unit in Ispra (Italy), to further explore the technical issues and opportunities presented by the need for new approaches and technologies in a future verified nuclear weapons dismantlement regime.

Nuclear warheads must contain radioactive material and, by their nature, gamma rays and neutrons are likely to penetrate to the outside of the warhead casing and even metal containers. Therefore radiation signatures should be detectable by appropriate pieces of equipment. For this reason, researchers in the field of technical verification of nuclear warhead dismantlement have studied and developed technologies for Non-Destructive Assay (NDA).

This paper presents a generic dismantlement pathway for verified nuclear warhead dismantlement, based on the scenario employed by the UK-Norway initiative for their exercise in 2008/9. Using this as a framework the types of measurement challenge likely to be presented to a verifying inspector are discussed. The problem of intrusiveness of measurements in relation to the issue of proliferative release of classified information about the warhead attributes is discussed and the concept of 'information barriers' is introduced as a possible solution to this issue. A list of candidate technologies for use in verification activities, with or without information barriers is then presented and, since most of these are new or novel approaches to the issue, an already-established system for classifying them – in terms of state of development and complexity of use in this context – is proposed. Finally, the concept of capturing this information as a library of 'datasheets', designed for periodic review as development proceeds, is presented.

Keywords: nuclear; weapons; disarmament; verification; technology; NDA; datasheets

1. Introduction

Within the ESARDA family, arms control applications and the common ground shared with safeguards has always been on the agenda. For instance the Working Group on Verification Technologies and Methods, the DA Working Group and the NDA Working Group, have long had an eye on nuclear weapons issues as well as civil material safeguards technology.

A newer Working Group (New Approaches/Novel Technologies) has recently begun to take a great interest in this subject, in parallel with a focus on Nuclear Safeguards technology. A topic-based meeting of members of the NA/NT Subgroup was hosted at the Joint Research Centre (JRC), ITU-Nuclear Security Unit in Ispra (Italy), to further explore the technical issues and opportunities presented by the need for new approaches and technologies in a future verified nuclear weapons dismantlement regime.

One of the outputs of that meeting was that the NA/NT focus group on nuclear disarmament verification technologies, would develop a structure for further consideration of technology R&D requirements - in such a way that the items of interest could be categorized, for example in the following way:

1. Constraints on technology and deployment in real situations
2. Fissile material attribute measurements
3. Fissile material template measurements
4. Quality assurance of the measurements and analysis
5. Warhead dismantlement assurance
6. Information barriers
7. Information security scenarios
8. "Spoofing" detection
9. Sampling of non-fissile materials as 'signatures'.

Part of developing a structure for further work is first to understand what warhead dismantlement is like and what the challenges are. While historically there is a significant body of work on these issues¹⁻⁸ the following sections describe the scenarios and challenges generically.

2. The role of technology in verifying nuclear disarmament

In a future nuclear disarmament activity, under a treaty or other agreement, the deployment of inspectors to witness nuclear warhead dismantlement is likely to be the principal, and most effective, approach to verification.

But nuclear warheads and components are a special class of object. Because the design of a nuclear weapon is information which, if passed on to a non-nuclear-weapon state would be proliferative, it is highly unlikely that any person attempting to verify its presence or identity would be allowed to view any of its design details.

There may be exceptions, where the visual appearance of the outer shell of a warhead, viewed from a minimum distance, could be classified as non-proliferative. However, actual measurements of such features as dimensions and weight will probably always be classified.

During the process of dismantlement, where parts of the warhead are being removed and the inner components revealed, the situation would be even more problematic. This is because the appearance of internal structures would be even more sensitive and potentially proliferative if revealed. Thus, the likelihood of an inspector witnessing dismantlement procedures or having eye contact with any of the components emerging from dismantlement is, at this date, vanishingly small.

2.1 Non-destructive assay

There is a saving grace, however, and that is that all nuclear warheads must contain radioactive material. What

that means is that ionising radiation is constantly being emitted from the radioactive components inside the warhead.

By the nature of them, gamma rays and neutrons, if emitted, are likely to penetrate to the outside of the warhead casing and even metal containers containing the warhead for transport and storage. Therefore radiation 'signatures' may be detectable by appropriate pieces of detection equipment. For this reason, researchers in the field of technical verification of nuclear warhead dismantlement have studied and developed technologies for Non-Destructive Assay (NDA). This has centred on the radiometric measurement of gamma rays and neutrons, which will be discussed more fully later in this paper.

3. Nuclear warhead dismantlement processes

Although most nuclear weapons appear follow the same general principles, in that nuclear yield is achieved by compressing fissile material to prompt criticality, diversity in design appears to apply across the world's various nuclear-armed states.

Given the many types and sizes in which nuclear weapons come, dismantlement processes are likely to be varied. Despite that, some generic processes must be common to all such dismantlement activities and an attempt will be made here to define a generic overall process, with a view to verification.

3.1 Removal from deployment

First, a nuclear warhead must be removed from its deployed location (e.g. on a missile, in a heavy bomber aircraft, in storage at a bomber base, or on board a naval vessel) and transported, perhaps via an interim storage location, to the facility at which it will be dismantled.

It is possible (though currently thought to be unlikely) that an inspector could be allowed to make some kind of measurement of radiation emissions from the warhead at the deployment site. However, they may be allowed to apply a tamper-indicating device (TID) or other 'unique identifier' to the outer warhead casing at this stage. Or they might be allowed to do both.

We note that this is the location at which the NEWSTART treaty⁹ between the US and Russia, provides for some verification activities.

3.2 Receipt at the dismantlement facility

The area receiving the warhead at the generic, future dismantlement facility would be the next key location in the chain. This, realistically, might be the area where an inspector is first allowed to interact with a warhead ready for

¹ Weapons Evaluation and Control Bureau (1969) *Demonstrated Destruction of Nuclear Weapons*, Washington DC: US Arms Control and Disarmament Bureau.

² Cochran, TB (1989), *Black Sea Experiment Only a Start*, Bulletin of the Atomic Scientists, 45 (9), pp.13-16.

³ Fetter S, Frolov V A, Miller M et al (1990), *Detecting Nuclear Warheads in the USSR-US Black Sea Experiment*, Science and Global Security, 1, pp. 225-327.

⁴ Office of Arms Control and Nonproliferation (1997), *Transparency and Verification Options: An Initial Analysis of Approaches for Monitoring Warhead Dismantlement*, Washington, US Department of Energy.

⁵ *Technology R&D for Arms Control*, Office of Nonproliferation research and Engineering, US Department of Energy/NNNSA, Spring 2001.

⁶ National Academy of Sciences Report, 2005, *Monitoring Nuclear Weapons and Nuclear-Explosive materials*, National Academies Press, Washington DC, (2005).

⁷ Cliff D, Elbahtimy H, and Persbo A; *Verifying warhead Dismantlement, Past, present, future*, VERTIC Research Report, Number 9, September 2010, (includes a detailed account of the UK-Norway Initiative activities from 2005 to 2010).

⁸ Eberhart J *inter alia*, *Technical challenges in verifying nuclear disarmament*, 25 Oct 2013, Briefing co-organized by the Permanent Mission of United Kingdom and the United States Mission (First Committee experts) on the UK-US collaborative research programme on nuclear arms control verification. <http://webtv.un.org/watch/technical-challenges-in-verifying-nuclear-disarmament/2769294424001/>.

⁹ www.state.gov/t/avc/newstart/index.htm.

dismantlement, though the warhead might well be inside a container at the time.

Again, some sort of measurement might be allowed here, and application of a tamper-indicating device (TID) or checking of a previously-applied TID might be allowed at this point.

3.3 Dismantlement

As far as can be judged, the disassembly of nuclear warheads seems to be a de-construction process, where components are unfastened using simple tooling, rather than a violent process using power tools and cutting equipment to destroy the structure.

The arrangement of nuclear materials and high explosives and associated firing devices at the heart of a nuclear warhead tend to be collectively referred to as a weapon's 'physics package'. To remove the fissile components from a nuclear warhead, it seems inevitable that the physics package would first have to be exposed by the removal of outer casings and ancillaries. As far as can be judged, every type of removed component would be separately packaged before it emerged from the dismantlement workshop. This was the model followed by the UK-Norway Initiative exercise in 2008/2009¹⁰.

According to the US Department of Energy, nuclear warhead 'dismantlement' refers essentially to *the separation of a weapon's explosive components from its fissile material components*.

3.4 Disassembly of the nuclear physics package

Considering the stage at which the conventional explosives must be removed and separated from the fissile material part of the warhead. It is not at all clear that any access to this process would ever be possible for verification inspectors. For this reason it may be necessary to find a way of maintaining 'continuity of knowledge' of the treaty-accountable item, or items, while they are inside the dismantlement processing area. Other than the confidence-building measure of inspection of the empty workshop before and after the dismantlement, the author is not yet aware of any satisfactory proposal of how this can be done.

After disassembly of the physics package is complete, its various components are likely to be packaged in dedicated, specially-designed containers, then stored or processed further, as appropriate to the future plans of the owner state.

Were the dismantlement to be a verified one, the alternative end points shown on Figure 1 would be monitored,

subject to negotiation and agreement between treaty partner(s). These end points are theorised here, based on publications over the last 20 years which have suggested these main possible end-points for fissile materials removed from nuclear warheads.

3.5 Post-dismantlement fissile component pathways

Figure 1 shows generic possible pathways that the fissile components might follow, ending in four possible main states:

1. Components stored whole in a long-term store;
2. Components shape-destroyed and stored long-term
3. Components processed into fissile material and stored long-term;

For one end-option on this diagram — the processing of fissile components into fissile material — there might also be further stages, leading to IAEA Safeguards, such as emerging fissile material, being blended with other fissile material (not from the declared weapon) stored long term, then possibly transferred to safeguards. Again, depending upon the treaty negotiations and outcomes, any one of these options might involve a *jointly-monitored* store, where the owner state and other parties to a treaty would have joint custody and monitoring rights to the store and its systems¹¹. The setting up and equipping of such a jointly-trusted facility might take some years to realise. In the case of civilian fissile materials however, there are of course many jointly-monitored systems in operation for reactor-associated material, under Safeguards.

¹⁰ Cliff D, Elbahtimy H and Persbo A; Verifying Warhead Dismantlement, past, present, future, VERTIC Research Report Number 9, September 2010, *The UK-Norway Initiative*, pp 64-85.

¹¹ A jointly-monitored store could include joint monitoring by a State and the IAEA, for which there is a precedent, in the Republic of South Africa.

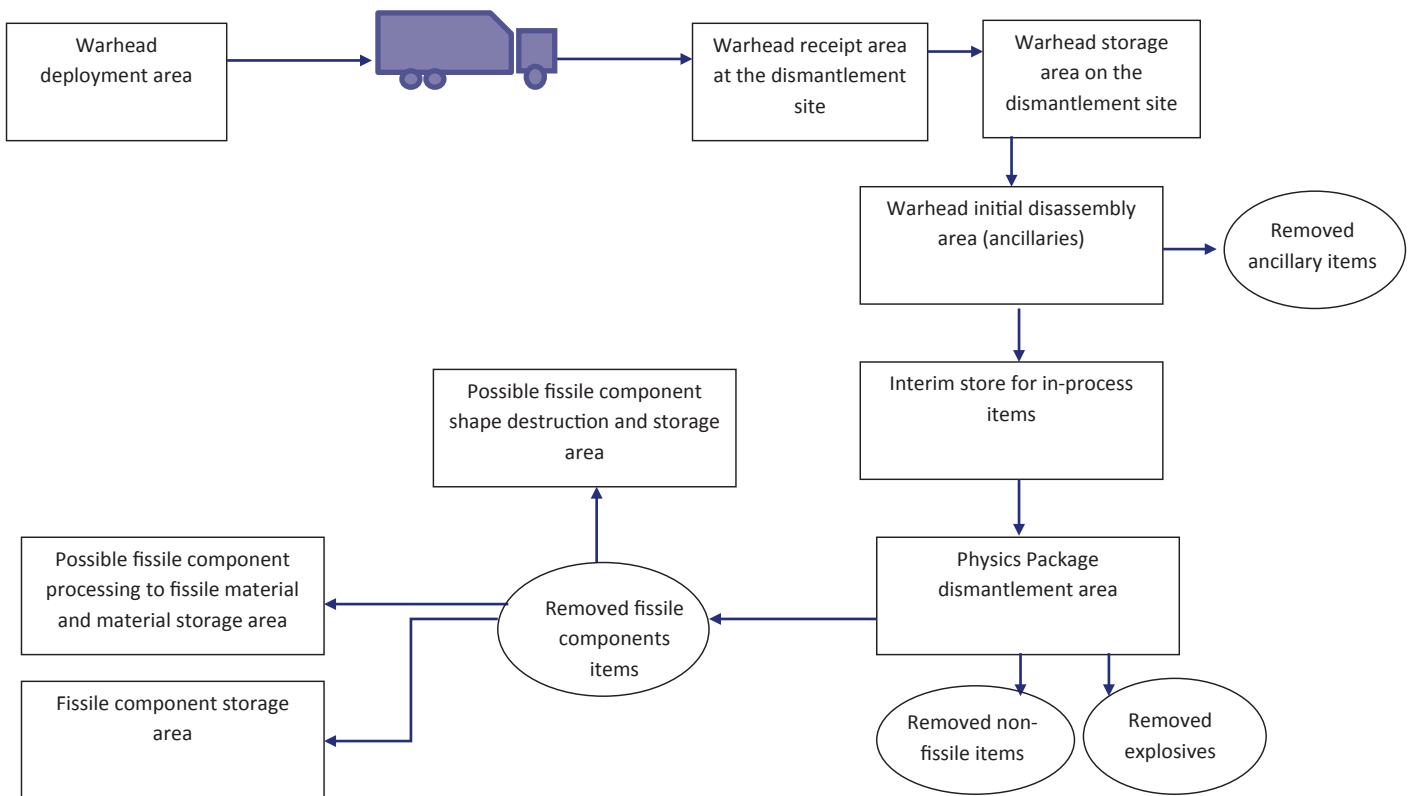


Figure 1: Possible nuclear warhead dismantlement pathways

4. Challenges for Non-Destructive Assay technologies

What really matters, as far as the operators of NDA systems are concerned, is what they are presented with and what they are being asked to measure. The latter will be determined by what declaration has been obtained by negotiators – because it will probably be necessary, as a minimum, to verify the declaration. The key factors in these measurement challenges are likely to be:

(i) For ‘passive techniques’: how much radiation or heat signature is being emitted and what does it have to pass through before reaching the detector itself? We note that the amount of attenuating material in a warhead is likely to be significantly more than is encountered in Safeguards-type NDA measurements of fissile material in cans. This means that low-energy gamma rays, for instance, may not be detected at all.

(ii) For ‘active’ techniques: What is the nature of the whole presented object and its container and can an active technique feasibly (and safely) stimulate an emission signature that will be interpretable?

The following is a list of the possible presented object scenarios:

- Warheads in/on delivery systems;
- Complete warheads inside multiple (i.e. Russian Doll) transport containers, inside road or rail vehicles;

- Complete warheads in multiple containers removed from road or rail vehicles;
- Complete warheads in innermost storage containers;
- Bare complete warheads (i.e. the re-entry body or outer casing is visible);
- Bare physics packages;
- Fissile components in single shell process containers;
- Fissile components in multiple (i.e. Russian doll) storage or transport containers
- Shape-destroyed fissile components in containers;
- Weapons-derived fissile material in process or storage containers (possibly blended with other fissile-containing material);
- Weapons-derived fissile material; possibly blended with other fissile-containing material; in multiple (i.e. Russian doll) containers.

5. The problem of intrusiveness

The release to inspectors of any design information about the nuclear warheads or components involved in a verified dismantlement regime would only be possible and legal if the inspector party were themselves from NPT Nuclear Weapons States. Even then, it may be that national security requirements of the dismantling State would require that no information of this sort were released.

So how can an inspector from a Non-Nuclear-Weapons State verify that a nuclear weapon is being dismantled if

he/she is not allowed to know the identifying characteristics or attributes of that weapon?

Several of the technologies appearing in Table 1 below will have the potential to reveal design information. In fact the Inspector does not really require to know this sort of information at all. What he/she is being asked to verify is 'is this a: nuclear warhead, nuclear component, nuclear material etc. - of the type declared, yes or no?'

So, the inspector essentially needs *decisional* information that will allow them to conclude yes or no, (with some measure of confidence). They also need to minimise the chance that they will later be shown to have been wrong. This being so, a mechanised way of getting that decisional data to the inspector directly, without the inspector having access to numerical data, can be devised. Potentially, this is what an 'Information Barrier' can do.

5.1 Information Barriers

An information barrier in this context should contain within itself the mechanism to consider the data it collects, compare it to the declared data (or data threshold) and then to output a **logical** result—which contains no proliferative information, it is just a 'yes' or a 'no'. This can then be used directly by the inspector to make a decisional statement to their superiors and thence to the rest of the world.

The devil in the detail however, comes down to the following:

- Is the information barrier system collecting and processing **appropriate data, directly related to attributes of concern** (such as the mass of a specific radioisotope present) and comparing it to a sufficient and **appropriate declaration** to make the verification decision valid?
- Is the information barrier receiving the true input data from the object in question?
- Is the information barrier and all its inner workings exactly what both parties believe it to be (**authentication**)?
- Has the information barrier been isolated from any possible tampering?

5.2 Types of information barrier in existence

There appear to be several types of information barrier system currently in operation or under consideration in the nuclear field. For warhead dismantlement verification, the main types discussed are:

Multiple technology analysis systems, which internally handle classified attribute-derived data, such as high-resolution spectra and/or multiplicity numbers; all physically isolated from the outer world by a robust, tamper-proof cabinet with just an output line for red or green lights.

Simplified systems, which look at only limited pieces of data and which make their yes/no decisions on the

basis of an agreed threshold match to a pre-agreed criterion—this criterion being directly-related to an important attribute (such as Pu-239:Pu-240 isotope ratio). An example of this is the prototype information barrier developed by the UK-Norway initiative over the last four years.

Template systems, which are essentially black box devices that collect an array of data being emitted from the object in question, and store it securely, but are then only asked subsequently whether a match has been achieved to the template data in a later situation.

The following sections deal with novel and emerging technologies *per se* and do not consider the ways in which they could be interfaced with an information barrier. That remains outside the scope of this paper.

6. Non-Destructive Assay technologies for nuclear warhead dismantlement verification

In this specific area, the ESARDA NA/NT Sub-Group has collected together a list of emerging technologies with potential use for disarmament verification inspectors, who will have to deal with the classified objects, and containerised components described in earlier sections of this paper. The following table is a list of non-destructive assay technologies that the author is aware of, either because they are being worked on now as possible tools for future verification, or because they appear as development ideas in the historical literature from START-3 preparation or from US-Soviet-IAEA Trilateral Initiative days^{12,13}. The techniques are grouped by the type of radiation detection they use. Finally, some examples which are non-radiometric are included.

As an attempt to capture what is known, by whom, and at what stage of development some of these technologies sit, the development of a collection of Data Sheets has begun. A prototype example of one such datasheet appears in the information box below, illustrating the important items of information such a datasheet should hold. This boils down to a description; an indication of the personnel involved who can supply more details; assessments of the maturity of development as applied to the problem of warhead dismantlement verification; and the complexity of operation required to achieve useable results.

¹² Shea T; Report on the Trilateral Initiative: IAEA verification of weapon-origin material in the Russian federation & the United States, IAEA Bulletin, pp. 49-53.

¹³ Shea T; The Trilateral Initiative: A model for the future? <http://www.armscontrol.org/act/2008-05/PersboShea.asp%2523Sidebarl>.

Passive techniques using gamma emission detection	
1	Identification of specific isotope presence by gamma spectrometry – (Ortec and Canberra HPGe)
2	Identification of specific isotope presence by calorimetric gamma spectrometry
3	Isotopic ratio determination (Pu) by gamma spectrometry
4	Isotopic ratio determination (U) by gamma spectrometry
5	Imaging of size and shape of radioactive component by gamma camera (commercially-available)
6	Imaging of size and shape of radioactive component by gamma auto-radiography (with pinhole?)
Passive techniques using neutron emission detection	
7	Mass estimation (Pu/U) by direct neutron multiplicity counting – (e.g. fission meter by Ortec)
8	Mass estimation (Pu/U) by neutron time-correlation assay /Feynman Analysis etc. of multiplicity
9	Identification of fissile material by neutron spectrometry
10	Estimation of organic material thickness by attenuation neutron counting
11	Imaging of size and shape of radioactive components by neutron auto-radiography with pinhole
12	Imaging of size and shape of radioactive components by “neutron camera”
13	Estimation of organic material thickness by time-correlated neutron assay/decay series time constant measurement
Passive techniques using two or more types of radiation measurement	
14	Determination of shielding configuration by gamma spectrum modelling with data fusion
15	Scintillation counting of gamma and neutron emissions
Techniques using ‘active’ irradiation of the presented object	
16	Active methods – LINAC beam on and off - Die-away analysis
17	Identification of fissile material type and mass by Time-of-flight neutron assay (NMIS)
18	Neutron time of flight imaging of internal structures (3-D Imaging NMIS)
Techniques using sample collection from facility environments	
19	Identification of Pu isotopics in the area by near-field environmental particle sampling
20	Identification of U isotopics (U) in process area by near-field environmental particle sampling
Techniques not employing measurement of ionising radiation from the warhead/component	
21	Identification of fissile heat source by thermal imaging
22	Imaging of high-Z materials by muon detectors
23	Xe detection in the warhead storage or processing area
24	Stand-off detection of processes by emissions from facilities (e.g. using hyper-spectral infrared imaging).

Table 1: NDA technologies for consideration

The datasheets initiative was another topic discussed at the 2012 special meeting of members of the NA/NT Working Group and other parties concerned with nuclear weapons dismantlement verification, at JRC Ispra.

It is proposed that the Data Sheets, once developed under a funded work-stream, could be held on behalf of the NA/NT Subgroup, subject to on-going maintenance and updating. They will thus constitute an information resource, or knowledge library, specifically for newer technologies as applied to nuclear disarmament verification.

DATA SHEET EXAMPLE - Quantum Calorimeter Gamma Ray Detector for verification measurements**1. Illustration of the System****1. A Brief Description**

This claims to be a higher resolution gamma-ray spectrometer than any yet available, based on quantum calorimeters, aimed at better nuclear safeguards measurements. The authors specifically suggest that the most promising applications include passive, non-destructive assay of nuclear materials such as plutonium isotopic mixtures and spent uranium fuel assemblies (as well as precise determination of the Lamb shift in heavy hydrogen-like atoms). Small, transition-edge thermometers, made of Mo/Cu superconductor crystals, cryogenically-cooled, represent the sensitive volume. Instead of electrical pulses analysed by a Pulse height Analyser and then displayed as No. of pulses in a series of energy bins (as in convention High Resolution Gamma Spectrometry) this approach uses temperature pulses in the sensitive volume to derive the gamma ray energy spectrum. It is proposed by the developers that an array of these sensitive volumes will be constructed, towards achieving a workable spectrometer.

This is a multi-collaborator project, involving US university and National Laboratory input and has been supported by the US Department of Energy's NNSA organisation, amongst others.

2. Technology Readiness Level = {3}**3. Complexity of Operation Level = {Inventor}**

4. Who is developing this technology (give key references)?: Barry L. Zink, Dept. of Physics & Astronomy, University of Denver. Collaborators: NIST, LANL, DOE/NNSA.

Array-Compatible transition-edge sensor microcalorimeter gamma-ray detector with 42 eV energy resolution at 103 keV, B L Zink, J N Ullom, J A Beall, K D Irwin, W B Doriese, W D Duncan, L Ferreira, G C Hilton, R. D. Horansky¹, C D Reintsema and L. R. Vale¹, Appl. Phys. Lett. **89**, 124101 (2006).

5. Discussion of data interpretation – is modelling required?

Not known, but likely to be amenable to the same modelling approaches as conventional HRGS.

6. Is it available to buy and how much would the technology cost to obtain?

Only one manufacturer: the inventor/developer. Cost unknown.

7. Other known fields of application?

Proposed for non-proliferation work. Also, according to the developers: This technology yields a higher resolution gamma-ray detector than before, offering reduced peak overlaps, better peak-to-background ratios, more accurate measurements of age & enrichment of uranium, more accurate measurements of plutonium isotopic mixes, and better determination of mass of plutonium in spent uranium fuel.

8. Is it possible to certify this technology (i.e. for use in radiation or explosives areas)?

This system should be deployable directly for safeguards applications, once developed further. It is a cryogenically operated system, so liquid nitrogen coolant is required.

As it is similar to conventional HRGS, but more accurate and sensitive, it would undoubtedly require an information barrier in a nuclear arms control treaty scenario. However, the same information barrier could potentially be used for this as for conventional HRGS.

10. Data Sheet last updated by whom and when?: David Keir, VERTIC, London, 16th October 2012.

7. Conclusion

A variety of relevant technologies exist, many available commercially. A considerable amount of work has also been completed in the development of scientific models, and software, for the interpretation of measurements made with these instruments.

However, in the special case of nuclear warheads and their components, the level of detail that would be revealed by these techniques would also, if revealed to a NNWS inspector, constitute a breach of Articles One and Two of the Nuclear Non-Proliferation Treaty. The challenge remains to devise information barriers that are sufficiently well-designed to bridge this gap.

There is also a requirement that the technologies themselves are fit for the purpose. In the context of nuclear warhead dismantlement verification, this will mean there are physical limits on use, such as time constraints and personnel limits. Thus, it is important to understand what level of expertise is required to effectively operate NDA equipment and the time needed to obtain useful results. To try to accommodate the requirements of prospective users and developers, it is proposed that a series of data sheets be prepared by the NA/NT WG and held as up-datable items of information, a knowledge library specifically for newer technologies as applied to nuclear disarmament verification. Each of these datasheets will include an assessed Technology Readiness Level (TRL) and Complexity of Operation Level (COL) as described in Appendix A and Appendix B.

Appendix A, NASA Technology Readiness Levels

In the research and development world, all new technologies must pass through a number of stages before they are accepted as a viable tool. At NASA these stages have been formalised and called ‘technology readiness levels’, or TRLs. Each TRL represents the evolution of an idea from a thought, perhaps written on the back of an envelope, to the full deployment of a product in the marketplace.

Various modified scales have been developed; by the US DoD, DOE and by ESA, but here we will use the current-day NASA approach. The figure below is a schematic of the NASA TRL scale¹⁴.

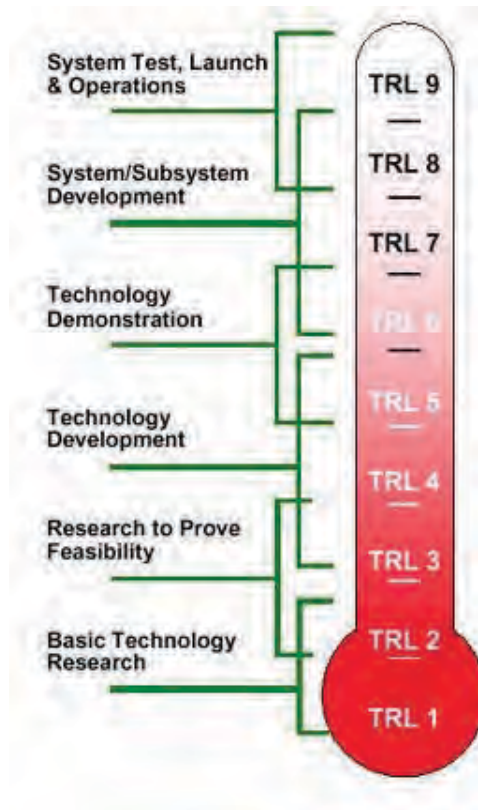


Figure A1: NASA Technology Readiness Diagram¹⁵

Technology Readiness Level

1. Basic principles observed and reported
2. Technology concept and/or application formulated
3. Analytical and experimental critical function and/or characteristic proof of concept
4. Component and/or breadboard validation in laboratory environment

Description

This is the lowest “level” of technology maturation. At this level, scientific research begins to be translated into applied research and development.

Once basic physical principles are observed, then at the next level of maturation, practical applications of those characteristics can be ‘invented’ or identified. At this level, the application is still speculative: there is not experimental proof or detailed analysis to support the conjecture.

At this step in the maturation process, active research and development (R&D) is initiated. This must include both analytical studies to set the technology into an appropriate context and laboratory-based studies to physically validate that the analytical predictions are correct. These studies and experiments should constitute “proof-of-concept” validation of the applications/concepts formulated at TRL 2.

Following successful “proof-of-concept” work, basic technological elements must be integrated to establish that the “pieces” will work together to achieve concept-enabling levels of performance for a component and/or breadboard. This validation must be devised to support the concept that was formulated earlier, and should also be consistent with the requirements of potential system applications. The validation is “low-fidelity” compared to the eventual system: it could be composed of ad hoc discrete components in a laboratory.

¹⁴ http://esto.nasa.gov/files/trl_definitions.pdf , for the *definition of Technology Readiness Levels*.

¹⁵ <http://www.hq.nasa.gov/office/codeq/trl/trlchrt.pdf>.

5. Component and/or breadboard validation in relevant environment	At this level, the fidelity of the component and/or breadboard being tested has to increase significantly. The basic technological elements must be integrated with reasonably realistic supporting elements so that the total applications (component-level, sub-system level, or system-level) can be tested in a 'simulated' or somewhat realistic environment.
6. System/subsystem model or prototype demonstration in a relevant environment (ground or space)	A major step in the level of fidelity of the technology demonstration follows the completion of TRL 5. At TRL 6, a representative model or prototype system or system - which would go well beyond ad hoc, 'patch-cord' or discrete component level breadboarding - would be tested in a relevant environment. At this level, if the only 'relevant environment' is the environment of space, then the model/prototype must be demonstrated in space.
7. System prototype demonstration in a space environment	TRL 7 is a significant step beyond TRL 6, requiring an actual system prototype demonstration in a space environment. The prototype should be near or at the scale of the planned operational system and the demonstration must take place in space.
8. Actual system completed and 'flight qualified' through test and demonstration (ground or space)	In almost all cases, this level is the end of true 'system development' for most technology elements. This might include integration of new technology into an existing system.
9. Actual system 'flight proven' through successful mission operations	In almost all cases, the end of last 'bug fixing' aspects of true 'system development'. This might include integration of new technology into an existing system. This TRL does not include planned product improvement of on-going or reusable systems.

Appendix B, Complexity of Operation Level (COL) - i.e. the level of expertise required

In order to judge the practicability of a system, specifically for arms control applications, where the deployment scenario would be somewhat restricted, a proposed additional classification, to accompany the TRL, is proposed. In the absence of anything else, the author proposes a simple descriptive classification, as follows:

INVENTOR = Only the inventor or his/her immediate team can make the system work for appropriate measurements. Several days of setup and calibration may be required prior to measurement.

SPECIALIST = A small group of post-graduate scientists with relevant experience, training and telephone "reach-back" can follow manual instructions and get useful results in a few days.

TECHNICAL = A small group of graduate scientists can, with a manual and technician support, achieve useful results in a day or two.

LAYMAN = A single, competent lay person with minimal training can push a button and retrieve useful results on a first try, and consistently thereafter for the length of a measurement campaign.

Confirmation of Nuclear Treaty Limited Items: Pre-dismantlement vs. Post-dismantlement

Duncan MacArthur, Danielle Hauck, Morag Smith

Los Alamos National Laboratory - Los Alamos, New Mexico 87544 USA

E-mail: dmacarthur@lanl.gov, hauck@lanl.gov, mks@lanl.gov

Abstract:

*One of the key factors in the verification of future nuclear disarmament treaties will be the confirmation, by a monitoring party, that declared treaty limited items (TLIs) are consistent with the declaration made by the host country. A significant part of this confirmation may be supplied by a radiation measurement system that confirms the declared radiation characteristics of the TLI. These radiation measurements can take the form of measuring declared characteristics (or attributes) of the TLI, comparing declared TLIs with a pre-existing template, or some combination of the two techniques. Treaties covering TLI dismantlement form an important subset of general disarmament treaties. In a dismantlement scenario, the confirmation radiation measurements can be performed either before or after the TLI is dismantled (or at both times). Pre-dismantlement measurement may generate additional confidence that the item is truly a TLI but may be technically challenging, while post-dismantlement measurement can offer additional confidence that the dismantled item **was** truly the declared TLI. Since repeated measurement increases monitoring party confidence and there are technical advantages to both measurement times, a combination of pre-dismantlement and post-dismantlement measurement will lead to the highest overall confidence. The relative importance of the two types of measurement is directly dependent on the specifics of the treaty under discussion.*

Keywords: nuclear; disarmament; attribute; template; dismantlement

1. Nuclear Arms Reduction Treaties

Most treaty monitoring situations can be reduced to two requirements, one for the owner of the nuclear material or item (the host) and one for the organization confirming the treaty declarations (the monitor):

- The host party makes a declaration concerning a treaty-limited item (or TLI) and/or its disposition to the monitoring party.
- The monitoring party must confirm this declaration without observing any sensitive information. By sensitive information, we mean classified information that the two parties do not intend to share.

The crux of this treaty-monitoring measurement challenge lies with the phrase “without observing any sensitive information.” Traditional nondestructive assay techniques, based on gamma-ray detection, neutron detection, or calorimetry, are widely and successfully used in numerous scenarios (e.g., waste assay and spent fuel monitoring) that do not involve classified information. [1]

Nuclear arms reduction treaties in force today are generally based on counting or limiting the number of delivery vehicles. [2] The use of radiation detection in the verification of these treaties is limited to confirming that items are not weapons — lack of radiation levels above background is taken as evidence that an item is not a nuclear weapon. However, it is possible that future monitoring regimes will include warhead confirmation and/or confirmation that warheads have been dismantled (monitored dismantlement). In both cases, it is necessary to confirm that a declared TLI is indeed a warhead. In the remainder of this paper, we address some of the issues surrounding warhead confirmation in a monitored dismantlement scenario.

The host party must trust the measurement system — the process of host trust-building is termed certification. One aspect of certification is that the host must trust that the measurement will not reveal sensitive information. The certification challenges associated with allowing a monitor to confirm that an item is a warhead are much more complex than those associated with confirming that an item is not a warhead. In particular, warhead confirmation potentially includes declaring characteristics of sensitive nuclear items and performing radiation measurements on these items, both of which could reveal sensitive information.

Similarly, the monitoring party is responsible for all steps required to build monitoring party confidence in the measurement system and its use within the monitoring regime; this process is generally termed authentication. The constraints imposed on the monitoring party by the need for simultaneous certification make it more difficult for the monitoring party to maintain confidence in the monitoring regime and its results.

Although many of the specific examples in the remainder of this paper refer to the monitored dismantlement scenario, the concepts, and in particular the measurement concepts, apply more generally to treaties involving warhead

(as opposed to delivery vehicle) confirmation. In sections 2 and 3, we will review dismantlement and measurement concepts while in section 4 we move on to a discussion of the timing of confirmation measurements.

2. Dismantlement Treaty Verification

As noted above, verification of arms control treaties generally involves confirmation that TLIs meet the declarations and/or confirmation that the TLIs have been disposed of as declared. Within a monitored warhead dismantlement treaty, these two confirmation steps are known as warhead confirmation and dismantlement confirmation.

For the purposes of this discussion, dismantlement of a nuclear weapon is defined as the separation of fissile material (FM) from high explosive (HE). Given this definition, dismantlement confirmation can be achieved by demonstrating (1) FM presence as well as the absence of HE in the declared FM container and (2) absence of FM in the dismantlement area and other containers. If HE were tracked, similar confidence could be achieved by confirming presence of HE as well as the absence of FM in the declared HE container and no HE elsewhere — however,

“no HE elsewhere” is very difficult to confirm practically. It is easier to detect and track undeclared FM in containers and large areas. Dismantlement confirmation, regardless of method, obviously must occur “post-dismantlement.”

As described above, a combination of presence and absence measurements can be used to confirm that a nuclear item has been dismantled. Confirming that that a declared item is a nuclear warhead is the more difficult of the two confirmation challenges. As shown in Figure 1, there are four points at which confirmation measurements might be performed on a declared warhead: (1) upon entering the monitoring regime, (2) somewhere within the regime where chain of custody (CoC) of the declared item has been maintained, (3) immediately before dismantlement, or (4) immediately after dismantlement. We will discuss each of the options for when to perform warhead confirmation measurements and the influence of other aspects of the monitoring regime (such as the requirement to maintain CoC) on these timing choices (and *vice-versa*). Warhead confirmation measurements are important not only to confirm that the item being monitored is indeed a warhead, but also to confirm that the item that is dismantled was indeed a warhead.

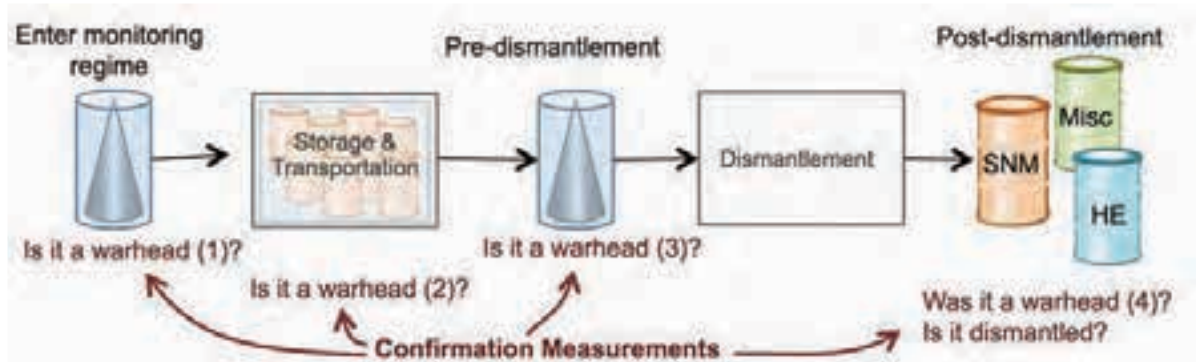


Figure 1: Schematic representation of a potential dismantlement regime identifying four options for warhead confirmation measurements. The dismantlement process is shown as a black box because it is anticipated that the host country will consider the details of this process to be sensitive.

3. Confirmatory Measurements

We have identified three primary methods to warhead confirmation. These are:

- **Attribute measurements:** Are the characteristics of the declared item consistent with it being a warhead?
- **Template comparison:** Is the item consistent with other items known or believed to be warheads?
- **Provenance:** Has the item undergone movements or come from a location consistent with being a warhead?

The first two methods are measurement-based and are described in detail below. The third approach is to use the provenance of the item as evidence that it is a warhead, and to maintain CoC of the item throughout the remainder of the monitoring regime. Even if any particular one of these methods produces relatively low assurance, all three

can be used in combination to increase monitor confidence. The host’s definition of “sensitive information” limits all three techniques, but each is limited in a different way.

In this paper, we focus on measurement methods (both attribute and template) and mention provenance only in passing, even though provenance may be an important source of confidence and can be used in conjunction with the warhead confirmation measurements discussed here. [3]

3.1 Information Barriers

Confirmatory measurements often involve the collection of sensitive data. In order to maintain certification, the measurement system must report the non-sensitive results, while simultaneously protecting any intermediate data required for the measurements. A key component of these confirmation measurement systems is the

information barrier or IB. [4] The IB is a series of controls that ensures that no sensitive information is released during a measurement and, simultaneously, that the monitoring party is able to independently confirm the host's declaration concerning the measured TLI.

A conceptual drawing of a generic certifiable measurement system incorporating an IB is shown in Figure 2. In practice, the IB would not be the single shell shown below — a practical IB includes layers of hardware, software, and procedural protection to provide a barrier system that, as a whole, are fault resistant and the components of which are fault tolerant.

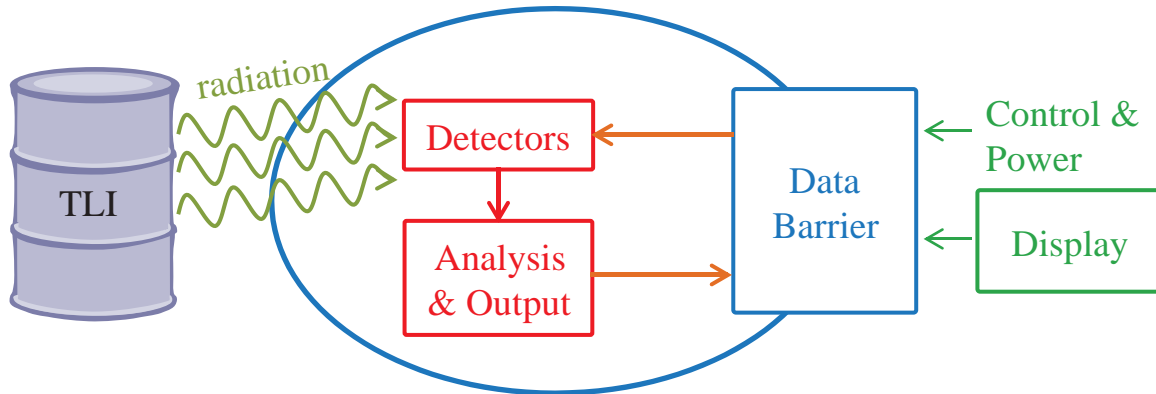


Figure 2: Schematic representation of an information barrier (IB) for a generic measurement system. All potentially sensitive information (contained in parts of the system shown in red) is contained within the IB (blue) while the monitors (green) are outside of the IB. In an attribute measurement system the IB prevents the release of any information other than the attribute results. In a template comparison system, the IB prevents the release of any information other than positive or negative results of a successful comparison.

Unfortunately, the same IB system that excels at protecting the host party's sensitive information also excels at "protecting" the monitoring party from any information that could be used to confirm the host party's declaration. Attribute measurement (discussed in section 3.2) and template comparison (discussed in section 3.3) are both ways of presenting useful non-sensitive results based on potentially sensitive data.

3.2 Attribute Measurement

One approach to confirming that an item is consistent with a warhead with a carefully controlled release of information about the TLI is to use an attribute measurement system or AMS. [5] Attribute measurement, as defined here, results in a non-sensitive indication of potentially sensitive measurement results. Potentially sensitive data can be made into a non-sensitive display by comparing the data with a mutually-agreed threshold, i.e., the display represents "quantity above threshold." Potential attributes displays include:

- the presence of nuclear material,
- having a nuclear material mass above a threshold,
- having a plutonium isotopic ratio below a threshold, or
- having a uranium enrichment above a threshold.

In any fielded implementation of an AMS, the host and monitoring parties would agree on the attributes to be measured (as well as the details of the AMS itself). The confidence generated by an AMS is only as high as the confidence that the chosen attributes uniquely define a warhead. The choice of attributes is very important — not

only must the attribute display be non-sensitive, but the reason for choosing that attribute must also be non-sensitive. Thus, negotiated attributes are often bounded by sensitivity concerns and may not be capable of providing a high level of confidence in warhead identity.

A number of AMSs have been built and demonstrated for international audiences in the last 15 years. Three significant examples are:

- *Trilateral Initiative Demonstration system* – Designed and built in the U.S.; this system measured three attributes, was demonstrated for IAEA and Russian representatives, and focused on information barrier capability. [6]
- *Fissile Material Transparency Technology Demonstration (FMTTD)* – Designed and built in the U.S.; this AMS measured six attributes; was demonstrated to Russian and U.S. government representatives, and focused on certification and information security. This is the only AMS demonstration where a classified weapon component was measured in front of an uncleared audience. [7]
- *Attribute Verification system for Neutrons and Gammas (AVNG)* – This trilaterally designed (VNIIEF, IAEA, and LANL/LLNL) designed AMS was jointly developed by VNIIEF, LANL, and LLNL and built in Russia. The AVNG measured three attributes, was demonstrated for a U.S. audience, and focused on Russian certification. [8]

An AMS performs independent measurements on each item. Thus, the confirmation (or lack thereof) of each declared item is completely independent of measurements on other items. Since each measurement stands alone, no long-term storage of potentially classified information

is required. As long as the same attributes are declared in each case, the measurement system can be used with several types of TLI or the same TLI in different containers. Finally, there can be a good match between the declared characteristics of the TLI and what is actually measured.

3.3 Template Comparison

Another approach to the challenge of generating monitor confidence is to use template matching. In this case, a potentially sensitive signature [typically (but not exclusively) a radiation signature] from a declared TLI is compared with a similar signature from an item known to be a TLI. This comparison can generate a high level of confidence that two items are identical or that a given item is unchanged. Since the template and individual results are not shown to the monitoring party, the template itself may (but is not required to — see for example ref. [9]) contain sensitive information.

Several template-matching demonstrations occurred over the same 15-year time frame as the AMS development discussed above. Of note are:

- *Trusted Radiation Identification System* (TRIS) was a U.S. developed system designed to provide a means to use low-resolution gamma-ray spectral measurements from sodium iodide (NaI) detectors to confirm the identity of declared material. TRIS compares the radiation signature of an inspected item with a known standard for a weapon or component of the same type. [10]
- A *template-matching demonstration* with classified canned subassemblies in containers was held in the U.S. in 1999. In this demonstration reference signatures were acquired for two containers with different items with the Russian delegation present. The signature was obtained for a third item in the third container and it was shown to match one of the reference signatures. This comparison was displayed on the computer screen for viewing by a Russian delegation with the ordinate scrambled. (As with the FMTTD, this demonstration required host certification.)
- A similar *template-matching demonstration* was performed with three classified plutonium metal parts in containers at VNIIEF for a US delegation with the same display of the ratio of signatures with the ordinate scrambled. (As with AVNG, this demonstration required Russian certification.)

In a template comparison, two items can be compared without ever releasing the template itself. The major advantage of this is that a template can incorporate a broad range of potentially sensitive radiation signatures (or other item features) and can result in high confidence that two items are nominally identical. However, template comparisons may require long-term jointly controlled storage of sensitive information.

Since template comparison can result in high confidence that two items are identical, templates have a large potential role in maintaining CoC. [11] However, for the purpose of warhead confirmation, confidence in a template-based confirmation is only as high as confidence that the comparison item is legitimate. In addition, whereas attribute measurements result in independent confidence levels for each warhead, template comparisons result in correlated confidence levels for each item. Confidence (or lack thereof) in the legitimacy of the comparison copy automatically transfers to the level of confidence in the accuracy of warhead confirmation for an entire series of items.

4. Timing of Warhead Confirmation Measurements

As illustrated in Figure 1, warhead confirmatory measurement can be performed at four different times within the dismantlement process. As described below, each of these times has specific advantages and disadvantages from the monitoring party's point of view. The different approaches to warhead confirmation (templates, attributes, provenancing or a combination thereof) offer different levels of authentication confidence at different times; thus, the details of a warhead confirmation measurement will influence optimum timing of that measurement.

The timing of a confirmation measurement can also result in a trade-off between measurement complexity and the complexity of maintaining CoC. The availability of CoC tools and item provenance must be taken into account when determining the optimum times to perform warhead confirmation measurements. CoC can be maintained during storage and transportation using a combination of visual observation and tags and seals. Maintaining CoC throughout the dismantlement process requires more elaborate measures such as the "room within a room" discussed in another paper at this conference. [12]

4.1 Pre-dismantlement – Entry into Monitoring Regime

We define entry into the monitoring regime as the time when the monitoring party has the option to begin maintaining CoC on the item. We do not assume that warhead confirmation measurements are necessary to "initialize" an item into the monitoring regime but that this entry time is one potential time to perform confirmation measurements. Confirmation measurements could be based on attribute measurement or template comparison or both.

Performing confirmation measurements upon entry into the monitoring regime provides the monitor with immediate confidence that an item is consistent with the host's declaration. Otherwise, an item may be present (and

potentially tracked) within the monitoring regime for many years before achieving confidence that it is a TLI. In addition, if the item has a known useful provenance (in this case, useful means that the provenance provides evidence that the item is a warhead), then immediate warhead confirmation measurements together with the provenance may be the best way to provide strong confidence that the item is as declared.

The timing of the warhead confirmation measurements has ramifications for the importance of maintaining CoC. If

confirmation upon entry into the monitoring regime is the only warhead confirmation measurement prior to dismantlement, then CoC between entry into the regime and dismantlement is extremely important. If, on the other hand, the item does not have a useful provenance and if the movements within the regime are not useful for confirming that the item is a warhead, then it may not be as important to perform warhead confirmation measurements at entry into the monitoring regime; in this case, the importance of CoC at any time prior to the first warhead confirmation measurements is minimized.

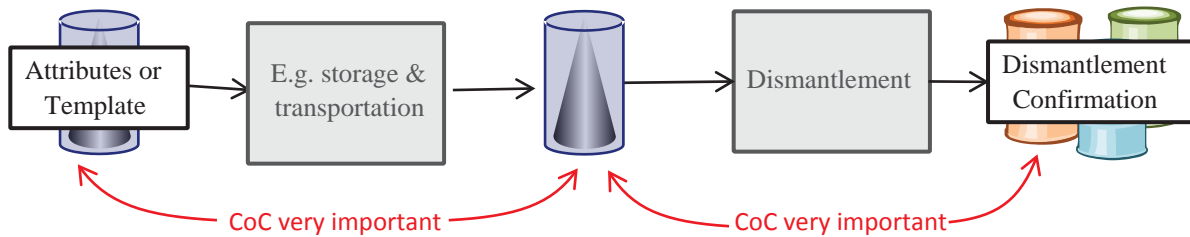


Figure 3: Ramification on CoC for performing warhead confirmation measurements upon entry into the monitoring regime. If there is only one set of warhead confirmation measurements, CoC between those measurements and dismantlement confirmation is extremely important. If the confirmation measurements are performed upon entry into the monitoring regime, there may be a relatively long amount of time (up to years) between the warhead confirmation and dismantlement.

Confirmation made upon entry into the regime has the strongest tie to warhead provenance but requires long-term CoC within the regime to connect this confirmation with eventual dismantlement, which may occur many years later. In addition, confirmation at this time involves the relatively difficult technical challenge of measuring assembled weapons where nuclear signatures may be shielded by explosive material and/or the casing of the weapon itself. Information security concerns may also be heightened for measurements of an assembled weapon.

4.2 Pre-dismantlement – Immediately Pre-dismantlement

Another potential time for warhead confirmation measurements is immediately prior to dismantlement. Such a

measurement may or may not represent the first set of confirmation measurements made on the declared TLI. Confirmation measurements made immediately prior to dismantlement provide added confidence that the item entering the dismantlement process is truly a warhead. The more time that elapses between the most recent warhead confirmation measurement and the dismantlement process, the more difficult it will be to maintain CoC.

If the confirmation measurements are only performed immediately pre-dismantlement, then maintaining CoC prior to this first set of measurements is only valuable if one is relying on provenance and/or movement of the item is a source of confidence in item legitimacy.

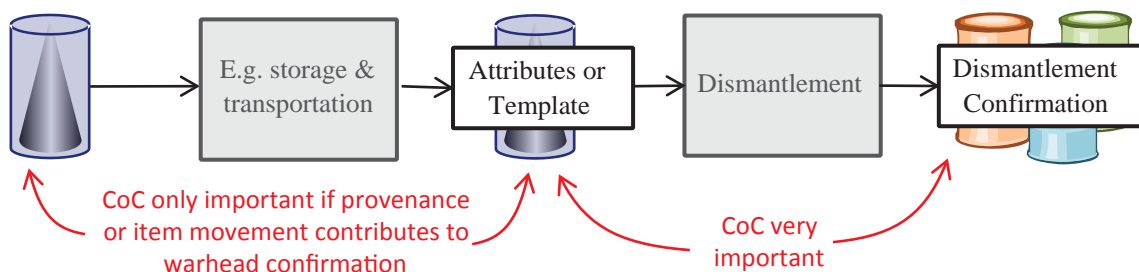


Figure 4: Ramifications on CoC for attribute measurements pre-dismantlement only. If the provenance or item movement is a source of confidence, then CoC prior to the first warhead measurement is very important. If provenance and item movement do not provide confidence, then the value of maintaining CoC prior to confirmation measurements is questionable.

If confirmation is made immediately prior to dismantlement, the tie to dismantlement is much stronger, but the link to the original declaration, and entry into the regime, requires extensive CoC. As the warhead is still assembled at this point in time, the measurement challenge is probably no different than that described in section 4.1.

4.3 Pre-dismantlement – During transportation and storage

Warhead confirmation could also occur at any time during the pre-dismantlement storage and transportation. For the most part, the strengths and trade-offs inherent in such a measurement time fall on a sliding scale between the “Entry into Regime” described in section 4.1 and the “Immediately Pre-Dismantlement” described in section 4.2. However, the one significant exception is that a robust CoC connection is now required for linking to both end points — the direct tie to either provenance or dismantlement has been lost with no specific compensating gain. For this reason, all else being equal, we would advocate making the primary confirmation measurements at one end or the other, and not at an intermediate position.

However, all else is seldom equal. If the CoC regime can begin on the delivery vehicle itself, practical and access limitations may prevent the warhead confirmation measurement from being made at this time. In this case, performing a confirmation measurement as soon as possible following entry into the CoC regime may increase monitor confidence.

In addition, random “challenge” measurements during transportation and storage can increase the monitoring party’s confidence that the TLI remains as declared throughout the process. These intermediate measurements would not replace the confirmation measurements, but would increase confidence that the item being tracked remains a TLI. Even if attribute measurements and/or provenance are used for initial confirmation, a template comparison may be the most effective way to perform these challenge measurements.

Another use of “intermediate” confirmation measurements is to re-establish CoC on an item if CoC has been lost at some point during the transportation and storage operations. It is never the intention to lose CoC, but it is important to have a recovery mechanism, such as re-confirmation, in case such a loss occurs. In addition, the access constraints discussed further in section 4.5 may have a significant impact on confirmation timing.

4.4 Post-dismantlement

There are two potential types of confirmation measurement that may take place post-dismantlement. The first, and most obvious, is to confirm that an item is dismantled,

i.e., that the HE and the FM are separate. Although the dismantlement confirmation itself presents challenges (as touched upon in section 2), the timing of dismantlement confirmation is not in doubt.

Following dismantlement, the TLI confirmation measurement is significantly changed and may be simplified. However, some of the critical characteristics that “make a weapon a weapon” may be lost in the dismantlement process:

- By definition, the shielding effects of HE need no longer be considered post-dismantlement. In addition, since the FM is no longer part of a warhead, the storage and packaging requirements will be changed. If the relevant characteristics are primarily nuclear, like the attribute examples given above, then the reduction in shielding may make nuclear measurements faster, more effective, and more discriminating.
- However, if other characteristics, such as relative FM and HE geometry, are important in the definition of a warhead, then post-dismantlement confirmation adds little or no confidence to an attribute measurement. The effectiveness of this type of warhead confirmation depends explicitly of the declared characteristics of the warhead and the mix of attribute measurement, template comparison and provenance used to make this confirmation.

The CoC requirements for confirmation that a declared item has been dismantled are essentially non-existent as warhead confirmation and dismantlement confirmation are occurring simultaneously (or nearly so). Conversely the CoC requirements for tying the dismantled TLI to the originally declared TLI become more extreme — in particular, the required CoC link now passes through the dismantlement “black box.”

4.5 Comparisons and Analysis

All four potential times for performing warhead confirmation measurements illustrated in Figure 1 have advantages and disadvantages for authentication — some of which have been discussed above. The determination of which confirmation timing is most suitable will depend directly on the details of the particular treaty being confirmed. Two limiting examples can illustrate this concept:

- If a treaty is purely concerned with item dismantlement, then post-dismantlement confirmation provides the strongest link between the item and the dismantlement process. In this extreme, CoC prior to dismantlement becomes less important as the link to regime entry is not a major goal.
- Conversely, if a treaty is purely concerned with keeping track of warheads within a monitoring regime, then confirmation upon entry into the regime provides the strongest, and most timely, tie to the warheads themselves.

In practice, it seems unlikely that a monitored dismantlement treaty would fall into either of these extremes cases. Some of the factors used in determining the most effective times to perform warhead confirmation measurements are: (1) the treaty importance of accepting warheads into the regime, (2) whether a useful provenance of the warhead is available, (3) whether the movements of the item through the monitoring regime provide additional confidence that the item is a warhead, (4) the relative confidence in CoC during different stages of the monitoring regime, (5) the planned types of warhead confirmation measurements (templates or attributes), (6) practical considerations such as the measurement difficulty due to amount of shielding around the item at different points in the monitoring regime, (7) the degree of host sensitivity concerning the container details and/or geometry of the item at different points in the monitoring regime, (8) safety requirements for measuring the item at different points in the monitoring regime, and (9) accessibility of the item, measurement equipment and/or radiation test sources at different points in the monitoring regime.

As *regime acceptance* (1) becomes more important in treaty verification, warhead confirmation at entry into the monitoring regime also becomes more important. If *item provenance* (2) is used as a source of confidence that the dismantled item was indeed a warhead, then it is necessary to maintain CoC continuously from entry into the monitoring regime to post dismantlement regardless of when warhead confirmation measurements are performed. Similarly, if *item movements* (3) through the monitoring regime add confidence in item legitimacy, then CoC must be maintained continuously starting before the movements until after dismantlement. The optimum timing of confirmation measurements may still be influenced by confidence in CoC (as discussed below) but may be dominated by considerations of measurement ability, safety and security.

If item provenance and movements provide only limited confidence and must be supplemented with confirmation measurements, then the timing of warhead confirmation greatly influences (and is influenced by) the *type of CoC* (4) required during different phases of the monitoring regime. The availability of CoC tools influences the optimum timing of warhead confirmation measurements, and maintaining CoC during dismantlement is relatively more difficult than maintaining CoC during storage and transportation.

A good example of a trade-off between CoC and confirmation timing results from the differences of performing confirmation measurements either before or after dismantlement. Regardless of timing, maintaining CoC between the most recent warhead confirmation measurements and post-dismantlement is necessary in order to confirm that the item that is dismantled does (or did) meet warhead confirmation criteria. If the warhead confirmation

measurements are performed before dismantlement, then CoC must be maintained through the dismantlement process. Performing warhead confirmation measurements post-dismantlement avoids the relatively difficult task of maintaining CoC during dismantlement.

There is interplay between the timing of different *types of warhead confirmation measurements* (5). In particular, a template comparison may be best performed prior to dismantlement due to the changes in radiation signatures that accompany dismantlement. Although the attribute examples given in this paper can be measured either before or after dismantlement, some other potential attributes, such as ones based on relative geometry of FM and HE, could only be performed before dismantlement. Attributes that must, by their nature, be performed before dismantlement may provide a stronger indication that an item is a warhead. However, such attributes could also be more sensitive and have not been used in measurement systems to date.

There are *practical* (6) and *security* (7) ramifications of measuring assembled weapons pre-dismantlement or components post-dismantlement. Before dismantlement, the assembled item may have more shielding, thus complicating the technical ability to make the measurement and the geometry of the assembled weapon may be more sensitive than the geometry of the disassembled components increasing security concerns. The *safety* (8) ramifications depend on the item and the facility. An assembled weapon is usually in a highly stable (and safe) state and it may be easier to perform confirmation measurements on an assembled weapon than on a disassembled component containing HE. On the other hand, confirmation measurements on a disassembled FM component may have fewer safety considerations than measurements on an assembled system containing HE. Safety considerations will influence access (and in particular the required distance between detectors and TLI) to the item for the measurement equipment.

The *accessibility* (9) of an item through the various stages of monitored dismantlement can have a very direct influence on the optimum confirmation timing. Measurement techniques such as neutron multiplicity counting and image generation can require large detectors, which are physically incompatible with some locations.

Perhaps the best combination (from an authentication point of view) of measurement strengths, CoC strengths, and efficiency would be achieved by performing warhead confirmation upon entry into the regime (or as soon as practical), immediately pre-dismantlement, and post-dismantlement, with a monitoring party option to perform confirmation measurements at various points during the storage and transportation phases. Steps back from this ideal would be made after considering

the nine factors described above. One possible way to decrease the measurement burden while maintaining monitor confidence would be to give the monitoring party the option of performing measurements at any of these times while still requiring that the confirmation measurements be performed a certain percentage of the time.

5. Acknowledgements

The authors would like to acknowledge the support of Los Alamos National Laboratory in writing and presenting this paper.

The authors would like to acknowledge the support of The U.S. Department of Energy, Office of Nuclear Verification in developing the concepts reported here.

The authors would like to acknowledge discussions with Jacob Benz, Malte Göttsche, John Mihalcz, Paul Rocket, Kevin Seager, Jennifer Tanner, Jonathan Thron, and Tom Weber.

6. References

- [1] Radiation Detection Equipment: An Arms Control Verification Tool, <http://dtirp.dtra.mil/pdfs/211p.pdf>
- [2] Johnson, M W *et al*; *Recovering START Institutional Knowledge*; *Proceedings of the INMM 52nd annual meeting*; Palm Desert, CA; July 17–21, 2011.
- [3] Committee on International Security and Arms Control, [US] National Research Council; *Monitoring Nuclear Weapons and Nuclear-Explosive Materials: An Assessment of Methods and Capabilities*; ISBN: 0-309-54889-6; (<http://www.nap.edu/catalog/11265.html>); 2005; p 45-47.
- [4] Williams, R *et al*; *Advances in Information Barrier Design*; *Proceedings of the INMM 46th Annual Meeting*, Phoenix, AZ; July 10-14, 2005.
- [5] MacArthur, D *et al*; *The Attribute Measurement Technique*; *Proceedings of the INMM 51st annual meeting*, Baltimore, MD, July 11-15, 2010.
- [6] Puckett, J *et al*; *General Technical Requirements and Functional Specifications for an Attribute Measurement System for the Trilateral Initiative*; *Proceedings of the INMM 42nd Annual Meeting*, Indian Wells, CA; July 15-19, 2001.
- [7] Fissile Material Transparency Technology Demonstration; http://www.lanl.gov/orgs/n/n1/FMTTD/index_main.htm.
- [8] Razinkov, S *et al*; *AVNG System Objectives and Concept*; *Proceedings of the INMM 51st annual meeting*, Baltimore, MD; July 11-15, 2010.
- [9] Glaser, A, Barak, B, and Goldston, R J; *Toward an Inspection System for Nuclear Warhead Verification Without Information Barrier*, *Proceedings of the 54th annual INMM Meeting*, July 14-18 2013.
- [10] Tolk, K *et al*; *Trusted Radiation Identification System*; *Proceedings of the INMM 42nd annual Meeting*; Indian Wells, CA; July 15-19, 2001.
- [11] Benz, J and Tanner, J; *Templating As A Chain Of Custody Tool For Arms Control*; *Proceedings of the 35th Annual ESARDA Symposium*; Bruges, Belgium; May 28-30, 2013.
- [12] Tanner, J *et al*; *The 'Room Within A Room' Concept for Monitored Warhead Dismantlement*; *Proceedings of the 35th Annual ESARDA Symposium*; Bruges, Belgium; May 28-30, 2013.

Panel Discussion: Disarmament Verification - a Dialogue on Technical and Transparency Issues

Malte Götsche¹, Götz Neuneck²

¹ Carl Friedrich von Weizsäcker-Centre for Science and Peace Research (ZNF), University of Hamburg, Beim Schlump 83, 20144 Hamburg, Germany, malte.goettsche@physik.uni-hamburg.de

² Institute for Peace Research and Security Policy (IFSH), Beim Schlump 83, 20144 Hamburg Germany

During the ESARDA Symposium 2013, a panel discussion on dismantlement verification took place, where technological and political issues were debated. As specified in this article, the major discussion points were the benefit of multinational, in particular European, technical engagement and correspondingly possible implications and future work that could be done in the context of ESARDA. The discussion was hosted by the ESARDA Novel Approaches / Novel Technologies and Verification Technologies and Methodologies Working Groups as well as the German Network for Nuclear Disarmament Verification (see www.disarmament-verification.org)

The purpose of this discussion was to promote a European debate on dismantlement verification. It was found desirable to create a dialogue between the European arms control and technical communities. Given the diversity of national perspectives within Europe on these issues, the question was what could be jointly done. The panelists represented a heterogeneous group from those nations which are currently major stakeholders in this debate. Among the panelists were Mona Dreicer (US, Lawrence Livermore National Laboratory), David Keir (UK, VERTIC, formerly Atomic Weapons Establishment), Ole Reistad (Norway, Institute for Energy Technology), Annette Schaper (Germany, Peace Research Institute Frankfurt) and Sergey Zykov (Russia, IAEA). The panel was moderated by Götz Neuneck (Germany, Institute for Peace Research and Security Policy).

Discussions on the Panel

The panelists stressed that international engagement between the potential actors should be promoted as the way to find solutions to verification development challenges. If methods and tools were developed unilaterally, how could the other party trust them? Joint research and development was proposed as a way to enable maximum trust in the functionality by all involved parties. The panelists found that one must strive for balances and compromises here. In particular, according to the Nonproliferation Treaty's Articles I and II, no proliferative information may be disclosed to non-nuclear weapon states. Further reasons such as national security and others further limit the amount of information the host party is willing to give. The inspecting party would therefore have incomplete knowledge about

the verification situation which makes the development of methods and tools more difficult. The inspecting state would therefore be interested in a maximum of (non-proliferative) information. This dilemma must be solved cooperatively for joint research and development to succeed. This might require a change of attitudes on both sides through understanding the other's needs: Nuclear weapon states could revisit if helpful non-proliferative information could possibly be declassified. Non-nuclear weapon states must accept that not all information can be given to them and that sometimes explaining why access to certain information is denied cannot be given.

The main question of the discussion was then how to trigger such engagement that would enable such joint activities – as a capacity - and confidence-building measure in its initial state. Keeping in mind the European focus, engagement was largely discussed in the context of nuclear weapon state – non-nuclear weapon state cooperation, though noting that initiatives among nuclear weapon states are also valuable, such as the Trilateral Initiative between the US, Russia and the IAEA. A strong European precedence for such cooperation is the UK-Norway-Initiative, which continues to look into relevant issues such as the development of an information barrier for warhead authentication as well as managed access of inspectors in a high security host facility. While Norway is a key player in this regard, some other non-nuclear weapon states appear to be silent, though this issue could be more relevant to them because of the Nonproliferation Treaty's Article XI calling for disarmament “under strict and international control”. One panelist asked that – given there are few such initiatives - how to convince non-nuclear weapon states that verification is “for them”. How can academia play a part? The role of the International Atomic Energy Agency was also discussed, finding that in particular in the past, the Agency was rather committed to this topic through the Trilateral Initiative and that there could be a future role. In regard to getting more states involved, it was stressed that inclusion requires careful discussions without mirror-imaging, i.e. assuming that the other states' interests would be the same.

Everybody agreed that a good start would be informal or formal cooperation at a scientific or technical level. Many verification issues are of hard scientific nature. It was

stressed that meaningful research can be conducted without access to classified information through working on principal issues of measurement technology or managed access. The benefit of technical collaboration would not only be the research results, but furthermore that the respective research communities are often linked to political decision-makers which could become convinced of the importance of this topic. Scientific engagement could have the form of international exercises and workshops; one participant advocated a “nuclear disarmament laboratory” including purpose-made research programs.

Besides scientific collaboration, the panelists agreed that political needs should be discussed and analyzed. One participant raised the question of what level of intrusive verification is expected and what political boundary conditions must be considered. How much verification is enough? Another participant argued that one should step back and analyze risk paths to find out where verification must be the strongest, somewhat like the Safeguards state-level approach discussed in the IAEA.

An overriding problem identified during the discussion was the lack of funding. Some panelists criticized that funding is often only made available when there is an immediate need for verification solutions, for example because of on-going treaty negotiations and that there are only few actors who currently perceive the need for immediate action. The panelists agreed though that research need for arms control verification is indeed immediate, given that problems have a sincere complexity both from a technical and an implementation point of view, therefore requiring much research and development. Efforts should therefore be strengthened now so that solutions would be available until politically desired.

Precedence of such an approach is the Group of Scientific Experts that researched monitoring technologies and data analysis methods relevant for the Comprehensive Test Ban Treaty verification long before treaty negotiations. Furthermore, one participant argued that the easiest way to hide warheads was now, so that dismantlement verification could become relevant much sooner than Global Zero. All in all, the participants saw a sincere lack of needed funding for such activities, especially in non-nuclear weapon states.

Potential Engagement for ESARDA

According to the panelists, ESARDA would be an excellent forum for further deliberations on dismantlement verification. Firstly, ESARDA participants have the needed expertise, ranging from nuclear detection and Safeguards experts to researchers with an interdisciplinary orientation, emphasizing that much expertise from Safeguards are helpful to develop dismantlement verification methods and tools. Secondly, ESARDA provides a heterogeneous international (European) forum consisting of both nuclear weapon and non-nuclear weapon states. Therefore, it appears that ESARDA could be a good platform to broaden efforts and to encourage experts with relevant expertise to start thinking about this topic. Already now, the Novel Approaches / Novel Technologies and the Verification Technologies and Methodologies Working Groups have dismantlement verification on their agenda and plan to continue to work on that subject. Efforts like this could mark the beginning of a more comprehensive European engagement with dismantlement verification which should be supported given the wealth of technical expertise that already exists within Europe.

Focused Working Group Activities on the Subject of Measurement Uncertainties and Reference Material Needs

J. Tushingham

In November 2011, the ESARDA Working Group on Standards and Techniques for Destructive Analysis (WG DA), in close collaboration with the International Atomic Energy Agency (IAEA), held a dedicated workshop on 'Uncertainties in Nuclear Measurements'. The workshop facilitated an exchange on the concepts and methods of measurement uncertainty estimation among reference material institutes, safeguards laboratories, nuclear and environmental material analysts and, in particular, operators on estimation of measurement uncertainty in nuclear measurements. Plenary lectures on fundamental metrological concepts for the estimation of uncertainty in nuclear measurements; and measurement uncertainty in material balance verification were followed by sessions on nuclear material analysis – for both accountancy and non-accountancy purposes – and environmental swipe sample analysis. A number of important recommendations were made on conclusion of the workshop, including a proposal to hold a dedicated workshop involving the ESARDA WG DA; the Working Group on Techniques and Standards for Non-Destructive Analysis (WG NDA); and the Working Group on Novel Approaches/Novel Technologies (WG NA/NT).

The three Working Groups WG DA, WG NDA and WG NA/NT subsequently held a joint workshop in March 2013. The workshop addressed the needs for standards/reference materials supporting DA and NDA instrument metrology and conformity assessment, and their application in estimation of measurement uncertainty, including uncertainty in nuclear data in view of new approaches in safeguards and needs for improvement of accuracy of existing DA and

NDA techniques. A plenary lecture on Euratom safeguards was followed by sessions on inspections and evaluations, destructive analysis, non-destructive analysis and novel technologies. The findings and points of discussion from these sessions were formulated into a series of recommendations including priority needs for reference materials, strengthening the understanding of metrological principles, compliance with international standards and the need to address the requirements of traceability at the outset of measurement development. A particular outcome of this workshop was that all participants recognised the need and the benefit of intensifying cooperation and exchange between safeguards; operators; research; and metrology communities, and follow-up activities were suggested.

Two detailed reports, providing summaries of the discussions held during the workshops and recommendations arising from the workshops, are now available. The abstracts are presented on the following pages, whilst the full reports may be downloaded from the ESARDA website:

<https://esarda.jrc.ec.europa.eu>

The Chairs of the Working Groups involved anticipate further collaboration in the future, with a joint meeting currently under discussion for Luxembourg 2014. Meanwhile, the Working Group Chairs take this opportunity to express their appreciation to all participants of the 2011 and 2013 workshops, and to the IAEA and DG Energy, respectively, for hosting the workshops.

Report on the Workshop on UNCERTAINTIES IN NUCLEAR MEASUREMENTS Organised by the ESARDA Working Group on Standards and Techniques for Destructive Analysis (WG DA)

Y. Aregbe⁽¹⁾, J. Tushingam⁽²⁾, K. Mayer⁽³⁾, G. Granier⁽⁴⁾, D. Donohue⁽⁵⁾, S. Balsley⁽⁵⁾, T. Prohaska⁽⁶⁾, S. Vogt⁽⁵⁾

⁽¹⁾ European Commission-Joint Research Centre-Institute for Reference Materials and Measurements, Geel, Belgium

⁽²⁾ National Nuclear Laboratory, Oxfordshire, United Kingdom,

⁽³⁾ European Commission-Joint Research Centre-Institute for Transuranium Elements, Karlsruhe, Germany

⁽⁴⁾ Commissariat à l'Énergie Atomique - DEN/DRCP/CETAMA, Marcoule, France

⁽⁵⁾ International Atomic Energy Agency - Office of Analytical Services, Department of Safeguards – IAEA-SAL, Seibersdorf, Austria

⁽⁶⁾ University of Natural Resources and Applied Life Sciences BOKU, Vienna, Austria

Abstract:

The ESARDA Working Group on Standards and Techniques for Destructive Analysis (WG DA), in close collaboration with the International Atomic Energy Agency (IAEA), organised a dedicated workshop on 'Uncertainties in Nuclear Measurements'. The workshop was held in conjunction with the annual working group meeting at the IAEA Safeguards Analytical Services (IAEA-SGAS) Seibersdorf Laboratories (SAL), Austria, on 8-9 November 2011. The focus of the workshop was to exchange concepts and methods of measurement uncertainty estimation among reference measurement institutes, safeguards laboratories, nuclear and environmental material analysts and, in particular, operators on estimation of measurement uncertainty in nuclear measurements. Participation was open to ESARDA WG DA members and to a limited number of invited participants from expert and research institutes. Forty-eight representatives from the main European and international nuclear safeguards organisations, nuclear measurement laboratories, nuclear industry and experts from environmental sciences institutes, participated in this workshop. Fundamental metrological concepts for the estimation of uncertainty in

nuclear measurements were presented by Roger Wellum, retired from Institute for Reference Materials and Measurements (IRMM) in the first plenary lecture. The second plenary lecture was given by Claude Norman from the IAEA on measurement uncertainty in material balance verification. The plenary lectures were followed by three sessions, the first on nuclear material analysis for accountancy purposes, the second on nuclear material analysis for non-accountancy purposes, and the third session was dedicated to Environmental Swipe Sample Analysis. The findings and points of discussion from these sessions were further discussed in a working group using the 'World-Café' approach around three selected topics, ensuring that all participants could benefit from the 'collective intelligence'. This report is a summary of the points of discussion raised during the sessions and in the working group, with main emphasis on the recommendations for the topics of approaches to uncertainty, sources of uncertainty, and knowledge of uncertainty. As in previous workshops organised by the ESARDA WGDA, all participants recognised the need and the benefit of intensifying cooperation between the nuclear safeguards and nuclear forensics communities, nuclear industry and environmental sciences institutes.

Report on the Workshop on Reference Material needs and Evaluation of Measurement Uncertainties in Destructive (DA) and Non-Destructive Analysis (NDA)

Y. Aregbe⁽¹⁾, H. Toivonen⁽²⁾, A-L. Weber⁽³⁾, J. Dackner⁽⁴⁾, P. Klumpp⁽⁴⁾, T. Prohaska⁽⁵⁾, E. Zuleger⁽⁶⁾, O. Alique⁽⁴⁾, R. Bencardino⁽⁴⁾, R. Jakopic⁽¹⁾, P. Peerani⁽⁷⁾

⁽¹⁾ European Commission-Joint Research Centre-Institute for Reference Materials and Measurements, Geel, Belgium

⁽²⁾ STUK - Radiation and Nuclear Safety Authority, Helsinki, Finland

⁽³⁾ Institut de Radioprotection et de Sûreté Nucléaire, Fontenay-Aux-Roses, France

⁽⁴⁾ European Commission Directorate General Energy, Nuclear Safeguards, Luxembourg

⁽⁵⁾ University of Natural Resources and Applied Life Sciences BOKU, Vienna, Austria

⁽⁶⁾ European Commission-Joint Research Centre-Institute for Transuranium Elements, Karlsruhe, Germany

⁽⁷⁾ European Commission-Joint Research Centre-Institute for Transuranium Elements, Ispra, Italy

Abstract

The ESARDA Working Groups on Techniques and Standards for Destructive Analysis (WG DA); on Techniques and Standards for Non-Destructive Analysis (WG NDA); and on Novel Approaches/Novel Technologies (WG NA/NT) organised a dedicated workshop on 'Reference material needs and evaluation of measurement uncertainties in Destructive (DA) and Non-Destructive Analysis (NDA)'. This workshop was hosted by the European Commission Directorate General Energy (DGENER) Nuclear Safeguards in Luxembourg from 5-7 March 2013. The workshop addressed the needs for standards/reference materials supporting DA and NDA instrument metrology and conformity assessment, and their application in estimation of measurement uncertainty including also uncertainty in nuclear data in view of new approaches in safeguards and needs for improvement of accuracy of existing DA and NDA techniques. The focus was to establish a regular exchange on these topics relevant to all three working groups with a special emphasis on supporting the needs of safeguards inspectors and evaluators. Participation was open to members and observers of the three ESARDA WGs, to DGENER and to a limited number of invited participants from expert and research institutes. Forty-nine representatives from the main European and international nuclear safeguards organisations, reference measurement institutes, metrology institutes, nuclear measurement laboratories, nuclear industry and from environmental sciences institutes participated in this workshop. The plenary lecture

on 'Euratom safeguards – inspections – evaluations' given by DGENER was followed by four sessions, the first on 'Safeguards – Inspections and Evaluations', the second on 'Destructive Analysis', the third on 'Non-Destructive Analysis', and the fourth session on 'Novel Technologies'. The findings and points of discussion from these sessions were further discussed in a working group using the 'World-Café' approach around five selected topics, ensuring that all participants could benefit from the 'collective intelligence'. This report is a summary of the points of discussion raised during the sessions and in the working group. The WS participants proposed recommendations for setting priorities on needs of reference materials in DA and NDA, for strengthening the understanding based on metrological principles and the Guide to the expression of uncertainty in measurement (GUM) between different approaches in uncertainty estimation for DA/NDA, and in the evaluation of reported results. Furthermore recommendations were given in view of compliance with international standards and the implementation of quality systems. Research and development towards new methods, new instruments, novel technologies, and modelling should be carried out having in mind right from the outset the requirements of feasibility, transparency, traceability and accuracy of measurement results. A particular outcome of this workshop was that all participants recognised the need and the benefit of intensifying cooperation and exchange between the safeguards; operators; research; and metrology communities, and follow-up activities were suggested.

